Manipulation of Mesenchymal Stem Cell Differentiation via Gold Nanoparticle-mediated Delivery of AntagomiRs

Shijoy Mathew

Submitted in fulfilment of requirements for the degree of Doctor of Philosophy (PhD)

Centre for the Cellular Microenvironment

Institute of Molecular, Cell and Systems Biology

School of Medical, Veterinary and Life Sciences

University of Glasgow, University Avenue

Glasgow, G12 8QQ

January 2020

Abstract

The human body is a complex piece of organic machinery, and as such, can be prone to faults and deterioration. There are many medical conditions that can be attributed to bone or cartilage deterioration and damage, like osteoporois and osteoparthritis. Regeneration of these tissues is an on-going challenge, which have been targeted in many different ways.

MicroRNAs are short sequenced RNAs that are involved in the regulation of nearly 60 percent of the genes in the body. This project aims to exploit their function to promote differentiation into different cell lineages. To do so, the implication of several microRNAs in osteogenesis, adipogenesis and chondrogenesis is investigated, and key microRNAs selected. Then, gold nanoparticles (GNPs) are used as a platform to deliver to the MSCs, anti-microRNAs (antagomirs) and microRNAs mimics, which are nucleotide sequences that can bind to the microRNA, preventing or promoting their function, respectively. The use of nanoparticles in medicine has picked up at a rapid rate, and its small size, non-toxicity and multi-valency allows for a safer and customizable method of cargo delivery.

In addition, the novel nanokicking technology, based on applying nanovibrations to the cells, which has been previously proven to induce osteogenesis, will be combined with the delivery of the miRNA-functionalised GNPs with the purpose of triggering a synergistic effect that enhances the osteogenic differentiation process.

Table of Contents

Acknowledgements

Firstly, I would like to thank my supervisor, Dr. Catherine Berry. She has provided me with the opportunity to tackle this innovative and exciting project and has excellently guided me through my PhD. She has helped me improve all aspects regarding scientific research and also helped me improve as a person. Her kind and caring nature helped with all the stresses that comes with a PhD and I will forever be grateful to her.

I would also like to thank my second supervisor, Prof. Matthew Dalby. By always willing to lend a second opinion has improved my way of thinking. His intelligence and nature always puts a smile on my face. The lectures during my Masters course conducted by him helped shape my interest in stem cell research.

A special mention to Dr. Mathis Riehle as the embodiment of a scientist. His wide range of expertise and interests is truly enlightening and watching him work with cells to plastic knobs is always a pleasure. His explanation of complex non-biological concepts has helped me with understand my work with clarity.

Mrs. Carol-Anne also deserves all my praise for always helping me with any issues I have had. She has provided support at the expense of her own time and I was able to obtain everything I needed due to her quick and effective methods.

I would also like to thank all the members of CCE (currently CeMi). From Dr. Monica Tsimbouri, who always lent a hand with all my work, to Dr. Aviral Vasta, whose guidance through the initial stages of my PhD, everyone has in one way or another, brought joy to this long journey. Also, a special thank you to Dr. Ross Gurden, who was a wizard with programming.

Finally, I would like to thank my parent for supporting me through this endeavour. Their belief in me helped to push me to achieve greater things.

Of course, a thanks to all my friends who help me forget about all this PhD business.

Authors Declaration

I hereby declare that the research reported within this thesis is my own work, unless otherwise stated, at the time of submission is not being considered elsewhere for any academic qualification.

Shijoy Mathew

6th January 2020

List of Tables

List of Figures

Chapter 1: Introduction

1.1 **Stem Cells**

The human body consists of cells that originated from stem cells. Stem cells are progenitor cells that can generate the specialised cells that form tissue and organs. Stem cells are also involved in the repair mechanisms of most multicellular organisms (Pittenger *et al.*, 1999; Ullah, Subbarao and Rho, 2015). The two main properties that define a stem cell are self-renewal and multipotency. Self-renewal is the ability of a cell to replicate itself without losing any of its information i.e., forming a perfect copy of itself (Bianco and Robey, 2001). Multipotency is the capacity of the cell to transform into specific types. The two main types of stem cells are embryonic stem cells and adult stem cells (Bianco, 2014).

Stem cell self-renewal occurs by two mechanisms. Obligatory asymmetric replication is when a cell divides into an undifferentiated mother cell, similar to its original state and a differentiated cell (Knoblich, 2008). Alternatively, stochastic differentiation is where the cell divides into either two undifferentiated or differentiated cells depending on the signals received (Sun and Komarova, 2015). Both methods of stem cell replication result in different cell pools, which are illustrated in fig. 1.1.

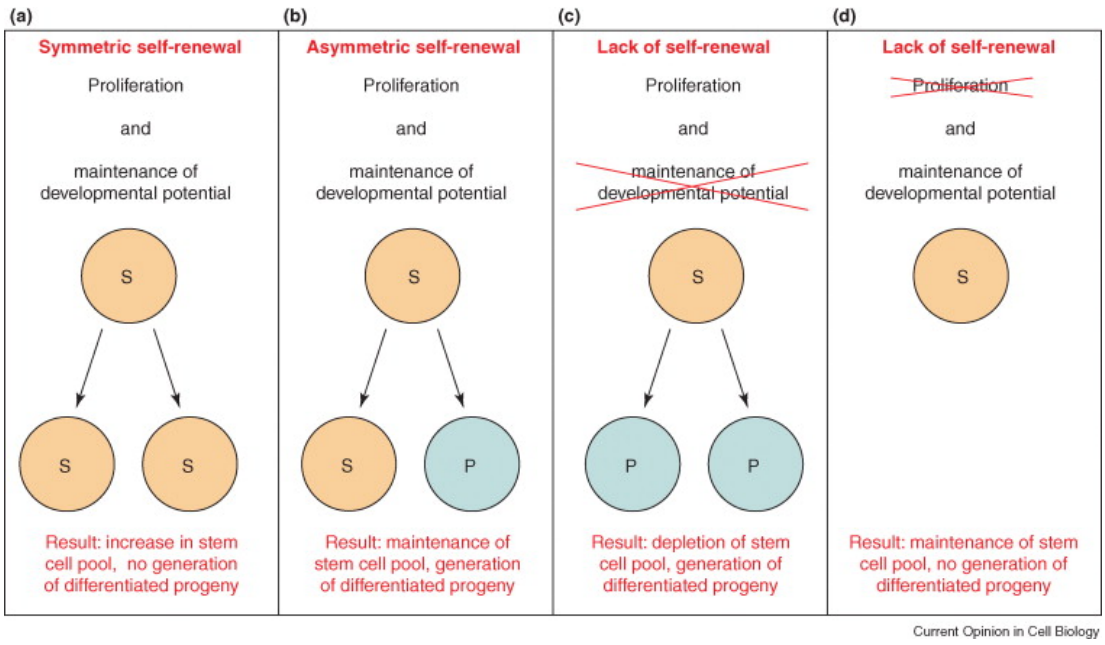

Fig. 1. 1 MSC self-renewal. The different self-renewal pathways are illustrated. The **S** indicates undifferentiated stem cell, while **P** shows differentiated progeny. The cell divides by either symmetric self-renewal generating two stem cells (**a)** or by asymmetric self-renewal producing a differentiated cell and one stem cell (**b)**. Over time, stem cells lose either their maintain stemness (**c)** or proliferate (**d)**, leading to depletion of stem cell pool or differentiated cells (Fig. adapted from Molofsky, Pardal, & Morrison, 2004).

Potency is the property of the stem cell to differentiate in different cell types. Some cells are pluripotent, such as embryonic stem cells, and they differentiate into nearly all types, while other adult stem cells, such as, mesenchymal stem cells (MSCs), can only differentiate into a more limited number of cell types (Samsonraj *et al.*, 2015).

Embryonic stem cells are cells derived from the blastocyst phase of embryos. They are pluripotent and can differentiate into cells found in the three germ layers; endoderm, ectoderm and mesoderm (Odorico, Kaufman and Thomson, 2001). Through gene transcription, either from the body or manually (through chemical induction) *in vitro*, these cells have the capacity to differentiate into any cell type (Reubinoff *et al.*, 2000). They are in high demand for use in regenerative therapy, but research is limited due to the ethical dilemmas brought about due to the procurement process of these cells (Avior, Sagi and Benvenisty, 2016).

Adult stem cells can be classified into two types; haematopoietic stem cells (HSCs) and mesenchymal stem cells (MSCs) (Chamberlain *et al.*, 2007; Vaidya and Kale, 2015). Mesenchymal stem/stromal cells or MSCs are found in different parts of the body such as bone marrow, adipose tissue and umbilical cord tissue (Mushahary *et al.*, 2018). MSCs are known to differentiate into several key cell types, the prominent ones being osteoblasts (bone), adipocytes (fat) and chondrocytes (cartilage) (Phinney and Prockop, 2007). MSCs were initially used for supporting HSC cultures due to the limited knowledge of them (Eastment *et al.*, 1982). Due to the arrival of recombinant growth factors and further understanding of their properties, bone-marrow derived MSCs are now routinely cultured and widely used in regenerative therapy, due to their comparative ease of procurement and differentiation profile (Richardson *et al.*, 2010).

1.1.1 Mesenchymal Stem Cells

MSCs are fibroblastic cells that were first isolated from guinea pig bone marrow (Friedenstein, Chailakhjan and Lalykina, 1970). Researchers were able to produce clonal colonies that could generate bone and reticular tissue. Further advancements and studies demonstrated that MSCs could also differentiate into other cells such as adipose and cartilage

cells. Their self-renewing nature and ability to differentiate into multiple cell types has allowed research into the capabilities of MSCs and showed the potential for regenerative medicine (Ding, 2011).

MSCs are primarily located in the bone marrow, adipose tissue and umbilical cord, from where they can be isolated for research purposes. The bone marrow stroma includes all the tissue within the bone marrow that are not involved in the function of haematopoiesis, the generation of new blood cells form HSCs. Within the bone marrow, MSCs reside in what is termed a 'niche', existing as cells lining the compact bone (endosteal niche) and cells surrounding vascular areas (perivascular niche) (Friedenstein, Chailakhyan and Gerasimov, 1987; Young *et al.*, 1995; Cordeiro-Spinetti, Taichman and Balduino, 2015; Grayson *et al.*, 2015).

There are many cellular markers that can be used to identify MSCs. The Mesenchymal and Tissue Stem Cell Committee of the International Society Cell & Gene Therapy (ISCT) defined the major markers that must be present to consider the cells as MSCs. The positive markers that must be present are CD73, CD90 and CD105, with the CD45 being a negative marker. Since MSCs exhibit several other markers which may or may not be present it all cells, it is extremely difficult to isolate a "pure" population of MSCs (Deans and Moseley, 2000; Dominici *et al.*, 2006). A mixed population is obtained and all the properties of each of these subtypes is yet to be understood.

Typically, isolation of MSCs from bone marrow involves either the explant culture method or the enzymatic method. In case of the former, the source tissue is rinsed with buffer to exclude blood cells and cut into tiny pieces and cultured on a cell culture plate. In enzymatic isolation, the small pieces are incubated in an enzyme solution which degrades the extracellular matrix. This allows release of small cell aggregates which are plated. The cells are sorted using flow cytometry, which shows if the cells have the pertinent markers mentioned above. They can be further separated based on the different markers allowing for isolation of specific phenotypes from the mixed population (Li *et al.*, 2016; Mushahary *et al.*, 2018).

1.1.2 MSC Differentiation

Mesenchymal stem cells are able to differentiate into multiple cell types (Dominici *et al.*, 2006; Ding, 2011; Bianco, 2014). When appropriate signals are received, the MSCs will drive toward a defined lineage (Bhaskar *et al.*, 2014). MSCs can differentiate into osteoblasts, adipocytes, chondrocytes, myoblasts and even neuron-like cells (Augello and De Bari, 2010). Research has shown that through specific interactions, the MSCs can differentiate into other cell types similar to the ones mentioned (Ye *et al.*, 2018; Leeman *et al.*, 2019). The most widely studied lineages are osteogenesis, adipogenesis and chondrogenesis, due to their impact in regenerative medicine and potential for therapy (Wang, Qu and Zhao, 2012).

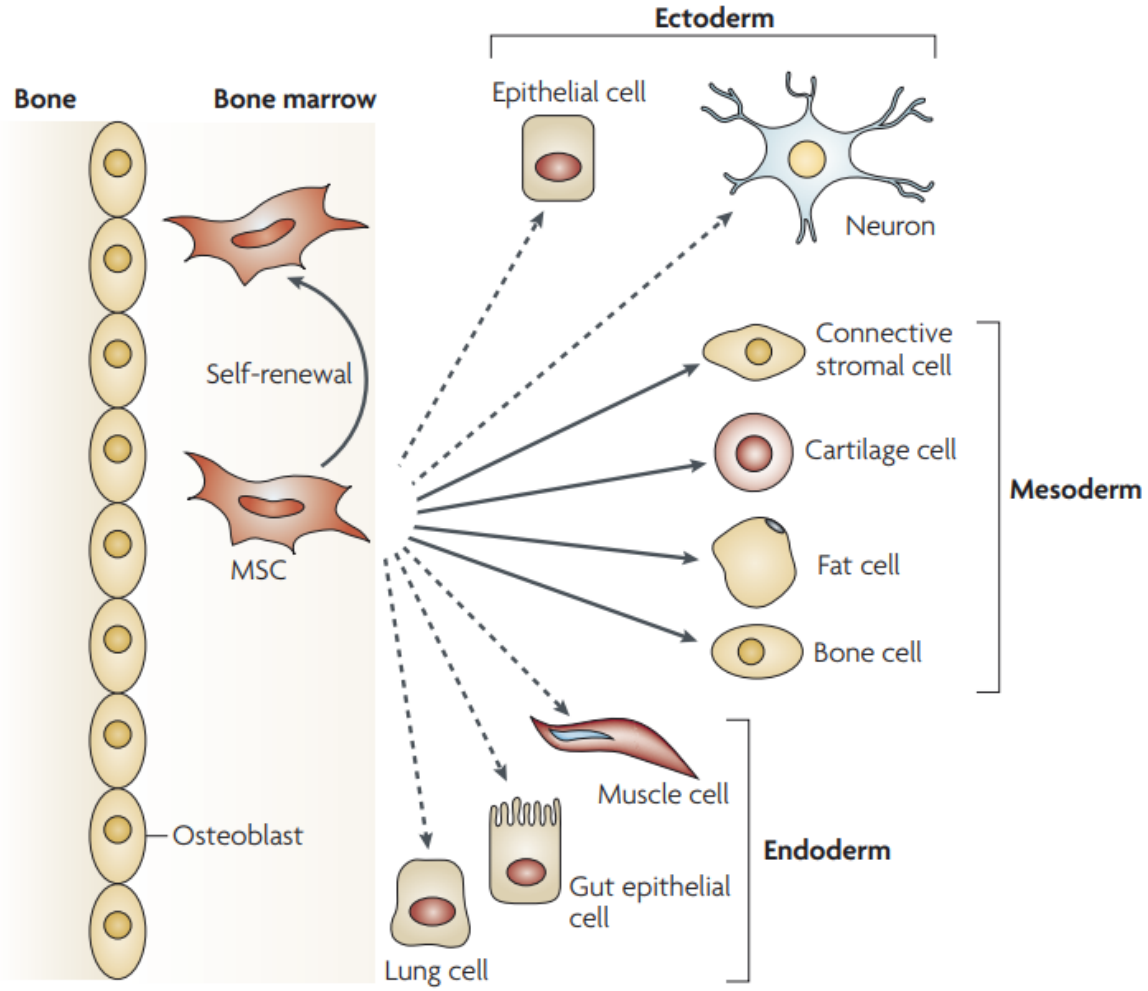

Fig. 1.2: MSC differentiation in the Bone Marrow. The key differentiation pathways are illustrated with solid arrows indicating differentiation *in vivo*, while the dashed arrows show reported pathways of differentiation through *in vitro* research studies (Fig. adapted from Uccelli, Moretta, & Pistoia, 2008).

1.1.2.1 Osteogenesis

Osteogenesis is defined as the differentiation of MSCs into osteoblasts or bone cells. This is a tiered process wherein the MSC becomes a pre-osteoblast and then into a mature osteoblast. During differentiation down the bone lineage, MSCs begin to synthesis and secrete an extracellular matrix consisting of fibronectin and type 1 collagen among other proteins. Indeed, osteoblast maturation can be characterised by the phases of proliferation, maturation, matrix synthesis and matrix mineralization (Neve, Corrado and Cantatore, 2011). Once the bone matrix has mineralized, it can be realised as bone as shown in fig. 3. The osteoblasts trapped in their mineralization are known as osteocytes (Bonewald, 2007). These cells make up most of the cells in the bone tissue, being involved in the signalling and bone resorption (Metzger and Narayanan, 2019).

Several signalling and transcription factors are involved in osteogenesis. The key transcription factor is the Runt-related transcription factor 2 (Runx2). Studies on Runx2 knockout mice have shown a lack of bone formation due to insufficient osteoblasts (Bruderer *et al.*, 2014). Other important bone matrix protein gene inducers are osterix and β-catenin. Immature and mature osteoblasts can be differentiated by the increased presence of either osteopontin (OPN) or osteocalcin (OCN) proteins respectively. The β-catenin dependent Wnt signalling pathway is an integral pathway, wherein β-catenin accumulates in the nucleus and heterodimerizes with lymphoid enhancer-binding factor/T-cell factor (Lin and Hankenson, 2011). This induces gene transcriptional activity leading to determination of MSC fate. Hedgehog signalling (HH) pathway is another important signalling pathway (Yang *et al.*, 2015). Other important pathways for bone formation are the BMP pathway and NELL-1 signalling pathway (Lin and Hankenson, 2011; Hayrapetyan, Jansen and van den Beucken, 2014). These pathways can collectively be visualised in fig. 1.3.

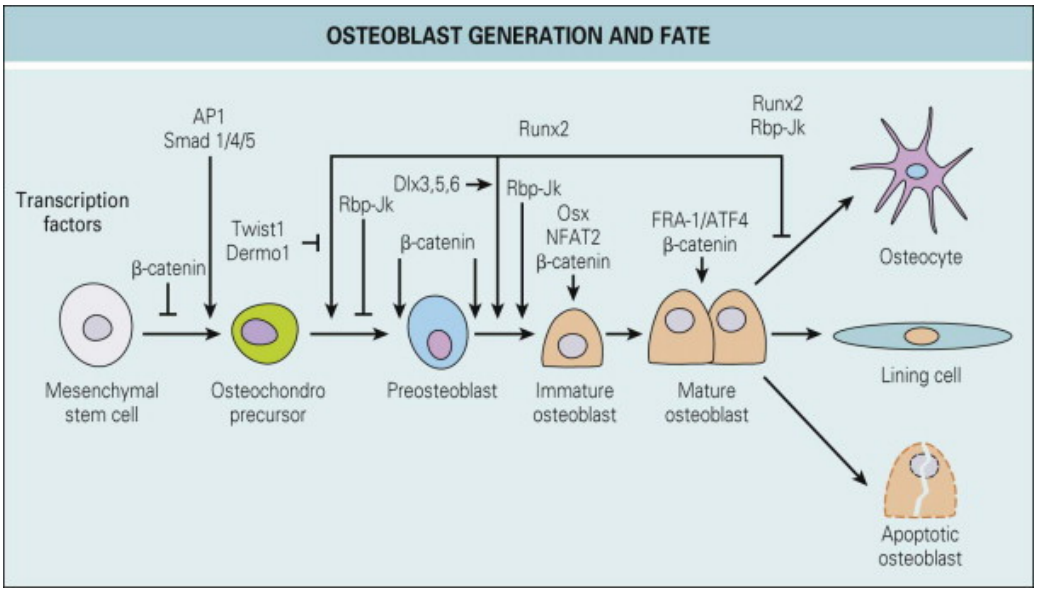

Fig. 1. 3: The key Signalling Pathways Involved in Osteogenesis. Adapted from (Burr, Bellido and White, 2015).

1.1.2.2 Adipogenesis

The maturation of MSCs to adipocytes is termed adipogenesis. This can be characterized by two phases; the determination phase and the terminal differentiation phase (Rosen and MacDougald, 2006). In the determination phase, MSCs commit to the adipocytic lineage and differentiate into pre-adipocytes. They have a fibroblastic structure and are thus indistinguishable from undifferentiated MSCs. In the terminal phase, the pre-adipocytes differentiate into adipocytes and become larger and rounder due to the presence of lipid vacuoles, where their functions include lipid synthesis and storage (Muruganandan, Roman and Sinal, 2009).

Peroxisome proliferator-activated receptor gamma (PPARγ) is the main transcription factor for inducing adipogenic competence, and thus it is also known as the master regulator of adipogenesis(Masanobu, 2013). Loss of PPARγ function leads to absence of adipogenic capacity of MSCs (Kamon *et al.*, 2003). Adipogenesis involves various sequential processes that converge at the PPARγ transcription level. . The other main proadipogenic transcription factor is the CCAAT/enhancer binding proteins (C/EBPs); PPARγ and C/EBPα induce gene expression for insulin sensitivity, lipogenesis and lipolysis (Darlington, Ross and MacDougald, 1998). The Kruppel-like factor (KLF) family of proteins which function

cooperatively to trigger the appropriate genes and induce the differentiation into preadipocytes and eventually adipocytes (Darlington, Ross and MacDougald, 1998; Masanobu, 2013).

Adipogenesis, has an inverse relationship with osteogenesis; the signals and pathways that promote adipogenesis inhibit the osteogenic lineage. The regulation of Wnt and HH signalling pathways are essential for adipogenesis (Fontaine *et al.*, 2008; D'Alimonte *et al.*, 2013). The inhibition of these pathways prevents osteogenesis and thus direct the differentiation of MSCs toward adipocyte formation. Other proosteogenic pathways such as Notch signalling, and BMP pathways must be blocked for adipogenesis(James, 2013).

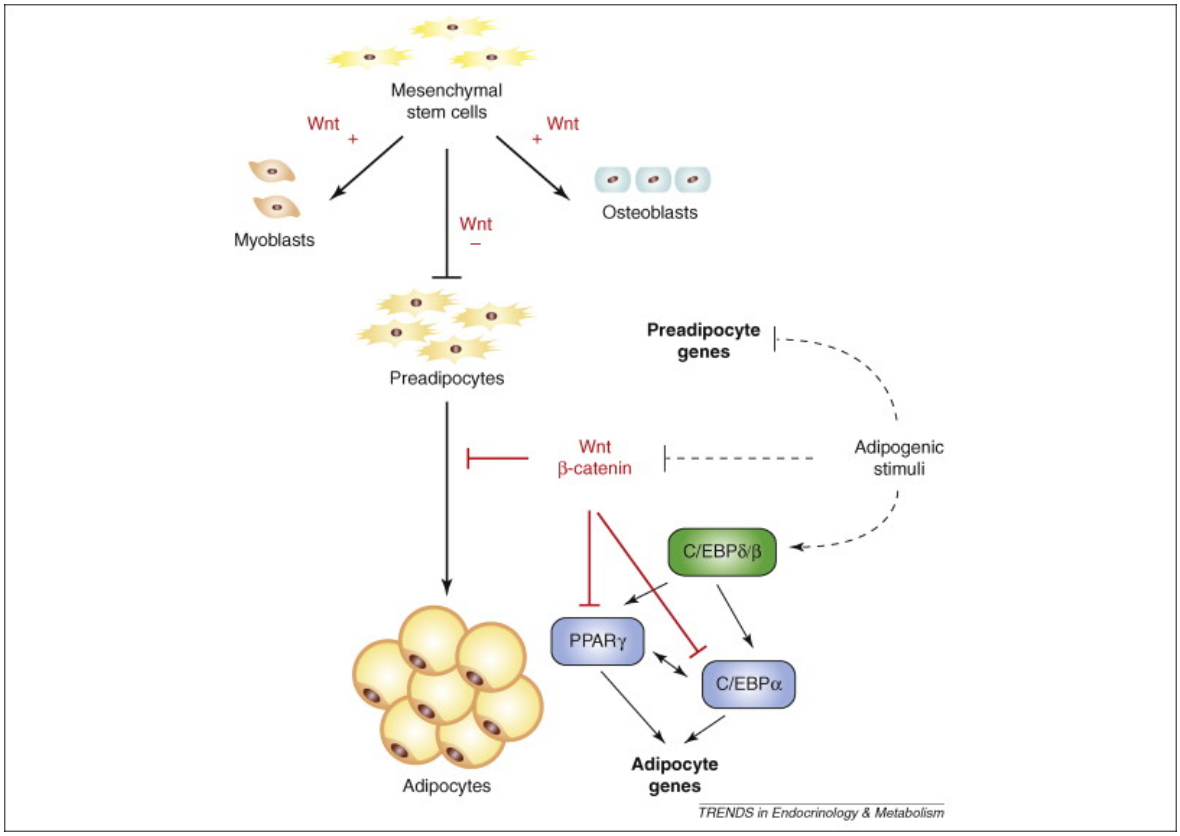

Fig. 1. 4: Key signalling pathways in Adipogenesis: Adapted from (Christodoulides *et al.*, 2009)

1.1.2.3 Chondrogenesis

Chondrogenesis is the differentiation of MSCs to chondrocytes, responsible for the development of cartilage in the body. MSCs need to be in a condensed form to be able for the change to occur. Extracellular matrix formation is vital, and the concentrated nature of

the cells is also essential for this. Mineralization is the next step, leading to the formation of calcified cartilage at a much later stage (Lefebvre and Smits, 2005).

Chondrocyte formation is a comparatively lesser known differentiation pathway. Although some molecular signals have been identified, the processes that lead to chondrogenesis are still not completely understood. A member of the HH signalling family, sonic hedgehog (Shh), is integral in expression of Sox9, the master regulator of chondrogenesis (Akiyama, 2008). Sox9, an early chondrogenic marker, is crucial for the differentiation and maturation of MSCs into chondrocytes as it leads of expression of Sox5 and Sox6, which together allow expression of type-II collagen, which is essential for chondrogenesis (Wuelling and Vortkamp, 2010). Sox9 is also integral in preventing hypertrophy of chondrocytes, although the exact mechanisms of which are not completely understood (Martinez-Sanchez, Dudek and Murphy, 2012). Runx2 is also involved, but only at the later stages to induce endochondral ossification (hypertrophy) (Liao *et al.*, 2014). Similarly, BMP-2 is also a later stage transcription factor that also shift chondrogenesis towards hypertrophy (Michigami, 2014). Cell-cell interactions are essential for development of cartilage, and although the exact mechanisms are still unknown, connexin-43 has been linked to osteoprogenitor chondrogenesis (Guillotin *et al.*, 2004; Zhang *et al.*, 2010). This may carry over to MSCs, but further study is required to be conclusive.

Collagens II, IX and XI are expressed during extracellular matrix formation (Chen *et al.*, 2005). The process of chondrogenesis is regulated by several growth factors such as fibroblast growth factor (FGF), transforming growth factor beta (TGFβ), BMP and Wnt pathways (Mariani, Pulsatelli and Facchini, 2014). The blocking of FGF and Wnt signalling pathways patently directs differentiation towards chondrocytes (Ito *et al.*, 2008; Qu *et al.*, 2013), however the role of TGFβ pathway is less clear, as studies have shown it to help with chondrocyte formation in joints, but it does not seem to be involved in the lineage direction during the initial stages of chondrogenesis (van der Kraan *et al.*, 2009).

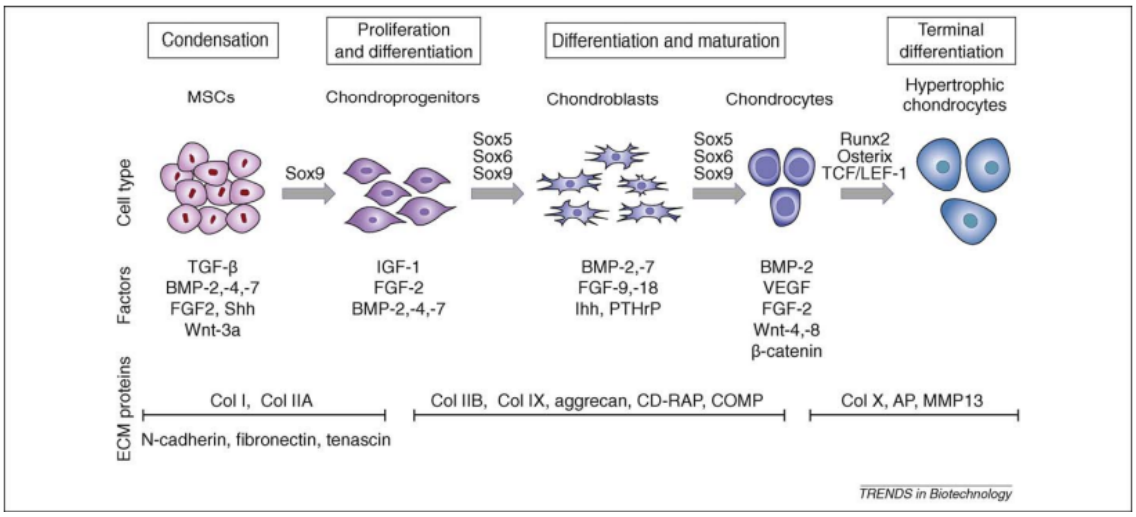

Fig. 1. 5: Key signalling pathways in Chondrogenesis. Adapted from (Vinatier *et al.*, 2009)

1.1.3 Artificial MSC Differentiation

The multipotent nature of MSCs has been exploited to artificially induce differentiation due to the potential for regenerative medicine. Chemical inducers were the primary method used to artificially trigger differentiation *in vitro*, due to their potency and relative ease of application (Lai *et al.*, 2017). As these are potentially toxic and difficult to administer *in vivo*, other methods of differentiation have been discovered and studied. Following the advent of micro- and nanotechnology, physical methods have also shown great promise. These methods can involve the use of physical forces to trigger certain mechanisms for differentiation, while others use proteins and other biological signals to induce differentiation (Li *et al.*, 2011; Tsimbouri *et al.*, 2014). Indeed, due to their non-intrusiveness, physical induction of differentiation is sought after for implants to be used in bone healing (Heydari Asl *et al.*, 2018).

1.1.3.1 Chemical Induction of MSC Differentiation

The most commonly used method to induce differentiation in nearly all cell types is to use soluble chemical factors, or agonists, that can trigger the various pathways for differentiation. Chemical inducers are widely used in laboratory settings to study differentiation.

For induction of osteogenesis, dexamethasone, ascorbic acid and β-glycerophosphate are the most commonly used supplements (Kuznetsov *et al.*, 1997). Dexamethasone is an essential corticosteroid, whose increased concentration can induce osteogenesis, while decrease in its levels can induce adipogenesis of MSCs. Dexamethasone enhances Runx2 expression (Viti *et al.*, 2016). Ascorbic acid is required for increased collagen type I production and β-glycerophosphate provides the phosphates needed for mineralization (Langenbach and Handschel, 2013).

Adipogenesis can be achieved by using dexamethasone, insulin and 3-isobutyl-1-methylxanthine (IBMX) (Pittenger, 1998). Insulin mimics insulin-like growth factor (IGF), which is an important signal in adipogenesis. Dexamethasone, in tandem with IBMX, stimulates the master transcription factor PPARγ expression (Scott *et al.*, 2011).

With regard to chondrogenesis, dexamethasone, transforming growth factor beta (TGFβ) and insulin (along with certain supplements) are used (Yoo *et al.*, 1998). Dexamethasone increase the collagen II levels with the cells and also the mRNA expression of aggrecan. Insulin, through the insulin receptor, acts as an inducer for chondrogenesis. TGFβ signalling pathways are essential for cartilage formation and maintenance (Zhang *et al.*, 2010).

There have been studies conducted to utilize proteins to trigger differentiation pathways of MSCs. An example includes the use of bone morphogenetic proteins (BMPs) such as BMP-2, either in their native form or as mimics. By binding these to implant surfaces or within hydrogel matrices, osteogenic differentiation can be triggered (Noël *et al.*, 2004; He *et al.*, 2014).

1.1.3.2 Physical Induction of MSC Differentiation

Over the past decade, research has shown the importance of physical cues and stimulation in cell behaviour (Higuchi *et al.*, 2013). Mechanical stimuli are key regulators of cellular structure and function and cells respond to these cues and illicit responses that include

motility, differentiation and proliferation. These cues can also cascade along neighbouring cells causing wide scale changes within cells (Wang and Chen, 2013). By exploiting these mechanical factors, differentiation can be directed towards a preferred lineage allowing *in vivo* translation of these techniques (Guilak *et al.*, 2009).

1.1.3.3 Differentiation induced by the physico-chemical properties of the substrate

The stiffness of substrates can be used to direct MSC fate. Engler et al. showed that MSCs are able to "feel" their environments and respond to the physical cues around them. Hard matrices cause the MSCs to be more secretory in terms of production of factors key for osteogenesis, while soft matrices are the opposite (Engler *et al.*, 2006). This can be attributed to the motor appendages, such as myosin II, pulling the against the matrix, which causes the cellular mechano-transducers to release signals to cope with this stress (Pelham and Wang, 1997). By inhibiting the action of the activities of myosin isoforms, the cells do not undergo the necessary stress changes to illicit a response (Kim *et al.*, 2005).

Several studies have shown that matrices of various stiffnesses can be used for multiple differentiations (Wen *et al.*, 2014). Extracellular matrix (ECM) simulation using collagen, laminin or fibronectin proteins is well established (Lin *et al.*, 2010; Llopis-Hernández *et al.*, 2015). A harder/stiffer substrate, preferably agarose or agarose blends, stimulates osteogenesis while a softer substrate can induce adipogenesis (Duarte Campos *et al.*, 2014). Alginate gels have been widely used to trigger chondrogenic differentiation in MSCs (Kavalkovich *et al.*, 2002). It has been theorised that non-muscle myosin (Nmm) II stimulation may be the cause of this, due to its presence in cell function (Parekh *et al.*, 2011).

1.1.3.4 Control of Cell Shape

Another myosin related stimulation is the control of cell shape. By growing cells in specific shapes, actin-myosin generated tension leads to differentiation of MSCs. Electron-beam lithography (EBL) can be used to print structures on the nanoscale. By printing certain

patterns outlined by nanopillars or nanopits, mini-islands can be created that can keep the cell within its confines and fill out the specific shape. Studies using this technique have shown that flattening and spreading the cells can induce osteogenesis while rounding the cells triggers adipogenesis (Kilian *et al.*, 2010; Duarte Campos *et al.*, 2014). Using similar techniques, micro-channels can be created, aligning MSCs placed in them and directing them towards a chondrogenic lineage (Chou *et al.*, 2013). By manipulating the 3D environment by encapsulating cells in gelatin or poly (lactic-co-glycolic acid) (PLGA) microfibers, cell stemness and viability were maintained for extended periods of time (Steele *et al.*, 2012; Tamayol *et al.*, 2013).

In the above cases, the physical properties of integrin and integrin ligands are exploited to achieve differentiation, especially in the case of bone formation. Integrins link the extracellular matrix (ECM) and actin cytoskeleton across the plasma membrane (Rowlands, George and Cooper-White, 2008). The interaction between the integrins and ligands physically bind the cells with their cytoskeleton, and the signals from this enable the cell to react to the chemical and mechanical cues from their microenvironment (Chaudhuri and Mooney, 2012). By using this as a base, artificially created structures can be used to achieve the same effect. A commonly used ligand is the arginine-glycine-aspartic acid (RGD) sequence, which are present in many ECM glycoproteins such as fibronectin, vitronectin and osteopontin (X. Wang *et al.*, 2013). By controlling cell adhesion using this concept, the appropriate signalling pathways are triggered, allowing us to mediate the direction of cell differentiation. Thus, cytoskeleton manipulation can have a great impact on differentiation.

Studies using nanotopographies have also shown the importance of integrin interactions in cell function. By causing actin and vinculin stresses due to reaching around nanopits and nanopillars, osteogenesis can be stimulated. Strain on adhesion proteins may also be the reason for these changes (Dalby *et al.*, 2007; McNamara *et al.*, 2010).

1.1.3.5 Mechanical stimulation of MSCs

Biomechanical stimulation is essential for development of cartilage and skeletal development. Paralysis of chick embryos showed the inhibition of progenitor chondrogenesis and even joint cavity formation (Hall, 1979). Dynamic forces act on

cartilage, with shear and hydrostastic stresses regulating ossification of the cartilage (Carter *et al.*, 1987). Shear stresses have been shown to direct migration of MSCs *in vitro* and mechanical loading stress has shown to improve angiogenic capacity of MSCs and also their proliferation (Kasper *et al.*, 2007; Yuan *et al.*, 2013; Wang *et al.*, 2015). As such, observing the MSC secretome due to mechanical stresses is a developing frontier.

An exciting and novel form of stimulating differentiation is the use of vibrations at the nano-scale. Using nanovibrations, Dalby's group was able to trigger osteogenesis in hMSCs (Nikukar *et al.*, 2013). These vibrations act on the actin-myosin of the cell, causing contractions. These contractions trigger the Rho-kinase activated (ROCK) pathway (Robertson *et al.*, 2018). SMAD proteins, such as SMAD1 and SMAD4 are activated and dimerize, which then translocates to the nucleus initiating the SMAD activated BMP/TGFβ pathway (Attisano and Wrana, 2002). This stimulates the osteogenesis of the cells leading to the formation of osteoblasts. The use of nanovibrations to stimulate osteogenesis has been coined 'nanokicking'. A special bioreactor containing piezoelectric conductors is used to induce the vibrations and cell cultures can be placed on top of the bioreactor, making it an easy and useful tool for bone-related research.

1.1.3.6 The Role of microRNAs in MSC Differentiation

MicroRNAs (miRNAs) are small non-coding RNAs of around 22 nucleotides in length that have been shown to be involved in around 60% of all gene functions. They function by post-transcriptionally inhibiting or degrading target mRNAs, thus promoting or inhibiting certain pathways (Bartel, 2009; Wahid *et al.*, 2010). As such, there is a new-found interest in studying the effects of miRNAs in the differentiation of MSCs and if this function of miRNAs can be exploited for regenerative medicine.

1.1.4 MicroRNAs and MSC Differentiation

Recently, miRNAs have been shown to be active in nearly every step of the different paths of differentiation of MSCs (Clark *et al.*, 2014). Multiple miRNAs work in tandem to inhibit multiple steps in a pathway, causing great impact in cell function. Although the exact

mechanisms of miRNA regulation are not fully understood, significant progress has been made in understanding their targets and methods of action. By using prediction methods, initial targets can be identified and studied to understand their role in differentiation (Lai *et al.*, 2003; Baglìo *et al.*, 2013).

A plethora of studies have been conducted to discover the role of specific miRNAs in each differentiation process. A few important studies can be seen in table 1. The main problem in exploiting these miRNAs is their fragile nature due to their small size and the fact that they are RNAs. The need for protection is essential in this case. The use of transfection molecules, dendrimers and nanoparticles to act as a delivery platform can be used to mitigate this (Ebert and Sharp, 2010). Due to the nature of miRNAs, off-target effects need to be studied to prevent side-effects such as immunotoxicity and even degradation. MiRNAs functions through binding of the ribosome induced silencing complex (RISC) with the target sequence (Chendrimada *et al.*, 2005). Addition of these extrinsic miRNA sequences through therapeutics may compete with the intrinsic miRNAs, leading to the decreased expression of the therapeutics (Formstecher *et al.*, 2006). Such problems need to be dealt with *in vitro* to confirm the required dosage for eliciting the required changes. Different delivery platform can mitigate some issues and this will be elucidated further on.

miRNA	**Effect in MSC**	**MSC source**	**Target (s)**	**Ref.**
let-7	Inhibits adipogenesis and migration of cell lines	h-BM	IL6	(T. Sun *et al.*, 2009)
miR-21	Promotes osteogenesis	h-BM	SPRY1/2	(Trohatou *et al.*, 2014)
miR-23a	Promotes chondrogenesis	h-BM	PRKACB	(Hassan *et al.*, 2010; Kang *et al.*, 2016)
	Inhibits osteogenesis	m-cell line	SATB2	

miRNA	Effect in MSC	MSC source	Target (s)	Ref.
miR-26a	Inhibits adipogenesis	h-AT, m-cell line	Fbxl19	(Acharya *et al.*, 2019)
miR-27a	Promotes immune regulation	r-AT	SDF-1α	
	Promotes osteogenesis	h-BM	DKK1, KREMEN2, SFRP2	
miR-27b	Promotes adipogenesis	h-AT	RUNX2	(Karbiener *et al.*, 2009)
	Inhibits osteogenesis	m-BM	SMAD1	
miR-29a	Inhibits osteogenesis	h-BM	Ostrerix, n.d.	(Kapinas, Kessler and Delany, 2009)
miR-30	Inhibits osteogenesis	h-AT	BMPR2	(Gao *et al.*, 2011)
	Inhibits proliferation	h-BM	n.d.	
miR-31	Inhibits osteogenesis and proliferation	h-BM	SATB2	(Xie *et al.*, 2014)

miRNA	Effect in MSC	MSC source	Target (s)	Ref.
miR-126	Promotes proliferation	r-BM	n.d.	(Dorrance *et al.*, 2015)
	Inhibits osteogenesis	m-cell line	SMAD5	
miR-130a	Inhibits adipogenesis	h-AT	EID1	(Wei *et al.*, 2017)
miR-133	Promotes chondrogenesis	h-BM, m-BM, m-cell line	ADAMTS-5, HDAC4	(Y. Zhang *et al.*, 2011; Liao *et al.*, 2013)
	Inhibits osteogenesis	m-cell line	DLX5	
miR-138	Promotes osteogenesis	h-cell line	APC	(Ye *et al.*, 2012; Viti *et al.*, 2016)
	Inhibits chondrogenesis	m-BM	SOX9	
miR-140	Inhibits immune regulation	m-BM	PTGES2	(Miyaki *et al.*, 2010)
miR-143	Inhibits/promotes adipogenesis	h-cell line	MAPK5	(Chen *et al.*, 2014)
miR-145	Inhibits chondrogenesis	h-BM	Sox9	(B. Yang *et al.*, 2011)

miRNA	Effect in MSC	MSC source	Target (s)	Ref.
miR-194	Promote myogenesis	m-cell line	CX43	(Wang *et al.*, 2019)
miR-199a*	Inhibits adipogenesis	h-cell line	n.d.	(E. A. Lin *et al.*, 2009)

Table 1.1: Various microRNAs involved in differentiation and maintenance of MSCs along with the studied cell line and identified targets. Adapted from (Clark *et al.*, 2014)**.**

1.2 MicroRNAs:

MicroRNAs (miRNAs) are single stranded sequences, of roughly 22 nucleotides in length, that base pair with mRNA and thus post-transcriptionally repress gene expression. Their genes are present located in independent transcription units, with a quarter of all miRNA genes present in the introns (Ramalingam *et al.*, 2014). They are found endogenously and are only partially complementary to the messenger RNA (mRNA). miRNAs are transcribed from endogenous transcripts that can form a local hairpin structures, which are processed in such a way that a single miRNA molecule accumulates from one arm of a hairpin precursor molecule (Bartel, 2004). Although miRNAs are mostly involved in repression, there have been situations where they upregulate the expression of certain genes, such as the upregulation of hepatitis C virus (HCV) RNA by miR-122 (Vasudevan, 2012).

1.2.1 Biogenesis of miRNAs

In animals, RNA Polymerase II (Pol II) transcribes the gene encoding the miRNA, leading to the formation of the primary miRNA (pri-miRNA) (Axtell, Westholm and Lai, 2011). This primary transcript contains the miRNA sequences, which are present in its hairpin structure. The hairpin structure consists of a stem that is 33-35 base pairs (bp) long, a

terminal loop and single stranded RNA segments at both the 5' and 3' end. This pri-miRNA gets cleaved to form hairpin structures called precursor-RNA (pre-RNA). The Microprocessor complex achieves this (Ha and Kim, 2014). This complex consists of the DiGeorge Syndrome Critical Region 8 (DGSCR8) associated with the enzyme Drosha. The DGSCR8 orients the RNAse III region of the Drosha, which in turn facilitates cleavage (Landthaler, Yalcin and Tuschl, 2004). The pre-miRNA is then exported from the nucleus by the Exportin-5 protein (Bohnsack et al. 2004).

After exporting the pre-miRNA to the cytoplasm, another RNAse III enzyme, Dicer, cleaves it near the terminal loop (Abrahante *et al.*, 2003). This leads to the formation of the miRNA duplex, indicated by miRNA:miRNA* (Knight and Bass, 2001). miRNA* is the passenger strand, which is biologically less active than the other 'guide' strand (Ha and Kim, 2014). Although the guide strand is more commonly observed in the silencing process, the passenger strand has also been seen in certain situations. One such example is that mir-142-3p, is found frequently in embryo tissue samples, compared to mir-142-5p, found in ovaries, testes and brain (Wu *et al.*, 2009).

The miRNA duplex then loads on to the Argonaute (AGO) protein to form RNA induced silencing complex (RISC) (Wahid *et al.*, 2010). This effector complex is how the miRNA induces downregulation of genes. AGO is the catalytic engine of the RISC (Chendrimada *et al.*, 2005). After the duplex loads, the unwinding of the miRNA begins. The N domain of the AGO protein unwinds the duplex, which leads to the guide strand being stably incorporated. The passenger strand is usually discarded, while the guide strand remains in the protein. The endonuclease C3PO is involved in the removal of the passenger strand (Kwak and Tomari, 2012). Certain AGO proteins can cleave the duplex in some situations, but as the duplex contains mismatches, unwinding without cleavage is preferred. This complex is known as the micro-ribonucleoprotein (miRNP) (Valinezhad Orang, Safaralizadeh and Kazemzadeh-Bavili, 2014).

The miRNP that is obtained is involved in the downregulation process. This is done by either posttranscriptional repression or by cleavage of the mRNA. The posttranscriptional repression occurs when the miRNA does not completely bind to the mRNA. It has been established recently that the most commonly seen method of downregulation is mRNA

degradation (Wahid *et al.*, 2010). This is achieved by cleavage of the mRNA, which has been guided to by the miRNA, by the AGO protein. This occurs when the miRNA completely binds to the complementary mRNA. The silencing of mRNA, by its binding to the miRNA, is a phenomenon that has not been completely explored. Although there is a large amount of information on the molecular aspect of the process, the mechanism is not clearly understood (Jonas and Izaurralde, 2015). It has been shown that in the case of Arabidopsis, the mRNA silencing may in fact take place at the initiation of translation, and not at the posttranslational period (Djuranovic, Nahvi and Green, 2012). Further work needs to be done on multiple species to establish the mode of action.

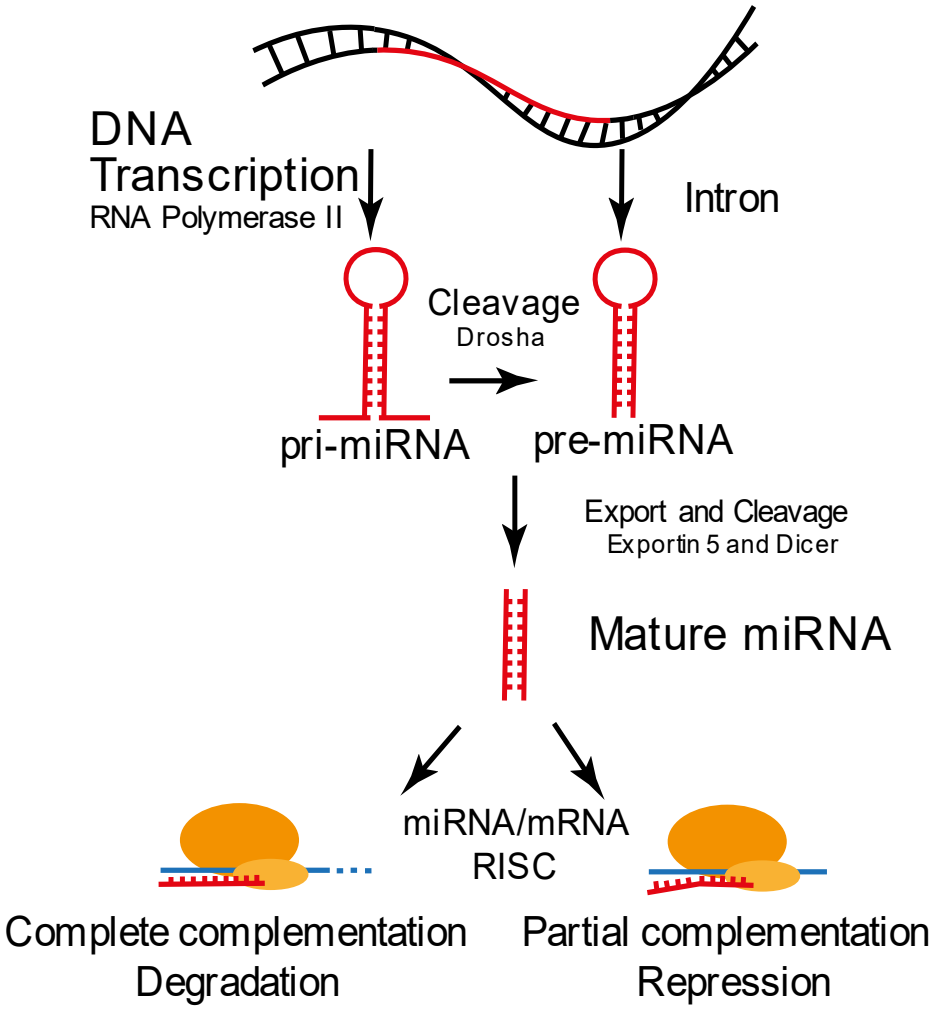

Fig. 1. 6: Biogenesis of miRNA occurs by transcription of intronal sequences by RNA polymerase II which produces either pri-miRNA or pre-miRNA. In the case of pri-miRNA, it is cleaved by Drosha to form pre-miRNA. The pre-miRNA is then cleaved by Dicer and forms a complex with the RISC, which binds to the mRNA, repressing it.

1.2.2 Functions of miRNAs:

As previously mentioned, miRNAs control the translation of proteins by binding to the mRNAs. This can be a broad statement and studies have shown this to be quite true. It has been noted that miRNAs are involved in around 60% of all genetic pathways (Jonas and Izaurralde, 2015). It has also been suggested by the Functional Annotation of the Mammalian Genome (FANTOM5) that for a specific cell type, nearly 50% of the miRNA pool is represented by the top five expressed miRNAs (de Rie *et al.*, 2017). This may suggest that miRNAs might mostly be involved in regulating expressional noise, indicated by the high mRNA to protein ratio observed during most experiments.

There has been a surge in miRNA studies over the last decade due to its large and varied functions. Over 2000 miRNAs have been discovered, but finding its exact role is a challenge (Friedman *et al.*, 2009). Computational target prediction is the initial practise to understand potential targets for miRNA action (Riffo-Campos, Riquelme and Brebi-Mieville, 2016). Once the targets have been identified, there efficacy is tested by amplifying and blocking the miRNAs. Potentially powerful ones are even taken to *in vivo* studies to understand its effects on development of relevant pathways.

The importance of miRNAs were first confirmed by mice models with the Dicer or DGCR8 deficiency (Kanellopoulou *et al.*, 2005; Wang *et al.*, 2007). Loss of either had shown embryonic lethality, indicating the importance of these to miRNA biogenesis, which in turn showed the impact in the growth of the embryo. Loss of specific miRNAs did not show complete loss of function, as in the case of miR-208. It was shown to be a vital component in cardiac tissue, but the mice with miR-208 knocked out still grew a heart. What was important to note was the role of the miRNA in homeostasis, as loss of miR-208 resulted in cardiac hypertrophy and defects in stress responses (Callis *et al.*, 2009).

The main reason for the increase in the attention to miRNAs was its role in cancer. Increase in certain miRNA families for different cancer types showed it role in cell differentiation state. Promoting or inhibiting these miRNAs during functional studies supported their role

in controlling cancer development (Hayes, Peruzzi and Lawler, 2014; Peng and Croce, 2016). miR-21 and miR-17-92 clusters were showed to be upregulated in cancer tissue, while others such as let-7 and miR-34 were downregulated (Pan, Wang and Wang, 2010; Concepcion, Bonetti and Ventura, 2012). This has also led to the use of miRNAs as markers for cancer.

1.2.3 MicroRNAs in MSCs

With their importance in cell state regulation, studies were conducted to see their effects on multiple cell types, including MSCs. Microarray studies provide a list of miRNAs that change their expression in MSCs. Most miRNAs discovered in this case tend to be from the let-7 family and miR-23-24-27 clusters, along with other families including, miR-10miR-29, miR-30 etc (Lim *et al.*, 2005; Thomson, Parker and Hammond, 2007). Since a large number of miRNAs from the same family share the same seed sequence, it has been hypothesised that co-expression of the different members may add to the robustness of their functions (Alberti and Cochella, 2017).

MSCs are mainly characterized by their ability to differentiate into osteoblasts, adipocytes and chondrocytes. While regular transcription factors are responsible for differentiation, it is emerging from the literature that miRNAs also play a major role in these pathways. Indeed, many miRNAs and their families have been discovered to be active during differentiation (Clark *et al.*, 2014).

In periodontal ligament tissue-derived MSCs, miR-17 was shown to target Smad ubiquitin regulatory factor-1 (SMURF1), promoting osteogenesis (Liu *et al.*, 2011). By targeting Osterix, miR-31 downregulates osteogenesis in human bone-marrow MSCs (Xie *et al.*, 2014). Certain families such as miR-30 and miR-24 families repress osteogenesis, and thus help in promoting adipogenesis (F. Sun *et al.*, 2009; Gao *et al.*, 2011). The miR-27 family targets PPARγ and C/EBPa, crucial to adipogenesis, inhibiting this pathway(Q. Lin *et al.*, 2009). Sox9 is targeted by miR-145 and SMAD1 is targeted by miR-199* (E. A. Lin *et al.*, 2009; B. Yang *et al.*, 2011). Both these genes are essential for chondrogenesis and inhibiting the translation of these stunt the chondrogenic development. There are a large number of

miRNAs that regulate the expression of important genes in MSC differentiation and a lot of studies are still being conducted to confirm their efficacy and potential therapeutic usage.

1.2.4 MicroRNA mimics and antagomiRs

MicroRNA based therapeutics can be classified into miRNA mimics and miRNA inhibitors. The more widely studied method is the inhibition using anti-sense oligonucleotides (ASOs), which can be used to directly target the miRNAs. These sequences are called anti-miRs or antagomiRs (Krutzfeldt *et al.*, 2005). By binding to the miRNAs, the antagomiRs prevent its translation, thus inhibiting it. Like antagomiRs, miRNA mimics are also used (Younger and Corey, 2011). These focus on copying miRNAs that have been shown to positively regulate important pathways.

Both these types of oligonucleotides need to be protected from enzymatic degradation, immune system, as well as requiring transport to the target location. Over the past few years, a lot of progress has been made to increase the affinity, stability and effects of these sequences. They can be made to be highly complementary to the target miRNA or match the sequence, but an efficient delivery method needed to be created.

The first miRNA based therapeutic experiments consisted of injecting miRNA mimics encoded in viral vectors directly at the target sites. This led to poor results due to degradation of the sequences, as well as poor target specificity (van Rooij and Olson, 2012). By modifying the sequences, they can be protected from the various nucleases in the body. 2'-O-methyl (2'-OMe) modifications to the sequences have been shown to provide increased resistance against nucleases and also improving the binding efficacy to the miRNA (Lamond and Sproat, 1993; Verma and Eckstein, 1998). Even with the improved resistance, the serum exonucleases can still affect the antagomiRs. This can be mediated by adding phosphorothioate bonds in place of the phosphate backbone (Krutzfeldt *et al.*, 2005). Replacing the non-bridging oxygen atoms with sulphur atoms can do this. This method requires that the replacement occur at specific intervals, as this modification lowers the binding affinity of the antagomiRs. Another modification that has been successful is the incorporation of 2'-O-methyoxymethyl (2'-MOE) group. This modification has shown

greater affinity and binding that is comparable to the phosphorothioate modifications (Manoharan, 1999). The advantage is that it is much easier to create, as only one modification is made to each strand. It was seen that these modifications were well tolerated at the 3' end, compared to the 5' end. This was due to the importance of molecular asymmetry and that the 5' end being important for its interference activity (Chiu and Rana, 2003). There are several other modifications that can be done, and the one to pick would depend on the target and the required effect, i.e. better binding or better stability.

1.2.5 Delivery of mimics and antagomiRs

Significant work has been done to increase the affinity and stability of the antagomiRs. But without a carrier, the oligonucleotide will not be able to reach its intended target. This could also potentially prevent the early excretion of the antagomiRs. This would allow for delivery *in vivo* without loss of the sequences.

The earliest foray into miRNA therapeutics were the use of viral vectors. Modified adenoviruses, lentiviruses and retroviruses were used with constructed vectors onto which the miRNA sequences were added on. They are then deployed in cells, so the miRNA is integrated into the cell's genomic DNA. This method showed promise as miR-138 induced a 1,000-fold expression increase, enhancing the production of pluripotent stem cells (Ye *et al.*, 2012). Another study showed a 2,500-fold increase in miR-143 expression in corneal epithelial cells (Lee *et al.*, 2011). Although the rewards are great, it carries the usual risks involved in viral vector use such as potential toxin production, immunological responses and mutations.

To go around this, non-viral methods were used next. Gene gun, electroporation, ultrasound and laser-based systems do not pose the same risks as viral-vectors, but their low transfection rate and relatively high apoptotic rate for cells may be a hinderance in developing this method (Nayerossadat, Maedeh and Ali, 2012). Lipid-based systems using a liposome covered cargo do not have any of the above issues, but their low half-life led to problems due to binding to non-specific serum proteins. By conjugating it with other compounds such

a polyethylene glycol (PEG) or cholesterol derivatives alleviate these issues (Vickers and Remaley, 2012).

A newer and safer delivery was achieved by using miRNA 'sponges' or by small molecules and oligonucleotides. MicroRNA sponges use vectors, such as with multiple binding sites, acting as a decoy or sponge for the miRNAs. The vectors express several sequences that allow binding of miRNAs that are antisense to them. This prevents the miRNA from being able to bind to the mRNA, allowing the mRNA to express itself (Ebert, Neilson and Sharp, 2007). This method has only been introduced in transgenic animals, where the target tissues overexpress the vectors, and as such are not a big focus in therapies (Ebert and Sharp, 2010). Small molecules have also shown to have an inhibitory effect on miRNAs, by disrupting its transcription. But due to its high EC_{50} (effector concentration for half-maximum response) and lack of knowledge on direct targets, this method has not been explored fully (Li and Rana, 2014).

Conjugation based methods were explored as a means of delivery. Cholesterol based conjugation was initially developed and it showed improved inhibition of microRNA action as well as being able to transport the antagomiRs mostly to the liver and also to the gut, kidney and steroidogenic organs to some extent (Krutzfeldt *et al.*, 2005; Wolfrum *et al.*, 2007). Liposome based delivery was also seen to show success. In this case, the antagomiRs were conjugated with lipids and this could also be modified to have high affinity for liver (Morrissey *et al.*, 2005; Akinc *et al.*, 2010). They can also be used for localized delivery as in the case where it was vaginally introduced in mice, and this prevented contraction of herpes simplex 2 for up to 9 days (Palliser *et al.*, 2006). Another approach consists of the use of the Fab domain of an antibody and conjugating it with the antagomiR. This confers it the ability to target specific locations, which are complementary to the antibody (Li and Rana, 2014).

There are several other methods available to transport antagomiRs, each having their benefits in terms of stability, specificity and effectiveness in general. The most promising mode seems to be the use of nanoparticles. These are widely recognized as the go to method for the future due to its high functionalization capabilities, allowing us to modify and choose the effect and properties we desire. They can be coated to shield against nucleases or bypass

the body's defences, have high loading capacity and be controlled during synthesis to obtain specific sizes and shapes, allowing for the required levels of biodistribution, cytotoxicity, imaging and excretion properties (Dreaden, Alkilany, *et al.*, 2012; Berry, 2013; Ding *et al.*, 2014).

The particles can be covalently or non-covalently conjugated to attain desired properties. The most commonly used conjugation is the covalently bound thiol conjugation, in the case of gold nanoparticles. The sulphur-gold interaction is a strong bond consisting of a partially covalent bond and mostly electrostatic bond (Roca and Haes, 2008). The antagomiRs can contain thiol modifications, and this can be used to form a bond with the nanoparticle, allowing for functionalization of the particle (Seferos *et al.*, 2009). Non-covalent methods can be used, but this applies only to unmodified oligonucleotides (Ding *et al.*, 2014). This principle requires that the GNPs be functionalized with cations, so as to bind with the negatively charged nucleic acids (McIntosh *et al.*, 2001). The covalent method is preferred as the oligonucleotides are synthetic and can be modified to include the thiol modification.

Once in the cells, this thiol modification helps in the release of the cargo, i.e. the mimic or antagomiR. The cell cytoplasm contains glutathione, a tripeptide antioxidant, that is essential for prevention of oxidation by reactive oxygen species in the cell (Pizzorno, 2014). They are essential in cargo release due to the binding of the cargo to the nanoparticle by a disulphide bond. The dithiol-disulphide exchange, catalysed by glutathione, cleaves the disulphide bond attaching the cargo, thus releasing it into the cell (Neves, Fernandes and Ramos, 2017). The chemical modifications mentioned above protect the cargo and allows it to bind to the mRNA, preventing its translation and thus promoting or inhibiting the targeted pathways. A study conducted with dye loaded nanoparticles showed its efficacy in both *in vitro* and cell cultures, showing the possibility of its use in therapeutics (Kumar, Meenan and Dixon, 2012).

1.3 Nanoparticles

Nanoparticles are organic or inorganic particles that usually have a size between the ranges of 1 and 100 nm in diameter (Sperling and Parak, 2010). Due to their extreme size, the properties they possess are distinct, compared to those of a larger scale. Nanoparticles that fall in the size range of biomolecules have attracted a lot of attention due to their unique properties and are widely studied for their use in biomedical applications.

There are many varieties of nanoparticles that are widely used. They are separated based on their constitution. Organic nanoparticles can be subdivided into liposomes, dendrimers, organic polymers and carbon nanomaterials (Romero and Moya, 2012). Inorganic nanoparticles consist of elemental metals, metal oxides, salts, alloys and quantum dots (Giner-Casares *et al.*, 2016). Each type brings a new property with it allowing for a diverse range of applications. Depending on whether imaging, delivery, biotoxicity, functionalization, etc. is the focus, multiple types are available, leading to a surge in studies of finding the optimal type for utilization in a specific area of research (Khan *et al.*, 2018).

The most commonly used inorganic nanoparticle is made from gold. Gold nanoparticles (GNPs) are widely used due to their relative ease of manufacture, non-toxic nature, photophysical and surface properties and inertness, among other desirable qualities (Ghosh *et al.*, 2008; Daraee *et al.*, 2016). These various properties have led to a surge in the use of GNPs in different fields, over the past few decades. Although various industrial applications have been the main destination for GNPs, its medical applications have been a very promising and attractive.

1.3.1 Optical properties of GNPs

Among its properties, GNPs exhibit enhanced radiative properties due to its surface plasmon resonance (SPR). This can be defined as the resonant oscillations of the free electrons on the nanoparticle surface caused by specific wavelengths of light. The condition of SPR is met when the frequency of incoming radiation matches the plasma frequency (oscillation of conduction electron due to a certain oscillation frequency). At this stage, the optical field is

highly localised and enhanced at the surface of the nanoparticle. This can be modified by changing the size of the nanoparticle, where an increase in the radius of the particle corresponds to an increase in the wavelength of the SPR peak (the colour exhibited) (Nilesh Kumar Pathak, Alok Ji, 2014).

The scattering cross-sections of GNPs has been seen to be around 10^5-10^6 times stronger than that of the emissions of a fluorescent dye molecule (Yguerabide and Yguerabide, 1998). As such, there is a large interest in its use as an imaging medium. Using a simple optical microscope, these GNPs can be visualised and thus allows easy tracking and localisation of the particles. Another important aspect is the virtually indefinite nature of its photostability, allowing less constraints on time and environment of experiments (Dreaden, Alkilany, *et al.*, 2012).

Due to their size, GNPs tend to preferentially accumulate in tumour cells. Tumour cells require more nutrients than regular cells, which in turn leads to formation of new vasculature, to supply more blood. Highly disordered endothelium and damaged lymphatic systems lead to preferential penetration of the nanoparticles and reduced elimination of the nanoparticles (Dreaden *et al.*, 2011). The photothermal properties of GNPs are very interesting as they have high absorption efficiency of light in the near-infrared (NIR) region. This allows photo-ablation of tumour cells, destroying them. Studies have shown the efficacy of GNPs and its various nanostructures in use for photothermal therapy and shows great future due to the accumulation of these particles in certain tumour sites (Loo *et al.*, 2004, 2005).

1.3.2 Biological application of GNPs

In regard to their biological application, GNPs have been found to have relatively low toxicity and good affinity for cellular uptake thanks to their inert nature. Due to their small size, GNPs are easily taken into the cell by several different internalization processes which are standard for the cells. These processes are necessary due to the size of the GNPs.

Endocytosis is the process by which cells internalize various macromolecules into the cell. This includes molecules that are not small enough to be diffused through the cell membrane. The two types of endocytosis are phagocytosis and pinocytosis (Dykman and Khlebtsov,

2014). Phagocytosis is the process in which the cell actin engulfs the molecule of a size above 500 nm, trapping it in a phagosome. The phagosome undergoes several pathways, which ends in the molecule being enzymatically degraded in the lysosome. Pinocytosis occurs when the cell uptakes molecules smaller than 500 nm. In this case the cell 'drinks' the molecule, thus taking in a small number of unwanted molecules. There are two types of pinocytosis, i.e., clathrin dependent and clathrin independent pinocytosis, with clathrin bring the protein that would coat membranes, eventually separating it off as vesicles, allowing for trafficking of particles (Royle, 2006). Macropinocytosis is another type, wherein the cell takes in a bulk amount and this type of endocytosis is receptor independent. This method of internalization is non-specific and so takes in foreign bodies too (Kafshgari, Harding and Voelcker, 2015).

The cell usually stores the foreign molecules in endosomal vesicles, which eventually get degraded in the lysosome, except in the case of macropinocytosis. This is not ideal as the cargo or ligands attached to the nanoparticles would also get destroyed. By using certain compounds (e.g. chlorpromazine and Dynasore) in tandem with the nanoparticle, we can promote the preferred endocytosis pathway, which would allow targeting of specific areas of the cell (Macia *et al.*, 2006). Blockage of a particular pathway usually entails the prevention of the formation of invaginations of the cell by attacking the pathways leading to it (Kafshgari, Harding and Voelcker, 2015).

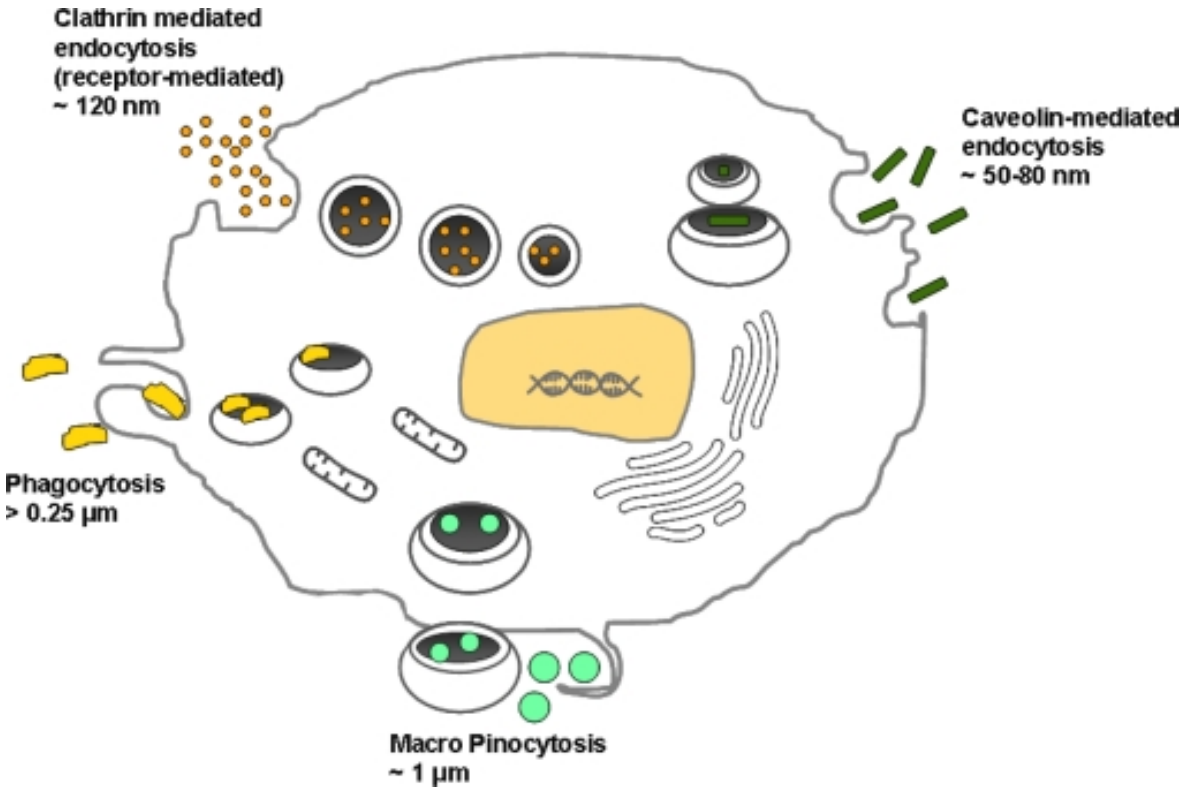

Fig. 1. 7: The different methods by which the cell intakes nanoparticles of different sizes. Adapted from (Kamaly and Miller, 2010)

There is a constant struggle to escape the vesicle and prevent transport to the lysosome. This can be remedied by using two methods, i.e. by either using specific coatings to facilitate escape, or adding other molecules in tandem with the particles to facilitate escape or target specific endocytosis pathways that would be detrimental to the nanoparticle or its cargo. Endosomal vesicle escape would allow the nanoparticle to leave its confines and deliver its cargo. This can be achieved by coating the nanoparticle with a cationic polymer or complexing the cargo with a liposome or a virus fusion protein. These work by damaging the vesicle causing the release of the nanoparticles. If the nanoparticle needs to target the nucleus, a nuclear localization signal can be conjugated with its coating, allowing transport into the nucleus.

The low toxicity of GNPs allows their accumulation up to a certain concentration without any ill effects. Several studies have been conducted to understand the pharmacological interactions of GNPs with cells and organs. A recent study showed the effect of nanoparticle

size and shape on toxicity. A concentration of up to 30 µM showed very little cell death and seemed to agree with conventionally accepted levels of GNP administration (Yang *et al.*, 2016). Another study showed no significant cell toxicity and organ changes in rabbit studies with administration after 24-hours (Park *et al.*, 2010). After an initial weight loss, dogs were shown to completely recover within 37 days without any signs of abnormalities (Abdoon *et al.*, 2016). GNPs have been shown to circulate in the blood stream for around 7 days, ending up in the liver. Due to the high surface area-to-mass ratio of the nanoparticles, care must be taken in these studies. This property allows for higher biological activity, which may lead to toxicity issues if not carefully followed.

1.3.3 Synthesis of gold nanoparticles:

There are various processes by which nanoparticles are synthesized, but the inherent concept for is same for all, i.e. the top-down technique. This involves obtaining smaller particles from a larger source (Dreaden, Alkilany, *et al.*, 2012). Chemical synthesis of nanoparticles is the most widely used technique. It usually involves the citrate reduction of chloroauric acid ($H[AuCl_4]$) using a reducing agent. This causes the reduction of Au^{3+} ions to Au^{+} ions. Further reactions lead to the formation of Au^{0} ions, which acts as the centre of nucleation (Jörg Polte *et al.*, 2010). At this stage, other chemicals must be added to prevent growth or agglomeration of the particle. A capping or stabilizing agent, like glutathione, prevents aggregation of the nanoparticles, but it can lead to the increase of particle size (Zhou *et al.*, 2011). A surfactant can be used instead, which would provide a charge to the particle, thereby repelling other particles and again, preventing aggregation. This does not increase particle size, which is essential for biological studies. Some chemicals, such as a citrate, can act as both the reducing and stabilizing agent (Dreaden *et al.*, 2011). Depending on the structure and dimension of the nanoparticle desired, the above method can be altered by changing the reducing and stabilizing agent and also the ratio of the gold ions to the agents (Dreaden, Alkilany, *et al.*, 2012). This is the most commonly used method as it allows monodispertion of the GNPs preventing aggregation, essential for biological applications. The size can be controlled by adjusting the pH of the reactants in the process (Ji *et al.*, 2007).

Laser ablation of the bulk metal in solution is also used to form GNPs. The nanoparticles are formed due to the condensation of the plasma plume of the metal (Amendola and

Meneghetti, 2009). Other physical methods such as sono-chemical, microwave irradiation, ultra-violet radiation, etc., can also be used (Khan, Vishakante and Siddaramaiah, 2013), but the laser ablation is preferred over other physical methods. A relatively newer method involves using supercritical fluid technology; gold can be micro-ionized and then precipitated, which would lead to the formation of nanoparticles (Thote and Gupta, 2005). Another method involves the use of 'green technology', i.e., using bacteria, fungi or plants, and their extracts, to produce nanoparticles. This involves the use of benign solvents or the microbe itself, and as such would be much safer and easier to dispose (Kharissova *et al.*, 2013; Hulkoti and Taranath, 2014). Although plenty of methods are available to synthesize nanoparticles, the citrate reduction method is preferred due to a larger output and greater control of the reaction process, and thus the formed nanoparticles.

1.3.4 Functionalization of nanoparticles:

The large surface area-to-mass ratio also allows functionalization of the GNPs. This is required to impart certain functions or load biological molecules onto the particles. It can also be used to passivate the GNPs against the immune responses of the cells. To load other molecules, ligand attachment is necessary, as it allows the attachment of the required cargo. It also allows the nanoparticles to target specific diseased areas and promotes selective interaction with cells or biological molecules. Although the tumour tissue allows preferential localization of the nanoparticles, the nanoparticles get localized in the liver and spleen due to the body's excretory mechanisms (Khlebtsov and Dykman, 2011). As such, it is always desired that the particles have specificity for problem regions. It also removes the toxic or undesired agents on the nanoparticle; for example, cetrimonium bromide (CTAB) is used as a surfactant during synthesis, but is harmful to cells or tissues (Alkilany and Murphy, 2010). By using a thiol-containing polyethylene glycol (PEG), the CTAB on the surface can be replaced by an inert and biologically advantageous compound (W. Wang *et al.*, 2013).

For the replacement to occur, the new ligand must have an affinity equal to or stronger than that of the ligand it is replacing. Another factor to consider would be the ligand structure and size in relation to the geometry of the nanoparticle, as this would indicate the density of the ligand around the particle, which would in turn affect the stability of the particle (Sperling and Parak, 2010).

The most commonly used ligand is the thiolated PEG (PEG-SH), as its hydrophobicity allows the dispersion of gold nanoparticles attached with a wide range of lipophilic molecules, along with increasing the circulatory half-life (Manson *et al.*, 2011). Thiolated nanoparticles can stay stably adsorbed for nearly 35 days under physiologic conditions. New research has shown that branched PEG has added benefits when conjugated with carbon nanotubes. This may be applied to gold nanoparticles in the future, providing better functionalization (W. Wang *et al.*, 2013).

1.3.5 Delivery of nucleic acids:

Nanoparticles can be used to deliver various cargos to a desired location. For the cargo to have the intended effect, it must reach the site of action intact. In the case of nucleic acids, they must be protected from enzymes such as nucleases. There are two ways of binding the load to the nanoparticles so as to protect them. These are the covalent and non-covalent conjugation to nanoparticles (Kafshgari, Harding and Voelcker, 2015).

Covalent conjugation is ideal when dealing with modified biological or synthetic compounds such as siRNAs. This bonding involves the anchorage of the cargo to the particle using a strong metal to sulphur bond (the cargo is thiolated to facilitate this). Protection from nucleases is a concern in this method, but recent advances have mitigated this issue by coating the conjugated nanoparticle with a copolymer. This coating was also shown to enhance cell internalization (Ding *et al.*, 2014).

Non-covalent conjugation is used to bind unmodified nucleic acids such as DNA or RNA to the nanoparticle. It uses different biotin binding proteins to conjugate the cargo to the surface of the nanoparticle. In DNA-GNP conjugates, the DNA is bent around the nanoparticle, which protects it from DNases (Ding *et al.*, 2014). The coated nanoparticles can be administered to cells using a gene gun, but a less invasive method would be to use the cellular uptake to transport the nanoparticles into the cell (Berry, 2013).

1.4 Aims and Objectives

Mesenchymal stem cells (MSCs) are multipotent and capable of differentiation into bone, cartilage and fat cells and therefore have great potential for regenerative medicine. MicroRNAs (miRNAs) are known to regulate differentiation, with key microRNAs being identified in this regard over the past 5-10 years. The aim of this project is to select and verify microRNA targets in MSC differentiation and to exploit their mechanism by delivery of miRNA and/or their antagomiRs to promote the differentiation process. The hypothesis is that by enhancing or repressing miRNA function, we can influence MSC differentiation. The specific objectives of this project are explained below:

- Confirm chemical induction *via* conditioned media (standard positive control for differentiation). Culture both commercially available Promocells and in-house isolated MSCs, obtained from the bone marrow of patients, in either DMEM or osteogenic / chondrogenic / adipogenic conditioned media for 21 days. Verify MSC differentiation.

- Complete a literature search to generate a catalog of established miRNAs that are expressed during MSC differentiation, in particular during osteogenesis (bone formation) and chondrogenesis (cartilage formation), but also adipogenesis (fat formation). This will inform on likely candidates for this study.

- Assess miRNA candidate expression in our differentiating MSCs. Both sources of MSCs will be cultured for 21 days in osteogenic / chondrogenic / adipogenic conditioned media. Isolate RNA and assess the expression levels of the candidate miRNAs using Fluidigm dynamic PCR.

- Confirm any strong candidates from the Fluidigm study in standard qPCR (which allows for higher cycling).

- Create oligonucleotides for several key miRNAs identified during Fluidigm and their antagomiRs (repression of miRNAs). Gold nanoparticles (GNPs) will be synthesized and functionalized with the sequences to deliver miRNA mimics/antagomiRs.

- Obtain the best combination of mimic/antagomiR to induce maximum shift towards differentiation with regards to osteogenesis, adipogenesis and chondrogenesis.

- In the final section of my PhD a dual osteogenic stimuli, both in comparison and in combination, will be used on MSCs to promote enhanced osteogenic stimulation. To do this, the miRNA approach of using antagomiR-31 treatment will be combined and compared with nanokicking, using within an established bioreactor in our laboratory.

Chapter 2: Materials and Methods

2.1 Cell Culture general protocol:

All experiments were conducted using human mesenchymal stem cells (hMSCs) obtained either from PromoCell® GmBH or Stro-1 selected MSCs donated graciously by Prof. Richard Oreffo and group (University of Southampton).

The MSCs were cultured in T75 flasks and maintained in growth media (13 ml) (section 2.1.2) at 37°C with 5% CO_2. Media was replaced every 3 days. Once nearing confluency, the media was removed and the cells were washed with HEPES solution (10 ml). The cells were detached using trypsin/versine solution (5 ml) at 37°C for around 5 minutes until cell detachment was seen. Fresh media was added to the cells to neutralize the trypsin/versine and the whole suspension was transferred to a universal tube and centrifuged at 1400 rpm for 4 minutes. A pellet was seen at the bottom of the flask and the supernatant was removed. The MSCs were resuspended in fresh media (1 ml) and transferred to new T75 flasks for subculturing or plated on well plates for experiments.

Before plating, 1 µl of the cell suspension was transferred to a haemocytometer with a coverslip on top to count the number of cells to maintain the initial seeding density across most experiments (excluding micromass cultures).

2.1.2 Growth Media:

Both the Promocell MSCs and the STRO-1 MSCs were cultured in a culture medium comprising of Dulbecco's modified Eagles media (DMEM, 430 ml), foetal bovine serum (FBS, 50 ml), antibiotics (Ab, 10 ml), sodium pyruvate (5 ml) and non-essential amino acids (NEAA, 5 ml). This DMEM is the standard culture media used throughout my project, unless otherwise stated.

The trypsin/versene solution used consisted of 1 ml trypsin in 20 ml of versene.

2.1.3 Conditioned Media for Differentiation:

For induction of differentiation, the base culture media described was used with added supplements, depending on the desired lineage, as follows:

(i) **Osteogenesis (OM):**

Dexamethasone (10 nM)

Ascorbic acid (100 μM)

β-glycerophosphate (20 mM)

(ii) **Chondrogenesis (CM):**

Ascorbate-2-phosphate (1 mM)

Transforming growth factor beta 1 (TGFβ1, 10 ng/ ml)

Dexamethasone (100 nM)

Insulin (6.25 μg/ ml)

(iii) **Adipogenesis (AM):**

Indomethacin (100 μM)

3-isobutyl-1-methylxanthine (IBMX, 500 μM)

Insulin (10 μg/ ml)

Dexamethasone (1 μM)

2.2 Micromass cultures of MSCs:

To enable differentiation of MSCs to chondrocytes, micromass cultures were required, as the high density of cells enables the release of essential factors for differentiation. This process is similar to the passaging of cells, up until the cell counting stage. After the cells were counted, the required number of cells, along with some media, were transferred to an Eppendorf. It was then centrifuged to obtain a pellet. The supernatant was discarded, and enough fresh media was added such that 10μl of the suspension would contain 100,000 cells. The cells were then plated by placing a 10μl drop in the middle of the well and left to attach for 2-4 hours. After the required time had passed, fresh media was added the cover the cells. After a couple of days, formation of spheroid like shapes indicated successful micromass culture.

2.3 MiRNA Extraction for Fluidigm and RT-qPCR:

MSCs were grown in DMEM, OM, AM and CM conditions for 3, 7 and 21 days of culture for both the Fluidigm study and the succeeding qPCR study. The total RNA was extracted

using the MagMAX^{TM}-96 for Microarrays kit. The cells were detached and lysed using TRI Reagent, which was subsequently spun at 12,000g for 10 minutes. The aqueous phase at the top of the samples was collected and plated on to the processing plate. 100% Isopropanol was added and placed on a shaker for 1 minute. RNA binding beads were added and the plates were shaken again for 3 minutes. The beads were collected to the bottom with the help of magnets and the supernatant was discarded. This process was repeated twice using a Wash Solution. It was then left to dry on the shaker. Finally, the Elution Buffer was added and placed on the shaker for 2 minutes and the supernatant containing the Total RNA was quantified using a UV spectrophotometer and was stored for Reverse Transcription.

2.4 RNA Extraction for RT-qPCR:

The MSCs were grown in DMEM and OM conditions for 7, 14 and 28 days of culture. The total RNA was extracted using the Qiagen RNeasy Mini Kit. The cells were harvested using RLT Buffer. The resulting solution was mixed with an equal volume of 70% ethanol and subsequently added onto a RNeasy MiniElute spin column, on a collection tube. This was then centrifuged at max speed for 1 minute. The flow-through was discarded and the samples were washed with Buffer RW1 by spinning at max speed for 1 minute. To remove any DNA present, the sample was incubated with DNase incubation mix for 15 minutes at room temperature. Buffer RW1 was added again and the samples were spun at max speed. Buffer RPE was added to the columns and spun at max speed. The columns were washed with 80% ethanol and spun again. The last remnants of liquid in the column were completely removed and dried by spinning again at max speed for 5 minutes. The spin column was moved to a fresh collection tube and RNase-free water was added. This was then spun at max speed for a minute to collect the elute where the RNA was present. The concentration was obtained using a UV spectrophotometer and was stored at -80°C for Reverse Transcription.

2.5 Extraction of protein and RNA for micromasses:

Due to the high number of cells required to test chondrogenesis, an Ambion® PARIS™ kit was used to extract protein and RNA from the same samples. The company suggested protocol was followed. Commercial Promocell MSCs were grown under DMEM and CM conditions for 7, 14 and 28 days. At each time point, the cells were harvested. The media

was removed, and the cells were washed with PBS. The cells were trypsinised and collected in an Eppendorf tube and washed again with PBS. Ice-cold Cell Disruption Buffer was added to lyse the cells. A plastic pestle was used to crush the micromasses as the addition of GNPs required an amount of force to break down the cultures. A portion of this lysate was stored, to use for protein analysis.

To obtain RNA, the remainder of the lysate was mixed with an equal volume of 2X Lysis/Binding Solution. A volume of absolute ethanol, equal to the initial amount of lysate, was added and the solution was mixed. This was then transferred to a filter cartridge assembled in a collection tube and centrifuged for one minute at 13,000 rpm. The flow-through was discarded and Wash Solution 1 was added and centrifuged at the same speed and time. It was then washed twice with Wash Solution 2/3. The filter cartridge was then transferred onto a fresh collection tube and Elution Buffer (preheated to 95-100°C) was added to the filter in sequential aliquots. The concentration was obtained using a UV spectrophotometer and was stored at -80°C for Reverse Transcription.

2.6 Reverse Transcription of Total RNA to cDNA:

The samples were reverse-transcribed using QuantiTect Reverse Transcription kit. The samples were aliquoted to obtain desired RNA concentration. Genomic DNA was eliminated from the sample by incubating with gDNA Wipeout Buffer for 2 minutes at 42°C. A master mix was made using the components provided, which included Reverse Transcriptase, RT Buffer and the RT primer mix. The master mix was added to the samples and finally loaded onto a thermal cycler. The parameters were as shown in table 1. The samples were stored at -20°C until further use.

Step	Time	Temperature
Hold	15 minutes	42°C
Hold	3 minutes	95°C

Table 2. 1: Parameter values used to program the thermal cycler.

2.7 qPCR of cDNA:

The cDNA obtained from the reverse transcription was also used in a standard qPCR. A master mix for each primer was made using SYBR Green, primers and RNase free water from the Quantitect SYBR Green PCR kit. This was pipetted into different wells along with their respective sample cDNA products. The plate was sealed and transferred onto the 7500 Sequence Detection System to obtain Ct values of the samples. Sequence Detection System to obtain Ct values of the samples. Quantification was done using the standard method. The endogenous controls used for the experiment were GAPDH. The machine was run as shown in table 2:

Step	Time	Temperature
Hold	2 minutes	50°C
Hold	10 minutes	95°C
Melt Step 1	15 seconds	95°C
Melt Step 2	1 minute	60°C
Melt Step 3	30 second	95°C
Melt Step 4	15 seconds	60°C

Table 2. 2: Parameter values used to program the 7500 Sequence Detection System.

2.8 Fluidigm Digital PCR:

Digital PCR using a microfluidics chip allows for a sensitive and time-saving PCR experiments. In this experiment, the 48.48 Dynamic Array^{TM} integrated fluidic circuit (IFC) was used, which conducted reactions for 48 samples along with 48 primers.

The digital PCR involved 3 major steps; Specific Target Amplification (STA), Exonuclease I (Exo I) Treatment and PCR.

In a DNA-free hood, the STA reaction solution was made using the TaqMan PreAmp Master Mix, pooled primers and DNase free water. This was equally transferred to a small volume of the samples and placed in a thermal cycler with the protocol as shown in Table 3:

Step	Time	Temperature
Hold	10 minutes	95°C
10-14 cycles	15 seconds	95°C
	4 minutes	60°C
Hold	∞	4°C

Table 2. 3: Time of one cycle and its respective temperature for Preamplification of sample cDNA.

The samples were cleaned up using Exo I treatment by adding Exonuclease I Reaction Buffer, Exonuclease I and water to each sample and ran in the thermal cycler as per Table 4:

Step	Time	Temperature
Digest	30 minutes	37°C
Inactivate	15 minutes	80°C
Hold	∞	4°C

Table 2. 4: Time of one cycle and its respective temperature for Exonuclease treatment of amplified sample cDNA.

The final products were diluted with TE Buffer, if required, and then carried over for the final PCR. SsoFast EvaGreen Supermix with Low ROX and DNA Binding Dye Sample were aliquoted to each sample. The primers were mixed with Assay Loading Reagent and Suspension Buffer to create the Assay Mix solution.

The IFC was fed with the control line fluid to lubricate the channels. The chip was primed in the IFC controller MX for the correct chip size and the samples and primers were pipetted onto their respective inlets on the chip. The chip was loaded back onto the controller which allowed the samples and assays to load into the chip. The IFC was finally placed in the Biomark HD PCR machine and the following program was run as per Table 5:

Segment	Step	Time (secs)	Temperature	BioMark HD Ramp Rate
1	Hot Start	60	95°C	2°C/s
2	PCR (30 cycles)	5	96°C	2°C/s
		20	60°C	2°C/s
3	Melting Curve	3	60°C	1°C/s
			60°C-95°C	1°C/3s

Table 2. 5: Time of one cycle and its respective temperature for the Digital PCR.

From the above run, a heat map was obtained, providing a quick look at the Ct values of each sample-primer combination. The endogenous controls used for the experiment were miR-191 ad U6 snRNA.

2.9 In-cell western assay:

To determine MSC differentiation, certain protein markers were assessed via in cell western. The protocol was followed according to the manufacturer's instructions.

The fixed cells were permeabilised with permease buffer at 4°C for 4 minutes. The buffer was then removed and blocking buffer (1% BSA) was added and shaken on a plate shaker for 1.5 hours. The blocker was then removed and the primary antibodies (diluted according to manufacturer's instructions) were added and incubated for 2.5 hours. The antibodies were removed and the wells were washed five times, for 5 minutes each, with wash buffer on a shaker. The secondary antibodies (1:500), for the respective animal, as well as the LICOR Cell Tag 700 (cell normalisation control) were added and incubated for 1 hour on a shaker. The previous wash step was repeated and subsequently wrapped in foil and stored at 4°C. The samples were imaged once dry using a LI-COR Odyssey® Sa.

2.10 Light Microscopy Staining (Histology)

To confirm the success of the differentiation media used, cells were grown on 24 well plates and stained appropriately. The MSCs were seeded on 24-well plates, at a cell density of 5000 cells per well (500 µl of DMEM per well). The cells were left to adhere for 24 hours and the media was replaced with the appropriate differentiation media (OM, CM and AM). Control groups of cells in DMEM were also included.

After 28 days culture, the cells were fixed in 4% formaldehyde (10 ml formaldehyde in 90 ml PBS with 2 g sucrose) and stained to assess differentiation. Von Kossa stain was used for osteogenesis, Safranin O stain for chondrogenesis and Oil Red O stain for adipogenesis. All these protocols were followed according to the manufacturer's instructions.

2.10.1 Von Kossa staining

The fixed cells were covered with 5% silver nitrate solution and exposed to Ultraviolet radiation using a U.V lamp, for 30 minutes. The wells were subsequently rinsed with deionised water and covered with 5% sodium thiosulphate solution for nearly 10 minutes. The cells were washed under tepid running tap water to clear and counterstained with nuclear fast red solution for 10 minutes. The wells were then rinsed with deionised water and 70% ethanol, ready to be viewed.

2.10.2 Oil Red O

The fixed cells were washed with distilled water and 60% isopropanol was added such that it covers the cells. After incubating for 5 minutes, the isopropanol was aspirated and the cells were covered with Oil Red O staining solution and incubated for 15 minutes. The solution was removed and the cells were washed with distilled water several times until the water was clear. After the water was removed completely, the wells were half-filled with PBS and then viewed.

2.10.3 Safranin O

The fixed cells were washed with distilled water and stained with Wiegert's iron haematoxylin solution for 10 minutes. It was then washed under running water for 10 minutes and subsequently stained with fast green solution for 5 minutes. It was then rinsed with 1% acetic acid solution for 10-15 seconds and then stained with 0.1% safranin O solution for 5 minutes. It was then dehydrated with 95% ethyl alcohol, absolute ethyl alcohol and xylene for 2 minutes each with 2 changes for each solution. Resinous solution was added and the plate was viewed.

2.11 Immunostaining for different markers of differentiation:

In addition to the histological staining, immunostaining was conducted to further confirm differentiation of the MSCs. All antibodies used in this protocol were diluted in PBS/1%BSA. The cells were plated and fixed similar to histological staining. The fixed cells were permeabilized for 5 minutes at 4°C using perm buffer. The cells were then incubated with PBS/1%BSA for 5 minutes at 37°C. The required primary antibody, along with phalloidin (actin stain) were added. The plate was covered in foil and incubated at 37°C for an hour. The antibody was removed and subsequently washed with PBS/0.5%Tween 20 thrice for 5 minutes each on a plate shaker. The secondary antibody, complementary to the species of the primary antibody, was added and incubated again at 37°C for an hour. It was removed and the plates were washed again. Streptavidin-FITC was added and incubated for 30 mins at 4°C. A final wash was done and a small drop of vectorshield-DAPI was placed on the cells. The cells were viewed under the microscope and then imaged.

2.12 Synthesis of gold nanoconjugates

Gold nanoparticles, with an average diameter of 13.7 ±2nm, were synthesized by the citrate reduction method (Jorg Polte *et al.*, 2010). Briefly, 250 ml of 1 mM hydrogen tetrachloroaureate (III) hydrate (Sigma) (98.46 mg) dissolved in 500 ml of distilled water were heated to reflux while stirring. Then, 25 ml of 38.8 mM sodium citrate dihydrate (285.28 mg) were added and refluxed for additional 30 minutes with vigorous stirring and

protected from light. The resulting red solution was cooled down and kept protected from light. Citrate capped GNPs were characterized by transmission electron microscopy (TEM) and UV-Vis spectroscopy (see Fig. 2).

These GNP were then functionalized with poly (ethylene glycol) (PEG). Briefly, 10 nM of the GNP solution were mixed with 0.003 mg/ ml of a commercial hetero-functional poly (ethylene glycol) (PEG) [O- (2-Mercaptoethyl)-O'-methyl-hexa (ethylene glycol), C15H32O7S, 356.48 Da, Sigma] in an aqueous solution of SDS (0.028%). Excess PEG was removed by centrifugation (14000g, 45min, 4ºC) and discarding the supernatant. This was repeated three times.

Four sets of NP-antagomiRs were prepared using modified 2'-ACE (2-bis (2-acetoxyethoxy) methyl) protected RNA oligonucleotides (Horizon Discovery Ltd). Briefly, the thiolated RNA oligonucleotides were suspended in 1 ml of 0.1M dithiothreitol (DTT), extracted three times with ethyl acetate and further purified through a desalting NAP-5 column (GE Healthcare) using 10 mM phosphate buffer (pH 8) as eluent. Following oligonucleotide quantification via UV/Vis spectroscopy, each RNA oligonucleotide was added to the GNP@PEG in a 100:1 ratio. AGE I solution (2% (w/v) SDS, 10 mM phosphate buffer (pH 8)) was added to the mixture to a final concentration of 10 mM phosphate buffer (pH 8), 0.01% (w/v) SDS, sonicated for 10 seconds using an ultrasound bath and incubated at room temperature for 20 minutes. Afterwards, the ionic strength of the solution was increased sequentially in 50 mM NaCl increments by adding the required volume of AGE II solution (1.5M NaCl, 0.01% (w/v) SDS, 10 mM phosphate buffer (pH 8)) up to a final concentration of 10 mM phosphate buffer (pH 8), 0.3M NaCl, 0.01% (w/v) SDS. After each increment, the solution was sonicated for 10 seconds and incubated at room temperature for 20 minutes. The solution was allowed to rest for additional 16 hours at room temperature, with mild agitation. Then, the functionalized NP-antagomiRs were centrifuged for 45 minutes at 14,000g, the oily precipitate washed three times with DEPC-treated H_2O, and redispersed in the same buffer.

The resulting NP-antagomiRs, were stored in the dark at 4 °C until further use.

Physical characterization of the NP-antagomiRs was performed by dynamic light scattering (Nanopartica SZ-100, Horiba), zeta potential (Nanopartica SZ-100,Horiba), UV/Vis spectroscopy and transmission electron microscopy.

2.13 Nanokicking Bioreactor setup:

The bioreactor surface area holds two standard 6-well plates. The design consists of an array of piezos sandwiched between an aluminium base block and a bimetallic top plate. The top plate of the platform used magnetic attachment to secure the 24-well plates using magnetic sheets stuck to the bottom of the plate. The static magnetic field produced has not been found to affect cellular function. However, these magnets, being halbach arrays, are only magnetic on the side facing the bioreactor and away from the cell culture, therefore any stray magnetic fields would be far smaller. A signal generator (GW Instek, New Taipei City, Taiwan) was used, which is capable of providing 10 $V_{pk–pk}$. The sine wave modulation of the amplifier output was provided by a signal generator (AD9833, Analog Devices, Massachusetts, USA). The frequency used was 1,000 Hz, controlled through a computer device connected to the bioreactors with a displacement amplitude of 30 nm (Campsie *et al.*, 2019).

2.14 Analysis of PCR data and statistics:

All PCR data was analysed using the standard Delta-Delta-Ct (DDCt) algorithm. Expression fold change (EFC) was calculated using the formula 2^{-DDCt}.

Statistical analysis of PCR was conducted using the GraphPad Prism software. A Kruskal-Wallis one-way ANOVA was used to compare samples. In all figs, * = $p<0.05$. Two-way ANOVA was conducted using the RStudio software for ICW.

Graphs were generated using Microsoft Excel for PCR and RStudio for ICW.

2.15 Western Blot:

After protein extraction, a Pierce™ BCA Protein Assay Kit was used to calculate protein concentration, following the protocol provided. A set of standards was created using supplied bovine serum albumin (BSA) with concentrations ranging from 2,000 µg to 25 µg. The standards were diluted with 1x PBS. Reagent A was mixed with Reagent B at a ratio of 50:1 to obtain a working reagent. On a 96-well microplate, 25 µl of sample or standard was added to each well and 200 µl of working reagent was added after. The plate was covered with aluminium foil and incubated at 37°C for 30 minutes. The plate was then cooled to RT

and was read on a Thermo Scientific™ Multiskan™ FC Microplate Photometer. A standard curve was displayed on the machine providing the final concentrations of all samples.

After calculating the concentrations of proteins, a volume containing 10 µg of protein was transferred to a new Eppendorf tube and 20 µl of 4x NuPAGE LDS sample loading buffer and 8 µl of 10x reducing agent (Invitrogen NP0004) was added. Finally, dH_2O was added to bring the final volume up to 80 µl. The samples were vortexed and boiled at 70°C for 10 minutes, after which they were ready to be loaded.

An Invitrogen Bolt gel (Bis Tris 4-12% NW04120) was loaded on to the gel cassette and assembled with Invitrogen Mini Gel Tank (A25977) to form the apparatus used for the western blot. 1x MES buffer was added and the tank was filled enough to just submerge the gel. The samples, along with a pre-stained marker (SeeBlue Plus 2 Prestained Marker), was loaded on to the wells. The samples were run at 150 V until the samples reached the near bottom of the gel.

Once the run is finished, a gel blot sandwich was made as shown in fig. 2.1. The filter paper and sponge were pre-soaked in transfer buffer and sandwiched with the rest of the apparatus, making sure no bubbles were present. The apparatus was then transferred on to the tank and transfer buffer was added to the brim of the core and run at 100V for 1 hour.

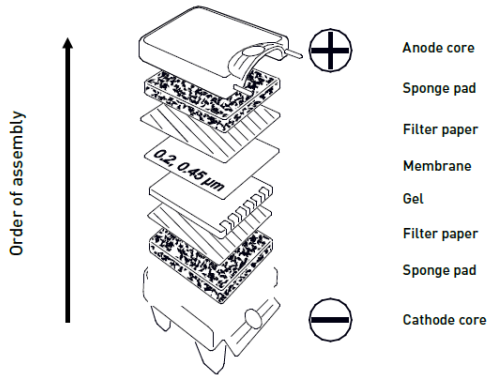

Fig. 2.1: Assembly order of the protein transfer apparatus. The membrane used is the nitrocellulose membrane, which would bind the proteins transferred from the gel.

Once the transfer step is completed, the apparatus was disassembled and the nitrocellulose membrane (containing the transferred proteins) was placed in a container. Blocking buffer (PBS with 5% milk powder) was added and transferred to a plate shaker for 1 hour at RT to allow blocking. Primary antibodies were added to blocking buffer at a concentration recommended by the manufacturers. Strips of the nitrocellulose membrane was cut in line with the size of studied proteins and placed inside 50 ml falcon tubes. The primary antibody solution was added, and the falcon tube was placed on a roller to allow binding of primary antibodies to the protein. The samples were left to bind at 4°C overnight.

The samples were then washed with washing buffer and secondary antibodies were added. The secondaries were diluted in the same process as the primary antibodies. The samples were placed on a roller again for 1 hour at RT. The samples were again washed and placed on saran wraps. ECL HRP substrate mix was added to the blots and taken to Thermo Scientific MYECL imager to develop the blot and obtain the images.

2.16 Materials List:

Materials/Reagents	**Supplier**
Cell culture	
Dulbecco's modified eagle medium (DMEM)	Sigma-Aldrich, UK
Foetal Bovine Serum (FBS)	Sigma-Aldrich, UK
Penicillin-streptomycin	Sigma-Aldrich, UK
Non-essential amino acids (NEAA)	Sigma-Aldrich, UK
L-glutamine	Invitrogen, UK
Sodium pyruvate	Life Technologies, UK
Dexamethasone	Sigma-Aldrich, UK
β-glycerophosphate	Sigma-Aldrich, UK
Ascorbic acid	Sigma-Aldrich, UK
Insulin	Sigma-Aldrich, UK
Ascorbate-2-phosphate	Sigma-Aldrich, UK
Transforming growth factor beta 1 (TGFβ1)	PeproTech, UK
Indomethacin	Sigma-Aldrich, UK
3-isobutyl-1-methylxanthine	Sigma-Aldrich, UK

Trypsin	Transforming growth factor beta 1
Versene	In-house
HEPES	Fisher Scientific, UK
Bovine Serum Albumin (BSA)	Sigma-Aldrich, UK
General Reagents	
Phosphate Buffer Solution (PBS)	In-house
Ethanol	VWR Chemicals, UK
Methanol	VWR Chemicals, UK
Acetic acid	VWR Chemicals, UK
Isopropanol	VWR Chemicals, UK
Hydrochloric acid (HCL)	VWR Chemicals, UK
Sodium Hydroxide (NaOH)	VWR Chemicals, UK
Formaldehyde	VWR Chemicals, UK
Sucrose	Fisher Scientific, UK
Dimethyl sulfoxide (DMSO)	Sigma-Aldrich, UK
Histology and Immunofluorescence	
Sodium Chloride	VWR Chemicals, UK
Magnesium chloride hexahydrate ($MgCl_2$)	VWR Chemicals, UK
Triton X-100	Sigma-Aldrich, UK
Tween 20	Sigma-Aldrich, UK
Rhodamine Phalloidin	Invitrogen, UK
Primary antibodies	Abcam, UK Santa Cruz Biotechnology, USA
Biotinylated anti-mouse secondary	Vector Laboratories, UK
Biotinylated anti-goat secondary	Vector Laboratories, UK
Biotinylated anti-rabbit secondary	Vector Laboratories, UK
Streptavidin-FITC	Vector Laboratories, UK
DAPI	Vector Laboratories, UK
Silver nitrate	Sigma-Aldrich, UK
Sodium thiosulphate	VWR Chemicals, UK
Nuclear Fast red	Sigma-Aldrich, UK
Oil Red O	Sigma-Aldrich, UK
Wiegert's iron haematoxylin solution	Sigma-Aldrich, UK
Safranin O	Sigma-Aldrich, UK

Xylene	VWR Chemicals, UK
In-cell western	
Donkey anti-mouse IR Dye 800	LI-COR Biosciences, UK
Donkey anti-rabbit IR Dye 800	LI-COR Biosciences, UK
Donkey anti-goat IR Dye 800	LI-COR Biosciences, UK
Cell Tag 700	LI-COR Biosciences, UK
Western Blotting	
Pierce™ BCA Protein Assay Kit	Thermo Fisher Scientific, UK
NuPAGE™ MES SDS Running Buffer (20X)	Thermo Fisher Scientific, UK
4x NuPAGE LDS	Thermo Fisher Scientific, UK
NuPAGE™ Sample Reducing Agent (10X)	Thermo Fisher Scientific, UK
Bolt™ 4-12% Bis-Tris Plus Gels, 10-well	Thermo Fisher Scientific, UK
SeeBlue™ Plus2 Pre-stained Protein Standard	Thermo Fisher Scientific, UK
Primary antibodies	Abcam, UK
NuPAGE™ Transfer Buffer (20X)	Thermo Fisher Scientific, UK
Goat anti-Mouse IgG (H+L) Secondary Antibody, HRP	Thermo Fisher Scientific, UK
Pierce™ ECL Plus Western Blotting Substrate	Thermo Fisher Scientific, UK
Quantitative Real-Time qPCR (PCR)	
RNeasy™ Micro Kit	Qiagen, UK
RNase-free water	Qiagen, UK
QuantiTect™ Reverse Transcription Kit	Qiagen, UK
Primers and Probes	Eurofins MWG Operon, UK Thermo Fisher Scientific, UK
QuantiTect™ SYBR Green PCR kit	Qiagen, UK
Protein Extraction for micromasses	
PARIS kit	Thermo Fisher Scientific, UK
Fluidigm	
MagMAX™ -96 for Microarrays kit	Thermo Fisher Scientific, UK
48.48 Dynamic Array™ integrated fluidic circuit (IFC)	Fluidigm, UK
12.12 Dynamic Array™ integrated fluidic circuit (IFC)	Fluidigm, UK
SsoFast EvaGreen Supermix	Bio-Rad, UK

TaqMan™ PreAmp Master Mix	Fisher Scientific, UK
Primers and probes	Fisher Scientific, UK

Table 2. 6: List of materials used and their supplier

The primers used for the Fluidigm study of microRNAs were purchased from Fisher Scientific, UK, and are proprietary. Primers used in the qPCR are listed below:

Primer	**Sequence (5'-3')**
GAPDH (endogenous control)	TCAAGGCTGAGAACGGGAA - Forward TGGGTGGCAGTGATGGCA- Reverse
Runx2	GGTCAGATGCAGGCGGCCC - Forward TACGTGTGGTAGCGCGTGGC- Reverse
ALP	ATGAAGGAAAAGCCAAGCAG - Forward CCACCAAATGTGAAGACGTG- Reverse
OCN	CAGCGAGGTAGTGAAGAGACC - Forward TCTGGAGTTTATTTGGGAGCAG- Reverse
PPARγ	CTATGGAGTTCATGCTTGTG - Forward GTACTGACATTTATTT- Reverse
GLUT4	GTATCATCTCTCAGTGGCTTGG - Forward ATAGGAGGCAGCAGCATTG- Reverse
AdipoQ	TATGATGGCTCCACTGGTA - Forward GAGCATAGCCTTGTCCTTCT- Reverse
Sox9	GCTCTGGAGACTTCTGAA - Forward GGTACTTGTAATCCGGGTG- Reverse
ACAN	GGCTTCCACCAGTGTGAC - Forward GTGTCTCGGATGCCATACG- Reverse
Col10	TGCCCACAGGCATAAAAGGCCC - Forward TGGTGGTCCAGAAGGACCTGGG - Reverse

Table 2. 7: List of primers used and their forward and reverse sequences

Chapter 3: Pilot study to identify potential miRNA targets

3.1 Introduction

3.1.1 Mesenchymal Stem Cell Differentiation

All the cells in the body are derived from undifferentiated stem cells that transform into other cell types as required (Bianco, 2014). In this regard, mesenchymal stem cells (MSCs) carry out repair and regeneration of bone, fat and cartilage. MSCs are primed to do this either by receiving external signals from other cells, or from the cell's internal gene regulatory systems. The differentiation process of MSCs is of great interest due to its potential in regenerative medicine (Bianco and Robey, 2001; Grayson *et al.*, 2015).

Osteogenesis is the process by which MSCs differentiate into mature osteoblasts. These osteoblasts are essential in replacing resorbed bone (by osteoclasts) in a process known as bone remodeling. Osteogenesis is controlled by key transcription factors such as Runx2 and Osterix (Zhang *et al.*, 2006; Vimalraj *et al.*, 2015). Controlling osteogenesis, allowing regulation of bone remodeling, has great therapeutic potential for the treatment of disease conditions such as osteoporosis and osteoarthritis, as well as bone difficulties including skeletal fracture healing (Dawson *et al.*, 2014).

Adipogenesis is the process by which MSCs differentiate into adipocytes. Adipocytes store energy in the form of free fatty acids during energy excess and this can be accessed later by the body when required (Gupta, 2014). It is mainly regulated by PPARγ, the master regulator of adipogenesis, as well as C/EBP alpha (Lefterova *et al.*, 2008). MSC commitment towards either osteoblasts or adipocytes is reciprocally regulated; both master transcriptional regulators, Runx2 (for osteoblasts) and PPARγ (for adipocytes) are present in low levels in undifferentiated MSCs and differentiation towards one lineage completely suppresses the genes associated with the other lineage [Pino, Biol Res, 4 (2012)]. The inverse relationship between adipogenesis and osteogenesis is a widely known interaction. By controlling adipogenesis, the direction of MSC differentiation can be shifted towards bone formation, which is more relevant in therapeutic studies.

Chondrogenesis is the process by which MSCs differentiate into chondrocytes. Cartilage tissue does not regenerate due to it being avascular and aneural (Akkiraju and Nohe, 2015). This causes it to be in a low metabolic state and requires nutrients through diffusion from

the articular surface (Simon and Jackson, 2018). Therefore, cartilage repair therapies are becoming commonplace, in particular for sporting injuries (Benthien and Behrens, 2010). Sox9 is the major transcription factor involved in the differentiation of MSCs to chondrocytes (Herlofsen *et al.*, 2011). Chondrocytes only make up about 1 -5% of the total cartilage mass, the remainder comprising the extracellular matrix (ECM) of collagen, proteoglycans and glycoproteins (Akkiraju and Nohe, 2015). A key research goal in controlling chondrogenesis is to achieve differentiation without hypertrophy, i.e., when the cells undergo endochondral ossification. As of yet, there is no clear method of achieving this and any development in this area would provide a major advance (Magne *et al.*, 2005).

3.1.2 MicroRNAs:

MicroRNAs are a recently discovered class of small RNAs that regulate gene expression post-transcriptionally , by either blocking mRNA translation or mRNA degradation (Chen and Rajewsky, 2007).. Recently, microRNAs have been shown to play a major role in MSC differentiation (Baglìo *et al.*, 2013). Emerging evidence now shows that microRNAs are crucial for bone development and osteogenesis as post-transcriptional regulators of Runx2 and PPARγ (e.g. miR-31, miR-34, miR-335, miR-26) with several exclusively identified in bone diseases such as osteoporosis (e.g. miR-705, miR-3077) [Liao, Cell Death Dis, 4 (2013)]. Thus, the control of microRNAs may prove a very powerful avenue of investigation for potential skeletal therapies.

Knock-out studies have been conducted on mice utilizing gene-editing techniques, which demonstrated the impact and importance of miRNAs in osteogenesis (E. A. Lin *et al.*, 2009; Yu *et al.*, 2010). MicroRNAs both positively and negatively regulate osteogenesis, targeting transcription factors and established pathways such as Runx2, Osterix, Wnt pathway and Hedgehog pathways. The main challenge, as with most miRNA studies, is the safe and targeted delivery of miRNAs and their antagomiRs.

Similarly, chondrogenic and adipogenic focused miRNAs have also been identified. As with osteogenesis, the main targets are transcription factors and key signaling pathways. For example, in chondrocytes miR-145 showed an inverse relationship with Sox9 expression, while miR-140 had a positive relationship (Miyaki *et al.*, 2010; B. Yang *et al.*, 2011). MiR-199a was also seen as a potent inhibitor by targeting SMAD1(E. A. Lin *et al.*, 2009). For

adipogenesis, miR-143 targeted ERK5, promoting adipogenesis and miR-138 was found to be a negative regulator(Esau *et al.*, 2004; Ye *et al.*, 2012).

In addition to the three main differentiation pathways, miRNAs are also involved with other differentiation processes such as myogenesis and neurogenesis in MSCs, as well as MSC self-renewal and proliferation (Peng and Croce, 2016). The let-7 family showed a possible influence on this process, but further work needs to be done to confirm its effects (Koh *et al.*, 2010). Fig. 3.1 illustrates the key miRNAs identified to date and their regulatory effects on MSC differentiation pathways.

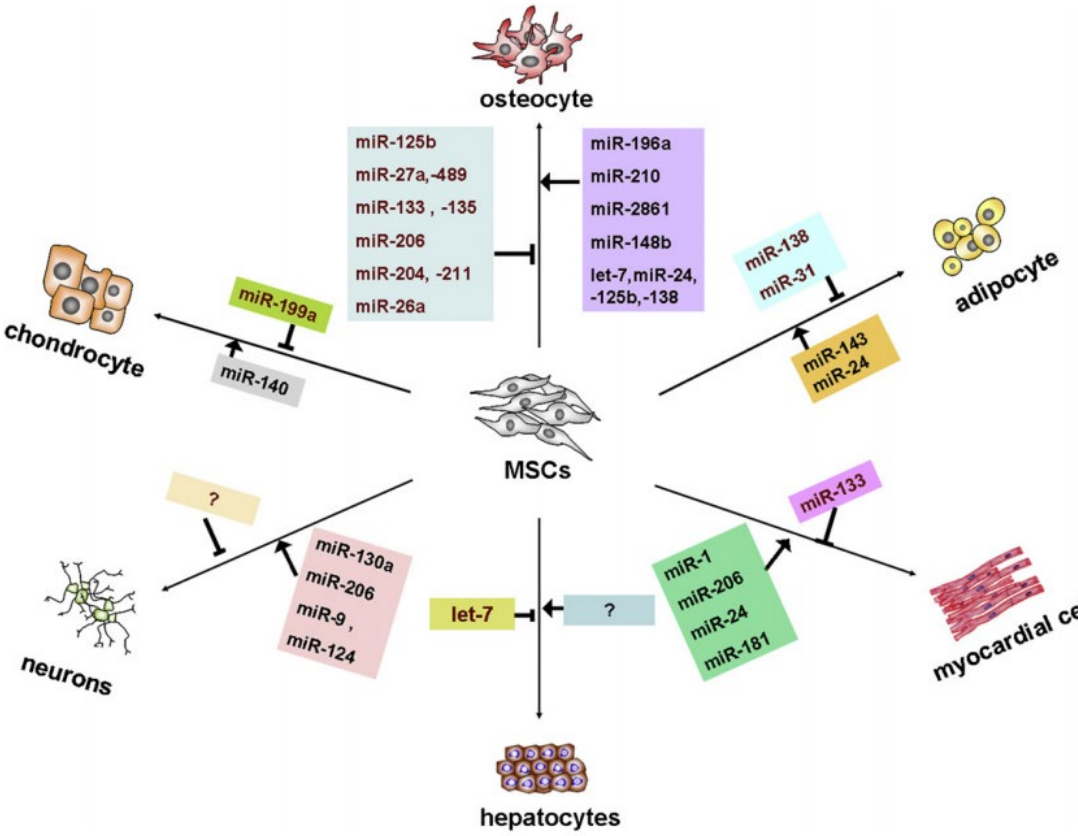

Fig. 3. 1: Differentiation pathways of MSCs and the miRNAs that target them. As research is continuously being conducted, further miRNAs are being discovered that may influence different pathways. Adapted from (Collino *et al.*, 2011).

3.2 Aims and Objectives:

The aim of this chapter is to identify miRNAs that target a specific differentiation transcription factor for each of the three main lineages. To achieve this, we must initially establish the multipotency of the two MSC populations, Stro-1 and Promocells, by confirming their ability to differentiate into osteoblasts, adipocytes and chondrocytes. Once this has been established, candidate miRNAs were selected following a literature review. Their expression levels were then determined during Stro-1 and Promocell MSC differentiation, confirming a final miRNA target for each differentiation lineage.

These aims were achieved by the following objectives:

- Confirming the potential of MSCs to differentiate via chemical induction using conditioned media. Two populations of MSCs are used in order to ascertain any differences between cell source; patient bone-marrow derived Stro-1 selected and commercially available Promocell® MSCs. The cells were cultured with either basal DMEM or osteogenic/ adipogenic/chondrogenic media. Differentiation was assessed via fluorescent staining and histology for appropriate markers.
- Completing a literature search to generate a catalog of miRNA candidates that are expressed during MSC differentiation, in particular during osteogenesis (bone formation), chondrogenesis (cartilage formation) and adipogenesis (fat formation). This will inform on likely candidates for our studies.
- Assessing miRNA candidate expression in our differentiating MSC populations. Using the conditioned media conditions and culturing MSCs for 21 days, we can isolate RNA and identify the candidate miRNAs using Fluidigm PCR, confirming their expression using RT-PCR.

3.3 Materials and Methods

3.2.1 Cell Culture

Two MSC populations were employed in this chapter. Both patient derived Stro-1 selected cells and commercial Promocells were cultured in T75 flasks in basal DMEM medium grown in an incubator at 37ºC at a CO_2 concentration of 5% (see section 2.1.1). All cells were expanded until approximately 80% confluent and used at passage 3.

For all experiments, the cells were seeded (5,000 cells per well) into appropriate cell plates, allowed to adhere to the bottom of the well plates over 24 hours whereupon the media was changed every 3 days to reflect the experiment conditions (see section 2.1.1). To trigger chondrogenic differentiation, it was necessary to coalesce the MSCs into a spheroid-like shape called a micromass for the duration of culture. The cells were cultured for 3, 7, 14, 21 or 28 days according to the experiment requirements.

3.3.2 Immunofluorescence microscopy

Both Stro-1 and Promocell MSCs were cultured in 24 well plates and allowed to grow for 28 days in basal DMEM, osteogenic, adipogenic and chondrogenic media, depending on the experiment conditions. The media was changed twice a week and at the end point, the cells were processed for immunofluorescence microscopy (section 2.11). The proteins of interest were osteocalcin (OCN, osteogenesis), fatty acid-binding protein (FABP, adipogenesis) and Sox9 (chondrogenesis). The images were then taken with a Zeiss Axiovert 200M fluorescent microscope and processed using the ImageJ software.

3.3.3 Histology (Light microscopy)

As above, both MSC populations were cultured on 24 well plates for 28 days, under appropriate conditions, at which point the cells were processed for histological staining. Von Kossa staining was conducted for osteogenesis, Oil Red O for adipogenesis and Safranin O staining for chondrogenesis, the protocols of which can be found in section 2.10 (1-3).

3.3.4 Fluidigm PCR for testing candidate miRNA expression during differentiation

Following a literature review to verify 3/4 miRNA targets per lineage pathway, the expression levels of each miRNA was assessed for both MSC populations upon differentiation. Both MSC populations were cultured within the appropriate media in 24 well plates for 3, 7 and 21 days. At the selected time points, the media was removed and the cells were washed. Using the MagMAX-96 kit, the cells were lysed and the RNA was extracted as described in section 2.4.

The concentration of the obtained RNA was initially measured using a UV spectrophotometer and then reverse transcribed with proprietary primers purchased from Thermo Fisher Scientific. The miRNAs tested are listed in table 3.1. A TaqMan MicroRNA Reverse Transcription kit was used for the reverse transcription (section 2.3) and the obtained cDNA was then amplified using a TaqMan PreAmp kit (see section 2.8). The samples were then loaded onto either a 12.12 Dynamic Array or 48.48 Dynamic Array integrated fluidic circuit (IFC) chip. The endogenous controls used were U6 snRNA and miR-191.

Section 2.8 describes the processes involved in the loading of the chip, where the chip was placed in a Biomark HD PCR machine and the program for the Fluidigm was run according to table 2.5. A heatmap was used to illustrate expression level changes and their Ct values (cycle threshold) were provided by the machine. Using the Ct values expression fold change (EFC) was calculated using the delta delta Ct method (section 2.13).

3.3.5 qPCR for confirming selected miRNA expression during differentiation

Based on their expression levels from the Fluidigm assessment, the miRNA candidates were short listed to 1/2 per differentiation pathway. As miRNA levels are transient and small, due to the restrictive nature (30 cycles) of the Fluidigm PCR, these sequences were further verified in both MSC populations using qPCR. Both types of MSCs were cultured on 24 well plates for 3 and 7 days in appropriate media, as published studies have indicated that miRNAs were most active during this early time period.

At the time points, the media was removed and the cells were washed with PBS. The cells were then lysed and the RNA was extracted using the MagMAX-96 kit, as described in section 2.3. The RNA was measured using a UV spectrophotometer and stored for reverse transcription.

The samples were reverse transcribed using a TaqMan MicroRNA Reverse Transcription Kit as detailed in section 2.6. The primers used were those previously used for the Fluidigm study. The cDNA was then processed using Qiagen SYBR Green qPCR kit (see section 2.7) and plated on to 96 well qPCR plates. The plate was then transferred onto the 7500 Sequence Detection System to obtain the Ct values of the samples. The endogenous control used was U6 snRNA. The results were calculated to obtain the EFC of each sample.

3.3 Results:

3.3.1 Confirmation of Stro-1 and Promocell MSC Differentiation

Treating the cells with different conditioned media and subsequently assessing appropriate markers at day 28 via immunofluorescence and histology confirmed Stro-1 and Promocell MSC multipotency.

3.3.1.1 Osteogenic Differentiation.

Osteogenic differentiation was noted in Stro-1 and Promocell MSCs cultured in osteogenic media. Positive Von Kossa staining of black deposits, indicating presence of silver phosphate (replacing calcium in calcium phosphate) (Fig. 3.2), whilst immunostaining demonstrated osteocalcin staining (late stage osteogenic marker), both supporting MSC differentiation down the osteogenic lineage (Fig. 3.3).

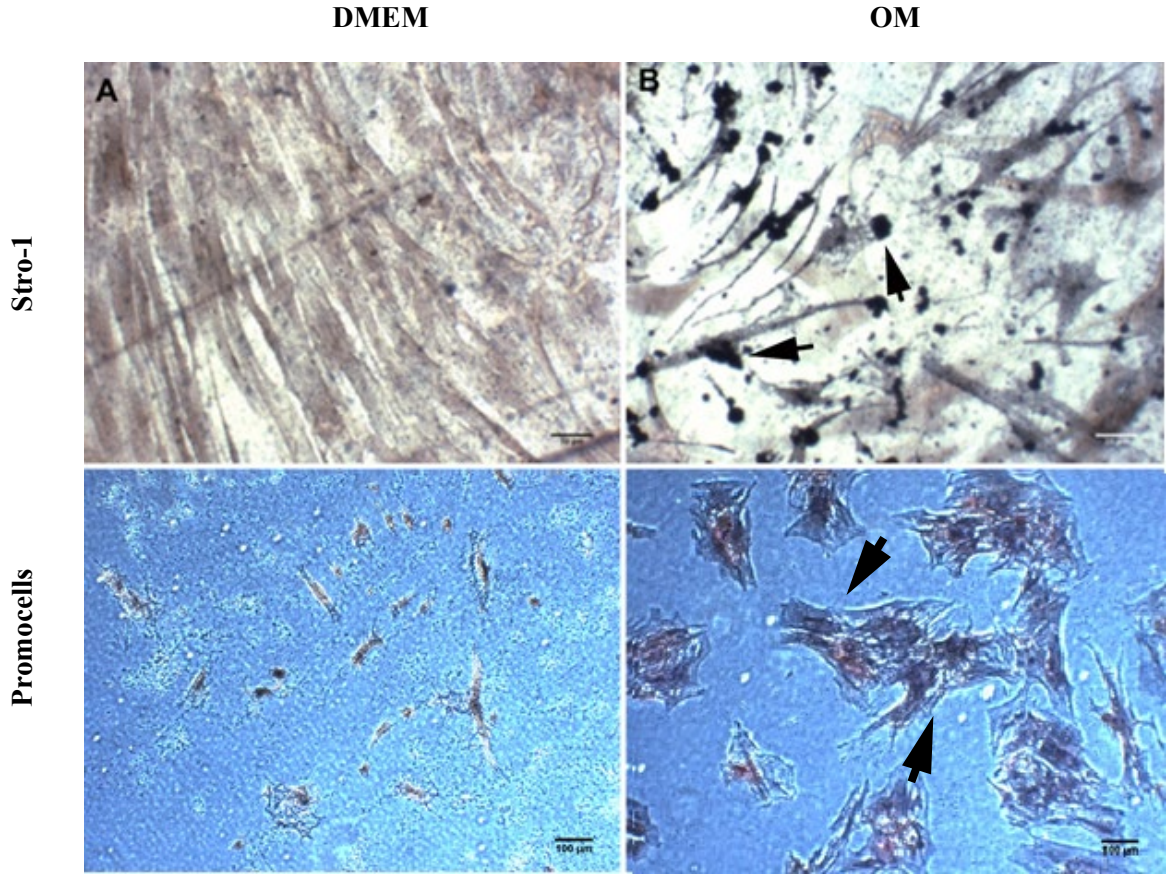

Fig. 3. 2 Von Kossa osteogenic staining of MSCs. Von Kossa staining after 28 days of culture within osteogenic media of (A) Stro-1 selected MSCs cultured in basal media, (B) Stro-1 selected MSCs cultured in osteogenic media, (C) Promocell MSCs cultured in basal media and (D) of Promocell MSCs cultured in osteogenic media. Arrowheads denote positive Von Kossa staining. Scale bar – 100 µm

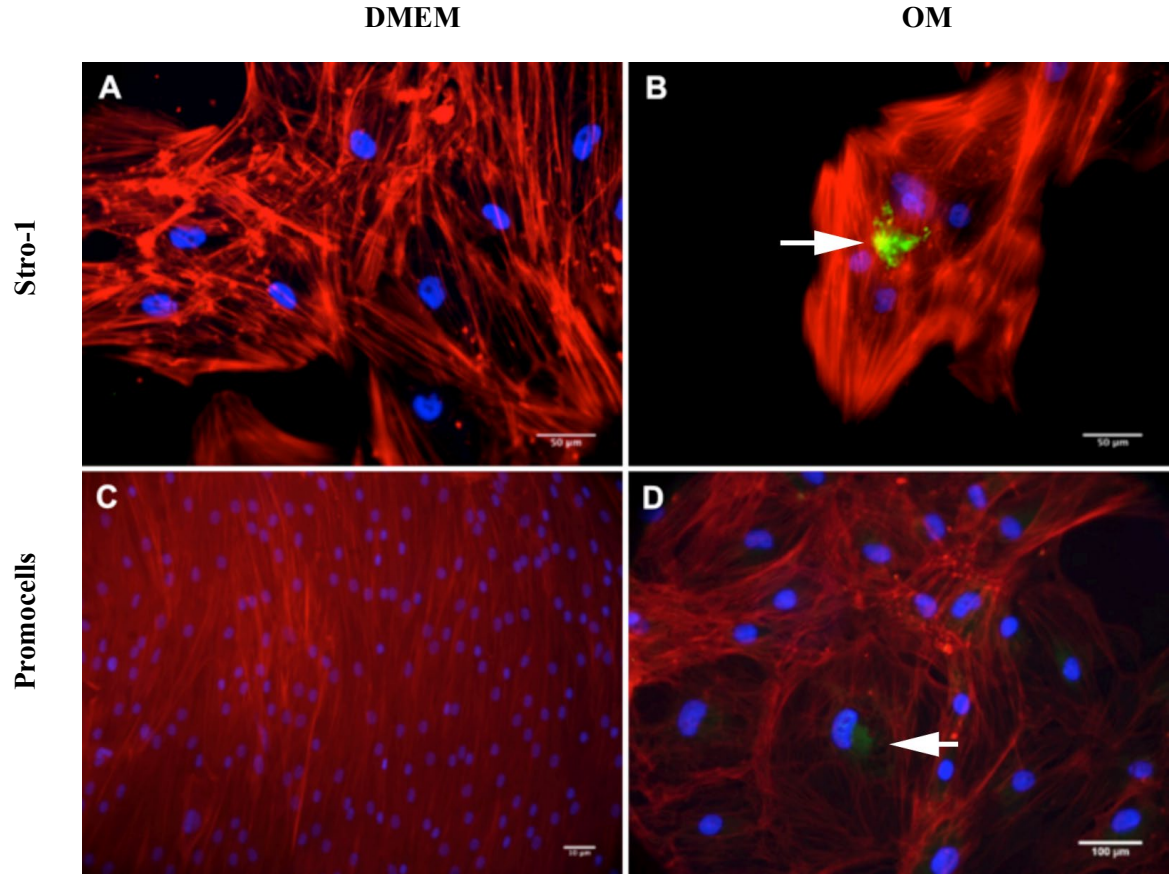

Fig. 3. 3 Fluorescence osteogenic staining of MSCs at day 28. Immunofluorescence staining of actin (red), OCN (green) and nuclei (blue) in (A) Stro-1 selected MSCs cultured in basal media, (B) Stro-1 selected MSCs cultured in osteogenic media, (C) Promocell MSCs cultured in basal media and (D) Promocell MSCs cultured in osteogenic media. Arrowheads denote positive OCN staining. Scale bar – A & B 50 µm; C & D 100 µm.

3.3.1.2 Adipogenic Differentiation

Adipogenic differentiation was observed in both MSC populations cultured in adipogenic media. Under light microscopy, fatty droplets were noted seen, whilst Oil Red O staining confirmed fatty acid deposits (Fig. 3.4) and immunostaining highlighted fatty acid binding proteins within cells cultured in adipogenic media (Fig. 3.5).

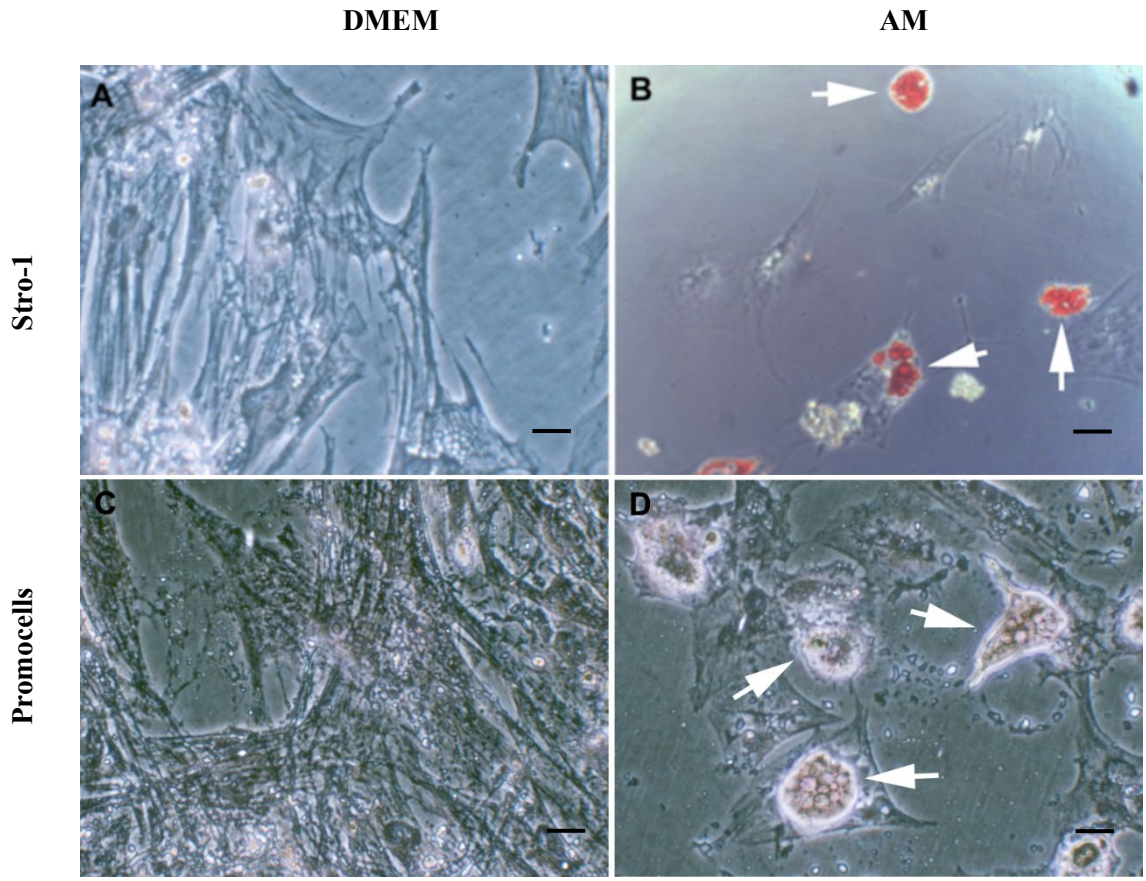

Fig. 3. 4 Oil Red O adipogenic staining of MSCs. Oil Red O staining after 28 days of culture within osteogenic media of (A) Stro-1 selected MSCs cultured in basal media, (B) Stro-1 selected MSCs cultured in adipogenic media, (C) Promocell MSCs cultured in basal media, (B) Promocell MSCs cultured in adipogenic media. Arrows denote fatty droplets within the cell. Scale bar -100 µm

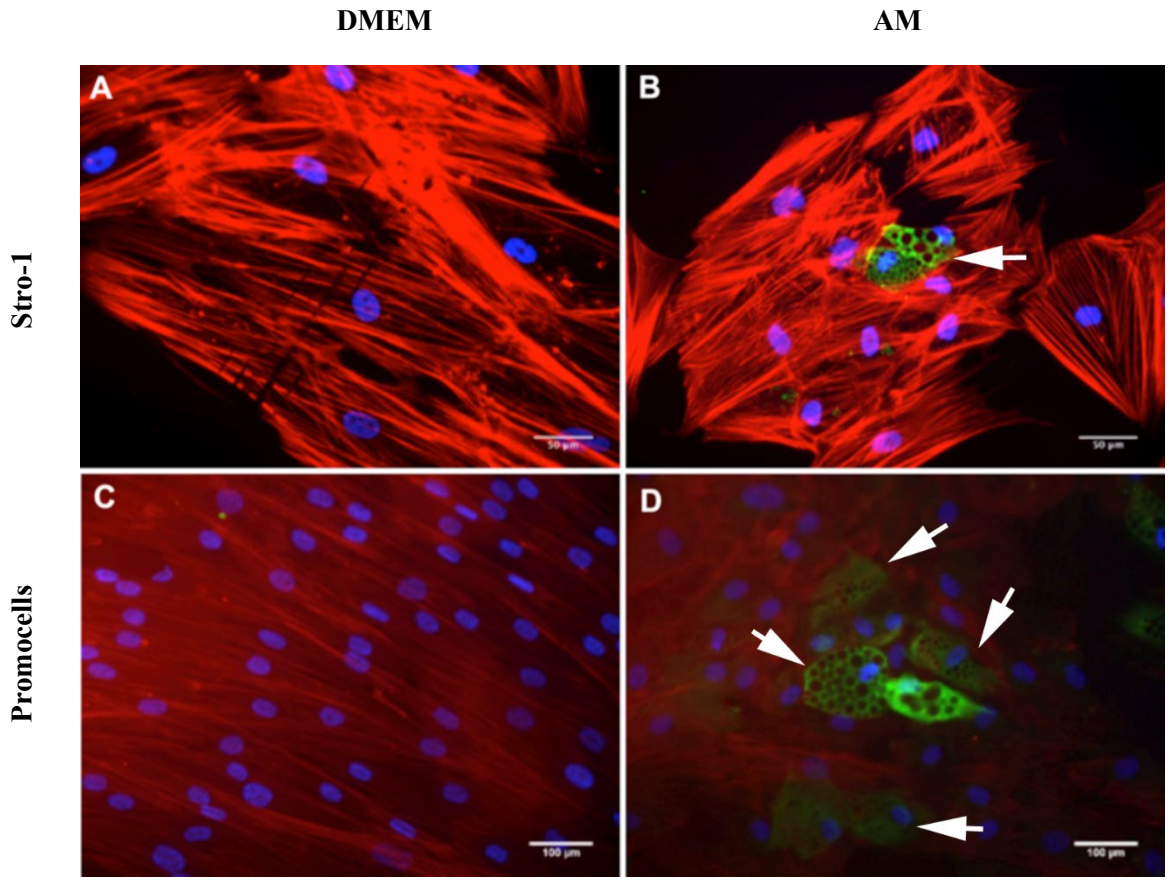

Fig. 3. 5 Fluorescence adipogenic staining at day 28 of FABP MSCs. Immunofluorescence staining of actin (red), FABP (green) and nuclei (blue) in (A) Stro-1 selected MSCs cultured in basal media, (B) Stro-1 selected MSCs cultured in adipogenic media, (C) Promocell MSCs cultured in basal media and (D) Promocell MSCs cultured in adipogenic media.

3.3.1.3 Chondrogenic Differentiation.

Chondrogenesis was also noted in both MSC populations when cultured with chondrogenic media. Safranin O staining was unsuccessful with Promocell MSCs, but was evident with Stro-1 selected MSCs (Fig. 3.6). The immunostaining process highlighted Sox9 (transcription factor) around the micromass, indicating chondrogenic lineage, shown in Fig. 3.7.

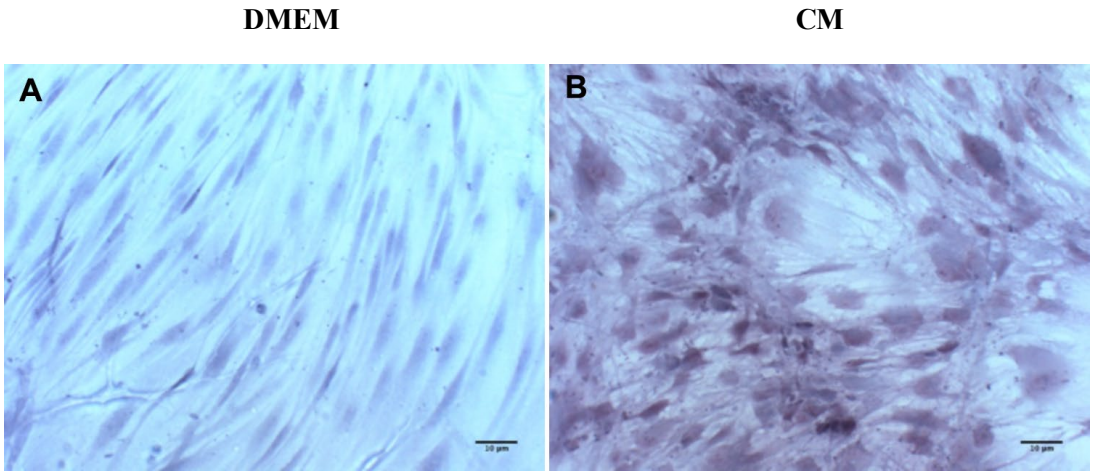

Fig. 3. 6 Safranin O chondrogenic staining of MSCs. Safranin O purple/red staining after 28 days of culture within chondrogenic media of (A) Stro-1 selected MSCs cultured in basal media, (B) Stro-1 selected MSCs. cultured in chondrogenic media. Arrows denote positive Safranin O staining.

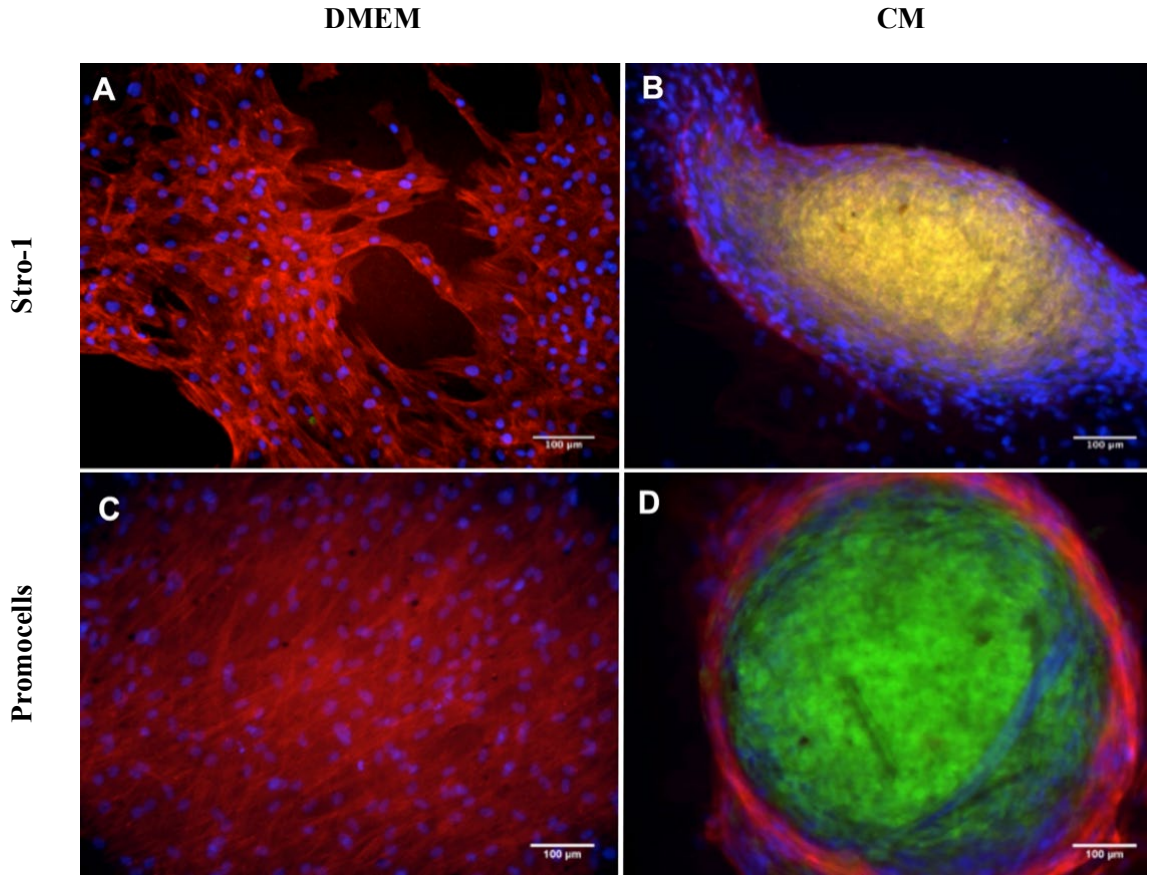

Fig. 3. 7 Fluorescence chondrogenic staining at day 28 of Sox9 in MSCs. Immunofluorescence staining of actin (red), sox9 (green) and nuclei (blue) in (A) Stro-1 selected MSCs cultured in adipogenic media, (B) Stro-1 selected MSCs cultured in basal media, (C) Promocell MSCs cultured in adipogenic media and (D) Promocell MSCs cultured in basal media.

3.3.2 MicroRNA Candidates Identification using Fluidigm PCR

To obtain an initial list of miRNA candidates involved in MSC differentiation, an extensive literature review was conducted. This included studies based on knockout and overexpression of miRNAs under osteogenesis, adipogenesis, chondrogenesis and also studies using standard growth media. From this, several key miRNA candidates, shown in table 3.1, were selected for expression studies within the two MSC populations via Fluidigm PCR.

MiR	Mechanism	Lineage	References
miR-31	**SATB2**	**Osteo (-)**	(Xie *et al.*, 2014)
miR-205	**Runx2**	**Osteo (-)**	(Hu *et al.*, 2015)
miR-133a	Runx2	Osteo (-)	(Liao *et al.*, 2013)
miR-135b	SMAD5	Osteo (-)	(Schaap-Oziemlak *et al.*, 2010)
miR27b	**PPARγ**	**Adipo (-)**	(Karbiener *et al.*, 2009)
miR-143	**ERK**	**Adipo (+)**	(Esau *et al.*, 2004)
miR-138	EID1	Adipo (-)	(Z. Yang *et al.*, 2011)
miR-145	**Sox9**	**Chondro (-)**	(B. Yang *et al.*, 2011)
miR-199a*	**Smad1**	**Chondro (-)**	(E. A. Lin *et al.*, 2009)
miR-140	Adamts-5	Chondro (+)	(Miyaki *et al.*, 2010)
miR-21	TGFβR2	Stem (+)	(Pan, Wang and Wang, 2010)
miR-30e	Ubc9	Stem (+)	(Yu *et al.*, 2010)

Table 3. 1: The miRNAs selected form a literature review for further Stro-1 and Promocell MSC expression studies by Fluidigm study. Those highlighted in bold were additionally selected for individual qPCR analysis.

Both patient derived Stro-1 and commercial Promocell MSCs were cultured in 24-well plates in similar conditions as section 3.2.1. The cells were lysed at three time points; at day 7, day 14 and day 21. The RNA was extracted and reverse transcribed to obtain cDNA. This was then pre-amplified and plated onto a 12:12 (for Promocells) and a 48.48 (for Stro-1) Dynamic Array™ integrated fluidic circuit (IFC) plate which holds 12/48 samples:12/48 primers (Please note that the larger 48:48 array was planned for use for the Stro-1 cells as our collaborator who gifts the cells was interested in a wider pool of miRNAs).

3.3.3 Promocell MSC Fluidigm PCR for candidate miRNAs

The microRNA candidates for expression during differentiation were all assessed in Promocell MSCs, cultured for 3, 7 and 21 days under basal and appropriate differentiation conditions. The cell samples were loaded onto the Fluidigm microfluidic chip and the PCR was run as explained in section 2.9 After running the Fluidigm PCR, a heatmap was obtained that illustrates an initial scan of the samples, allowing identification of successfully run samples and also potential data trends. Fig. 3.8 shows the Promocells 12:12 heatmap, where the colours indicate approximate Ct values (cycle threshold). Unfortunately, due to possible contamination, too low expression or low amplification, not all time points were successfully run (as indicated by black boxes in the heatmap).

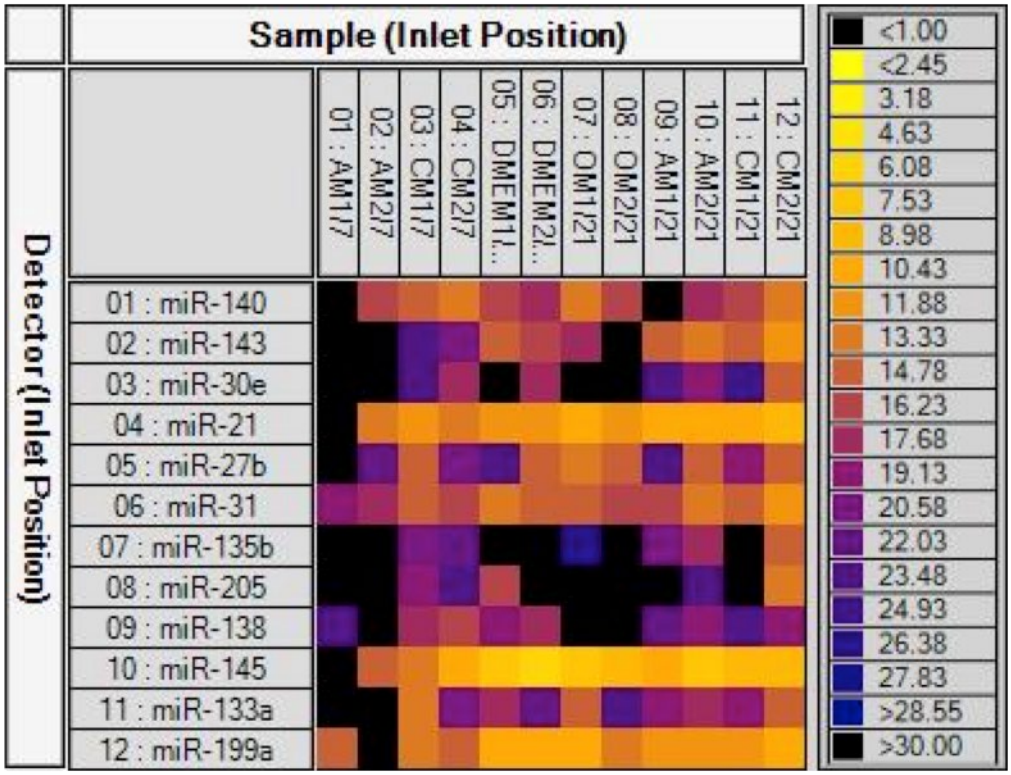

Fig. 3. 8 Promocell heatmap of a 12:12 Fluidigm chip assessing miRNA expression. The left column shows the miRNA primers used. The top row shows the samples denoted by media type/replicate number/time point in days (AM: adipogenic media; CM: chondrogenic media and OM: osteogenic media). The left column lists the miRNA sequences assessed and the right column shows the colours, which reflect the number of cycles required to provide a value, which is the cycle threshold or the Ct value.

From the Ct values obtained by Fluidigm, the expression fold change (EFC) for MSCs cultured under differentiation conditions normalised to cells cultured in basal DMEM was calculated and depicted in fig. 3.9. Only successful samples can be graphed, hence several are missing. Four selected miRNA expressions are shown below, other successful run samples can be found in the Appendix.

The expression of both osteogenic miRNAs (miR-31 and miR-205) was decreased with time in osteogenic media culture (Fig. 3.9 A,B), reflecting the literature, where both miRNAs are reported as being decreased during osteogenesis (Xie *et al.*, 2014; Hu *et al.*, 2015).

MiR-145 is reported as being decreased during chondrogenesis (B. Yang *et al.*, 2011). Here, miR-145 expression is massively reduced with time in chondrogenic culture, supporting the literature (Fig. 3.9 C).

Finally, miR-143 is reported as being increased during adipogenesis (Esau *et al.*, 2004). Here, miR-143 is clearly increased with time in adipogenic culture (Fig. 3.9 D).

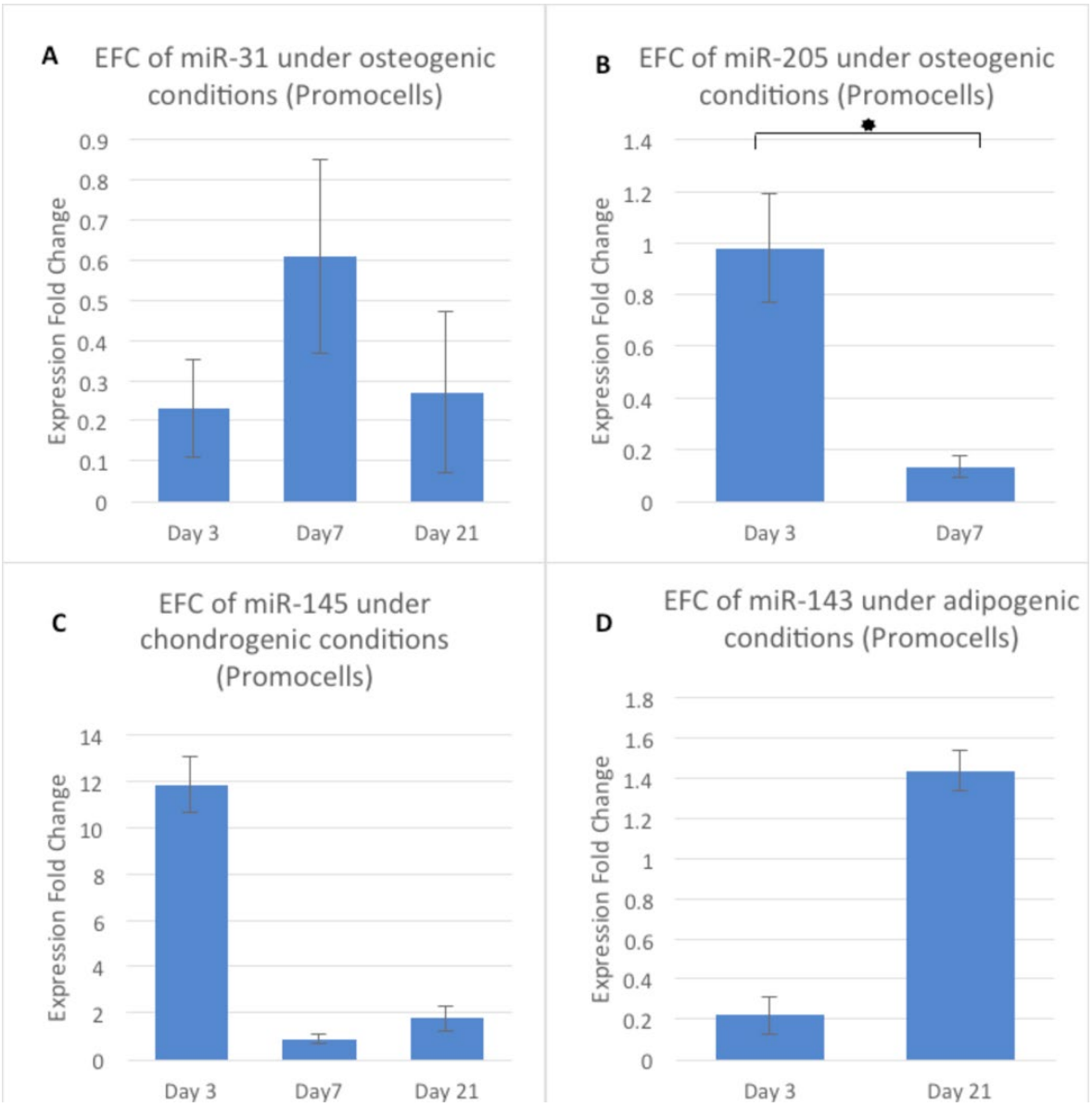

Fig. 3. 9 Expression fold change (EFC) of Promocell MSC miRNA sequences in differentiation media. (A) and (B) show the EFC of miR-31 and miR-205 respectively for Promocells cultured in osteogenic media. (C) is the EFC of miR-145 in chondrogenic conditions. (D) is the EFC of miR-143 in adipogenic media. (n=2; error bars indicate SD; $p<0.05$).

3.3.4 Stro-1 MSC Fluidigm PCR for candidate miRNAs

Stro-1 selected MSCs were cultured for 3, 7 and 21 days under basal and appropriate differentiation conditions. Fluidigm PCR for Stro-1 MSCs generated a heat map indicating

all the miRNA sequences (and several additional ones as requested by out collaborator), at time points days 3, 7 and 21, under appropriate differentiation conditions (Fig. 3.10) Unfortunately, due to the transient nature of the miRNAs and the potentially low expression levels, many samples were undetected (as indicated by black boxes in the heat map).

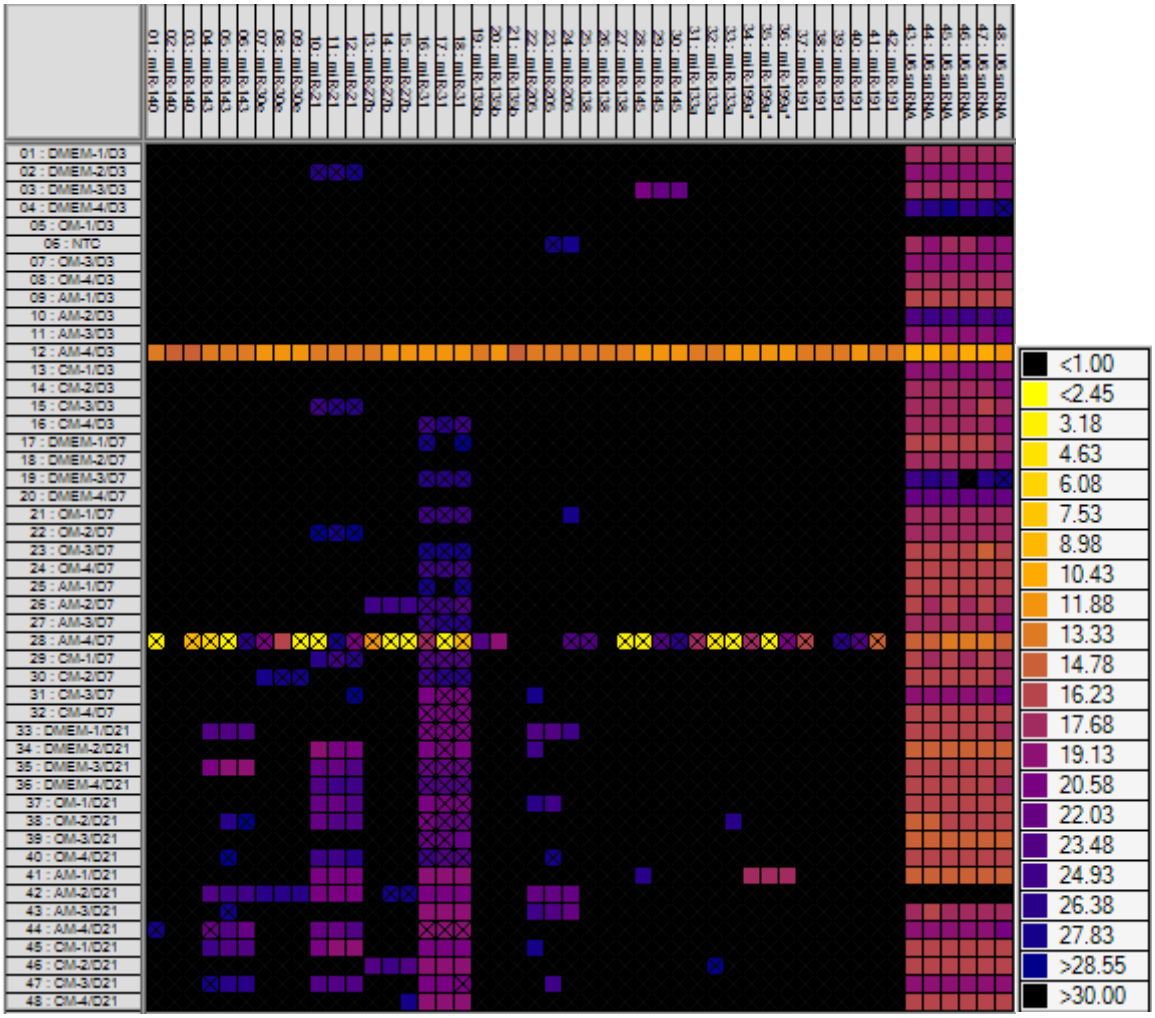

Fig. 3. 10 Stro-1 heatmap of a 48:48 Fluidigm chip assessing miRNA expression. The left column shows the miRNA primers used. The top row shows the samples denoted by media type/replicate number/time point in days (AM: adipogenic media; CM: chondrogenic media and OM: osteogenic media). The left column lists the miRNA sequences assessed and the right column shows the colours, which reflect the number of cycles required to provide a value, which is the cycle threshold or the Ct value.

Where sufficient readouts from the Fluidigm allowed, graphs were generated to indicate miRNA expression levels over time for MSCs cultured under differentiation conditions normalised to cells cultured in basal DMEM.

The expression of miR-31 was decreased with time in osteogenic media culture (Fig. 3.11 A), reflecting the literature. Unfortunately, whilst miR-205 is clearly expressed, only a single time point was identified, so timeline comparisons were not possible (Fig. 3.11 B).

Both miR-145 (chondrogenesis) and miR-143 (adipogenesis) are both expressed, but again only a single time point, thus no timeline comparisons were available (Fig. 3.11 C,D).

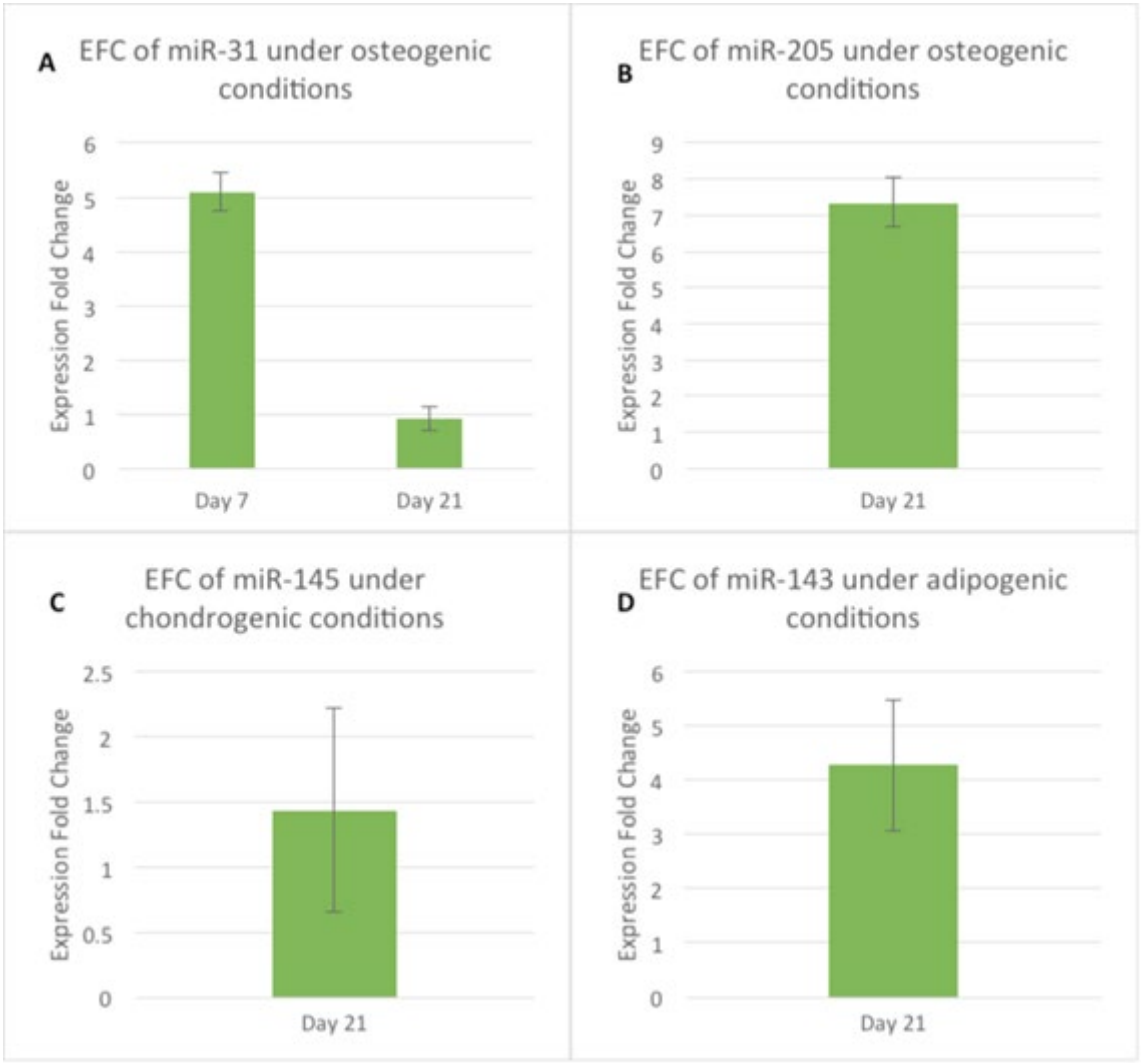

Fig. 3. 11 Expression fold change (EFC) of miRNA in differentiation media for Stro-1 selected MSCs. Due to the limited values obtained from the Fluidigm study, only few data points were obtained. (A) and (B) represent the EFC of miR-31 (n=4) and miR-205 (n=2) respectively for cells cultured in osteogenic media, (C) represents the EFC of miR-145 (n=2) in chondrogenic conditions, whilst (D) represents the EFC of miR-143 (n=3) in adipogenic media (error bars indicate SD; $p<0.05$).

3.3.5 Verification of final candidates MicroRNA expression via qPCR

Following on from the Fluidigm study, a final list of single candidate miRNAs per lineage were identified; these were further verified in Promocells and Stro-1 by qPCR. Two time points were assessed, days 3 and 7, as studies have shown that miRNAs are most active during the early time periods (Moreau *et al.*, 2013; Freiesleben *et al.*, 2016). The expression levels were calculated using the double delta Ct analysis.

3.3.5.1 MiRNA Expression in Promocell MSCs

The osteogenic miRNA expression levels, miR-31 and miR-205, are shown in figs 3.12. The expression of miR-31 decreases over time for Promocell MSCs cultured in osteogenic media, supporting the Fluidigm data and the literature. However, there was a surprisingly large significant increase in the expression of miR-205 from day 3 to day 7 (unlike the Fluidigm data and the literature).

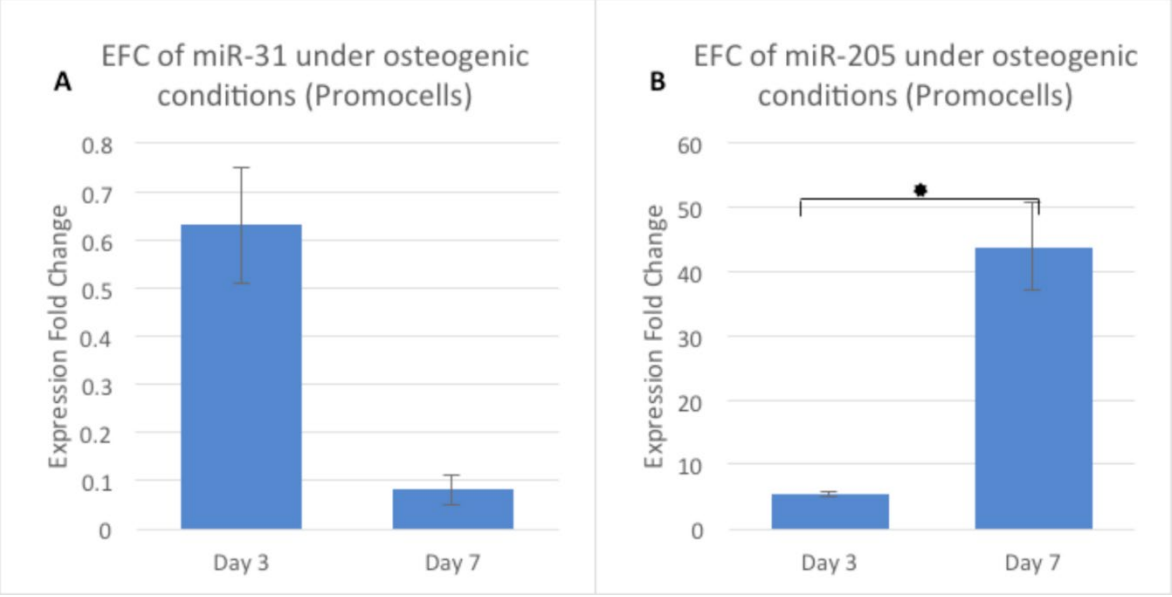

Fig. 3. 12 Expression fold change (EFC) of miRNA in Promocell MSCs cultured in osteogenic media. (A) miR-31 expression at days 3 and 7, and (B) miR-205 expression at days 3 and 7 (n=4, error bars indicate SD, $p<0.05$).

The chondrogenic expression levels for miR-145, are shown in fig.3.13 (A). There is a trend of decreasing expression with time, supporting the Fluidigm data and the literature (B. Yang *et al.*, 2011).

The adipogenic expression levels of miR-143 are shown in fig. 3.13 (B). Here, a significant increase in miRNA expression with time in adipogenic culture was noted, supporting the Fluidigm data and the literature stating that miR-143 is a promoter of adipogenesis (Esau *et al.*, 2004).

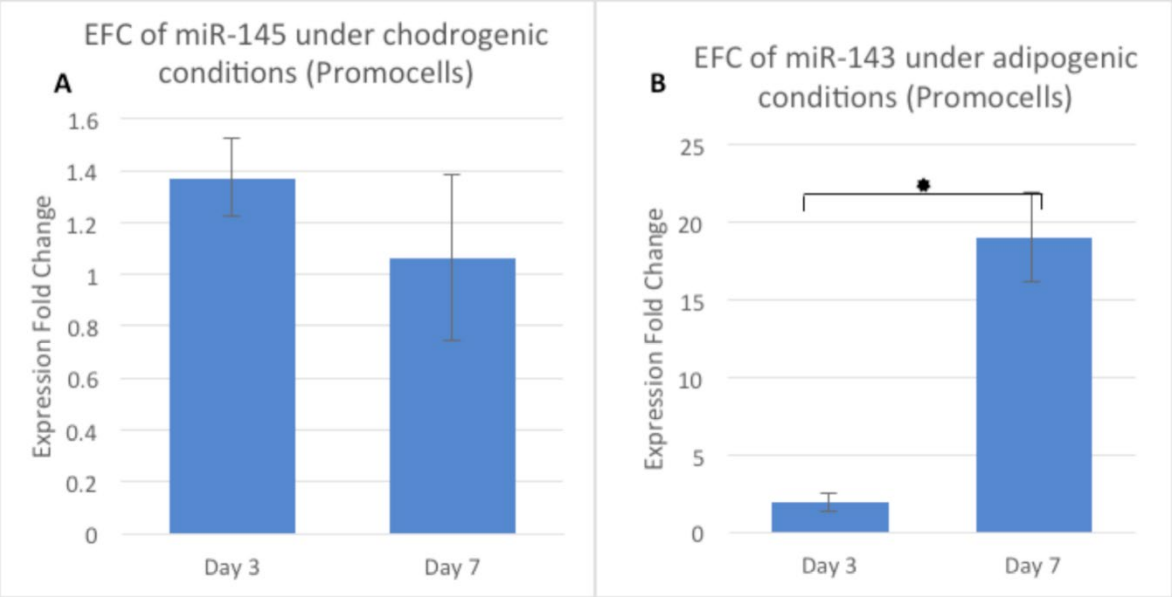

Fig. 3. 13 Expression fold change (EFC) of miRNA in Promocell MSCs cultured in chondrogenic or adipogenic media. (A) miR-145 under chondrogenic conditions, and (B) miR-143 in adipogenic media (n=4, error bars indicate SD, $p<0.05$).

3.3.5.2 MiRNA Expression in Stro-1 MSCs

The osteogenic miRNA expression levels, miR-31 and miR-205, are shown in figs 3.14. In both cases, the trend was for a decrease in miRNA expression with time in osteogenic culture. This mirrored the Fluidigm data and the literature, where both miR-31 and miR-205 are decreased during osteogenesis (bone formation), demonstrating that both may be considered inhibitors of osteogenesis (Xie *et al.*, 2014; Hu *et al.*, 2015).

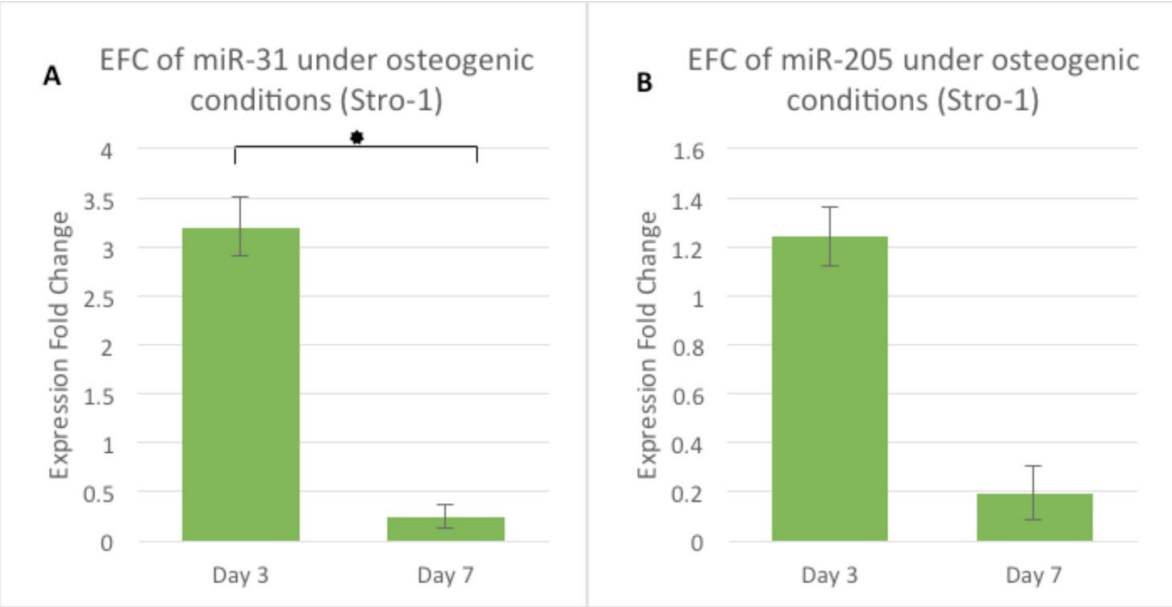

Fig. 3. 14 Expression fold change (EFC) of miRNA in Stro-1 cultured in osteogenic media. (A) miR-31 expression at days 3 and 7, and (B) miR-205 expression at days 3 and 7 (n=4, error bars indicate SD, $p<0.05$).

The miR-145 expression levels are shown in fig. 3.15. Here, the trend was for a decrease in miRNA expression with time in chondrogenic culture (Fig. 3.13 (A)), as expected from the literature, where miR-145 is decreased during chondrogenesis (cartilage formation) (B. Yang *et al.*, 2011).

The miR-143 expression levels are shown in fig. 3.15 and supported the Fluidigm data, with a significant increase in miRNA expression with time in adipogenic culture (Fig. 3.13 (B)). Again, this reflected the literature, where miR-143 is increased during adipogenesis (fat formation) (Esau *et al.*, 2004).

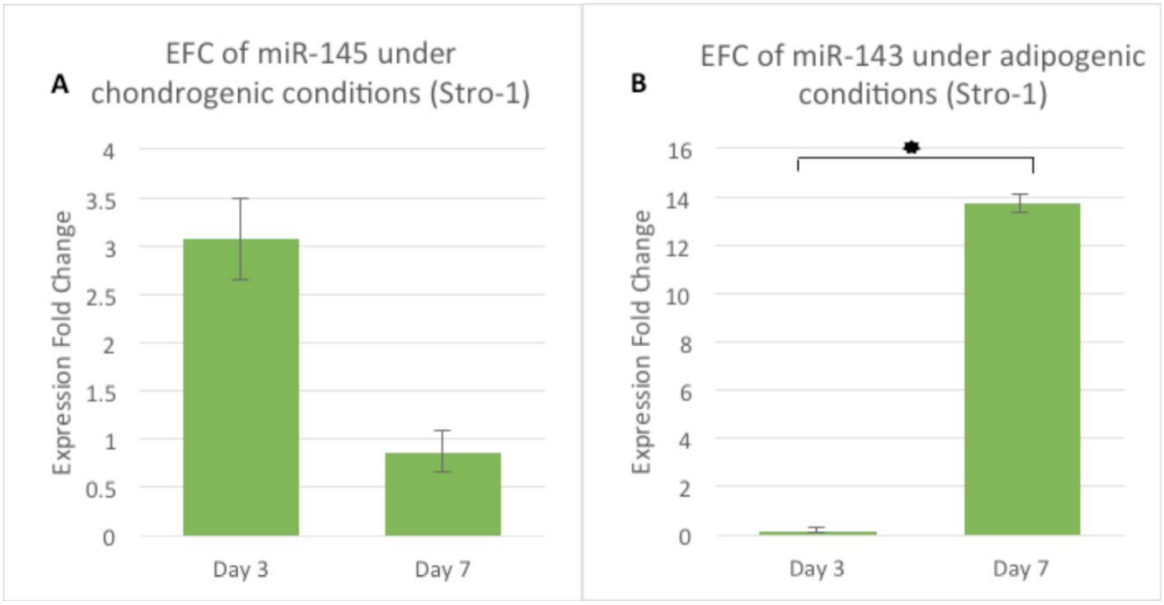

Fig. 3. 15 Expression fold change (EFC) of miRNA in Stro-1 cultured in adipogenic media and chondrogenic media. (A) shows miR-145 cultured in chondrogenic media while (B) is miR-143 in adipogenic media (n=4, error bars indicate SD, $p<0.05$).

3.4 Discussion:

MSCs are known for their ability to self-renew, as well as differentiate into other cell types (Pittenger *et al.*, 1999). There is a bulk of recent evidence supporting the role of miRNAs in the differentiation process (Oskowitz *et al.*, 2008; McGregor and Choi, 2011; Y. Zhang *et al.*, 2011). Within this chapter the aim was to employ two MSC populations and verify their capability to differentiate down the osteogenic, adipogenic and chondrogenic lineage. Subsequently, following a literature review of miRNAs and MSC differentiation, the expression of several highlighted miRNAs were assessed within our MSC populations over time during differentiation, with a view towards finalising a miRNA candidate for further study.

3.4.1 Confirmation of Stro-1 and Promocell multipotency

Two MSC populations were employed, an in-house bone marrow isolated population Stro-1 and the commercially available Promocells. MSCs are usually extracted from bone marrow (mostly from femoral heads from hip replacement surgeries) using density gradient centrifugation before mononuclear fraction and marker selection (Bieback *et al.*, 2008). This is a commonly used procedure and allows for selection of plastic adherent MSCs and also haematopoietic stem cells (HSCs), if needed. Commercially available MSCs, such as Promocell MSCs, are obtained through proprietary techniques. Although in-house derived cells, such as the Stro-1 cells used in this chapter, represent a true osteoprogenitor population depending on the isolation technique used, expansion culture is time-consuming and patient samples cannot be reliably obtained when required. In this chapter, by comparing both in-house derived and commercially available cells, it was demonstrated that both MSC populations have similar differentiation capacity and miRNA expression profiles and as such, be used interchangeably. In some instances, there were higher expression of markers in Stro-1 cells, but due to the benefits of Promocells, the latter was used for research.

To assess differentiation potential *in vitro*, the most widely established method utilises of chemical supplements added to standard growth media (Liu *et al.*, 2016). Depending on the chemicals used and their concentrations, we can direct their lineage towards the required direction. Chemical induction is widely used to differentiate different cell types under *in vitro* conditions. They cannot be easily directed to the required location (to prevent off-target

reactions) and can also cause toxicity. So whilst the chemicals cannot be used *in vivo*, it has proved to be an essential tool in research as it is a relatively reliable method of differentiating cells (Hwang *et al.*, 2008). The timeline of *in vitro* differentiation closely matches that of the body, as it takes around 4-weeks for cells to differentiate, which is close to the time it takes for bone fractures to heal (Funk *et al.*, 2000).

With regard to osteogenesis, both MSC populations clearly express calcium phosphate, as indicated by the black areas in the Von Kossa staining (Fig. 3.2). The black spots around the cells show silver phosphate, resulting from the exchange of calcium with silver present in the solution used during the staining protocol. Calcium phosphate is an essential component in bone formation. During this process, osteoblasts deposit mainly hydroxyapatite (insoluble salt of calcium and phosphorous) in the bone matrix. Other minerals such as magnesium and sodium are also deposited. Nearly 70% of the mineralization occurs within the first few days while complete mineralization can take up to five weeks (Funk *et al.*, 2000). In support of this is positive staining for osteocalcin (Fig. 3.2 (B&D)), which is a late stage osteogenic marker (Yang *et al.*, 2014). The image also shows a cluster of cells (9 using a nuclei count), which is necessary for differentiation as adhesion proteins like focal adhesion kinase (FAK) are involved in this process (Wrobel, Leszczynska and Brzoska, 2016). Collectively, this confirms the induction of osteogenesis by the differentiation media.

With regard to adipogenesis, again both MSC populations exhibit fatty acid deposits in their cytoplasm, as stained by Oil Red O (Fig. 3.4). The diazo dye works by staining neutral triglycerides and lipids in the cells (Mehlem *et al.*, 2013). Further evidence is shown with positive fatty acid binding protein (FABP) staining around the fatty deposits (Fig. 3.4 (B&D)). Both positive stains confirm the induction of adipogenesis.

Finally, chondrogenic differentiation was assessed in micromass cell culture. Micromass cell culture involves the culture of a high density of cells confined to a small area. This leads to the formation of a spheroid like structure. Micromass culture is necessary as the high cell to cell interactions are a required component for chondrogenic differentiation (Zhang *et al.*, 2010). Positive staining of Sox9, a master regulator of chondrogenesis was noted (Fig. 3.7 B&D) (Akiyama, 2008).

In summary, both cell populations are capable of differentiation down the three main lineages, with little difference noted between cell types.

3.4.2 Expression of key miRNAs within differentiating MSC populations

Over a thousand papers were published within the last two decades detailing the involvement of various miRNAs in MSC differentiation. Though this has not translated into any FDA approved research for miRNAs, companies and laboratories are involved in efforts to finalise phase 1 and phase 2 trials. Patisiran, a small-interfering RNA (siRNA) drug was granted FDA approval in 2018, paving the way for small RNA to be used in medical trials (Adams *et al.*, 2018). The promising field of miRNAs in therapeutics is an exciting endeavour and has large untapped potential in regenerative medicine and even cancer.

In order to develop a system whereby we can use a single miRNA to influence MSC differentiation, an initial screen of the expression of several miRNA candidates within both MSC populations was needed. Next generation sequencing (NGS) would be an excellent approach (Galván *et al.*, 2014; Manning *et al.*, 2015). NGS technology or high-throughput sequencing is a term used for a wide variety of modern techniques that are used to sequence either DNA or RNA. Although the term suggests NGS involves only sequencing, any next-generation techniques used to resolve multiple genetic loci can be considered as NGS. However, due to the cost restrictions, here the Fluidigm BioMark HD system was employed.

Fluidigm allows for the use of an integrated fluidic circuit (IFC) to conduct a high-throughput PCR. Several different sizes of microfluidic chips are available, allowing the calculation of up to 96 samples with 96 primers. As such, a large number of samples can be analysed, allowing for high-throughput experiments. Microfluidics is the science of controlling small volumes of fluids using channels in the size range of microns and has a wide range of applications. Due to the nature of microfluidics, only a small volume of sample and reaction mixes are required, allowing for cost and sample efficiency. The Fluidigm device used in this chapter also touts single-cell analysis, improving the range of experiments that can be conducted. For example, Wechsler et al. compared the effects of alternating current on differentiation of MSCs at the cell level using the above technique (Wechsler, Hermann and Bizios, 2016). After loading the samples onto the chip, automated systems control the rest of the process, allowing for better time management. All these benefits lower the workload of analysing single gene expressions in cells considerably, whilst providing accurate results.

By using the literature as a base, several miRNA candidates were selected that were identified in osteogenesis, adipogenesis, chondrogenesis and MSC 'stemness' retention. Both MSC populations were cultured for 7, 14 and 21 days under appropriate differentiation media conditions and the change in miRNA expression was assessed. Initially the data was presented as a heat map (Fig. 3.8 and Fig. 3.10). Heat maps are a form of representing data wherein the colours represent a value or its approximation from a given data set. Heatmaps are used as a preliminary form of analysis where the data is summarised simply and effectively, and as such has been used in several studies (Fu *et al.*, 2013; Kumar *et al.*, 2014). The endogenous control used was U6 snRNA, a widely used control in miRNA studies (Lou *et al.*, 2015; Masè *et al.*, 2017).

3.4.2.1 Osteogenic miRNA gene expression

The Promocell data from the 12:12 Fluidigm chip is shown in fig. 3.9 and the Stro-1 chip in fig. 3.10. There were several samples that did not yield values, but on the whole, the chip generated useful data that allowed the observation of the gene expression fold changes over time. The changes observed were mostly as expected and mirrored the literature.

In particular we were interested in miR-31 and miR-205, as both were referenced recently in the literature as being involved in osteogenesis (Deng *et al.*, 2014; Qiao, Chen and Zhang, 2014; Xie *et al.*, 2014; Hu *et al.*, 2015). In addition, two other relevant miRNAs, miR-133a and miR-135b, were also assessed (Schaap-Oziemlak *et al.*, 2010; Liao *et al.*, 2013). All four miRNAs assessed have been reported as negatively influencing osteogenesis (i.e. their expression is decreased during osteogenesis), as indicated in fig. 3.16. Both miR-31 and miR-133 directly inhibit osteogenesis via inhibiting Runx2 expression whilst miR-31 also inhibits osterix (Osx).

Both miR-31 and miR-205 were clearly expressed in Promocell MSCs and mirrored the literature, whilst only miR-31 was expressed in Stro-1 cells. However while miR-133a showed a decrease in expression, miR-135b showed an increase over time in Promocells (Appendix Fig. 3.18), whilst no data was generated for Stro-1 cells. As such, miR-31 and -205 were selected as inhibitors of osteogenesis for further study in subsequent chapters.

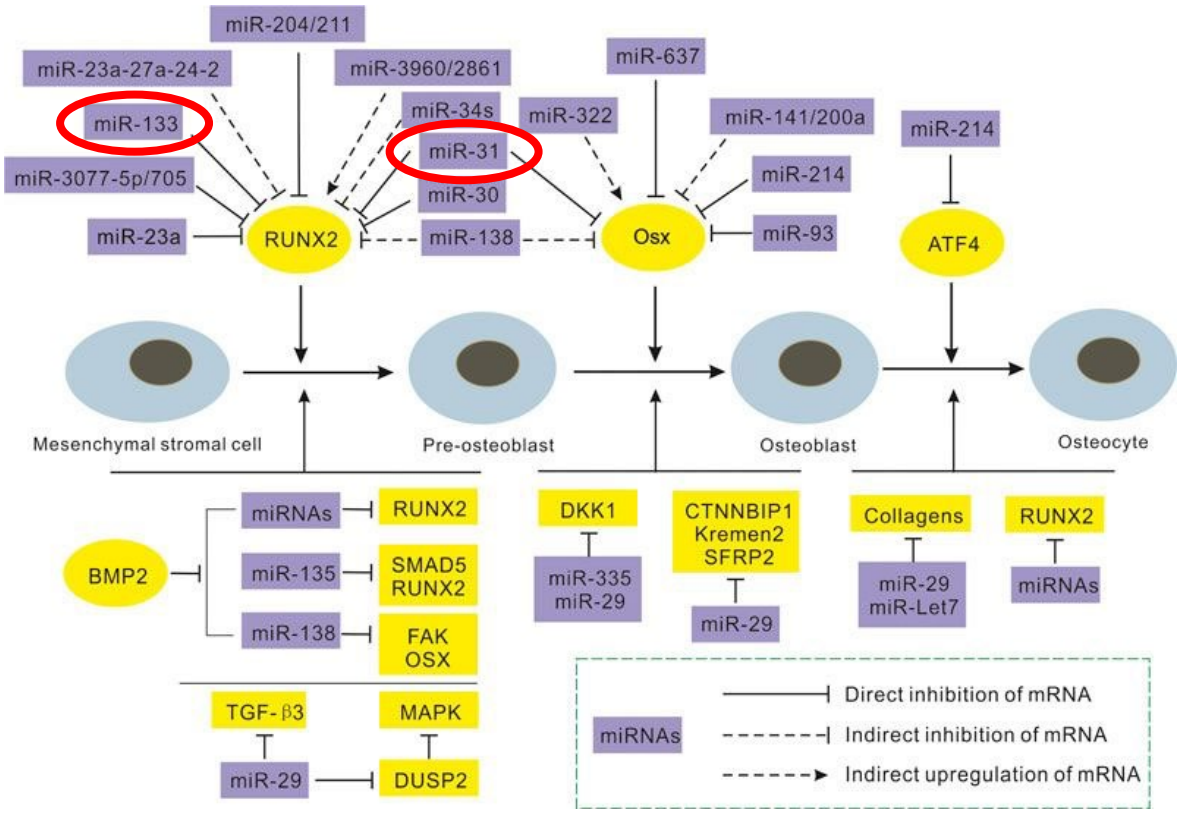

.

Fig. 3. 16: Schematic summary of the individual miRNAs involved in osteogenesis. The progression of osteogenesis from an MSC through to an osteocyte is illustrated, with miRNAs indicated in purple, relative to their targets in yellow. Both miR-31 and miR-133 are circled in red (adapted from (Jing *et al.*, 2015)).

3.4.2.2 Adipogenic miRNA gene expression

The main miRNAs stated in the literature as being involved in adipogenesis are miR-143, miR-138 and miR-27b (fig. 3.17). Both miR-138 and miR-27b were shown to be negative regulators of adipogenesis, while miR-143 being the positive regulator (Esau *et al.*, 2004; Karbiener *et al.*, 2009; Z. Yang *et al.*, 2011).

In these studies, miR-143 supported the literature and demonstrated a large, significant, increase in expression during adipogenesis (Fig. 3.13 D & 3.15 D) in both MSC populations. The other two adipogenic miRNAs are graphed in the appendix; only miR-27b showed a response for both Promocells and Stro-1 selected cells, with a slight increase noted. Therefore, miR-143 was selected for further study.

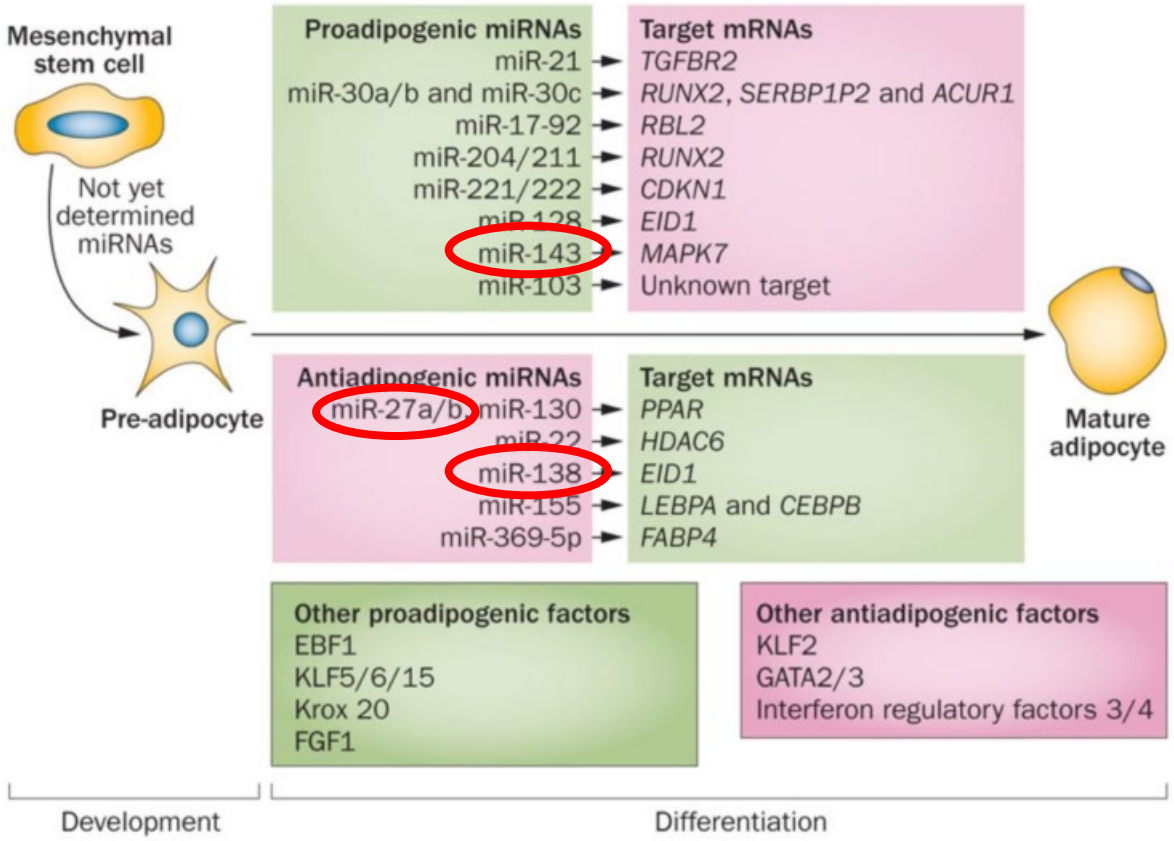

Fig. 3. 17: Schematic summary of the individual miRNAs involved in adipogenesis. The progression of adipogenesis from an MSC through to a mature adipocyte is shown, with positive miRNAs influencers in the upper panel and negative miRNA influencers in the middle panel; relative to their targets on the right-hand side panels. MiR-27a/b, miR-138 and miR-143 are circled in red (adapted from (Arner and Kulyté, 2015)).

3.4.2.3 Chondrogenic miRNA gene expression

For chondrogenesis, the main miRNAs studied to date are miR-145, miR-199a* and miR-138. Both miR-145 and miR-199a* decrease in expression over chondrogenesis, while miR-140 is a positive regulator (E. A. Lin *et al.*, 2009; Miyaki *et al.*, 2010; B. Yang *et al.*, 2011). Neither miR-140 or miR-199a* elicited a sufficient response in the Stro-1 selected cells but did show a response in Promocells as seen in the appendix fig. However, miR-145 clearly decreased in expression over time under chondrogenic conditions as expected.

3.4.2.4 The issues with using Fluidigm to analyse gene expression

The main problem with the Fluidigm technique is that it restricts itself to 30 cycles. This, along with the low levels of miRNAs (mostly being repressed), often cannot provide a suitable platform to obtain the expression levels. It did, however, allow the generation of an initial candidate list, verifying their expression where possible. Any miRNAs with a considerably high Ct value (>30) had to be neglected.

The formation of primer dimers is also a major concern, as the primers are not much larger than the miRNAs themselves. This can lead to problems with the interpretation of data, but by analysing the melting curves, this can be mitigated. There may be other reasons such as purity of the RNA or low reverse transcription rate that may cause the high Ct values. Perhaps there may also have been degradation of samples occurring. Due to the relatively new nature of this technique, troubleshooting was difficult. The technique was repeated, but most of the results remained the same.

Summary – using the data from both Fluidigm studies, a single target per lineage was selected for further study; osteogenic miR-205, adipogenic miR-143 and chondrogenic miR-145.

3.4.3 Confirmation of expression of single miRNA targets for osteogenesis, adipogenesis and chondrogenesis by qPCR

Following on from the Fluidigm data, real-time qPCR was carried out on the single selected miRNA target from each lineage. Real-time qPCR has the benefit of reaching up to 40 cycles, thus is better for amplifying small quantities of mRNA, however it can be prone to errors, due to the high number of samples and replicates involved.

3.4.3.1 Osteogenic study

MiR-205 was selected as the main target for osteogenesis. Expression levels of miR-205 were low in Stro-1 cells, but very high in Promocell MSCs, in particular at day 7 (nearly an 8-fold change increase compared to control). Mir-205 is involved in the ERK and p38

MAPK pathways, affecting Runx2 and leading to the negative regulation of osteogenesis; a study by Zhang et al. highlighted this reverse relationship between miR-205 expression and Runx2 (Y. Zhang *et al.*, 2011). Furthermore, Hu et al. confirmed that controlling the expression of miR-205 during osteogenesis influences the phosphorylation of ERK and p38 (Hu *et al.*, 2015). Both ERK and p38 phosphorylate several osteogenic factors such as Runx2 and even DLX5. DLX5 transactivates Osterix which is also essential for osteogenesis (Rodríguez-Carballo, Gámez and Ventura, 2016). ERK is involved in the proliferation, differentiation and apoptosis of cells. Inhibition of the ERK pathway promoted mineralization of cells, essential for bone formation (Doan *et al.*, 2012). Other studies also showed the importance of miR-205 in osteogenesis, **thus miR-205 was selected as an osteogenic miRNA for further study in subsequent chapters** (Tabruyn *et al.*, 2013; Qiao, Chen and Zhang, 2014; Zhao *et al.*, 2014; Hu *et al.*, 2015).

3.4.3.2 Adipogenic study

The expression of miR-143 in Promocells and Stro-1 MSCs increased significantly during adipogenesis (Figs. 3.13 D & 3.15 D). Unlike the other miRNA targets studied, miR-143 has a positive relationship in adipogenesis. An early study conducted by Esau et al. discovered the role of miR-143 in adipogenesis (Esau *et al.*, 2004). They showed that miR-143 expression increased during the differentiation and repressing its activity inhibited adipogenesis. It was further discovered that by targeting the MAPK and ERK, miR-143 promotes adipogenesis. As mentioned previously, these two pathways are also essential for osteogenesis. By taking into account the inverse relationship of these two differentiation paths, miR-143 can be seen to be an important factor in adipogenesis. MAPK is involved in the proliferation and differentiation of cells. In the early stages of adipogenesis, this pathway promoted the clonal expansion of cells. Although at the later stages, overexpression of miR-143 has been shown to limit adipogenesis, the ERK mediated phosphorylation of PPARγ due to miR-143 counteracts the mentioned effect, positively regulating adipogenesis (Chen *et al.*, 2014; An *et al.*, 2016). **Thus, miR-143 was selected as an adipogenic miRNA for further study in subsequent chapters**.

3.4.3.3 Chondrogenic study

The expression of miR-145 was decreased over time for both Promocell and Stro-1 MSCs (Fig. 3.13 C & 3.15 C). The expression levels did not show the same level of change across the two cell types, but this could be attributed to genetic variation between sources. The most essential transcription factor for chondrogenesis, Sox9, is targeted by miR-145; this was first reported by Yang B. et al. MiR-145 has also been reported to cause decreased collagen II and aggrecan protein expression, which are key constituents of the cartilage matrix (B. Yang *et al.*, 2011). As the master regulator of chondrogenesis, Sox9 is essential for chondrogenesis, triggering expression of genes such as Sox5 and Sox6, which along with Sox9, are often referred to as the chondrogenic trio (Akiyama *et al.*, 2002). Furthermore, miR-143 also prevents ossification of chondrocytes helping to maintain their cartilage state (Dy *et al.*, 2012). Although several transcription factors including TGFβ control the expression of miR-145, it has been shown in studies that inhibiting it also showed promising results (Kenyon *et al.*, 2019). **Thus, miR-143 was selected as a chondrogenic miRNA for further study in subsequent chapters** (Martinez-Sanchez, Dudek and Murphy, 2012).

3.5 Conclusion

The aim of this chapter was twofold; (1) to verify multipotency in two MSC populations and (2) to assess the expression of miRNAs during differentiation, with a view towards manipulating miRNA levels in MSCs to influence differentiation. A list of potential miRNA candidates was identified form the literature and their expression levels were established in both MSC populations during differentiation.

Both the in-house derived Stro-1 cells and commercially available Promocells were capable of differentiation down the three main lineages; osteogenesis, adipogenesis and chondrogenesis, thus verifying that both MSC populations used are multipotent. Due to the easily available nature of the commercial Promocell MSCs and the similarity of results between the two sample types, we will be using these cells for all further experiments.

Following an extensive literature review, a list of candidate miRNAs was obtained. To identify whether these miRNAs are present in the two cell types, a multiplex PCR was conducted. Using the Fluidigm BioMark HD system, we were able to conduct a large experiment of multiple samples and primers. Although it had its limitations, the ability to obtain a high throughput allowed us to screen several miRNA candidates.

A final miRNA target for each differentiation pathway was identified for further confirmation via qPCR in both MSC populations. Changes in expression of miRNAs were verified during differentiation. Both Stro-1 and Promocell MSCs showed similar changes in the levels of miRNA expression, further showing that either cell types were suitable for further experiments. The miRNAs chosen to be used in further stages were miR-31, miR-205, miR-145 and miR-143.

3.6 Appendix

A.1 Expression fold change of excluded miRNAs from the Promocell Fluidigm study:

A1.1 Osteogenesis. The Promocell Fluidigm study also included miR-133a and miR-135b, negative regulators of osteogenesis. MiR-135b showed a decrease in its expression overtime during osteogenesis as expected according to literature, however miR-133a demonstrated a significant increase over time in culture. Due to none or very little response for the same miRNAs in the Stro-1 study, these miRNAs were not taken for further experiments. As of yet, no studies have shown the expression of miR-135b till such a late time point, so it may have an unidentified interaction, which might be essential for cell development

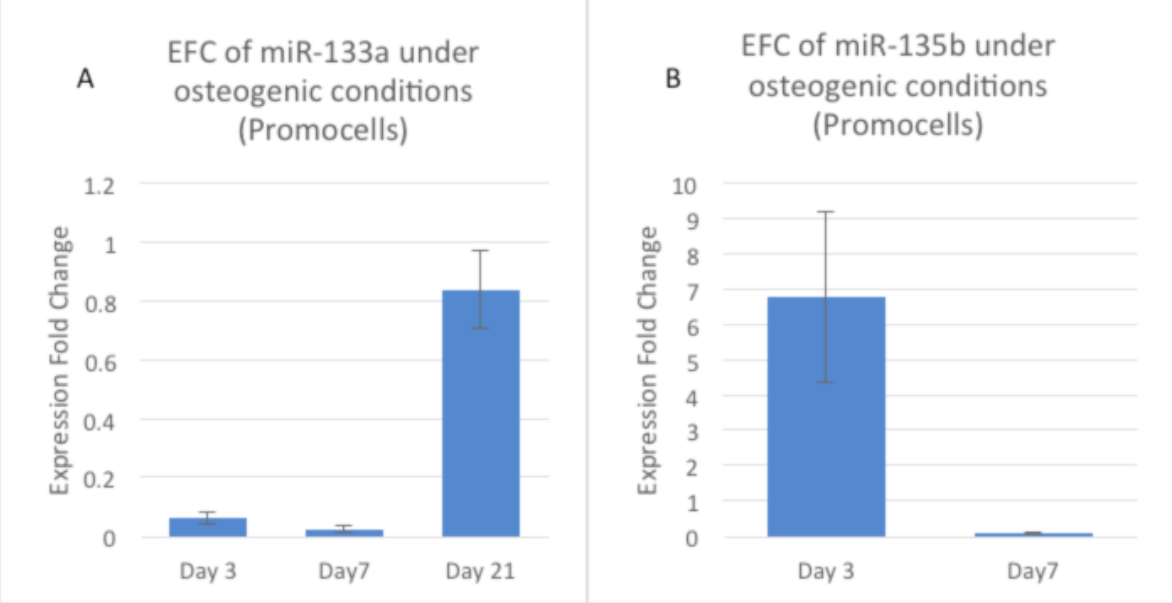

Fig. 3. 18: Promocell expression fold change (EFC) of miRNA cultured in osteogenic media. (A) miR-133a, and (B) miR-135b (n=3, error bars indicate SD, $p<0.05$).

A1.2 chondrogenesis. MiR-140 and miR-199a* expression was assessed in Promocells over time in chondrogenic culture. Being a negative regulator, miR-199a* showed a decrease in its expression from the earliest time point to the final. Although miR-140 is a positive regulator of chondrogenesis, it also showed a decrease in its expression. Both graphs indicated high variation, which, coupled with the opposing data trend for miR-199a in the literature, removed these miRNAs from further study.

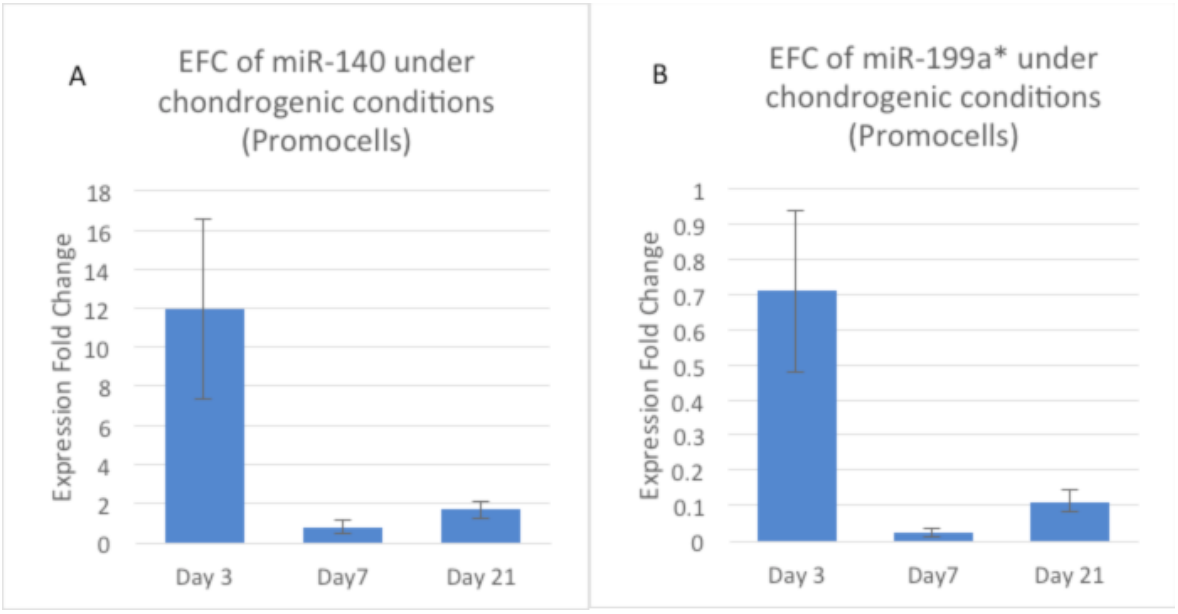

Fig. 3. 19: Promocell expression fold change (EFC) of miRNA cultured in chondrogenic media. (A) miR-140, and (B) miR-199a* (n=3, error bars indicate SD, $p<0.05$).

A1.3 adipogenesis. MiR-27b is a reported negative regulator of adipogenesis; the data supported this, with expression clearly decreased in Promocells over time in adipogenic culture (fig. 3.20). However, miR-143 showed large, significant increases in expression in both Promocell and Strol-1 MSCs, therefore it was selected for further study.

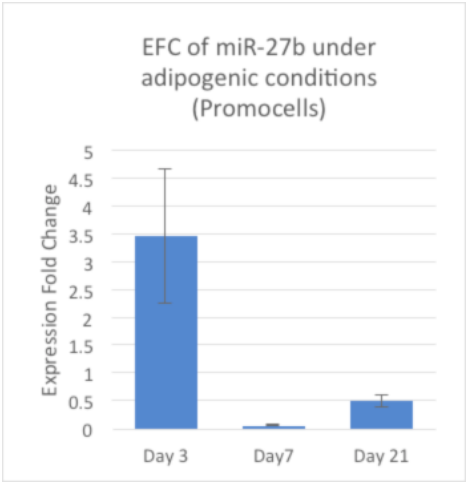

Fig. 3. 20: Promocell expression fold change (EFC) of miRNA cultured in adipogenic media. MiR-27b expression under adipogenic conditions (n=4, error bars indicate SD, $p<0.05$).

A.2 Expression fold change of excluded miRNAs from the Stro-1 Fluidigm study:

A2.1 Osteogenesis.

The Fluidigm study of Stro-1 selected cells did not show many positive results, as the heatmap illustrated. Only miR-27b, a negative regulator of adipogenesis, showed a response which can be visualised in fig. 3.21. Due to this, Promocells were selected for further study in subsequent chapters.

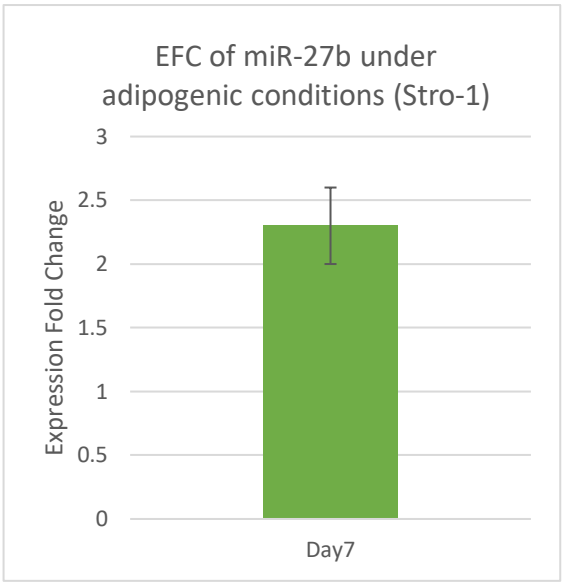

Fig. 3. 21: Stro-1 expression fold change (EFC) of miRNA cultured in adipogenic media. MiR-143 in adipogenic media (n=3, error bars indicate SD, $p<0.05$).

Chapter 4: Using miRNA antagomiRs/mimics to stimulate differentiation of MSCs

4.1 Introduction

4.1.1 MicroRNA and Mesenchymal Stem Cell Differentiation

MicroRNAs (miRNAs) are short RNA sequences of around 22 nucleotides in length. Their function is to regulate the expression of mRNAs through silencing or degradation through perfect or imperfect complementarity, respectively (Ha and Kim, 2014). Being found endogenously, they are formed through the transcription of endogenous transcripts forming a structure that is looped on one end and single stranded segments at the other end. This is called the primary miRNA (pri-miRNA). This structure is then cleaved by a microprocessor complex leading to precursor miRNA (pre-miRNA) with its loop intact, forming a hairpin structure. The Dicer enzyme cleaves the loop and forming miRNA:miRNA*, where the miRNA is the guide strand and miRNA* is the passenger strand (Ruby *et al.*, 2007). In most cases the guide strand functions more effectively and usually has the nomenclature of miR-X-5p, where X is an arbitrary number identifying the miRNA. This guide strand binds to the Argonaute protein which leads to a complex that can bind to mRNAs within the cell and regulate its expression (Meister *et al.*, 2004).

By repressing the function of mRNAs, the miRNAs can regulate many different pathways within the cell, with appropriate signaling leading to the repression of the required mRNA. MSC differentiation is of great importance due to their ability to differentiate mainly into osteoblasts, adipocytes and chondrocytes. This process has a multitude of chemical and physical pathways required to function (Bianco, 2014). One such process is the regulation by miRNAs. Recent studies have shown the importance of miRNAs in differentiation (Gao *et al.*, 2011; Baglìo *et al.*, 2013). Through over and under expression studies, an increasing number of miRNAs have been discovered that target various transcription factors for during mesenchymal stem cell differentiation. One can therefore assume that by manipulating the levels of miRNAs, the lineage of the cell can be directed towards a particular direction.

To identify the miRNA candidates, an extensive literature study was conducted. The ideal miRNA would have non-conflicting targets of action and be modestly studied for relevance of function. The previous chapter used the Fluidigm and qPCR studies to confirm the levels of initial candidate miRNAs during different time points of MSC differentiation.

4.1.2 MicroRNAs and Osteogenesis

Osteogenesis is the formation of osteoblasts and osteoclasts from MSCs, and they have important functions for bone formation and resorption, respectively (James, 2013). As osteogenesis is vital for skeletal development, understanding it is essential for the development of treatments for skeletal dysfunctions. MiRNAs control osteogenesis by interacting with its positive and negative regulators such as the main transcription factors Runx2 and Osterix. Multiple studies have identified targets of miRNA action at various stages of osteogenesis. MiRNAs such as miR-135 and miR-138 can act at the early stages, while miR-29 and let-7 can act at the later stages of osteoclast formation (Koh *et al.*, 2010; Y. Zhang *et al.*, 2011). It is necessary to understand the time of action and select the right candidates for potential therapeutic use. MiR-205 is an important candidate for osteogenesis. It acts on the master transcription factor, Runx2, and represses its function. Hu *et al.* showed the decrease of alkaline phosphatase (ALP) and bone sialoprotein (BSP) when miR-205 was overexpressed in MSCs (Hu *et al.*, 2015). A recent cancer study also showed miR-205 affecting Runx2 expression, inhibiting the progression of pancreatic cancer (Zhuang *et al.*, 2019). Targeting this microRNA, through the use of antagomiRs (anti-sense miRNAs) could lead to the repression of this miRNA, allowing unhindered functionality of Runx2. This could lead to increased osteogenesis in MSCs.

4.1.3 MicroRNAs and Adipogenesis

Adipogenesis is also influenced by miRNAs. The formation of adipocytes is essential for the eventual deposition of lipids to be used as a source of energy (Rosen and MacDougald, 2006). As adipogenesis and osteogenesis are inversely related, any insights into this process can be used to fortify osteogenesis. Esau *et al.* conducted a high throughput study of several miRNAs during adipocyte formation (Esau *et al.*, 2004). One of these miRNAs was miR-143. They continued their study into this miRNA and discovered its role as an adipogenesis promoter. Targeting the ERK pathway, by introducing antagomiRs of miR-143 they observed lower expression of adipogenic genes and also lowered triglyceride accumulation. By introducing mimics, we can potentially increase the rate of adipogenesis and control MSC fate.

4.1.4 MicroRNAs and Chondrogenesis

The formation of cartilage is also of great importance due to its role in the skeletal system. Injuries or diseases to the cartilage can lead to drastic quality of life changes (Herlofsen *et al.*, 2011). MiRNAs such as miR-140 and miR-145 positively and negatively regulate chondrogenesis (Wuelling and Vortkamp, 2010). MiR-145 was shown to target Sox9 expression through the use of plasmid reporter vectors with a Luciferase reporter. They showed the inverse relationship between miR-145 and Sox9. By creating antagomiRs to miR-145, chondrogenesis may be promoted, leading to quicker cartilage formation. (B. Yang *et al.*, 2011)

4.1.5 In-house MSCs vs commercial Promocell MSCs

MSC populations can be obtained from multiple sources such as bone-marrow and adipose tissue. These populations can exhibit differences in stemness, proliferation and differentiation properties, and as such, it is essential to identify the ideal phenotype of MSCs for research to translate it for medical use. In-house Stro-1 selected MSCs are patient derived, and as such are biologically relevant. Stro-1 is a common MSC marker and cells selected for this antigen are used for studies (Stewart *et al.*, 1999). There has been contention on its use due to the marker being prevalent in MSCs found in bone marrow and adipose tissue, but not in the endothelium of blood vessels. A certain section of these MSCs also do not show presence of essential MSC markers such as CD34 (Lin *et al.*, 2011). Commercially Promocell MSCs have been selected to show the recommended ISCT (International Society Cell & Gene Therapy) markers and are also commonly used for *in vitro* studies (Samsonraj *et al.*, 2015). Due to their ease of availability and meeting the criteria for MSCs, they are an ideal source for this work.

The previous chapter compared the differentiation potential and the presence of miRNAs in both cell types. The similarity in the results in most cases showed the possibility of using either cell types for clinical relevance. Due to the widely used nature and availability of Promocell MSCs in scientific studies, this study chose to use this cell types for future experiments.

4.1.6 Chapter Aims

We aim to deliver the miRNA antagomiRs/mimics to stimulate differentiation of MSCs. The main issue is the delivery of these sequences safely to the target. Several delivery vehicles

have been used in studies to deliver oligonucleotides to specific locations. Most *in vitro* studies conducted use transfection agents to deliver the sequences (Lee *et al.*, 2011; Jensen, Anderson and Glass, 2014). The issue with these methods is the toxicity of the agents *in vivo*. Newer methods of delivery such as dendrimers and lipids have been in the forefront, but to the relatively new nature of these platforms, a more robust and well-studied vehicle is required (Vickers and Remaley, 2012; Dzmitruk *et al.*, 2018).

The use of gold nanoparticles (GNPs) for medical research has been well established. From treating tumors through thermal ablation to biosensors, the relative safety of GNPs for biological use is already established (Dreaden, Alkilany, *et al.*, 2012). Cells have are known to easily engulf these GNPs through endocytosis, providing a route to cellular entry. In the case of delivering oligonucleotides, the sequences are bonded to the nanoparticle surface through the formation of a thiol bond. Therefore, by modifying oligonucleotides (thiolating), we can therefore attach them onto GNPs as cargo (Ghosh *et al.*, 2008). In addition, the sequences can be protected from intracellular enzymatic degradation by further modifying the GNPs using poly-ethylene glycol (PEG) coating which passivates the particle (Manson *et al.*, 2011). Once inside the cell, the thiol bond linking the sequences to the GNPs can be cleaved by the oxidative agent glutathione in the cell cytoplasm (Kumar, Meenan and Dixon, 2012). The above-mentioned points highlight the versatility of GNPs and we have taken this approach to deliver our sequences to the MSCs.

4.2 Methods and Materials:

4.2.1 Synthesis and functionalization of GNPs:

All GNP synthesis and characterization was carried out by our collaborators Professor Pedro Baptista and his team, based in Caparica, Portugal (Section 2.12). AntagomiRs of miR-205 and miR-145, along with mimics for miR-143 were purchased from Horizon Discovery Ltd.

4.2.2 Cell Culture:

All cells used in this section were hMSCs purchased from Promocell GmBH. They were cultured in basal DMEM and maintained at 37°C in 5% CO_2. At around 80% confluency the

cells were passaged, counted and 5,000 (for monolayer) or 200,000 (for micromass) cells were seeded on to 24-well plates for the experiments. All details of these processes can be found in section 2.1-2.2. Cells were cultured as monolayer for the osteogenesis and adipogenesis experiments and as micromasses for the chondrogenesis experiments.

4.2.3 Real Time qPCR Analysis:

Cells were cultured for 7, 14 and 28 days. At the end of the relevant time points for monolayers, the RNA was extracted using a Qiagen RNeasy kit. Micromass RNA was extracted using the PARIS kit. RNA concentration was measured using a UV spectrophotometer and reverse transcribed using a Quantitect reverse transcription kit. After obtaining the cDNA, the samples were plated onto 96-well qPCR plates and using a Quantitect SYBR Green PCR kit, the samples were prepared for qPCR. The plates were loaded onto the 7500 Sequence Detection System, which provided the Ct values. Using standard DDCt algorithm, the expression fold change of the samples was calculated. These protocols used can be found in section 2.3 to 2.7. Statistics was done using one-way ANOVA. The primers used are listed below. The primer sequences can be found in table 2.7.

Osteogenesis: Runx2, ALP, OCN
Adipogenesis: PPARγ, GLUT4, AdipoQ
Chondrogenesis: Sox9, ACAN, Col10
Endogenous control: GAPDH

4.2.4 In Cell Western Analysis:

Cells were plated onto 24-well plates as above, but the required time points, the cells were fixed with 4% Formaldehyde solution. Samples were permeabilized and incubated with primary antibodies relevant to the study.

Osteogenesis: Runx2, ALP, OCN
Adipogenesis: PPARγ, GLUT4, AdipoQ
Stemness: CD90

After incubation, the cells were washed and the secondary antibodies along with Cell tag was added and incubated again. Finally, the samples were washed again, dried and visualized

using the LICOR Odyssey Sa system. Relative expression of protein was calculated by obtaining the ratio of protein fluorescence to Cell tag fluorescence. Protocol can be found in section 2.9. Statistics was done using two-way ANOVA.

4.2.5 Histology and Immunofluorescence:

The cells were cultured as section 4.2.4 until the fixation stage. At this point, the cells were processed for histology and immunofluorescence as follows:

Osteogenesis: Von Kossa staining / Osteopontin immunofluorescence
Adipogenesis: Oil Red O staining / Fatty acid binding protein immunofluorescence
Chondrogenesis: Safranin O staining / Collagen II immunofluorescence

The protocols were followed as in section 2.10 and 2.11.

4.2.6 Western Blot

The detailed western blot protocol can be found in section 2.15. The primary antibodies used were GAPDH, Sox9, Aggrecan and Collagen X.

4.3 Results

4.3.1 Effect of GNPs functionalized with miR-205 antagomiRs

During osteogenesis, miR-205 has been reported to negatively target SATB2 and decrease Runx2 expression (Hu *et al.*, 2015). This leads to **inhibition of osteogenesis** and repression of differentiation. An antagomiR against miR-205 was therefore designed and conjugated onto GNPs with a view towards delivering to Promocell MSCs to reverse the inhibition of osteogenesis and encourage osteoblast formation. To achieve this, MSCs were cultured on 24-well plates, two media controls were used; (i) basal DMEM (control) and (ii) osteogenic media (positive osteogenesis control). After 24 hours culture the cells were then maintained in both media and challenged +/- antagomiR-205 (treatment) and a nonsense strand (negative control). The samples were then cultured for up to 28 days, during and up to which point they were assessed for osteogenic differentiation both at the gene and protein level.

4.3.1.1 Real time qPCR of MSCs treated with miR-205 antagomiRs

To assess the impact of the antagomiR-205 at the RNA level, MSCs were cultured for 7, 14 and 28 days and RT-qPCR was carried out (as section 2.8). Briefly, at each time point the cells were lysed and the RNA was extracted. After the RNA concentration was identified, they were reverse-transcribed and the samples were plated for qPCR. Three markers were assessed; Runx2 (an early osteogenic marker), alkaline phosphatase (ALP, a general osteogenic marker) and osteocalcin (OCN, a later osteogenic marker).

The MSCs cultured in osteogenic media demonstrated clear increases in all osteogenic markers across all three time points, with no difference depending on whether GNPs were present or not (orange bars in fig. 4.1). However, at all three time points the antagomiR-205 did not indicate any difference when compared to control MSCs (no NPs) or nonsense strand GNPs (NS) (blue bars in fig. 4.1). In summary, there was no evidence at the gene level to suggest that challenging MSCs with antagomiR-205 promoted osteogenesis.

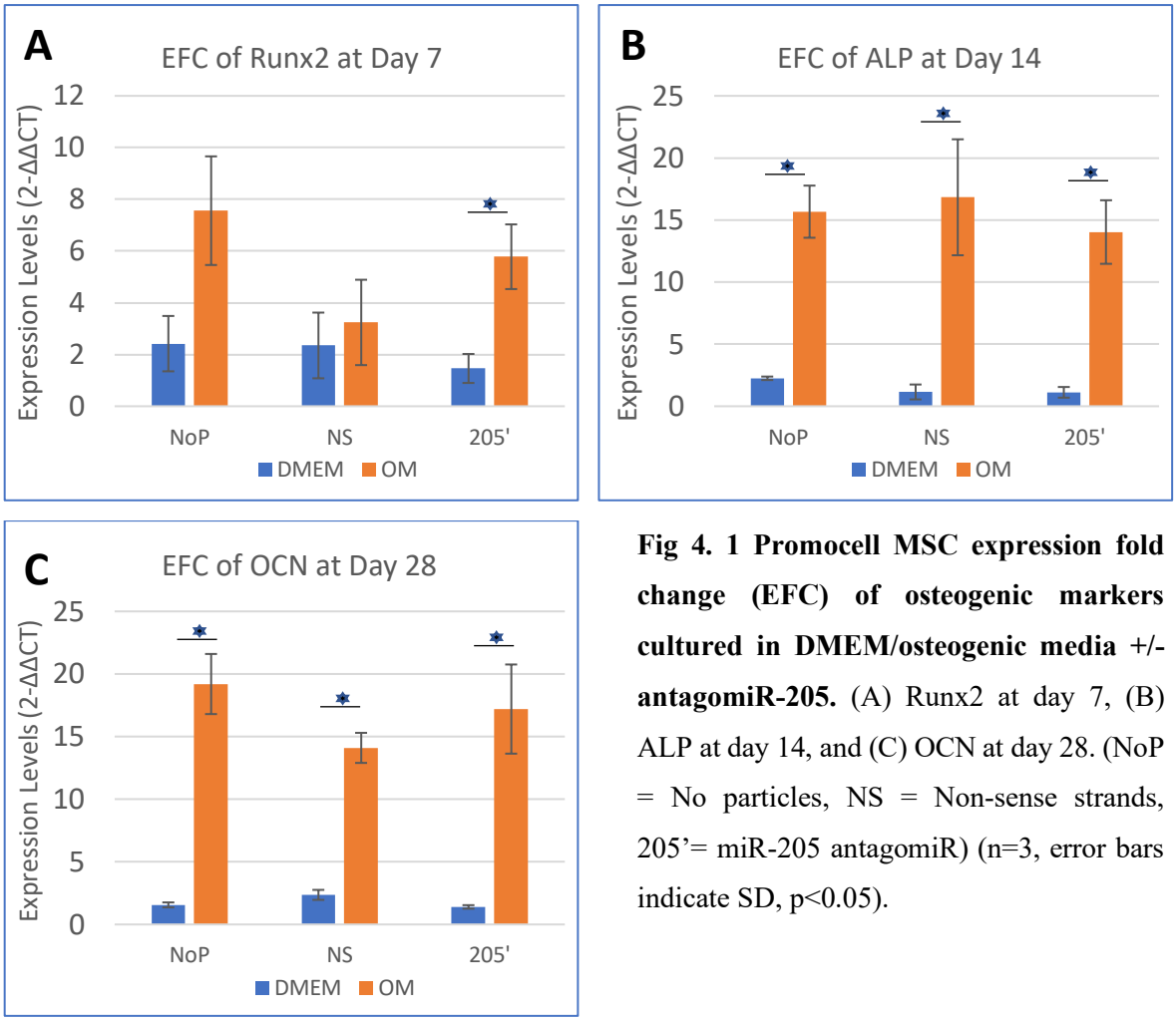

Fig 4. 1 Promocell MSC expression fold change (EFC) of osteogenic markers cultured in DMEM/osteogenic media +/- antagomiR-205. (A) Runx2 at day 7, (B) ALP at day 14, and (C) OCN at day 28. (NoP = No particles, NS = Non-sense strands, 205'= miR-205 antagomiR) (n=3, error bars indicate SD, $p<0.05$).

4.3.1.2 In-cell western of MSCs treated with miR-205 antagomiRs

To assess osteogenesis at the protein level, in-cell western was carried out on MSCs cultured for 7, 14 and 28 days (section 2.9). Briefly, cells were seeded in 24 well plates and cultured as for the previous PCR study (in DMEM, osteogenic media and +/- antagomiR-205 and nonsense strand). At the relevant time points, the samples were fixed with 4% formaldehyde solution and stained for the same three osteogenic markers, Runx2, ALP and OCN. In addition MSCs were also stained at all time points for the stemness marker CD90. The samples were then analysed to produce plots of relative marker fluorescence.

Fig. 4.2 indicates the osteogenic marker fluorescence in DMEM on the left panel and osteogenic media on the right panel. There are several key points from these graphs:

- In the case of Runx2, MSCs cultured without GNPs (no NPs) in osteogenic media have significantly higher levels than those cultured in DMEM, however later markers of ALP and OCN are similar.
- Under DMEM conditions (left panel), the addition of antagomiR-205 did not indicate any increase in osteogenic markers when compared to no particle control or nonsense negative control.
- Under osteogenic media conditions (right hand panel), the addition of antagomiR-205 showed a decrease in osteogenic markers when compared to no particle control. The nonsense negative control also showed a decrease compared to no particle control.
- Both Runx2 and OCN appear enhanced in MSCs when treated with antagomiR-205 in osteogenic media compared to DMEM media (i.e. comparing the 205 data in each panel). This may suggest a synergistic effect on osteogenesis.

A

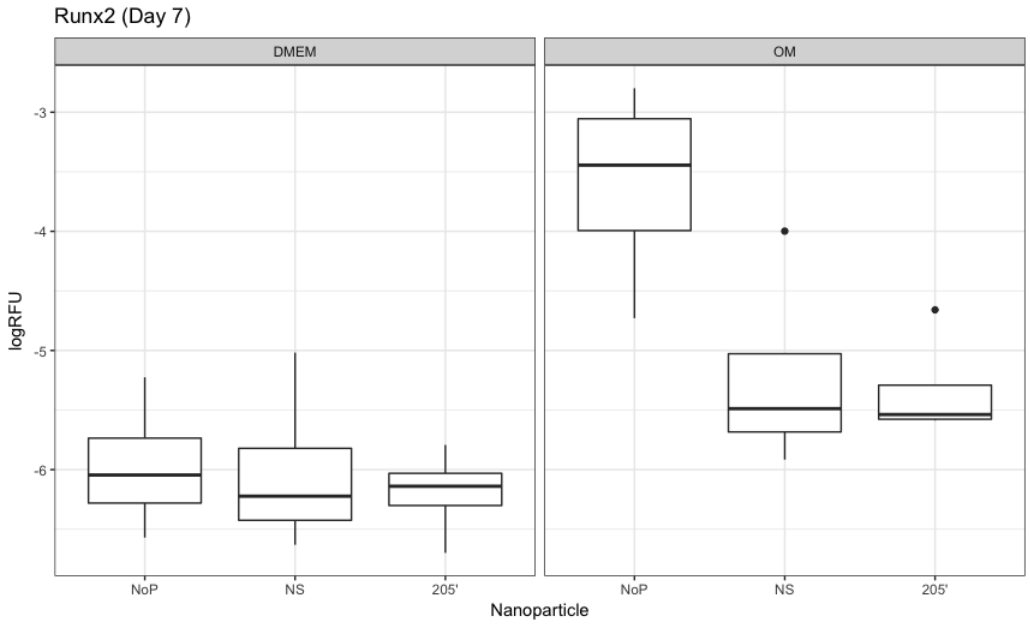

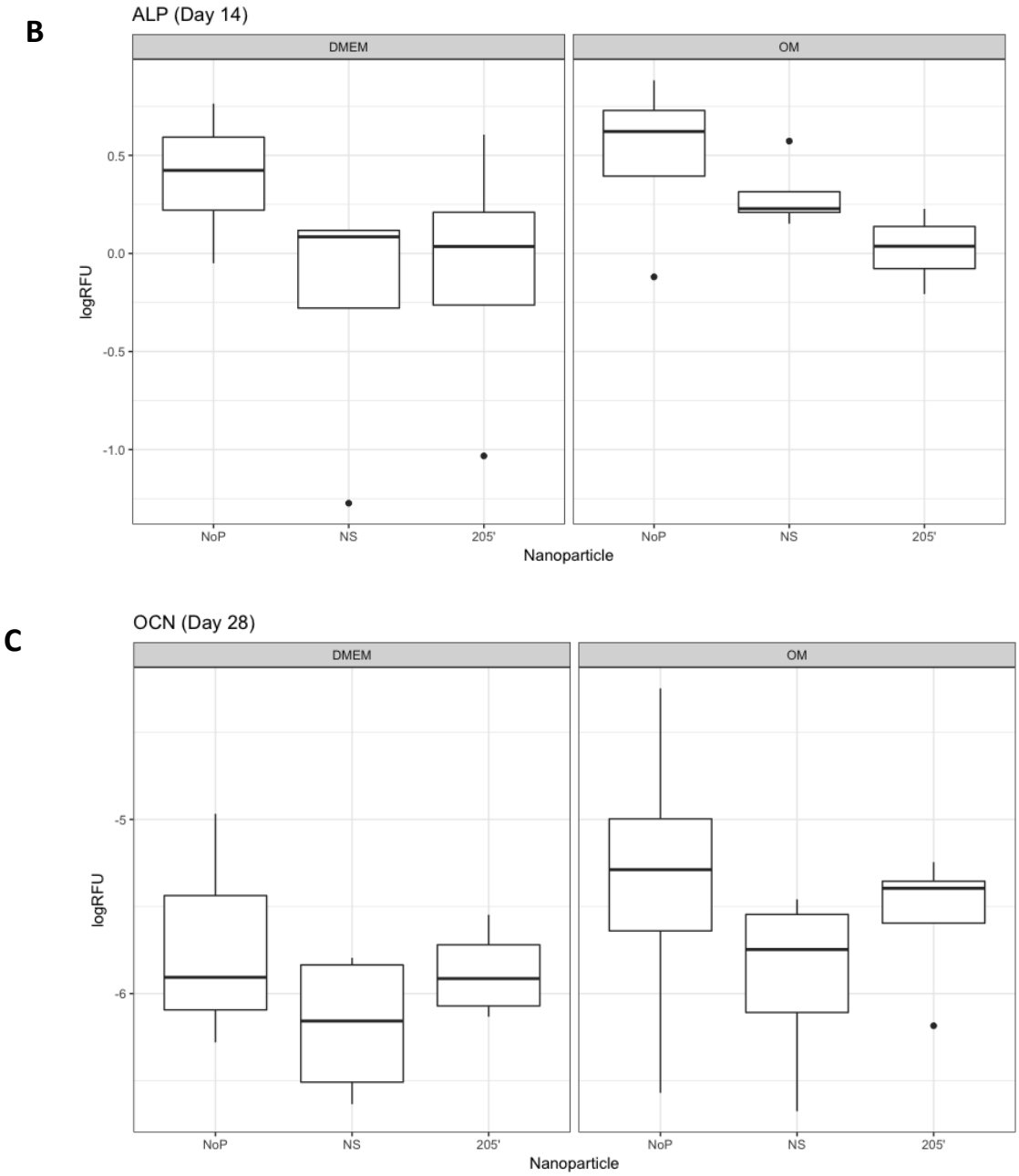

Fig. 4. 2 Logged relative fluorescence (RFU) values of osteogenic markers stained in Promocell MSCs after treatment with antagomiR-205. Each graph indicates a comparison of an osteogenic marker in both basal DMEM and osteogenic media; (A) Runx2 at day 7 day; (B) ALP at day 14; (C) OCN at day 28. NP indicates no particles, NS represents the non-sense strand (negative control) and 205' represents the miR-205 antagomiR. (n=4, dots indicate outliers, statistics done through two way ANOVA)

In addition to assessing osteogenic markers, CD90 was also verified as a measure of stemness (fig. 4.3). Stemness was clearly maintained to a greater extent at days 14 and 21 and in MSCs cultured in DMEM compared to those cultured in osteogenic media, as shown in fig. 4.3 B and C. No difference in stemness was noted when MSCs were challenged with

GNPs at any time point in DMEM media (left hand image). However, there was a data trend to suggest that addition of GNPs, in particular the antagomiR-205 GNPs, encouraged maintenance of stemness when MSCs were cultured in osteogenic media (right hand panel).

A

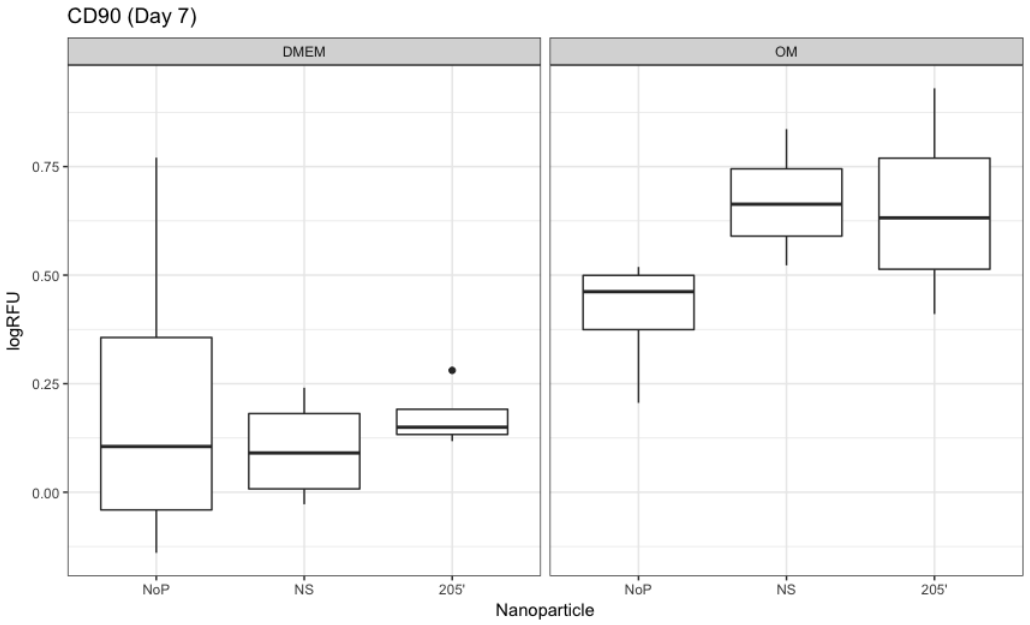

B

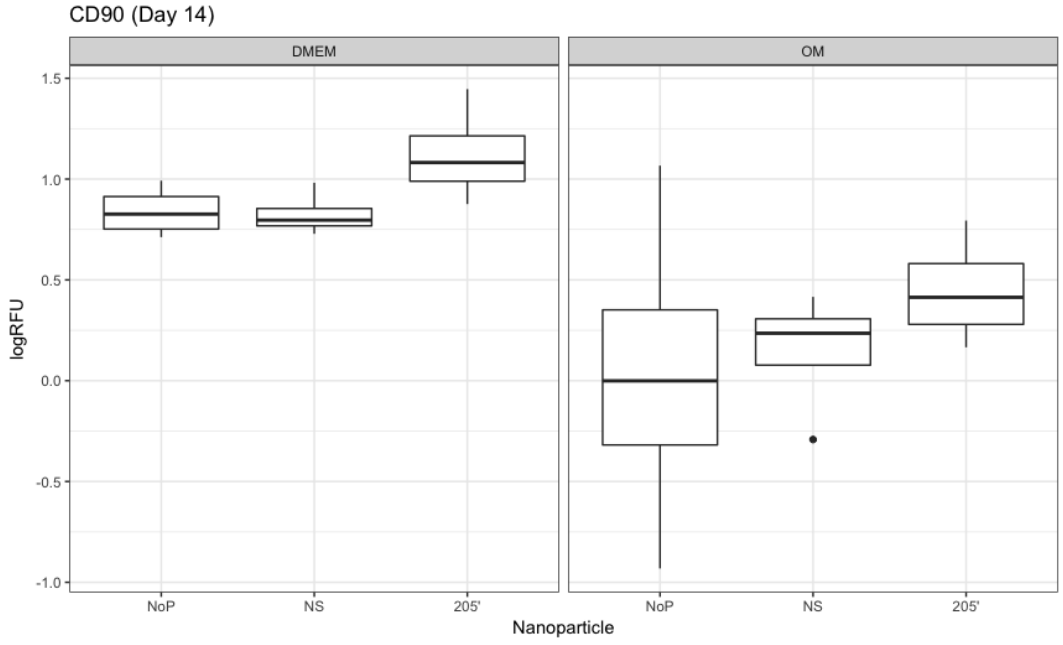

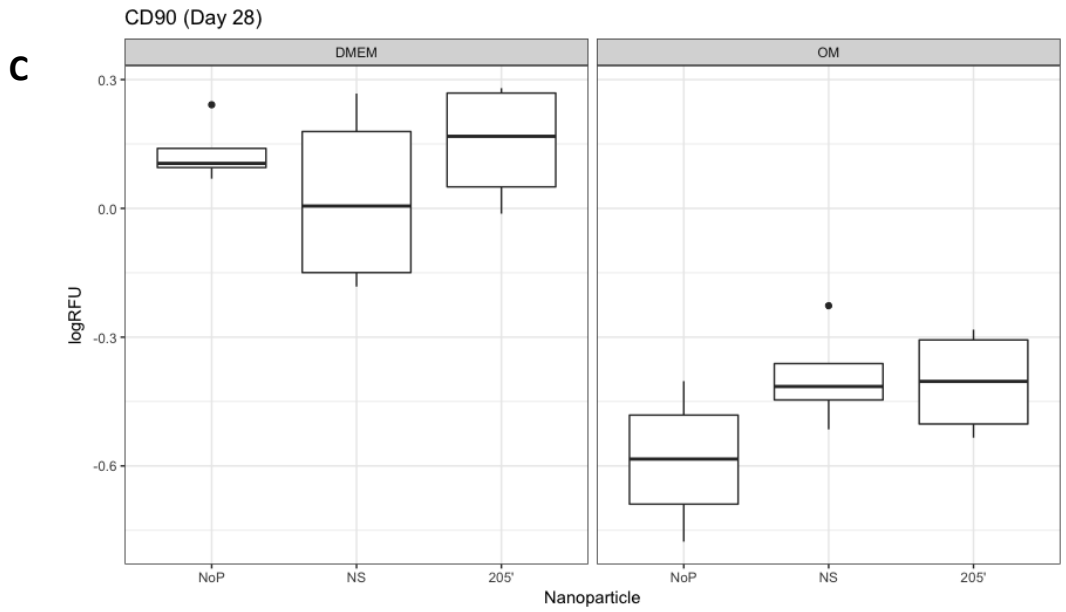

Fig. 4. 3: Logged relative fluorescence (RFU) values of the stemness marker CD90 stained in Promocell MSCs after treatment with antagomiR-205. Each graph indicates a comparison in both basal DMEM and osteogenic media; (A) at day 7; (B) at day 14; (C) at day 28. NP indicates no particles, NS represents the non-sense strand (negative control) and 205' represents the miR-205 antagomiR. (n=4, dots indicate outliers, statistics done through two way ANOVA)

4.3.1.3 Immunofluorescence and Von Kossa staining of MSCs treated with miR-205 antagomiRs

To further complement the qPCR and in cell western data, immunofluorescence and histology staining was carried out on MSCs cultured for 28 days. The MSCs were cultured as for the previous PCR and in cell western studies up to 28 days. At this point the samples were fixed with 4% formaldehyde and either underwent Von Kossa staining or standard immunofluorescence protocols.

The black stain in the Von Kossa images indicate silver phosphate that replaced the calcium phosphate present within the cells, reflecting a positive stain for osteoblast formation (fig. 4.4). MSCs cultured in DMEM media samples did not show any deposits of silver phosphate (fig. 4.4 A, C). However, MSCs cultures in osteogenic media clearly indicate positive staining (fig. 4.4 B, D). The presence of the antagomiR-205 did not appear to increase staining when compared to controls with no GNPs (fig. 4.4 C, D). The change in colour for fig. 4.4 D is due to the image being taken at a later date compared to the others.

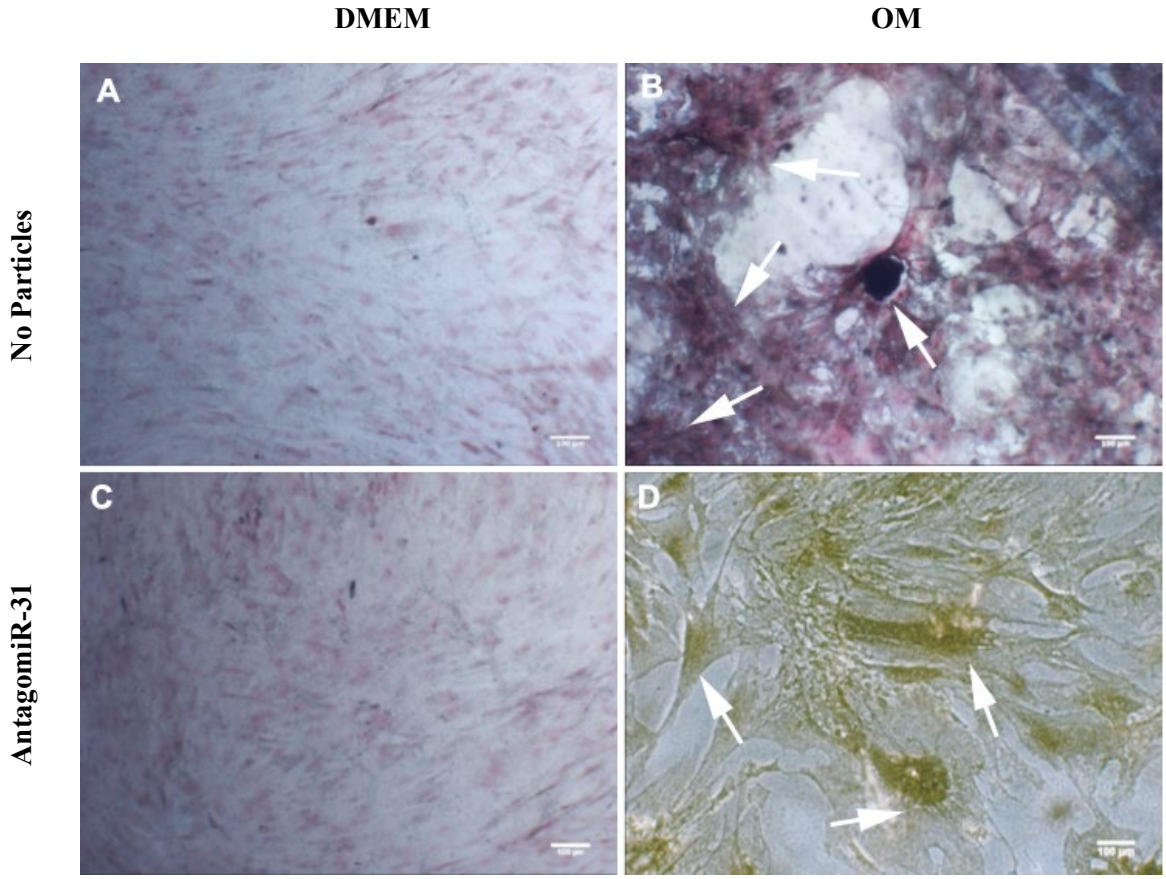

Fig. 4. 4: **Von Kossa staining of MSCs after 28 days of culture**. MSCS were (A) cultured in DMEM media, (B) cultured in osteogenic media, (C) cultured in basal media supplemented with miR-antagomiR-205 and (D) cultured in osteogenic media supplemented with antagomiR-205. Arrowheads indicate positive staining. Scale bar – 100 µm

There was no osteopontin (OPN, late stage marker) staining in MSCs cultured in DMEM alone (fig. 4.5 A), whilst MSCs cultured in osteogenic media showed strong OPN staining (fig. 4.5 B). Interestingly, OPN staining was visible for MSCs cultured with the antagomiR-205 in DMEM and in osteogenic media (fig. 4.5 C, D). This suggest that antgomiR-205 may have some osteogenic effect at the protein level. Fig. 4.6 corroborates this by measuring the fluorescence intensities of the images.

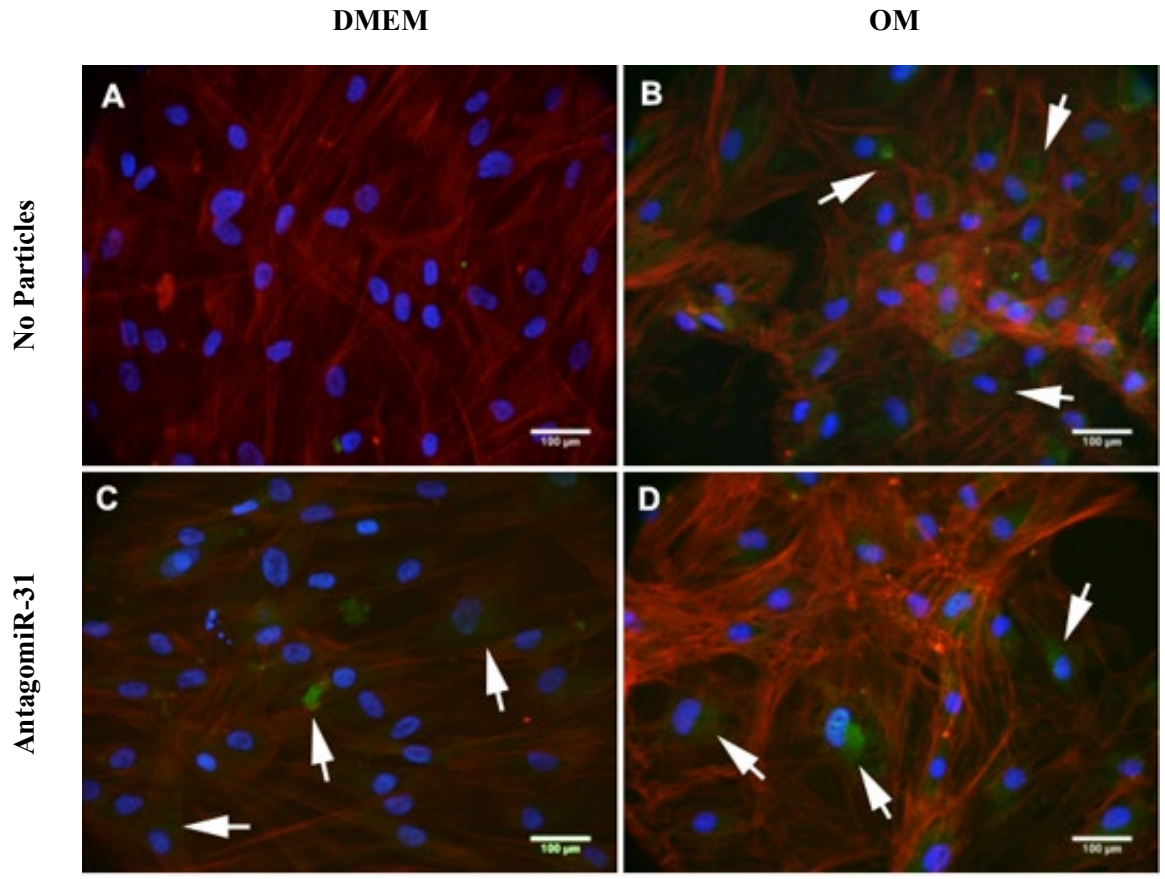

Fig. 4. 5: Immunofluorescence staining of osteopontin in MSCs after 28 days of culture. MSCs were (A) cultured in DMEM media, (B) cultured in osteogenic media, (C) cultured in DMEM media with antagomiR-205 and (D) cultured in osteogenic media with antagomiR-205. (Green = osteopontin (OPN), Blue = DAPI (nuclei), Red = actin staining). Arrowheads indicate positive staining.

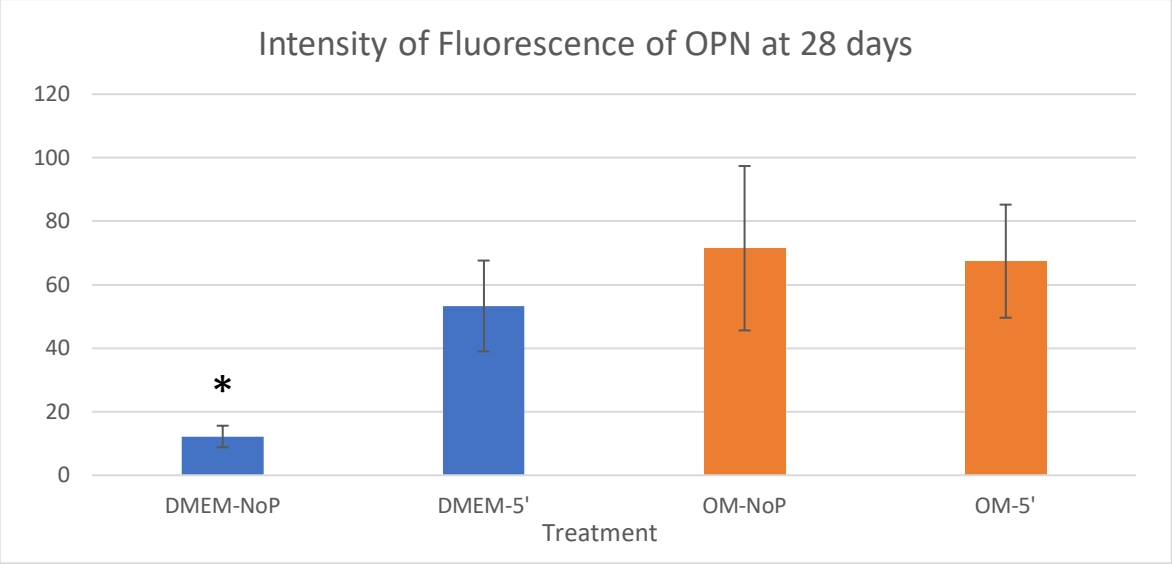

Fig. 4. 6: Semi-quantification of osteopontin staining in MSCs after 28 days of culture. Values were calculated using threshold analysis of the FITC channel. (n=3, error bars indicate SD, $p<0.05$)

4.3.2 Effect of GNPs functionalized with miR-143 mimics

By targeting the ERK pathway, miR-143 has shown to **positively regulate adipogenesis**. By increasing the levels of miR-143 in the cells, it is therefore hypothesised that this will lead to an increase in adipogenesis. MiRNA mimics provide the same functionality as its original miRNA and so to achieve this, miR-143 mimics were designed and conjugated onto GNPs. MSCs were cultured on 24-well plates, two media controls were used; (i) basal DMEM (control) and (ii) adipogenic media (positive adipogenic control). After 24 hours culture the cells were then maintained in both media, and challenged +/- miR-143 (treatment) and a nonsense strand (scrambled original sequence, negative control). The samples were then cultured for up to 28 days, during and up to which point they were assessed for adipogenic differentiation both at the gene and protein level.

4.3.2.1 Real time qPCR of MSCs treated with miR-143 mimics

To assess the impact of the miR-143 mimics at the RNA level, MSCs were cultured in both basal DMEM and adipogenic media (AM) for 7, 14 and 28 days. 24 hours after plating, GNPs for the non-sense strands (NS) and miR-143 mimics (143') were added. After the RNA concentration was identified, they were reverse transcribed, and the samples were plated for qPCR. Three markers were assessed; PPARγ (an early adipogenic marker), GLUT4 (a general adipogenic marker) and AdipoQ (a later adipogenic marker). GAPDH was used as the endogenous control.

MSCs cultured in adipogenic media clearly show increased levels of all adipogenic markers, with no difference on addition of the GNPs (orange bars in fig. 4.7). No differences were noted for MSCs incubated with the miR-143 mimics at any time point when compared to control (no GNPs) or the nonsense strand (negative control).

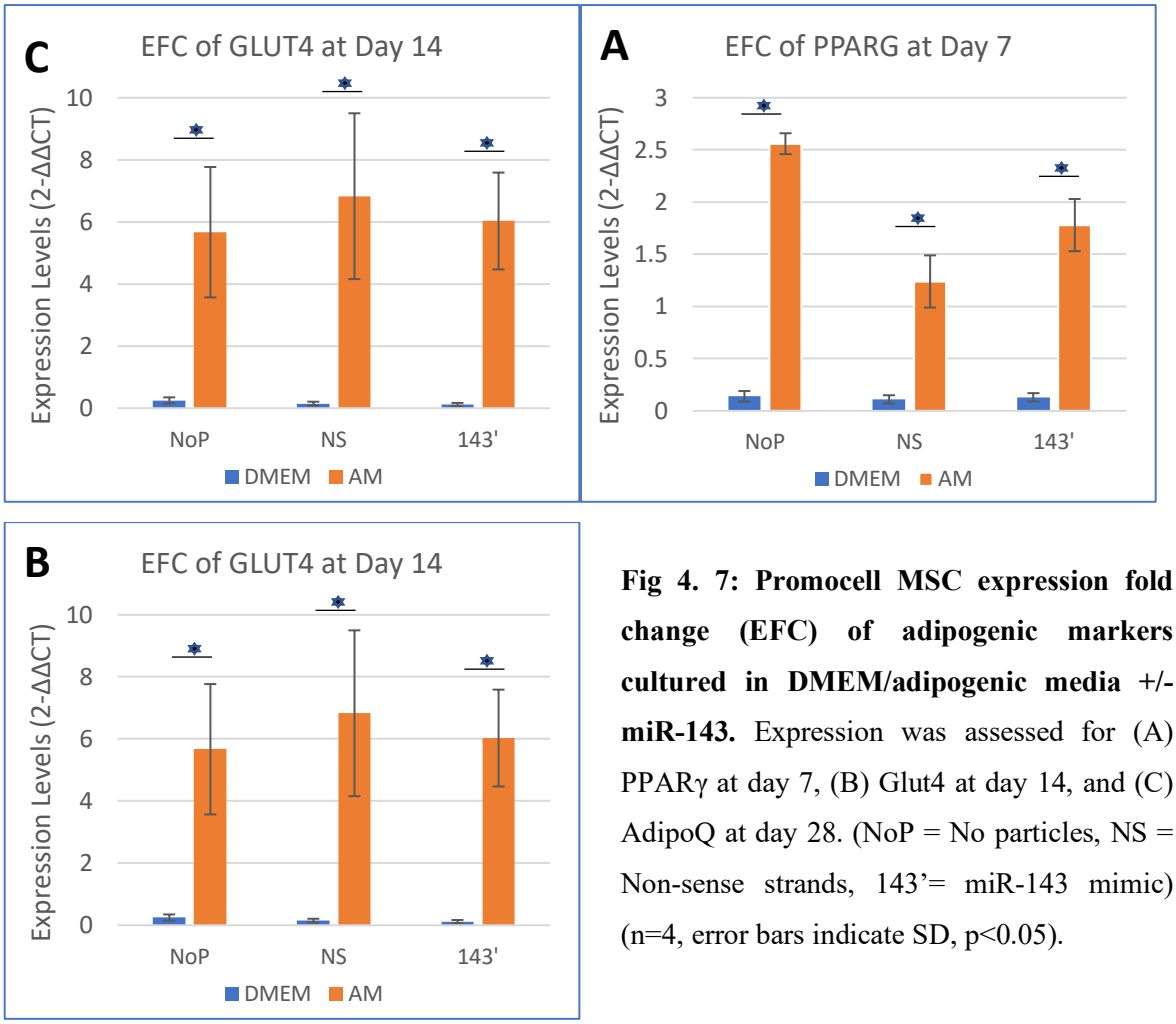

Fig 4. 7: Promocell MSC expression fold change (EFC) of adipogenic markers cultured in DMEM/adipogenic media +/- miR-143. Expression was assessed for (A) PPARγ at day 7, (B) Glut4 at day 14, and (C) AdipoQ at day 28. (NoP = No particles, NS = Non-sense strands, 143'= miR-143 mimic) (n=4, error bars indicate SD, $p<0.05$).

4.3.2.2 In-cell western of MSCs treated with miR-143 mimics

In cell western was conducted to determine whether any changes in adipogenic marker protein expression following treatment with miR-143. As for PCR, the cells were plated for 7, 14 and 28 days. The GNPs were added, and the cells were fixed at the required time points. Protein expression of PPARγ, GLUT4 and AdipoQ was assessed at their respective time points. The expression of CD90 (stemness marker) was also assessed at all time points.

Fig. 4.8 indicates the adipogenic marker fluorescence in DMEM on the left panel and adipogenic media (AM) on the right panel. There are several key points from these graphs:

- At all time points, the expression of adipogenic markers was higher in MSCs cultured in AM conditions compared to those of samples cultured in basal DMEM, indicating that the MSCS are differentiating appropriately.

- Under DMEM conditions (left panel), the addition of mimics appeared to increase PPARG expression at day 7 compared to no particles (control), with no further changes in expression at the later time points.
- Under osteogenic media conditions (right hand panel), no differences in marker expression were noted at any time point following the addition of miR-143 mimics.

A

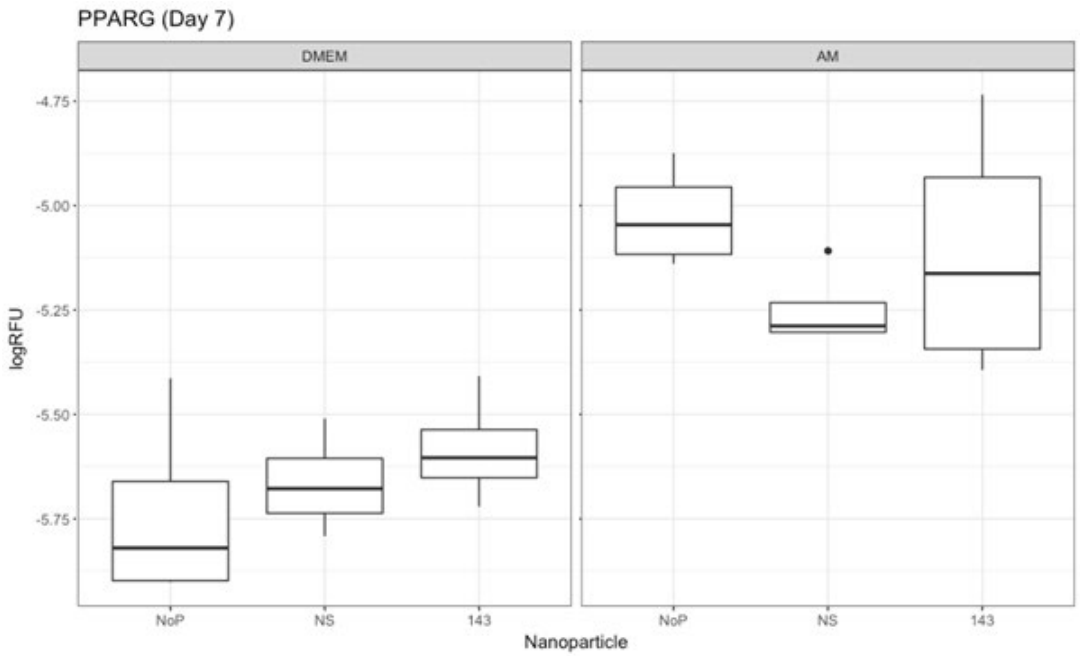

B

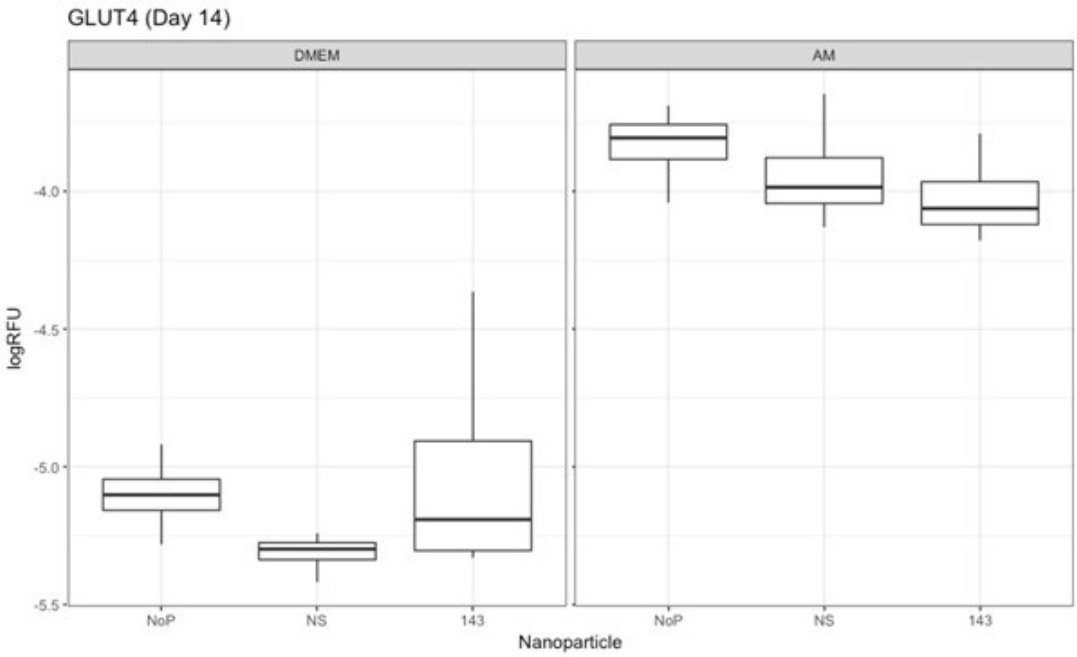

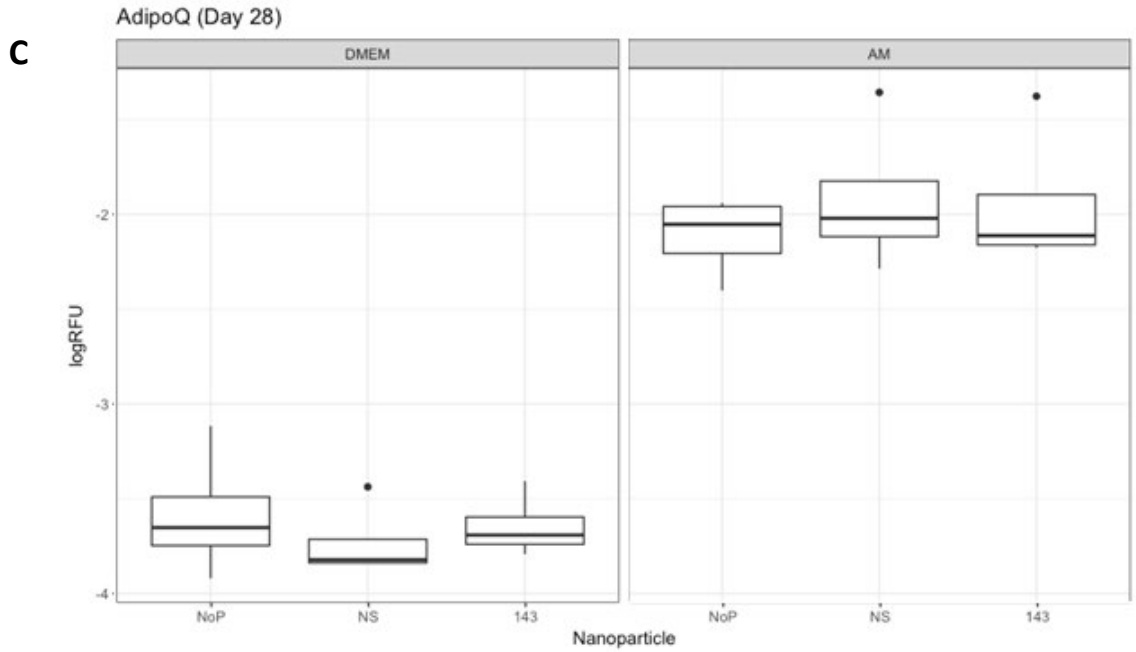

Fig. 4. 8: Logged relative fluorescence (RFU) values of adipogenic markers stained in Promocell MSCs after treatment with miR-143. Each graph indicates a comparison of an adipogenic marker in both basal DMEM and adipogenic media; (A) PPARG at day 7 day; (B) GLUT4 at day 14; (C) AdipoQ at day 28. NP indicates no particles, NS represents the non-sense strand (negative control) and 205' represents the miR-143 mimic. (n=4, dots indicate outliers, statistics done through two-way ANOVA)

In addition to assessing adipogenic markers, CD90 was also verified as a measure of stemness (fig. 4.9). Surprisingly, there was very little difference in stemness between MSCs cultured in DMEM compared to those cultured in adipogenic media (all time points). There was a data trend to suggest that incubation with the GNPs, in particular the miR-143 GNPs, encouraged maintenance of stemness when MSCs were cultured in AM compared to DMEM (right hand panel compared to left hand panel).

A

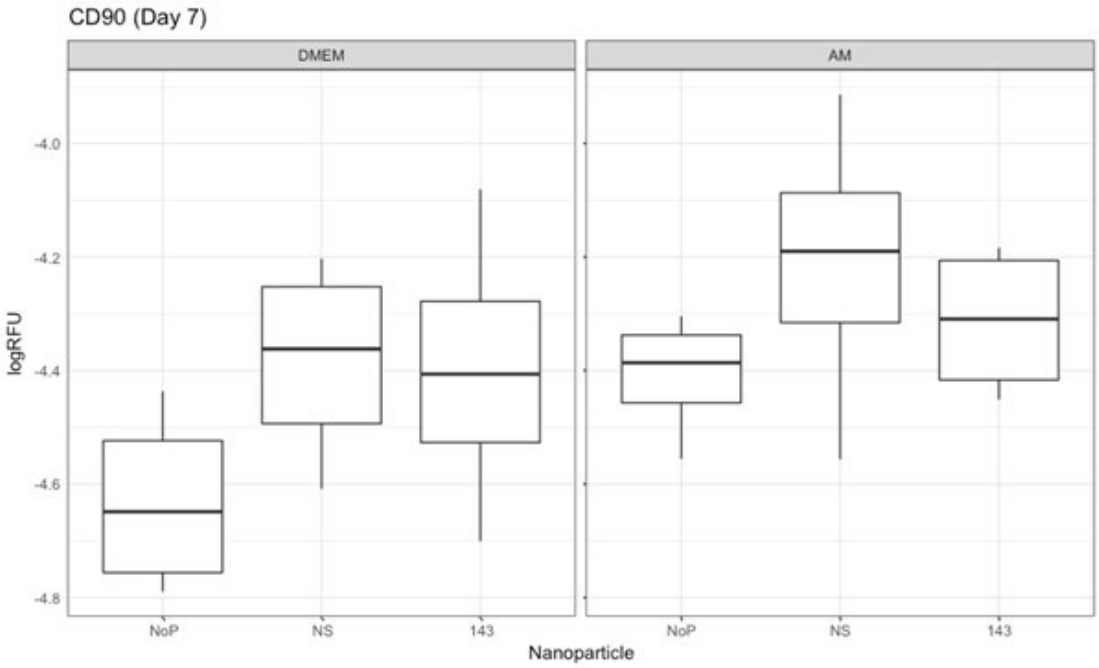
CD90 (Day 7)
DMEM
AM
logRFU
-4.0
-4.2
-4.4
-4.6
-4.8
NoP
NS
143
Nanoparticle

B

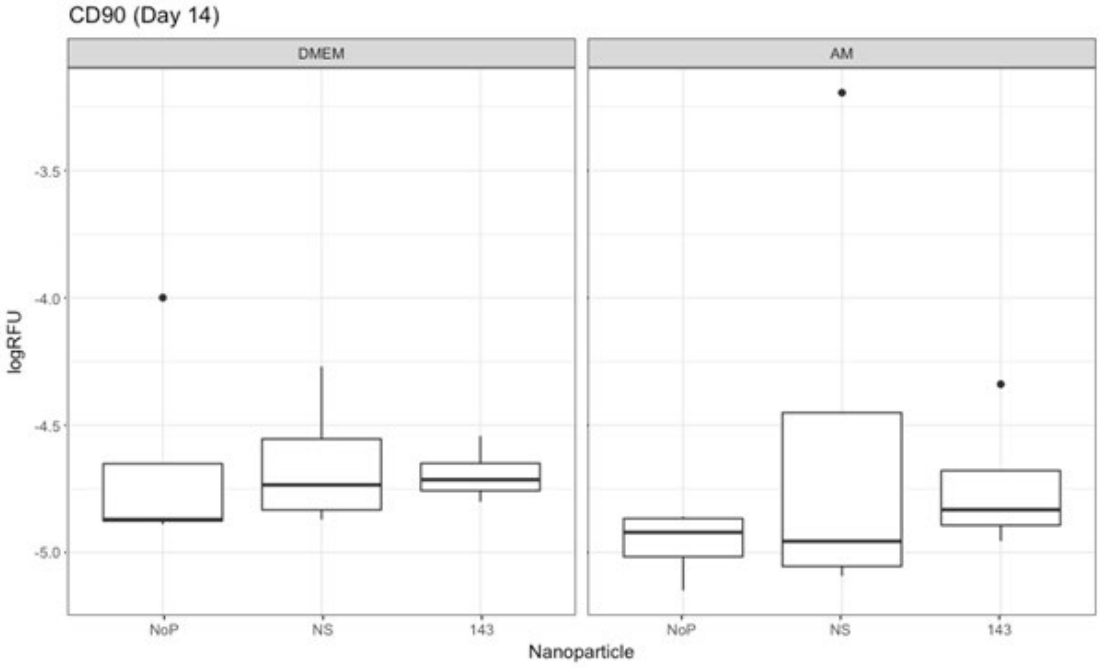
CD90 (Day 14)
DMEM
AM
logRFU
-3.5
-4.0
-4.5
-5.0
NoP
NS
143
Nanoparticle

C

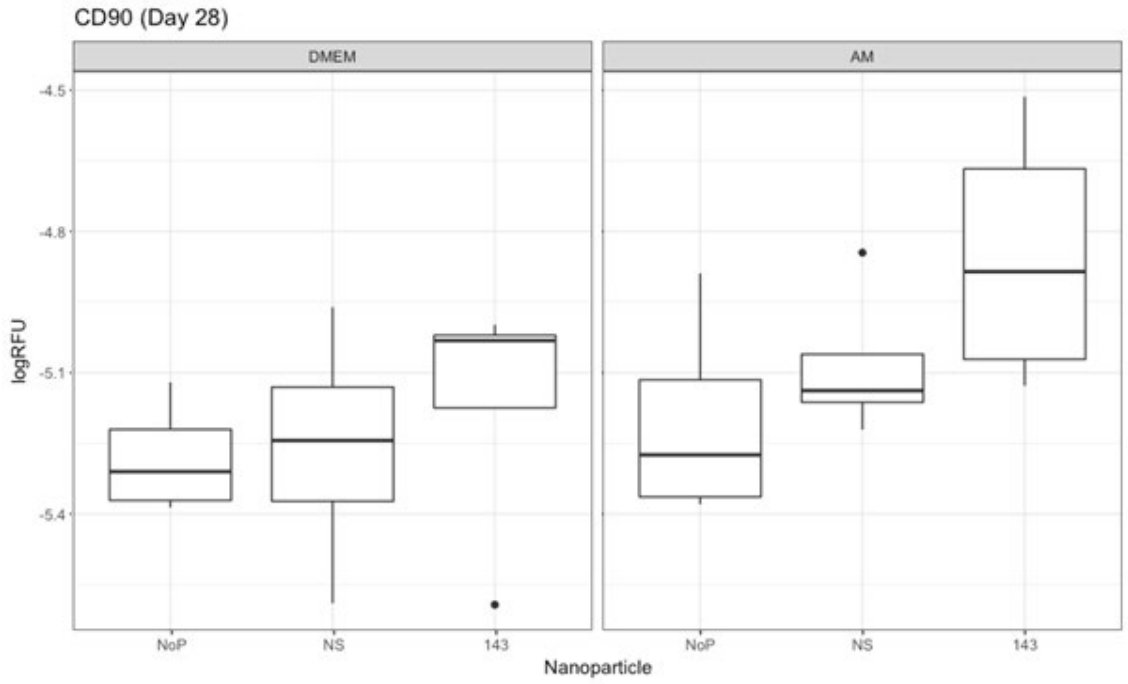

Fig. 4. 9: Logged relative fluorescence (RFU) values of the stemness marker CD90 stained in Promocell MSCs after treatment with miR-143. Each graph indicates a comparison in both basal DMEM and adipogenic media; (A) at day 7; (B) at day 14; (C) at day 28. NP indicates no particles, NS represents the non-sense strand (negative control) and 143' represents the miR-143 mimics. (n=4, dots indicate outliers, statistics done through two-way ANOVA)

3.2.3 Oil Red O staining and Immunofluorescence of MSCs treated with miR-143

To further complement the qPCR and in cell western data, immunofluorescence and histology staining was carried out on MSCs cultured for 28 days. The MSCs were cultured as for the previous PCR and in cell western studies up to 28 days. At this point the samples were fixed with 4% formaldehyde and either underwent Oil Red O staining or standard immunofluorescence protocols for adipogenic markers.

Oil Red O staining highlights the fat deposits present in adipocytes, staining them red, providing a great visual indicator of the presence of fatty acids (fig. 4.10). MSCs cultured in DMEM alone did not show any fatty acid deposits (fig. 4.10 A). Meanwhile, MSCs cultured in adipogenic media clearly indicate positive staining (fig. 10 B, D). MSCs challenged with miR-143 in DMEM indicated several fatty acid deposits in cells, suggesting that some cells on starting to differentiate (fig. 4.10 C).

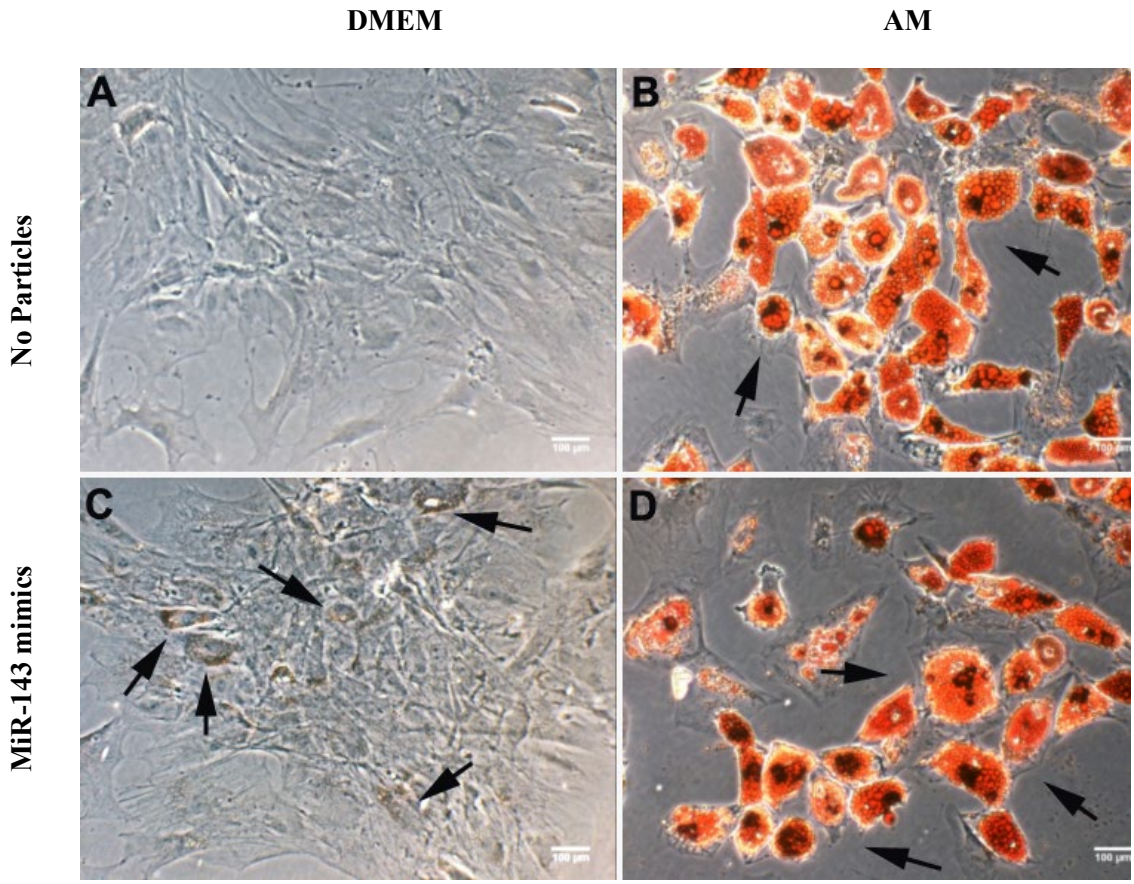

Fig. 4. 10: **Oil Red O staining of MSCs after 28 days of culture**. MSCs were (A) cultured in basal media, (B) cultured in adipogenic media, (C) cultured in basal media with miR-143 mimics and (D) cultured in adipogenic media with antagomiRs. Arrowheads indicate positive staining.

With regard to the immunofluorescence staining, there was no positive fatty acid binding protein (FABP) staining in MSCs cultured in DMEM alone (fig. 4.11 A), whilst MSCs cultured in adipogenic media showed strong FABP staining, with a clear change in cell morphology (fig. 4.11 B, D). The sample cultured in DMEM and treated with antagomiR-145 did not show any signs of FABP, suggesting that its effect was not strong enough to elicit a change. This is corroborated by the fluorescence intensities of the previous figs (fig. 4.12).

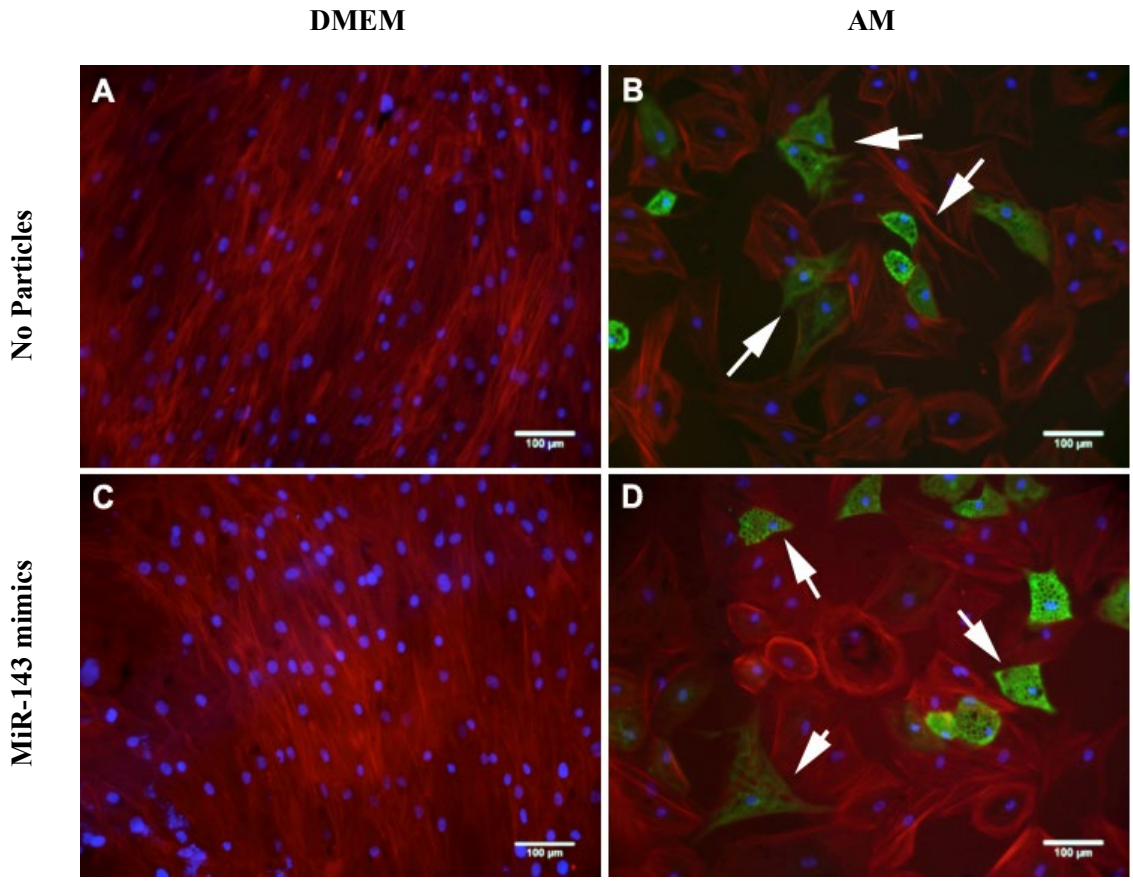

Fig. 4. 11: **Immunofluorescence staining for fatty acid binding protein in MSCs after 28 days of culture.** MSCs were (A) cultured in DMEM media, (B) cultured in adipogenic media, (C) cultured in DMEM media with miR-143 and (D) cultured in adipogenic media with miR-143. (Green = fatty acid binding protein (FABP), Blue = DAPI (nuclei), Red = actin staining). Arrowheads indicate positive staining.

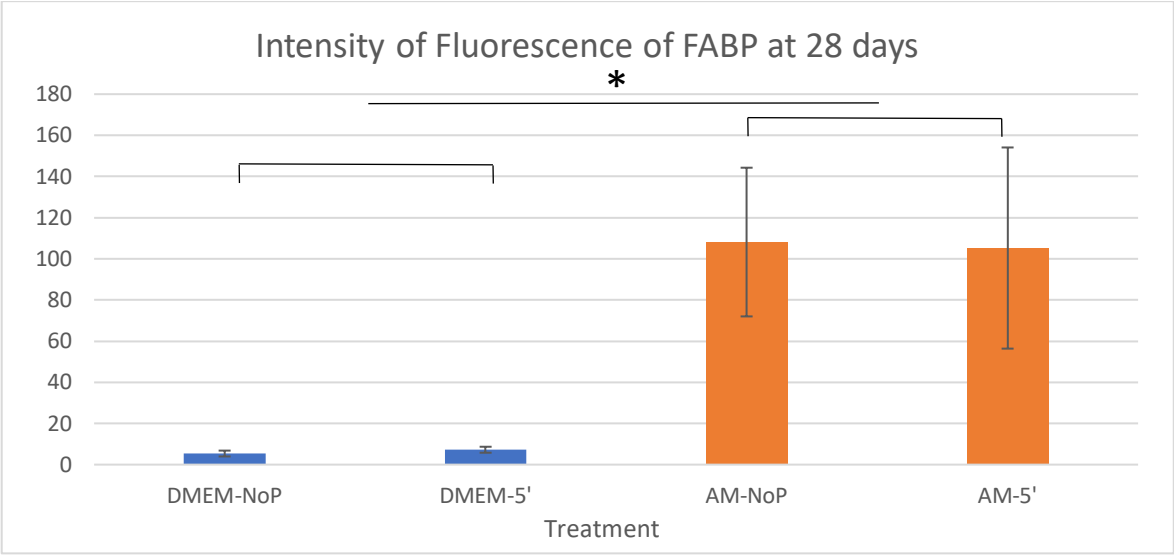

Fig. 4. 12: Semi-quantification of FABP staining in MSCs after 28 days of culture. Values were calculated using threshold analysis of the FITC channel. (n=3, error bars indicate SD, $p<0.05$)

4.3.3 Effect of GNPs functionalized with miR-145 antagomiRs

In MSCs, miR-145 targets Sox9 to **inhibit chondrogenesis**. By providing antagomiRs against miR-145 to MSCs, it is hypothesised that chondrogenesis can be enhanced. To achieve this, the MSCs were seeded as micromass cultures (as section 2.3). The high concentration of cell-to-cell contact and adhesion promote MSC differentiation towards chondrocytes.

4.3.3.1 qPCR of MSCs treated with miR-145 antagomiRs

To assess the chondrogenic marker gene expression, the cells were cultured as micromass cultures for 7, 14 and 28 days and evaluated for early, mid and late stage chondrogenic markers. 24 hours after plating, GNPs for the non-sense strands (NS) and antagomiR-145 (145') were added. After the RNA concentration was identified, they were reverse transcribed and the samples were plated for qPCR. Three markers were assessed; Sox9 (an early chondrogenic marker), aggrecan (ACAN, a general chondrogenic marker) and collagen 10 (Col10, late marker).

MSCs cultured in chondrogenic media show a trend towards increased levels of chondrogenesis, in particular at the later time point of day 28, with a variation observed at the early time of day 7 on addition of the antagomiR-145 GNPs (orange bars in fig. 4.13). When cultured in DMEM media, at both later time points (days 14 & 28) the addition of antagomiR-145 showed a trend for increased expression of chondrogenic markers (blue bars in fig. 4.13).

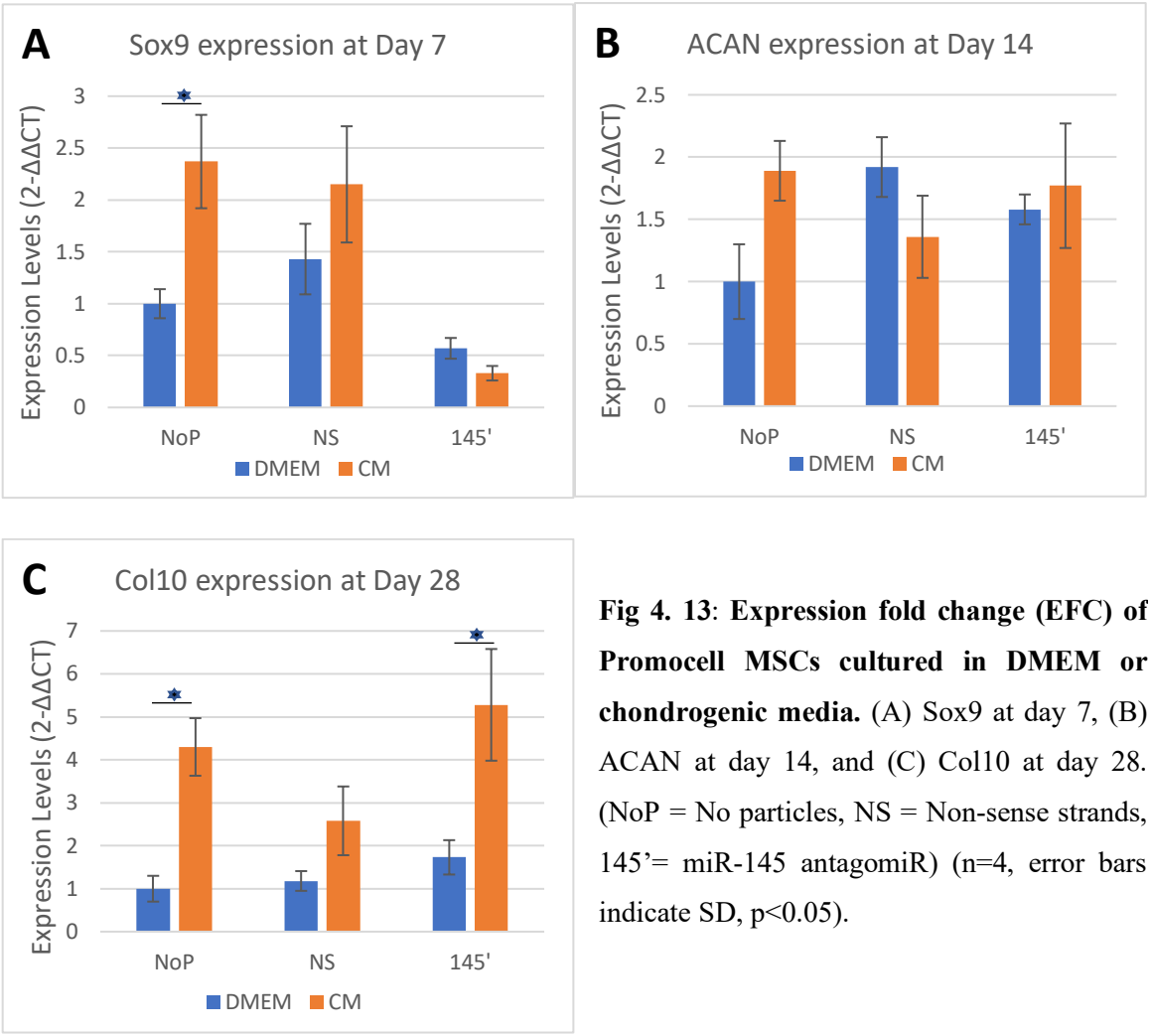

Fig 4. 13: Expression fold change (EFC) of Promocell MSCs cultured in DMEM or chondrogenic media. (A) Sox9 at day 7, (B) ACAN at day 14, and (C) Col10 at day 28. (NoP = No particles, NS = Non-sense strands, 145'= miR-145 antagomiR) (n=4, error bars indicate SD, $p<0.05$).

4.3.3.2 Western Blot of MSCs treated with miR-145 antagomiRs

To see whether the gene level changes matches the protein expression, a western blot was conducted. Due to the difficult nature of extracting proteins from the micromasses, a very low yield of proteins was obtained. Due to this we were not able to properly conduct the western blot and as such, were not able to complete our protein study.

4.3.3.3 Safranin O staining and Immunofluorescence of MSCs treated with miR-145 antagomiRs

To visualize the impact of miR-145 antagomiRs, Safranin O staining and immunofluorescence was conducted. Safranin O stains the proteoglycans and collagen II present in cells a deep red colour. Although all cells contain certain amounts of these proteins, the intensity of the colour is used as an indicator of chondrogenesis. All images

appeared to show positive staining (fig. 4.14), with the CM and miR-145 treated samples giving the strongest staining (fig. 4.14 D)

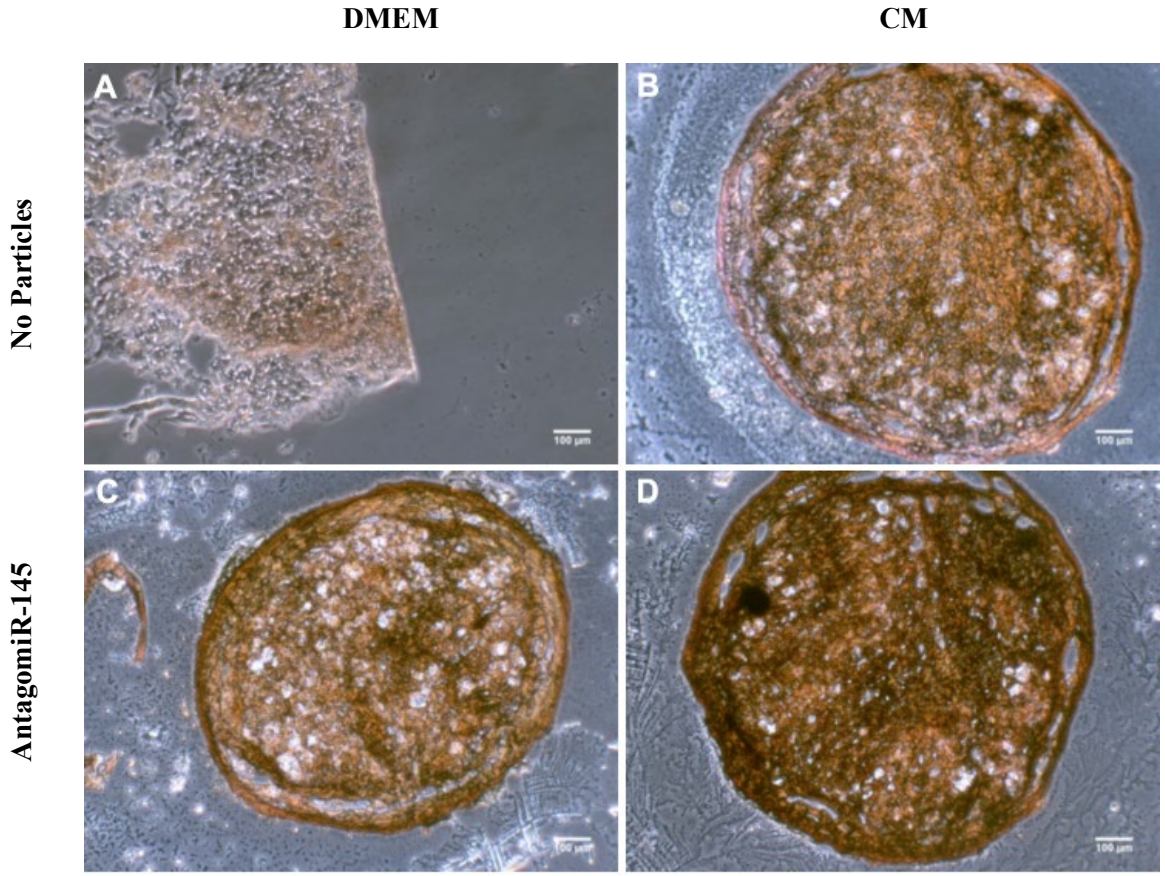

Fig. 4. 14: Safranin O staining of MSCs after 28 days of culture. MSCs were (A) cultured in basal media, (B) cultured in chondrogenic media, (C) cultured in basal media with miR-145 antagomiRs and (D) cultured in chondrogenic media with miR-145 antagomiRs.

The Safranin O stains the proteoglycans within the micromass sections red. The clear/grey colouring is that of the cytoplasm. The sample cultured only in DMEM shows light red colouring with most of the sample being clear, indicating a minimal or no chondrogenesis. In contrast, fig. 4.14 (C) shows a higher intensity of red with few clear spots. This shows the influence of the antagomiRs on samples cultured in basal media. The samples cultured in CM also showed a deep red colour with few clear spots indicating a shift towards chondrogenesis, as expected.

The immunofluorescence staining allowed us to visualize the presence of collagen II within the cells; here, the staining is viewed as green, or yellow due to red/green overlay. Positive staining was observed in samples cultured in CM (fig. 4.15 B, D). Positive staining was also

observed in MSCs treated with antagomiR-145 and cultured in DMEM, suggesting enhanced chondrogenesis (fig. 4.15 C)

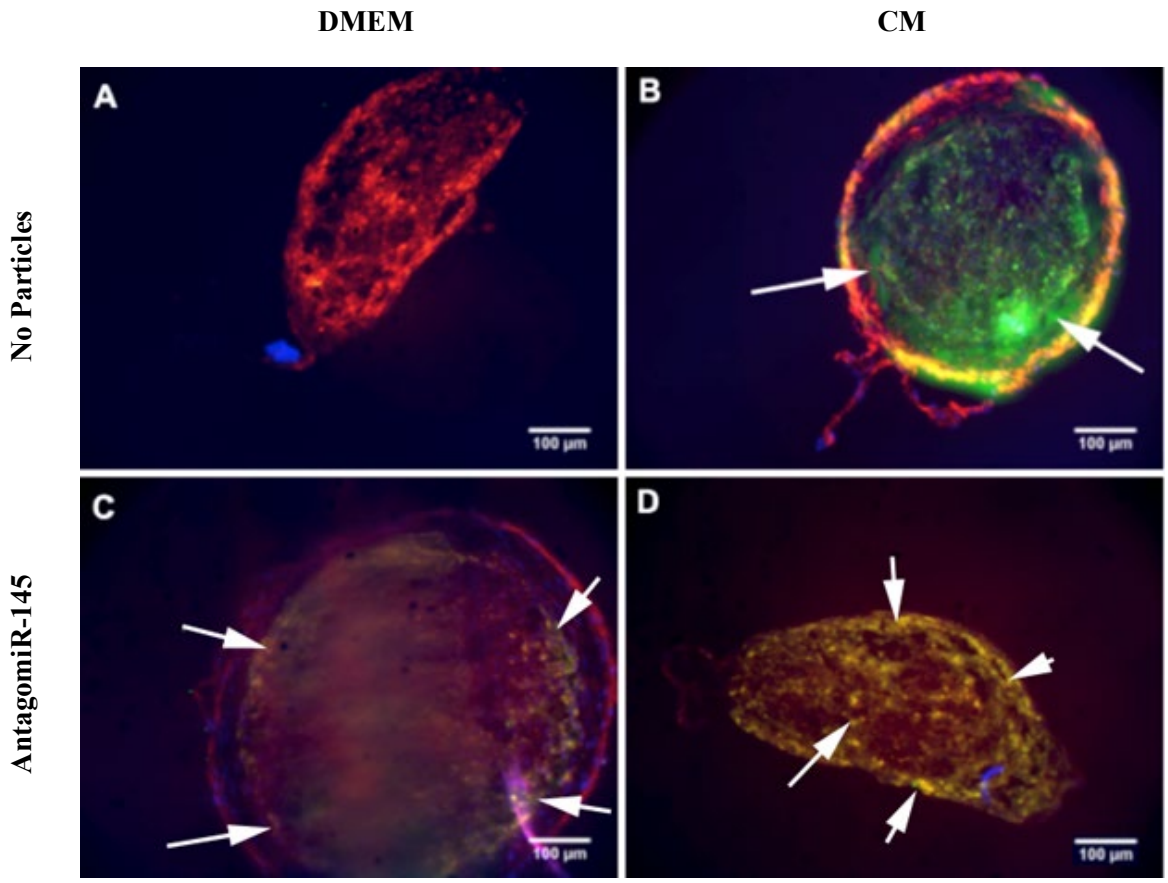

Fig. 4. 15: **Immunofluorescence staining for Collagen II protein in MSCs after 28 days of culture.** MSCs were (A) cultured in DMEM media, (B) cultured in chondrogenic media, (C) cultured in DMEM media with miR-145 antagomiR and (D) cultured in chondrogenic media with miR-145 antagomiR. (Green = collagen II, Blue = DAPI (nuclei), Red = actin staining). Arrowheads indicate positive staining.

4.4 Discussion

MicroRNAs have been highlighted as having a role during MSC differentiation, as summarised previously in fig. 4.1. Gold nanoparticles (GNPs) have been used a delivery platforms for small RNA sequences, as they protect the sequence from degradation in biological systems and can also detach sequences within the cell based on the chemistry of the conjugation (Berry, 2013). In our lab we have developed a system of using thiolated RNA sequences conjugated onto GNPs, which allows delivery and detachment via intracellular glutathione (Conde *et al.*, 2012; McCully *et al.*, 2015). Here, similar principles were used, whereby GNPs were used to deliver microRNAs identified as being involved in differentiation to MSCs, both control MSCs cultured in DMEM and differentiating MSCs, cultured in the appropriate media.

Therefore, miRNA sequences were conjugated onto GNPs. The GNPs were coated with poly ethylene glycol (PEG) to passivate the NPs and to protect the RNA sequences. *In vivo*, NP interaction with serum proteins forming a protein corona can lead to targeted uptake by cells such as macrophages (Giner-Casares *et al.*, 2016). PEG is a widely used passivating agent that also prevents aggregation of the GNPs *in vitro* (Manson *et al.*, 2011; Suk *et al.*, 2016).

4.4.1 Mir-205 and Osteogenesis

Many microRNAs are involved in cancer pathways and as such are used as markers for various cancers. Mir-205 has been implicated in breast cancer due to its additional role in mammary stem cell maintenance (De Cola *et al.*, 2015). It has also been found to have a role in osteogenic differentiation. Early work conducted on vascular smooth muscle cells showed that miR-205 may target Runx2 and Smad1 (Qiao, Chen and Zhang, 2014). Runx2 is the master regulator of osteogenesis. It targets several osteogenic genes. An important target is osteocalcin (OCN) whose levels have been correlated with increased bone mineral density (Yang *et al.*, 2003). MiR-205 also targets other osteoblast specific genes such as bone-sialoprotein (BSP) and osteopontin (OPN) (Hu *et al.*, 2015). Fig. 4.14 summarises the potential targets. Runx2 is also involved in the ossification of chondrocytes due to its consensus binding site present in collagen type X. This leads to bone formation from cartilage (important in bone repair and infantile bone formation) (Qiao, Chen and Zhang, 2014). As such, any miRNA targeting Runx2 should have an impact on osteogenesis.

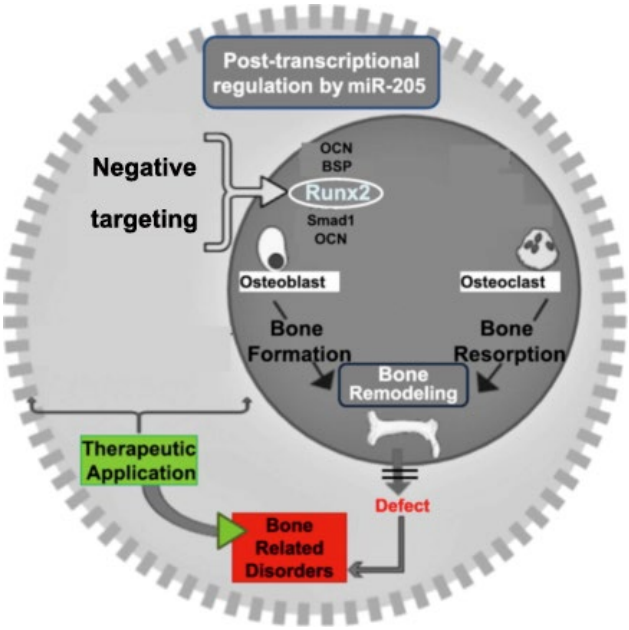

Fig. 4.16. MiR-205 targets in osteogenesis. MiR-205 has been reported to negatively target several osteogenic genes, including runx2, Smad1, osteocalcin (OCN), bone-sialoprotein (BSP) and osteopontin (OPN). Therefore, removal of miR-205 may encourage bone formation and remodelling, leading to new therapies (adapted from (Narayanan *et al.*, 2019)).

Another target of miR-205 is SATB2. SATB2 is important in osteoblast differentiation and craniofacial patterning (Zhao *et al.*, 2014). As shown by Zhang et al, SATB2 activates Runx2 dependent osteogenesis, therefore it is also essential in the process of bone formation (J. Zhang *et al.*, 2011). Here, the authors implanted SATB2 overexpressing cells on to mandibular bone defects. The overexpressing cells had an increased activity of BSP and underwent faster osteogenic differentiation, indicating SATB2's role as a potent transcription factor.

The Fluidigm study conducted in chapter 3 correctly identified a decrease in miR-205 expression in MSCs over time during osteogenesis. The subsequent qPCR in chapter 3 further supported this, confirming the inhibitory role of miR-205 in osteogenesis. Thus, collectively, miR-205 was an attractive candidate for study as it potentially targeted two important transcription factors, Runx2 and SATB2.

4.4.1.1 Manipulating Mir-205 Levels in MSCs

As miR-205 reportedly inhibited osteogenesis, it was hypothesised that inhibition of miR-205 should conversely encourage osteogenesis. An antagomiR sequence against miR-205 was therefore conjugated onto the GNPs and incubated with MSCs in both DMEM and osteogenic media (OM; positive control). Any potential osteogenic effects were investigated at both the RNA and protein levels.

4.4.1.1.1 MiR-205 antagomiR: impact at the RNA level

Initially, qPCR analysis was carried out to determine any effect of antagomiR-205 on the expression of osteogenic markers; Runx2 (early marker), alkaline phosphate (ALP, mid-phase marker) and osteocalcin (OCN, late stage marker). The MSCs cultured in OM did show higher expression of osteo-specific genes at the relevant time points, but the antagomiR did not induce a higher expression.

MiR-205 is known to influence both Runx2 (used as a marker here) and SATB2. The function of Runx2 has been extensively studied and its importance in osteogenesis has been established (Bruderer *et al.*, 2014). Knockout studies have shown that without Runx2, mineralization is absent and leads to severe skeletal abnormalities and high mortality rates pre-birth (Takarada *et al.*, 2013). SATB2 is also essential in bone formation as both a Runx2 enhancer as well as its inhibiting actions on several Hox genes, which are themselves inhibitors of osteogenesis (Dobreva *et al.*, 2006). Targeting either or both of these genes should theoretically lead to an effect in differentiation.

The antagomiR-205 treatment did not affect runx2 expression levels. Bearing in mind the number of potential targets for mir-205, it may have been more relevant to investigate levels of SATB2 expression (as SATB2 influences Runx2 expression). The antagomiR may have caused an increase in SATB2 levels, but this might not have translated to an increase in Runx2 expression due to post-transcriptional modifications and events. Hu *et al.* looked at SATB2 expression and noticed an increase in its levels when using miR-205 antagomiRs (Hu *et al.*, 2015).

4.4.1.1.2 MiR-205 antagomiR: impact at the protein level

The RNA environment is unstable and can be easily degraded, thus assessing marker protein expression is necessary. An in-cell western (ICW) was conducted to understand the changes

of the protein environment due to antagomiR-205. ICW uses fluorescently labelled antibodies to detect protein levels, compared to the cell number, using a cell tag, such that a single cell protein value can be calculated as relative fluorescence units (RFU). Here, the osteogenic markers Runx2, ALP and osteocalcin (OCN) were assessed.

Clear increases in bone markers were noted with MSCs cultures in OM, indicating that the MSCs were differentiating appropriately. No differences in markers were recorded for MSCs treated with antagomiR-205 in DMEM, however there appeared to be an increase in markers at day 14 and 28 for MSCs both cultures in OM and treated with antagomiR-205. This suggests that the antagomiR may have a synergistic effect when applied in combination with the OM, by enhancing or potentiating osteogenesis. This observation was further supported by the immunostaining, where the bone marker osteopontin (OPN) stained for a day 28 showed increased levels in MSCs treated with antagomiR-205 both in DMEM and also in OM.

As expected, the stemness marker, CD90, was increased in MSCs cultured in DMEM at the later time points of days 14 and 28 when compared to MSCs cultured in OM, indicating that the MSCs retain their phenotype better in basal media. However, it was also noted that treatment with antagomiR-205 also seemed to increase CD90 expression, when compared to parallel controls. Another target of miR-205 is phospholipase C beta 1 (PLCβ1). It is an important enzyme in nuclear lipid transduction as well as cell cycle progression (Fiume *et al.*, 2012). Zhao and his group showed that PLCβ1 was a target of miR-205 and by downregulating the expression of miR-205 using vectors, they discovered that the stemness of hepatocellular carcinoma cells increased (Zhao *et al.*, 2015). It can be said that this role of miR-205 may be present in MSCs too, recorded as an increase in CD90 expression levels. CD90 was chosen as the marker for stemness due to its prevalence in MSCs and recommendation by the ISCT as one of the criteria for defining MSCs (Samsonraj *et al.*, 2015). It may be pertinent to use other MSC markers such as CD105 or even Stro-1 and compare the fluctuations in its levels at different time points. Due to various factors such as time to reach confluency, the cells lose stemness overtime. This can lead to issues with expression of certain factors and using cells at an earlier passage point may provide more stable results.

4.4.1.1.3 Manipulating Mir-205 Levels in MSCs: Conclusion

In summary, whilst treatment with antagomiR-205 does not show a strong impact on osteogenesis, the protein expression evidence suggests that reduction of miR-205 during osteogenesis can **potentiate differentiation**.

4.4.2 Mir-143 and Adipogenesis

The impact of obesity on our lifestyles cannot be understated. This leads to multiple issues such as type 2 diabetes mellitus and cardiovascular diseases. Adipose tissue stores fat deposits within adipocytes. It is therefore crucial to understand the underlying mechanisms involved in this process. MiRNAs are able to indirectly regulate adipogenic differentiation of MSCs by targeting various genes that may be involved in balancing self-renewal and stem cell differentiation. Our study focused on using miR-143 mimics with a view towards shifting the lineage of MSCs to adipocytes. This may provide a better understanding of the process of adipogenesis and also potentially look towards using antagomiRs against adipogenesis as a clinical treatment.

Using a combination of expression data and functional assay results, Esau and co-workers first identified miR-143 as one of the regulators of adipocyte differentiation (Esau *et al.*, 2004). MiR-143 was identified as targeting extracellular signal-regulated kinase 5 (ERK5), also known as mitogen-activated protein kinase 7 (MAPK7) gene, which is involved in promoting growth and proliferation in response to tyrosine kinase signalling, boosting adipocyte differentiation (Nithianandarajah-Jones *et al.*, 2012). ERK5 mediates phosphorylation of PPARγ, the master regulator of adipogenesis and promotes adipogenesis, thus miR-143 indirectly enhances adipogenesis as seen in fig. 4.17 (Zhu *et al.*, 2014).

In chapter 3, the Fluidigm study correctly identified an increase in miR-143 expression in MSCs over time during adipogenesis. The subsequent qPCR in chapter 3 further supported this, with large significant increase in miR-143 recorded in both Promocell and Stro-1 MSC populations over time in adipogenic media (AM), confirming the positive role of miR-143 in adipogenesis. Thus, miR-143 was used in this study with a view towards enhancing adipogenesis.

4.4.2.1 Manipulating Mir-143 Levels in MSCs

As miR-143 reportedly enhanced adipogenesis, it was hypothesised that increasing miR-143 levels in MSCs should further encourage adipogenesis. A miR-143 mimic sequence was therefore conjugated onto the GNPs and incubated with MSCs in both DMEM and adipogenic media (AM; positive control). Any potential adipogenic effects were investigated at both the RNA and protein levels.

4.4.2.1.1 MiR-143 mimics: impact at the RNA level

To assess the effect of the miR-143 mimics on the RNA environment, qPCR was carried out. The expression of adipogenic markers; PPARγ (early stage marker), GLUT4 (mid-stage) and adiponectin (AdipoQ, late stage) were assessed.

The markers were all increased for MSCs cultured in AM, indicating that the cells are differentiating appropriately. However, there were no changes in marker expression for MSCs treated with the miR-143 mimics, either in basal DMEM or AM. Esau's study showed that by transfecting miR-143, they obtained higher levels of ERK5, and thus increased adipogenesis, but also by providing antagomiRs to miR-143, there was a decreased expression of PPARγ and GLUT4 expression. The use of a transfection agent may have led to a more pronounced localization of miR-143 within the cells (Esau *et al.*, 2004).

4.4.2.1.2 MiR-143 mimics: impact at the protein level

Protein expression of PPARγ, GLUT4 and AdipoQ were assessed at their respective time points to identify changes in protein adipogenic markers. Clear increases in marker expression were noted with MSCs cultured in AM over all time points, indicating that the MSCs were differentiating appropriately. The miR-143 mimics showed an increase in PPARG for MSCs cultured in DMEM, with no changes noted at later time points. The histology staining reflected this, with a small number of MSCs exhibiting fat droplets following miR-143 treatment. Whilst the evidence was not strong, it does suggest that miR-143 has a potential influence on adipogenesis

The CD90 expression was generally similar across MSCs cultured in either DMEM or AM, indicating no clear changes in retention of expression. Interestingly, there was an increase in CD90 expression following treatment of miR-143 at days 7 and 28 in both DMEM and AM, suggesting that MSC phenotype is preserved in MSCs treated with miR-143 mimics. The

opposite was identified on previous studies on cancer stem cells. For example miR-143 (along with miR-145) was shown to supress cancer stem cell markers/'stemness' factors including CD133, CD44, Oct4, c-Myc and Klf4 in cells from prostate cancer bone metastasis (Huang *et al.*, 2012). In addition, a further study demonstrated that increasing levels of miR-143 reduced cancer stem stemness, potentially signifying a greater role in stemness (Zhang *et al.*, 2015). Collectively, this evidence, along with our study, suggests a role for miRNAs in regulating stem cell characteristics.

4.4.1.1.3 Manipulating Mir-143 Levels in MSCs: conclusion

In summary, from the evidence presented here, the addition of miR-143 mimics to MSCs may slightly enhance adipogenesis, but also maintain MSC phenotype.

MiR-143 has been shown to be relevant during adipogenesis. It influences the MAPK pathway by possibly targeting ERK5 (Clapé *et al.*, 2009). ERK5 is vital in vascular development as target deletion of ERK5 in mice led to severe issues with cardiovascular development and vascular integrity. It was difficult initially to understand its effects in adipogenesis due to foetal lethality upon deletion of ERK5 (Nithianandarajah-Jones *et al.*, 2012).

Here, we see a slight increase in early stage adipogenesis following treatment of miR-143. Conversely, Chen et al. conducted a study to investigate the role of miR-143 in adipocyte derived stem cells (ADSCs) and found that miR-143 halted the progression of adipogenesis, along with cell proliferation during early stages of clonal expansion, but when introduced during the growth arrest/terminal differentiation phase, it promoted adipogenesis. In Chen's study, miR-143 was delivered using a lentivirus after 48 hours of culture, resulting in increased levels of PPARγ and larger amounts of fat deposits. Further study discovered that miR-143 also targets MAP2K5, another member of the MAPK family (Chen *et al.*, 2014). But by targeting MAP2K5, miR-143 inhibits adipogenesis. During the clonal expansion stage, DNA synthesis and cell division require the activation of the MAPK pathway. One of the factors controlling this is MAP2K5. By targeting this pathway, miR-143 may in fact be stunting the clonal expansion. This in turn cascades to suppression of C/EBPα (another important adipogenic transcription factor) leading to the decrease of adipogenesis, as shown in fig. 4.17 (Chen *et al.*, 2014). However, when introduced at the later stages, miR-143 did in fact block the MAPK pathway leading to lower phosphorylation of PPARγ. This is important as phosphorylation of PPARγ prevents differentiation of the cells. By preventing

this, more non-phosphorylated PPARγ remains, promoting adipogenesis. Therefore, the influence of miR-143 appears to be related to the timeline of adipogenesis.

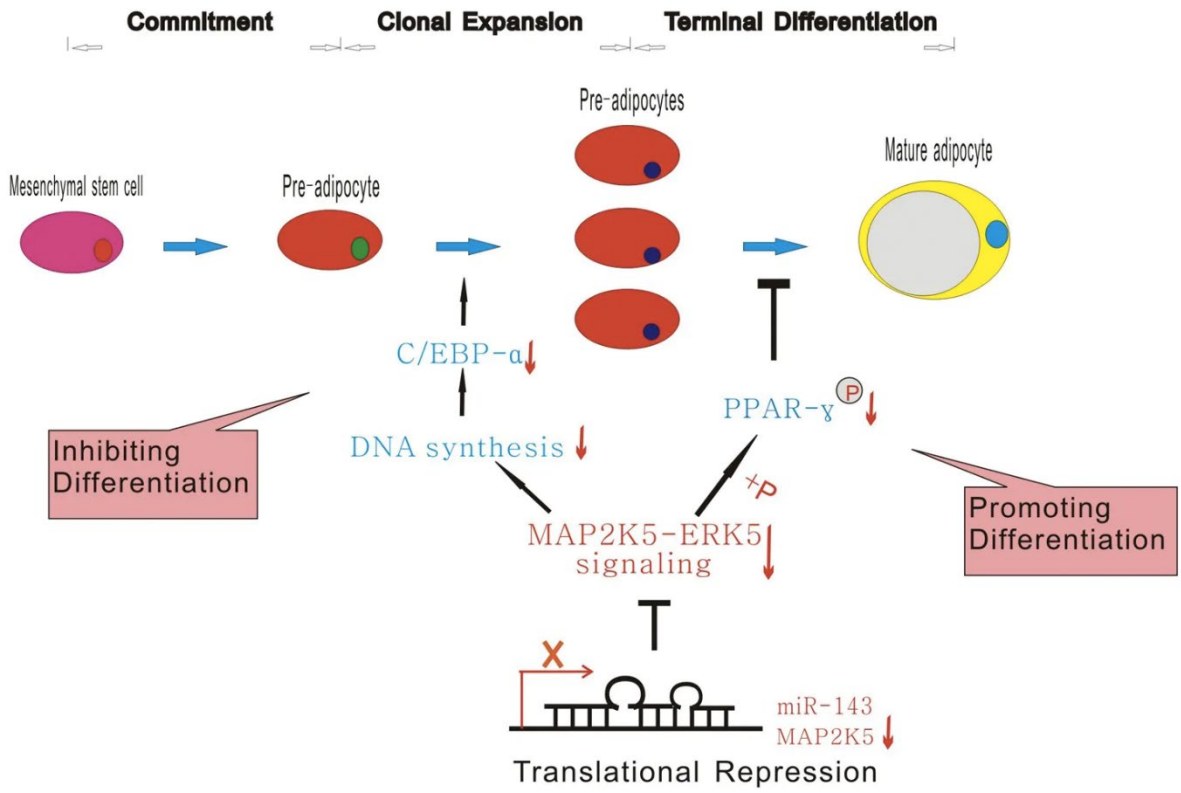

Fig. 4. 17: **Schematic of the proposed miR-143 and MAP2K5 regulation during ADSC adipogenesis.** ERK as a substrate of MAP2K5 trigger clonal expansion and activates C/EBP-a, thus overexpression of miR-143 in this phase blocks clonal expansion and subsequent differentiation (by inhibiting MAP2K5). However blocking MAP2K5 during the terminal differentiation stage reduces phosphorylation of PPAR-g and thus promotes adipogenic differentiation (taken from (Chen *et al.*, 2014)).

In our study, the miR-143 mimics were added 24 hours after seeding cells. As such, we were in fact introducing miR-143 during the early cell growth phase, which may have led to the prevention of clonal expansion, stunting differentiation during time in culture. It would be interesting to identify whether adding the mimics at a later time point, after cell growth was established, would better influence adipogenesis.

4.4.3 Mir-145 and Chondrogenesis

Cartilage degradation can be caused by either physical injury or osteoarthritis (Caplan *et al.*, 1997). As cartilage does not regenerate, techniques to promote cartilage production in clinic are a common aim in regenerative medicine. The main issue comes with maintaining the nature of chondrocytes. Chondrocytes, over time, become ossified and become part of the skeletal structure. This is essential is foetal development, but as one progresses with age, this becomes an issue (Mackie *et al.*, 2008).

As with the other differentiation pathways, miRNAs are involved in the regulation of chondro-specific genes (Crowe *et al.*, no date). The main regulator of chondrogenesis is Sox9, which controls the secretion of cartilage matrix proteins, leading to chondrocyte formation (Akiyama *et al.*, 2002). Sox9 knockout studies showed that loss prevented cartilage development and also repressed the expression of other cartilage specific genes such as Collagen II (Col2a1) and aggrecan (ACAN), both being part of the cartilage matrix (Lefebvre and de Crombrugghe, 1998). MiR-145 had been shown to target Sox9, by binding to it and causing repression. Thus, by introducing antagomiRs against miR-145, the aim is to prevent this action and thereby promote chondrogenesis.

4.4.3.1 Manipulating Mir-145 Levels in MSCs

As miR-145 reportedly inhibited chondrogenesis, it was hypothesised that inhibition of miR-145 should conversely encourage chondrogenesis (B. Yang *et al.*, 2011; Kenyon *et al.*, 2019). An antagomiR sequence against miR-145 was therefore conjugated onto the GNPs and incubated with MSCs in both DMEM and chondrogenic media (CM; positive control). Any potential chondrogenic effects were investigated at both the RNA and protein levels.

4.4.3.1.1 MiR-145 antagomiR: impact at the RNA level

To determine the effect of antagomiR-145 on chondrogenic gene expression qPCR was carried out. MSCs were expanded as micromass cultures and Sox9 (an early adipogenic marker), aggrecan (ACAN, a general adipogenic marker) and collagen 10 (Col10) expression was assessed at days 7, 14 and 28 days respectively.

The gene expression for all chondrogenic makers was increased in MSCs cultured in CM when compared to DMEM, indicating that the cells were differentiating appropriately. The antagomiR-145 GNPs were designed to target Sox9, but no changes in Sox9 expression were noted following treatment. Instead, there was an increase in gene expression at the later time points, supporting chondrogenesis (days 14 and 28). For example, collagen X (Col10) showed increased expression for the treated samples. This is an important matrix protein providing the network linkage present in chondrocytes (Shen, 2005). Although this is mainly expressed in hypertrophic chondrocytes, its increased expression in samples treated with antagomiRs is promising.

To date, all research conducted on the role of miR-145 in MSCs have demonstrated an inhibitory effect on chondrogenesis. In one such study, Yang *et al.* showed that introduction of miR-145 through overexpression did not cause any changes in the levels of Sox9 mRNA expression. However, subsequent protein analysis identified that protein levels of Sox9 were decreased (B. Yang *et al.*, 2011). It was hypothesized that miR-145 may be binding through imperfect complementation, thus not affecting the mRNA levels. Instead, it affected the translational process, leading to the eventual decrease in Sox9 protein levels. This might have led to the low purity of the RNA samples due to the presence of the antagomiRs. The antagomiRs would prevent the post-transcriptional silencing of the Sox9 proteins, leading to an increase in the expression of ACAN and Col10 at later stages.

4.4.3.1.2 MiR-145 antagomiR: impact at the protein level

Due to the nature of micromass culture, in cell western cannot be used, therefore a standard western blot was scheduled. Unfortunately, due to the low level of proteins obtained from the sample, we were not able to obtain a result from the western blotting. This was most likely due to the lysis step of the micromass culture. The RIPA buffer used for lysis was probably not able to lyse all the cells causing a low yield. As such, the protein concentration was compromised and the blot that was run did not provide any information.

As yet, there are no studies using antagomiRs of miR-145 to study the effect on late stage chondrogenesis. Instead, most research has been carried out to show the role of miR-145 in downregulating chondrogenesis. In these studies, authors showed that there was a decrease in the levels of chondro-specific proteins and also the their impact on cartilage formation (Lee *et al.*, 2011; Martinez-Sanchez, Dudek and Murphy, 2012). It would be interesting to

see if Sox9 expression is indeed decreased at the early stages and also if the production of collagen and proteoglycans are affected.

4.4.3.1.3 miR-145 antagomiR: Histology and Immunofluorescence:

Although we were not able to conduct a protein study, the Safranin O and immunofluorescence staining did show the presence of essential components of cartilage formation, i.e., proteoglycans and collagen II. The results were promising, as MSCs treated with antagomiR-145 demonstrated much higher levels of these proteins when compared to MSCs cultured without the antagomiRs.

4.4.3.1.4 miR-145 antagomiR: Conclusion

If research can regenerate cartilage without allowing a shift towards hypertrophy, treatments may be able to move away from arthroplasty (implanting a 'fake cartilage') or cartilage replacement from other parts of the body. Due to the common nature of injuries such as anterior cruciate ligament (ACL) tears and diseases including osteoarthritis, a consistent and safer option is in high demand.

Here, by targeting miR-145, the aim was to enhance chondrogenesis. As discussed, miR-145 targets Sox9, an important regulator of chondrogenesis. Our gene expression studies were consistent with Yang's study, which showed no changes for Sox9 expression. The specific binding of miR-145 to a unique 3'-UTR region of the Sox9 mRNA has been suggested to be the cause of this. The eventual increase in downstream protein expression of other chondro-specific genes in histology and immunofluorescence staining, such as ACAN and Col10, leads us to believe that there is in fact a change caused by the antagomiRs. This is promising, but it is essential to confirm whether the chondrocytes remain at this stage or become hypertrophic. The high Col10 expression is a potential sign of possible hypertrophy, but only after further protein expression studies in addition to identifying runx2 levels can this be determined.

4.4.4 The use of miRNA sequences to manipulate differentiation

Previous studies have shown that altering miRNA sequences can influence MSC differentiation, for example inhibiting miR-205 can cause an increase in the expression of osteo-specific genes (Baglìo *et al.*, 2013; Zhuang *et al.*, 2019). Often, transfection agents are used deliver the miRNA sequences, such as Lipofectamine 2000, which boasts a high

delivery rate, but is toxic to cells/tissues, thus cannot be used therapeutically. Here we used gold nanoparticles (GNPs) as a delivery platform, a method that is non-invasive and has been shown to cause minimal toxicity.

However, as we do not observe strong gene or protein expression changes when delivering the miRNA/antagomiR sequences to MSCs, it may be that the sequences are not reaching their target, for example they may be degraded in the cell after release. An established glutathione mediated response is used here to release the sequences following cellular uptake (McCully *et al.*, 2015). The thiol bond attaching the miRNA sequence to the GNP is cleaved by glutathione present within the cell cytoplasm. Whilst release should occur without any issues, perhaps the miRNA/antagomiR sequence may not be able to reach its target within the cell as it is degraded by the various RNases present. To adapt out protocols, we could potentially further modify the sequences to allow protection, without changing its activity or target selection.

Another factor that may affect the efficacy of these treatments may be the fact that the antagomiRs are not binding to the miRNAs, affecting the mRNA function. To understand this, ribosome profiling may be useful. It is based on next generation sequencing of ribosome protected mRNA fragments (Guo *et al.*, 2010). This provides data on whether the mRNA is being repressed or degraded due to the activity of our sequences. If we can identify the efficacy of the repression of target genes, we may indirectly understand if the sequences are affecting the population of miRNAs in the first place.

It is also highly likely that a single type of miRNA/antagomiR sequence may not be sufficient to cause a response. For example, miR-205 is one of many miRNAs that are involved in osteogenesis. The effect of single miRNA may be offset by other factors such as additional miRNAs and general autocrine/paracrine signals. This is supported by the evidence suggesting that antagomiR-205 enhanced osteogenesis when used in combination with OM. In future work it may be useful to combine treatments, using a miRNA/antagomiR sequence as an adjunct with another established differentiation technique.

4.5 Appendix

To confirm the uptake of nanoparticles within cells, Transmission Electron Microscopy images of MSCs were taken at 1 hour and 48 hours after incubation with GNPs.

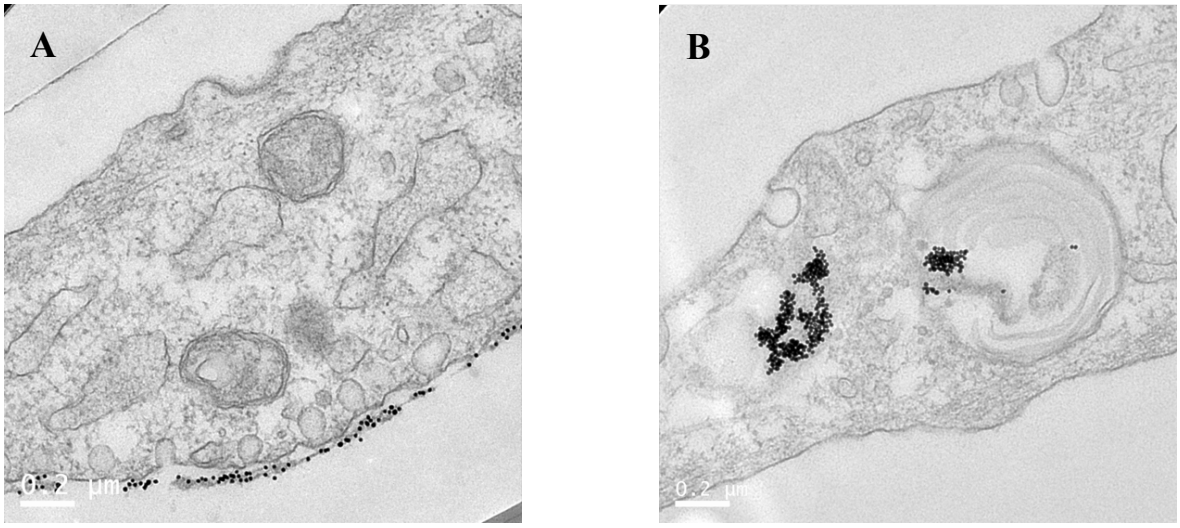

Fig. 4. 18: TEM images of MSCs cultured in DMEM for 24 hours. (A) shows GNPs after 1 hour of incubation with MSCs and (B) shows GNPs after 48 hours of incubation. Localization of GNPs at these multiple time points can be seen. (Scale bar - 0.2 µm)

Chapter 5: Using a combination of miR-31 antagomiR with nanovibrational stimulation to induce osteogenesis

5.1 Introduction

5.1.1 Osteogenesis via Physical Cues

The role of mesenchymal stem cells (MSCs) in regenerative therapeutics has been highlighted in previous chapters. In particular, the need for bone regeneration is paramount, both for skeletal issues such as non-union fractures and diseases including osteoporosis. Therefore, there has been much research into manipulating MSC differentiation towards bone.

As detailed in chapter 1, there are several techniques employed to encourage osteogenesis (1.1.3). The most established approach entails the use of chemical supplements, in the case of osteogenesis, a phosphate source (β-glycerophosphate) and a pathway (Runx2) trigger such as dexamethasone (Langenbach and Handschel, 2013). Growth factors can also be used to enhance bone formation, either directly to the media, or supplanting it onto implanted surfaces to promote growth or differentiation. This has shown to be a potent stimulant for osteogenic differentiation and has seen wide use in research, namely bone morphogenetic protein (BMP-2) (Noël *et al.*, 2004).

There are also physical means of inducing osteogenesis Cell-cell interaction can be mimicked by topography using nanopillars and nanopits. The topography can be presented to the cells using biomaterials (Li *et al.*, 2011). This technology is based on the importance that cell tension and adhesion play in cell function, due to the mechanotransductive mechanisms in the cell cytoskeleton caused by physical cues present in the environment (Dalby *et al.*, 2007; Guilak *et al.*, 2009).With MSCs, certain nanotopographies have shown to stimulate osteogenesis (Dalby *et al.*, 2007; Tsimbouri *et al.*, 2014; Yang *et al.*, 2014). Further to topography, manipulating MSC differentiation through substrate stiffness, for example by matching the stiffness of bone, triggers osteogenesis (Engler *et al.*, 2006; Parekh *et al.*, 2011). This technique of controlling the environment can be taken a step through the use of vibrations to induce changes within the cell.

5.1.2 Nanokicking and Osteogenesis

A more novel method of inducing osteogenesis through physical cues is using a technology termed ‘nanokicking’. Nanokicking uses nanovibrations, created by passing electric current

through piezoelectric actuators, to induce mechanical stresses to cells (Pemberton *et al.*, 2015). The amplitude of these vibrations are around 30 nm and this triggers the Rho-kinase (ROCK) pathway, which directs MSC lineage towards osteogenesis (McBeath *et al.*, 2004). By using specially made bioreactors (fig. 5.1), we can induce nanovibrations that cause actin-myosin contractions due to the ROCK pathway. Studies conducted using this technique have shown an increase in the levels of alkaline phosphatase (ALP) and Osterix (Pemberton *et al.*, 2015; Tsimbouri *et al.*, 2017). ALP is a robust indicator of bone formation and Osterix is an important transcription factor for osteogenesis (Marie, 2008). At the structural level, an increase in nucleus size and vinculin for 'nanokicked' cells evidence the phenotypic changes. Being a cytoskeletal protein, an increase in vinculin shows that the vibrations do in fact target the adhesion networks, causing stresses that trigger certain processes (Robertson *et al.*, 2018).

Further study demonstrated that the ROCK pathway was active during nanokicking (Robertson *et al.*, 2018). Inhibition of the ROCK pathway using inhibitors affected SMAD function within cells by preventing dimerization of SMAD1 with SMAD4 and also its translocation to the nucleus (Ji *et al.*, 2014). The importance of SMAD proteins in skeletal development is well established, as deletion of SMAD1 led to foetal lethality due to chondrodysplasia (Retting *et al.*, 2009). They are essential in triggering the BMP/TGFβ pathways, and as such, all the downstream processes involved with them. By promoting the ROCK pathway and in turn, SMAD mediated BMP/TGFβ pathway, nanokicking physically causes a response from the cells, which leads to osteogenesis (Retting *et al.*, 2009).

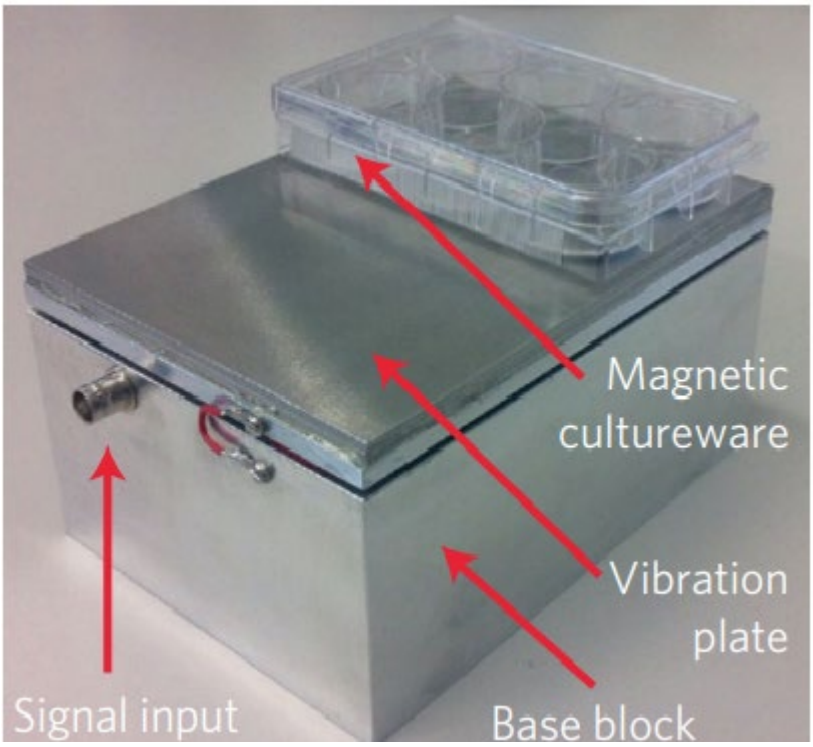

Fig. 5.1: The nanokicking bioreactor setup. The nano-vibrational bioreactor consists of a piezo-driven vibrational plate set on top of a heavy base block to direct vibration upwards. The culture-ware is magnetically attached to the top plate and vibrated at the nanoscale according to the input voltage signal. Adapted from (Tsimbouri *et al.*, 2017)

Although much work on vibrational studies in conjunction with nanoparticles have been to understand the physical properties of such a combination (changes in optical properties, plasmon resonance), Curtis and group tried to see whether using nanovibrations can stimulate uptake of nanoparticles in cells. They saw that by modulating the frequency, there was an increase in uptake of nanoparticles. Although the conditions of the experiment vary greatly with this study (they used a frequency between 2-10 Hz and magnetic particles of 500 nm), they showed that the combination did not affect particle uptake negatively (Vaidyanathan, Curtis and Mullin, 2011). Smaller nanoparticles will not be pulled physically when compared to larger sizes, but as it does not negate the uptake mechanisms of the cell, this study should have no issues (Smith *et al.*, 2010). No studies have been conducted on particle uptake using gold nanoparticles and nanovibrations, but there should be a comparatively lower effect of nanovibrations on gold particles compared to magnetic particles.

5.1.4 Chapter Aims

In the previous chapter, results suggested that whilst the application of miRNA sequences to MSCs was not sufficient to induce differentiation, there was evidence that the sequences could potentiate differentiation. This was investigated in this chapter by combining the nanokicking approach with miRNA-based therapeutics, to determine whether osteogenesis can be enhanced.

Previous work in our lab demonstrated that antagomiR-31 stimulated osteogenesis (McCully *et al.*, 2018). The literature reports that miR-31 targets the AT-rich sequence-binding protein 2 (SATB2), which is a positive influencer of Runx2 (Xie *et al.*, 2014). By acting on SATB2, Runx2 functionality is lowered, leading to a decrease in osteogenesis (J. Zhang *et al.*, 2011). In addition, Manochantr reported an increase in the expression of alkaline phosphatase (ALP) in the MSCs treated with miR-31 inhibitors (Manochantr *et al.*, 2017). Similarly, McCully *et al.* also noticed an increase of osteocalcin protein (McCully *et al.*, 2018). These studies showed that using miR-31 antagomiRs leads to an increase in osteogenesis through functional repression of miR-31. We therefore employed the application of antagomiR-31 along with nanokicking to determine investigate whether this provided a synergistic effect on MSC osteogenesis.

5.2 Materials and methods

5.2.1 Synthesis and functionalization of GNPs

All GNP synthesis and characterization was carried out by our collaborators Professor Pedro Baptista and his team, based in Caparica, Portugal (Section 2.12). AntagomiRs of miR-31 were purchased from Horizon Discovery Ltd.

5.2.2 Cell culture

HMSCs were cultured as the cell culture protocol in section 4.2.2 and section 2.1. All samples were cultured as monolayers.

5.2.3 Nanokicking bioreactor

The bottom of the plates of samples to be nanokicked were stuck to magnetic sheets to allow magnetic attachment to the bioreactor. After seeding of the cells, the plate was placed on top

of the bioreactor and incubated at 37°C with 5% CO_2. The nanovibrations were set at a frequency of 1,000 Hz with a displacement amplitude of 30 nm. The set-up of the reactor can be found in section 2.13.

5.2.4 Real Time qPCR Analysis:

RT-qPCR was followed as in section 4.2.3 and from 2.3 to 2.7. GAPDH was used as the endogenous control, while gene expression of Runx2, ALP and OCN was calculated at early, mid and late time points.

5.2.5 In Cell Western Analysis

Protocol was followed as in section 4.2.4 and section 2.9. Protein expression of Runx2, ALP and OCN was confirmed for early, mid and late time points, while CD90 was used as a stemness marker.

5.2.6 Histology and Immunofluorescence

Von Kossa staining was followed as section 2.10 and immunofluorescence protocol can be found in 2.11. OPN antibody was used as a visual indicator of OPN protein within cells.

5.3 Results

5.3.1 Effect of GNPs functionalized with miR-31 antagomiRs on MSCs with/without nanokicking

MiR-31 has been reported to repress osteogenesis by targeting SATB2 and thus affecting Runx2 expression. An antagomiR against miR-31 was generated and conjugated onto GNPs with an aim to delivering to Promocell MSCs to reverse the inhibition of osteogenesis and encourage osteoblast formation. Nanokicking is a novel technique of using nanovibrational stimulation to enhance osteogenesis. We aimed to use a combination of nanokicking along with miR-31 antagomiRs to determine the effect on MSC osteogenesis.

To achieve this, MSCs were cultured on 24-well plates, two media controls were used; (i) basal DMEM (control) and (ii) osteogenic media (positive osteogenesis control). After 24 hours culture the cells were then maintained in both media, and challenged with +/-

antagomiR-31 (treatment). The samples were then cultured for up to 28 days, during and up to which point they were assessed for osteogenic differentiation both at the gene and protein level at multiple time points.

5.3.2 Real time qPCR of MSCs treated with miR-31 antagomiRs

Initially the gene expression of osteogenic markers was investigated at early (7 days), mid (14 days) and late (28 days) time points for MSCs that were (i) cultured in DMEM or osteogenic media, (ii) treated with antagomiR-31 and (iii) nanokicked or not nanokicked. At the relevant time points, the cells were lysed and after cDNA synthesis, real time PCR was conducted. The osteogenic markers examined were Runx2, ALP and OCN expression at the respective time points. For nanokicked cells, the plates were placed on the bioreactor 4 hours after seeding to allow attachment of the cells to the plate. GAPDH was used as the endogenous control. The data was graphed to allow observation of whether any of the individual three approaches to stimulating osteogenesis were successful, as well as identifying any synergistic effects.

The Runx2 gene expression levels at day 7 are shown in fig. 5.2. Neither the osteogenic media nor the antagomiR-31 treatment enhanced Runx2 expression, however nanokicking significantly increased Runx2 expression. There was no synergistic increased observed for antagomiR-31 with either osteogenic media or nanokicking.

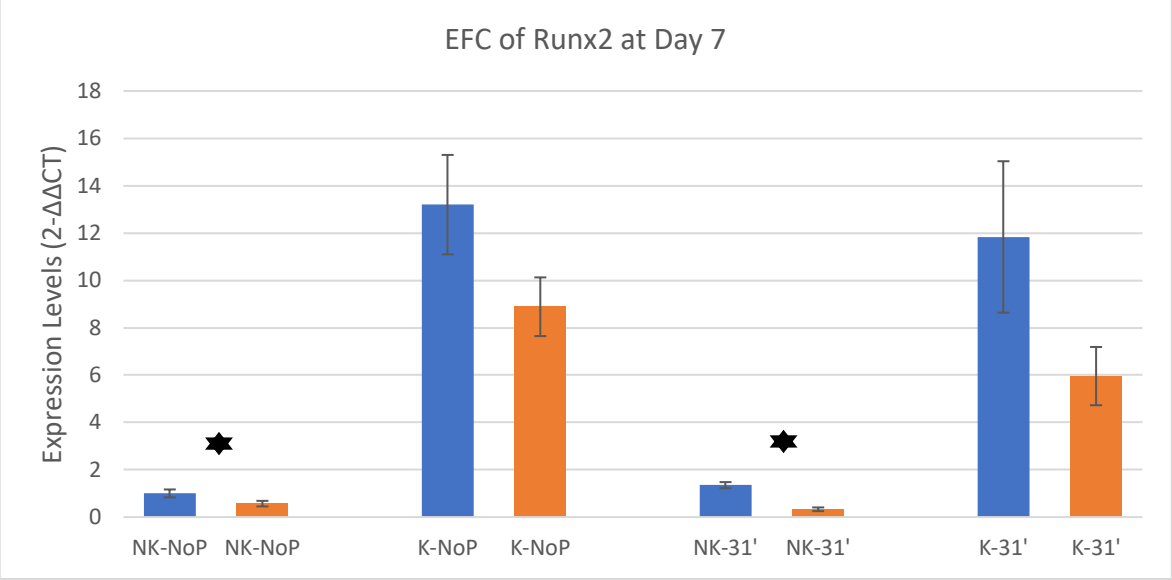

Fig. 5.2 Promocell MSC expression fold change (EFC) of Runx2 cultured in DMEM/osteogenic media +/- antagomiR-31, with and without nanokicking for 7 days. (Blue= DMEM, Orange= OM, NoP = No particles, 31'= miR-31 antagomiR, NK= Non-Kicked, K= Kicked) (n=3, error bars indicate SD, $p<0.05$) * is significance between kicked and non-kicked samples.

The ALP gene expression levels are shown in fig. 5.3. The results mirrored the Runx2 expression levels, neither osteogenic media nor antagomiR-31 influenced ALP expression, whereas nanokicking significantly increased expression. There was a potential data trend for further enhanced expression when nanokicking was applied in combination with antagomiR-31, however this was not significant.

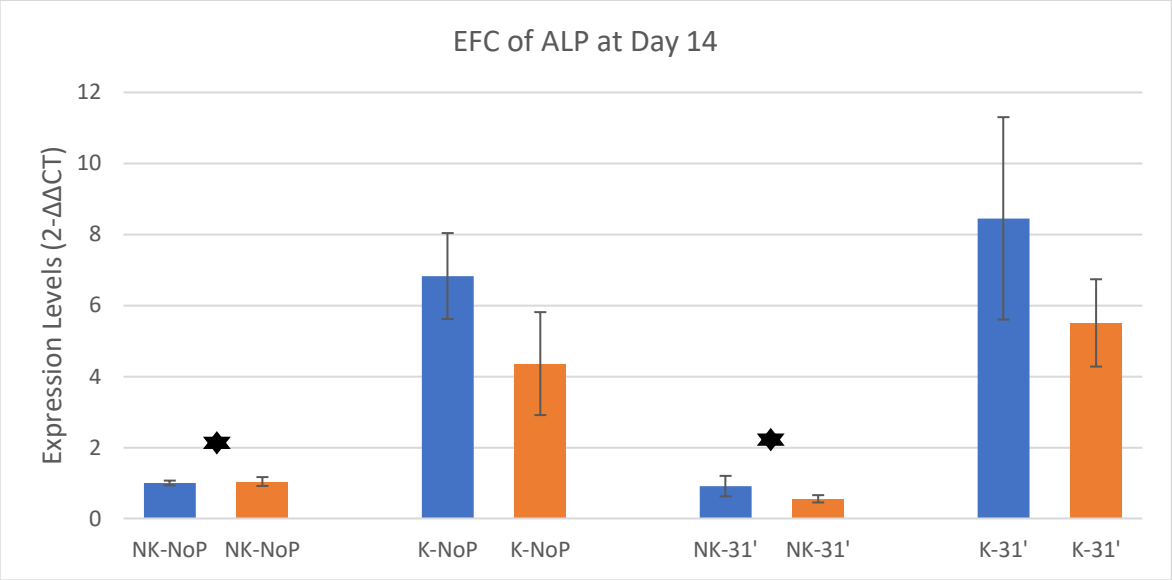

Fig. 5.3 Promocell MSC expression fold change (EFC) of Runx2 cultured in DMEM/osteogenic media +/- antagomiR-31, with and without nanokicking for 14 days. (Blue= DMEM, Orange= OM, NoP = No particles, 31'= miR-31 antagomiR, NK= Non-Kicked, K= Kicked) (n=3, error bars indicate SD, $p<0.05$). * is significance between kicked and non-kicked samples.

The osteocalcin gene expression levels are shown in fig. 5.4. Again, niether osteogenic media nor antagomiR-31 influenced expression levels, but nanokicking significant increased osteocalcin expression. There was no evidence for any synergistic effects.

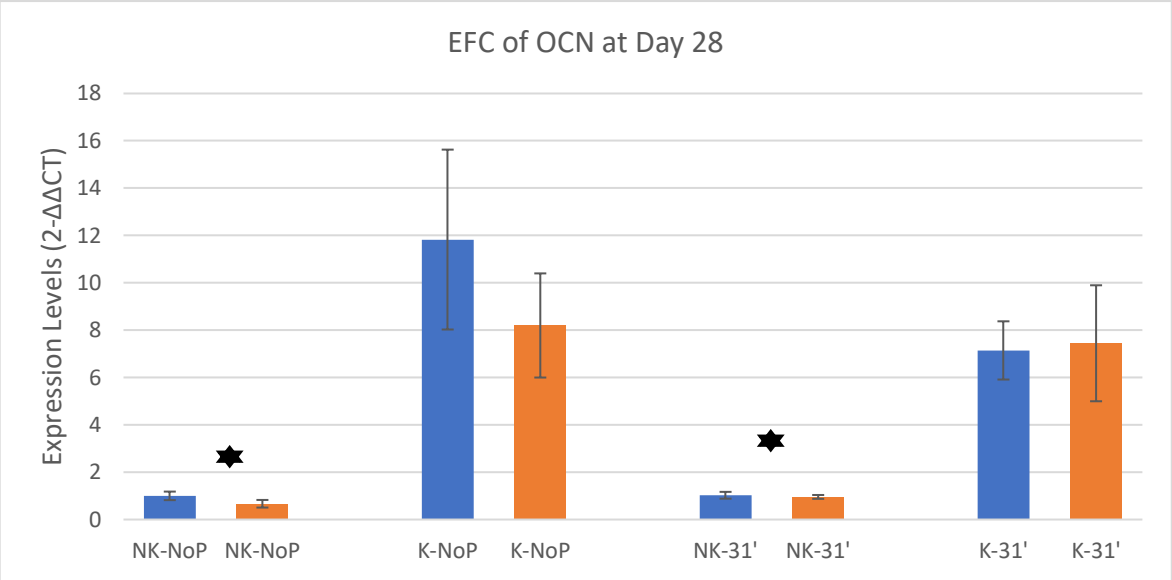

Fig. 5.4 Promocell MSC expression fold change (EFC) of OCN cultured in DMEM/osteogenic media +/- antagomiR-31, with and without nanokicking for 28 days. (Blue= DMEM, Orange= OM, NoP = No particles, 31'= miR-31 antagomiR, NK= Non-Kicked, K= Kicked) (n=3, error bars indicate SD, $p<0.05$). * is significance between kicked and non-kicked samples.

5.3.3 In-cell western of MSCs treated with miR-31 antagomiRs

After analysing the gene expression, an in-cell western (ICW) was conducted to determine any changes in protein expression of osteogenic makers. As previously, the cells were cultured in 24-well plates and the antagomiRs and appropriate media were added 24 hours after seeding. Samples to be nanokicked were placed on bioreactors 4 hours after initial seeding. After 7, 14 and 28 days, the samples were fixed and processed for in cell western, assessing Runx2, ALP and OCN protein expression after 7, 14 and 28 days respectively. CD90 antibody was used as a stemness marker.

MSCs which were not nanokicked are shown in fig. 5.3A, with kicked cells in fig. 5.3B. The cells cultured in osteogenic media indicated a general increase for Runx2 expression when compared to equivalent cells in DMEM culture. The addition of antagomiR-31 did not provide any increase in Runx2 expression in DMEM culture for non-nanokicked cells (fig. 5.5A, left panel), however there was a trend for increased Runx2 with antagomiR-31 treated cells in osteogenic media (fig. 5.5A, right panel). For nanokicked cells, antagomR-31 showed an increasing trend for Runx2 in DMEM and in osteogenic media. This suggests that the combination of antagomiR-31 with osteogenic media encouraged Runx2 epression, with is further increased in nanokicked cells.

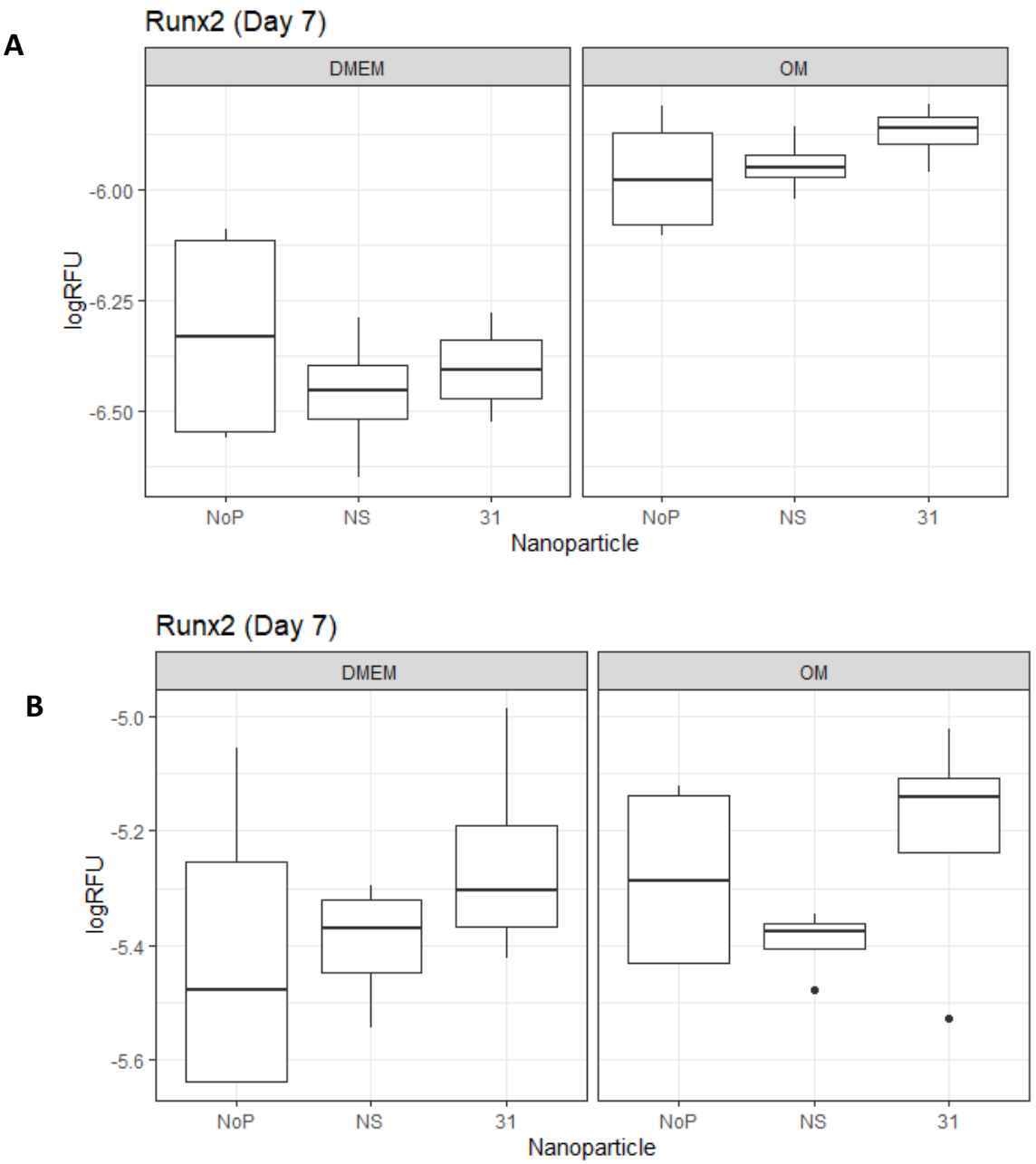

Fig. 5.5 Logged relative fluorescence (RFU) values of Runx2 expression in Promocell MSCs after treatment with antagomiR-31 +/- nanokicking. Each graph indicates a comparison of Runx2 in both basal DMEM and osteogenic media; (A) in control, non-nanokicked cells (B) in nanokicked cells. NP indicates no particles, NS represents the non-sense strand (negative control) and 31 represents the miR-31 antagomiR. (n=4, dots indicate outliers, statistics done through two-way ANOVA)

At day 14, there was no increase in ALP expression noted with any condition; osteogenic media, antagomiR-31 or nanokicking cells (fig. 5.6 A, B).

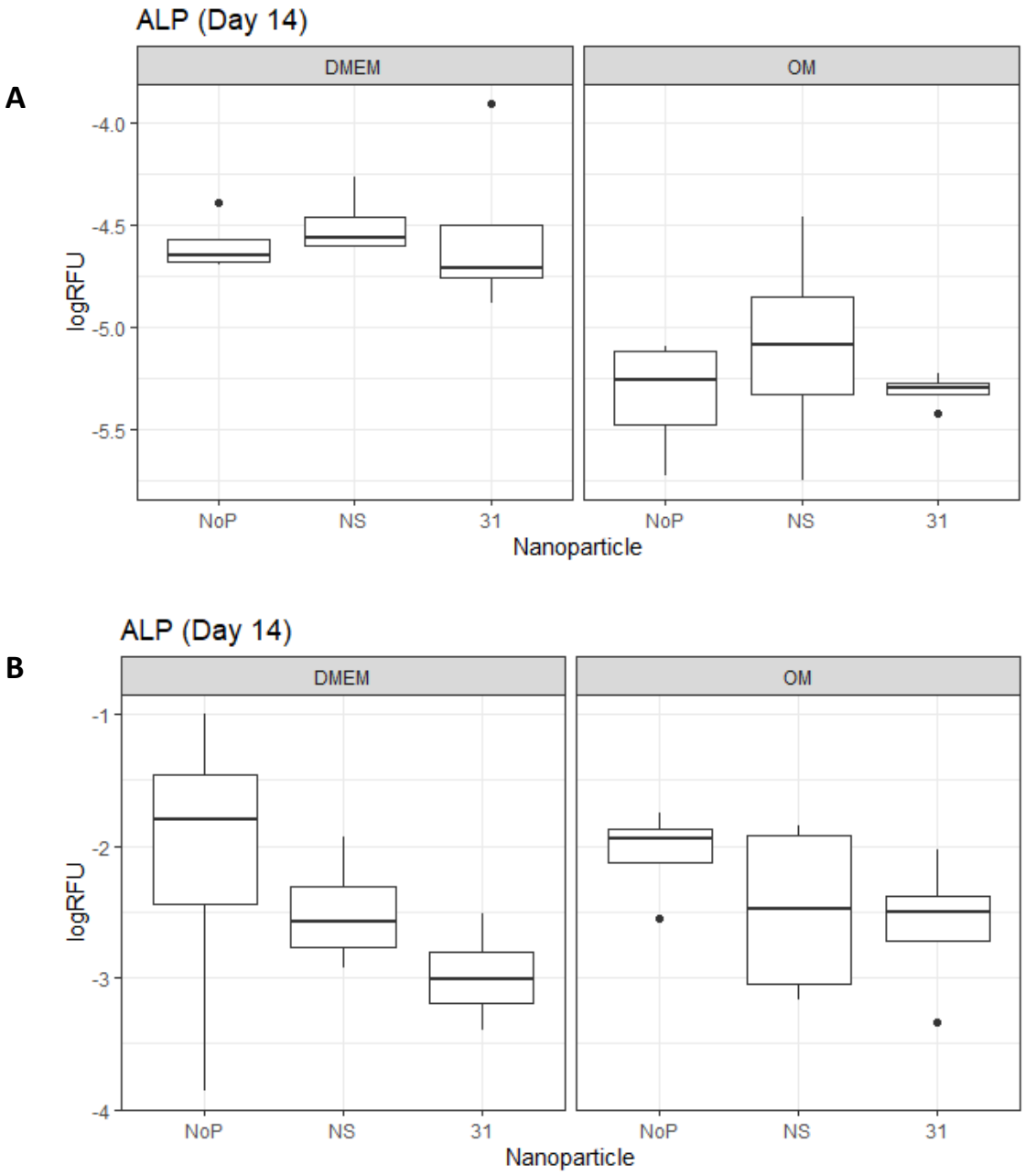

Fig. 5.6 Logged relative fluorescence (RFU) values of ALP expression in Promocell MSCs after treatment with antagomiR-31 +/- nanokicking. Each graph indicates a comparison of Runx2 in both basal DMEM and osteogenic media; (A) in control, non-nanokicked cells (B) in nanokicked cells. NP indicates no particles, NS represents the non-sense strand (negative control) and 31 represents the miR-31 antagomiR. (n=4, dots indicate outliers, statistics done through two-way ANOVA)

The expression of osteocalcin mirrored the ALP expression at day 14, with no increases in OCN identified under any treatment condition; osteogenic media, antagomiR-31 or

nanokicking (fig. 5.4 A, B). In fact, the osteogenic media actually caused a decrease in OCN expression in non-kicked cells (fig. 5.7 A, right panel).

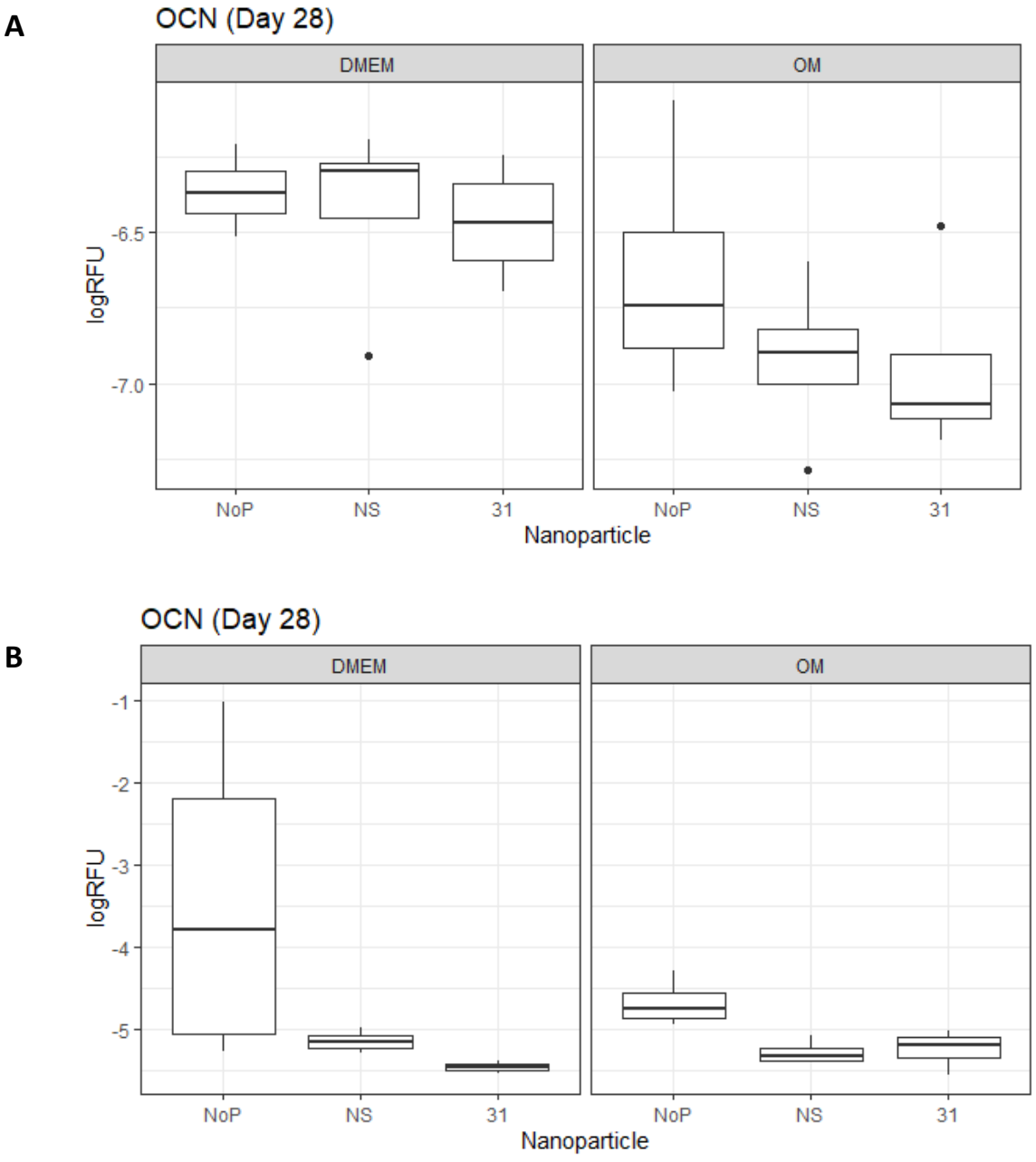

Fig. 5. 7 Logged relative fluorescence (RFU) values of OCN expression in Promocell MSCs after treatment with antagomiR-31 +/- nanokicking. Each graph indicates a comparison of Runx2 in both basal DMEM and osteogenic media; (A) in control, non-nanokicked cells (B) in nanokicked cells.NP indicates no particles, NS represents the non-sense strand (negative control) and 31 represents the miR-31 antagomiR. (n=4, dots indicate outliers, statistics done through two-way ANOVA)

The stemness marker, CD90, was assessed to determine maintenance of MSC phenotype. At day 7, CD90 expression was higher in non-nanokicked cells treated with antagomiR-31, in both DMEM and osteogenic media (fig. 5.8A). Conversely, a decrease in CD90 expression was noted with nanokicked MSCs treated with antagomiR-31 in DMEM and osteogenic media (fig. 5.4B).

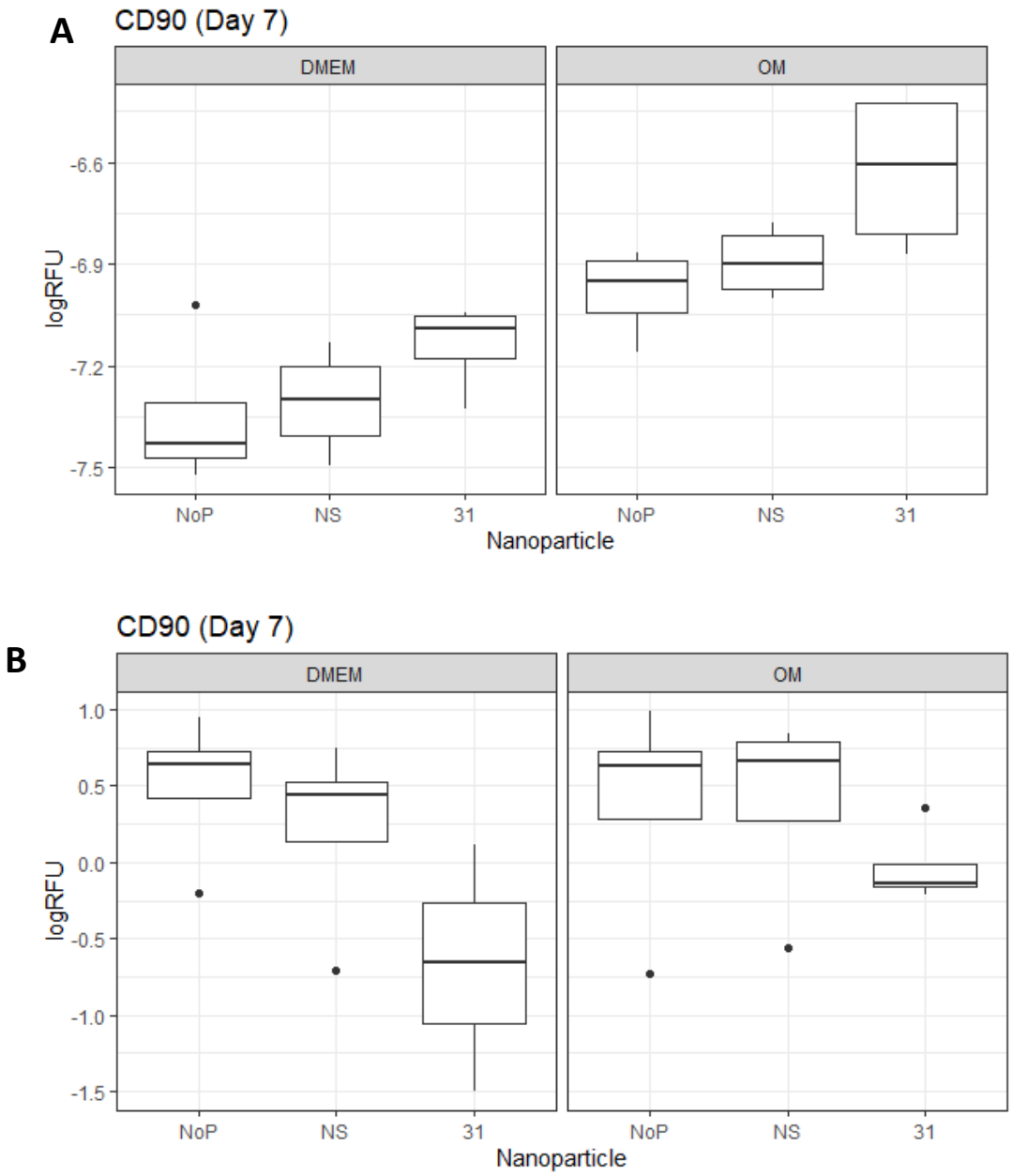

Fig. 5. 8: Logged relative fluorescence (RFU) values of the stemness marker CD90 stained in Promocell MSCs at day 7 after treatment with antagomiR-31. Each graph indicates a comparison in both basal DMEM and osteogenic media; (A) in control, non-nanokicked cells (B) in nanokicked cells. NP indicates no particles, NS represents the non-sense strand (negative control) and 31 represents the miR-31 antagomiR. (n=4, dots indicate outliers, statistics done through two-way ANOVA)

At day 14, CD90 expression in non-nanokicked cells was decreased in both DMEM and osteogenic media (Fig. 5.9A). Nanokicked MSCs again demonstrated a decrease CD90 expression in DMEM, with no change in osteogenic media (fig. 5.5B).

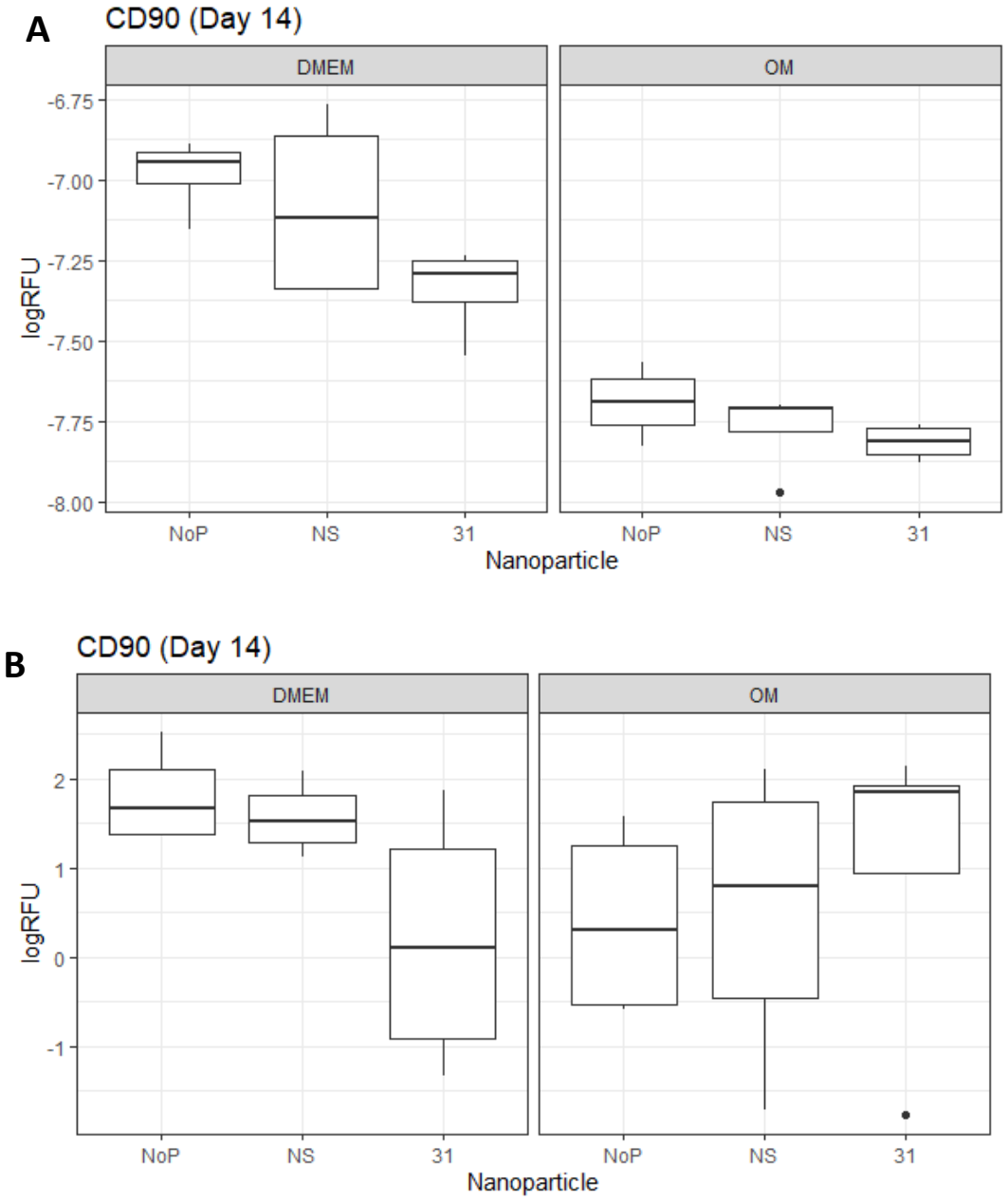

Fig. 5.9: Logged relative fluorescence (RFU) values of the stemness marker CD90 stained in Promocell MSCs at day 14 after treatment with antagomiR-31. Each graph indicates a comparison in both basal DMEM and osteogenic media; (A) in control, non-nanokicked cells (B) in nanokicked cells. NP indicates no particles, NS represents the non-sense strand (negative control) and 31 represents the miR-31 antagomiR. (n=4, dots indicate outliers, statistics done through two-way ANOVA)

By day 28, CD90 expression levels were being maintained in both non-kicked and nanokicked MSCs regardless of media or antagomiR-31 treatment (fig. 5.10).

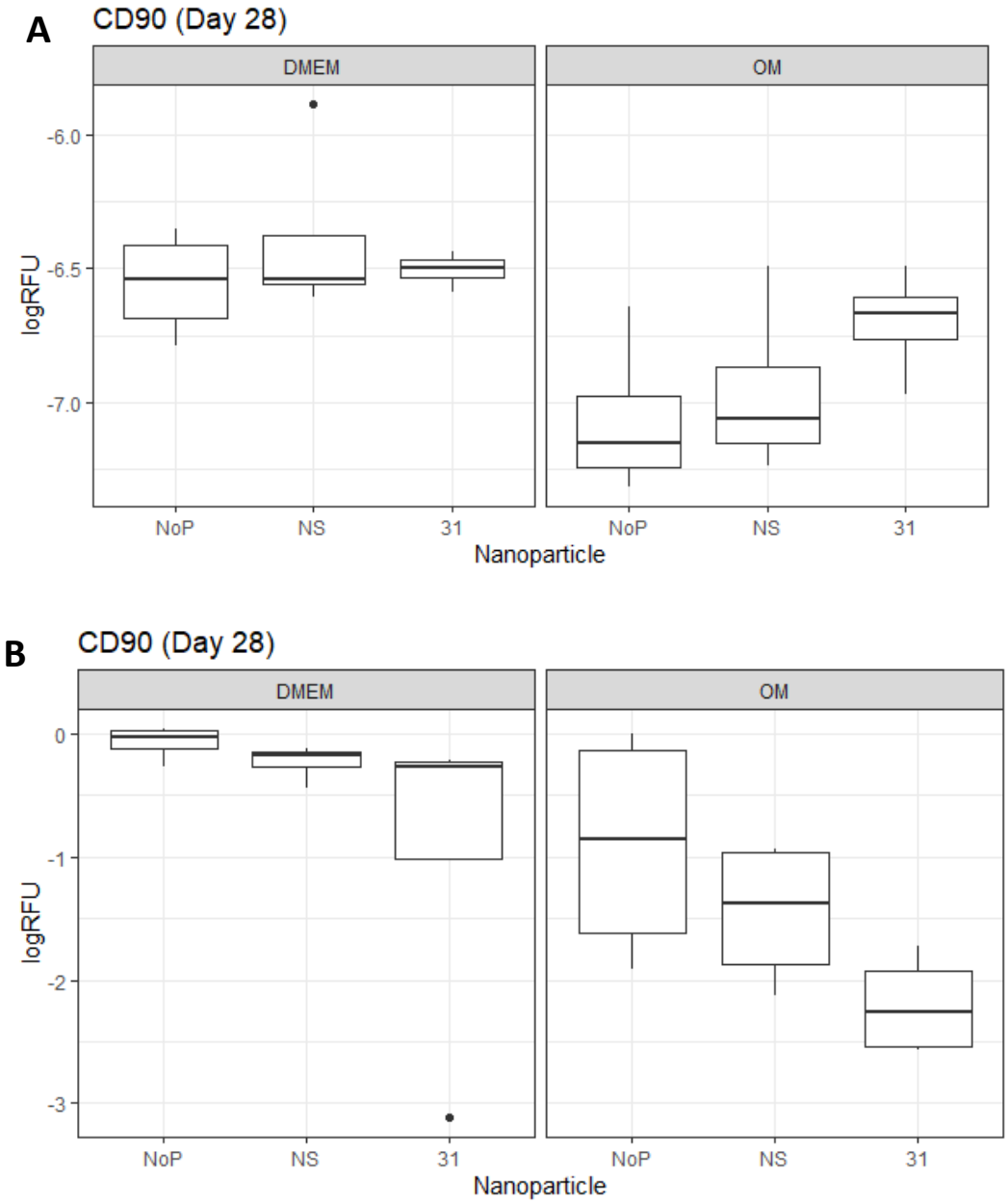

Fig. 5.10: Logged relative fluorescence (RFU) values of the stemness marker CD90 stained in Promocell MSCs at day 28 after treatment with antagomiR-31. Each graph indicates a comparison in both basal DMEM and osteogenic media; (A) in control, non-nanokicked cells (B) in nanokicked cells. NP indicates no particles, NS represents the non-sense strand (negative control) and 31 represents the miR-31 antagomiR. (n=4, dots indicate outliers, statistics done through two-way ANOVA)

5.3.4 Immunofluorescence and Von Kossa staining of MSCs treated with miR-31 antagomiRs

In addition to the gene and protein expression studies, Von Kossa staining and immunofluorescence were conducted on both non-kicked and nanokicked MSCs cultured for 28 days.

5.3.4.1 Von Kossa staining for non-kicked and nanokicked MSCs

In the control, non-nanokicked MSCs, positive Von Kossa staining was only detected in cells cultured in osteogenic media, indicating a shift towards osteogenesis (fig. 5.11 B, D). The cells treated with antagomiR-31 cultured in DMEM did not show any indication of staining.

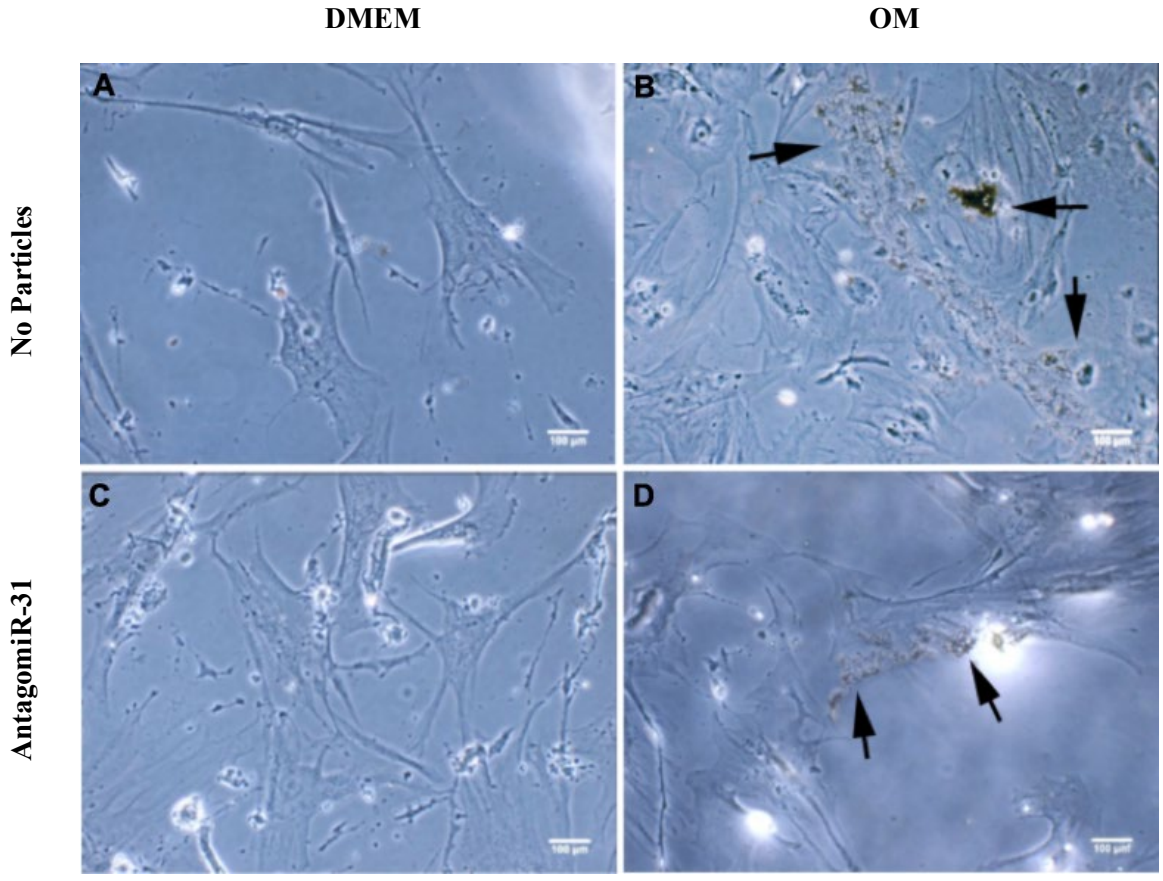

Fig. 5.11: Von Kossa staining of MSCs after 28 days of culture with antagomiR-31. MSCs were cultured in (A) DMEM media, (B) osteogenic media, (C) DMEM supplemented with antagomiR-31 and (D) osteogenic media supplemented with antagomiR-31. Arrowheads indicate positive staining.

Conversely, MSCs that were cultured on top of nanokick bioreactors, we see the presence of silver phosphate deposits on all samples (fig. 5.12). This indicates a shift of cell lineage towards osteogenesis in response to nanokicking.

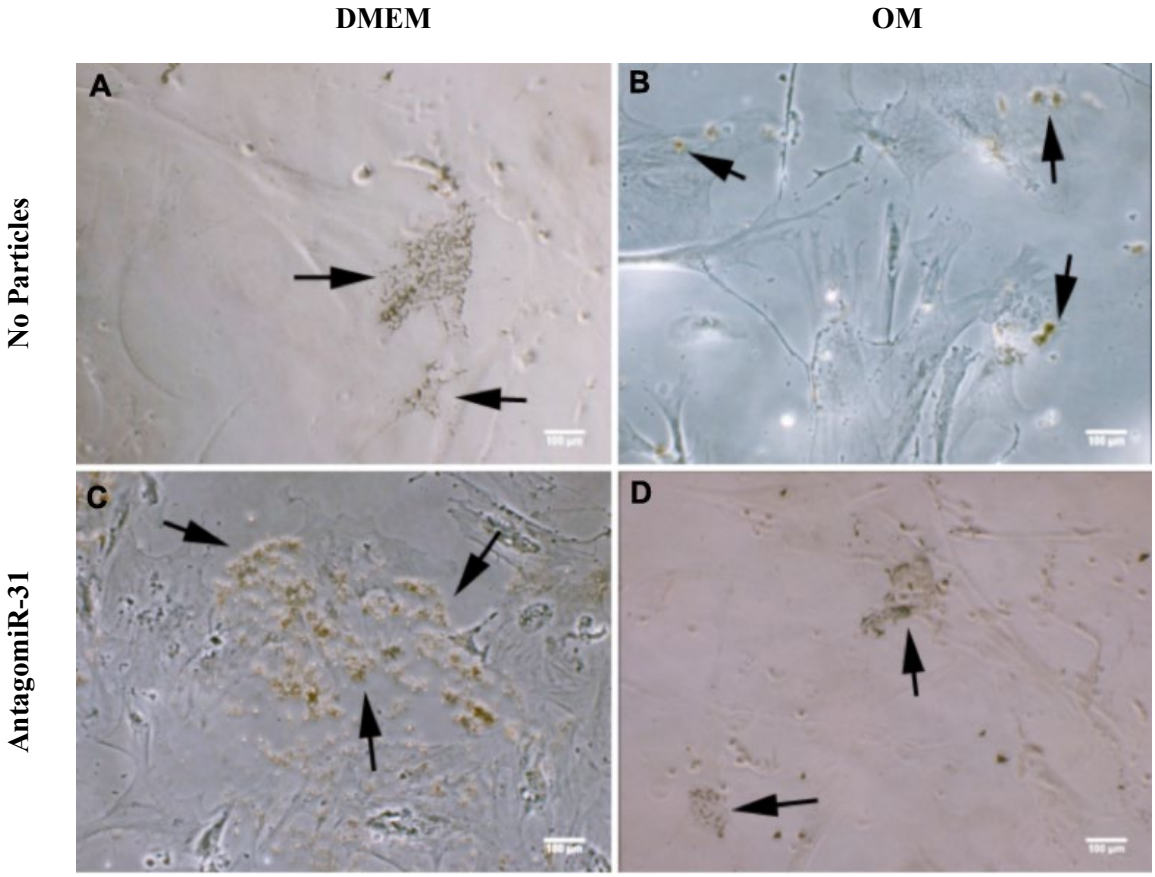

Fig. 5. 12**. Von Kossa staining of MSCs after 28 days of culture with antagomiR-31 after nanokicking**. MSCS were cultured in (A) DMEM media, (B) osteogenic media, (C) DMEM supplemented with antagomiR-31 and (D) osteogenic media supplemented with antagomiR-31. Arrowheads indicate positive staining.

5.3.4.2 Immunofluorescence staining for non-kicked and nanokicked MSCs

To visualize the cell protein, immunofluorescence was conducted on MSCs after 28 days of culture using both DMEM and osteogenic media, treated with antagomiR-31 and either non-nanokicked or nanokicked. At 28 days the cells were fixed with 4% formaldehyde, processed for immunofluorescence and osteopontin (OPN) was visualised as an indicator of osteogenesis.

The immunofluorescence for non-kicked samples mirrored the Von Kossa results, where OPN was indicated for MSCs cultures in osteogenic media (fig. 5.13 B, D), but no positive

staining was observed with the antagomiRs (fig. 5.13 C). This can lso be seen in the fluorescence intensities as in fig. 5.14.

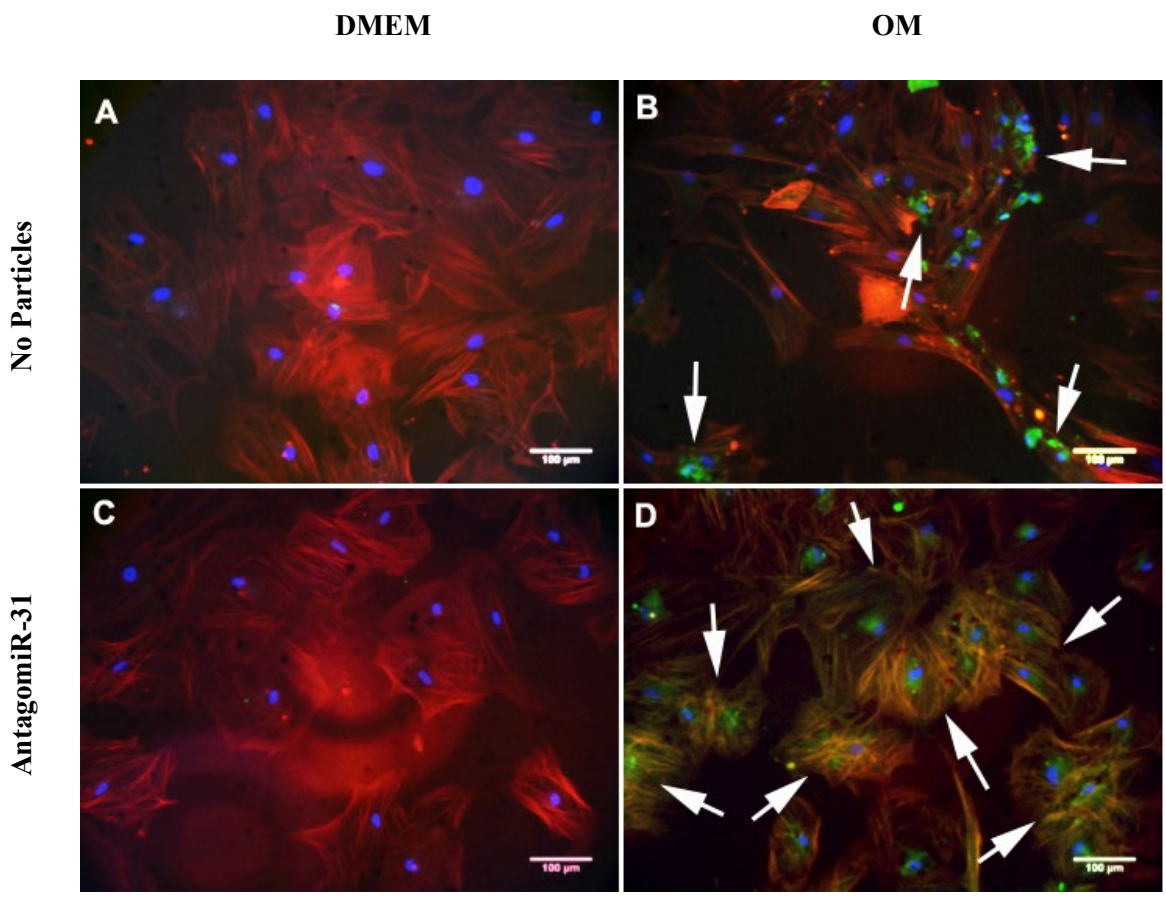

Fig. 5.13**: Immunofluorescence staining of osteopontin in MSCs after 28 days of culture**. MSCs were cultured in (A) DMEM media, (B) osteogenic media, (C) DMEM with antagomiR-31 and (D) osteogenic media with antagomiR-31. (Green = osteopontin (OPN), Blue = DAPI (nuclei), Red = actin staining). Arrowheads indicate positive staining.

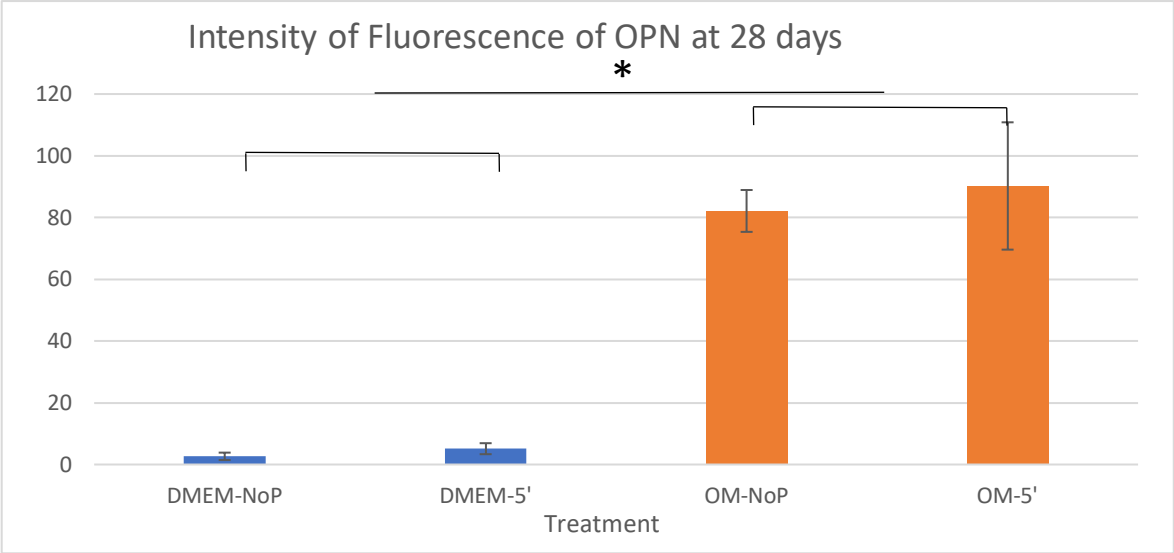

Fig. 5. 14: Semi-quantification of osteopontin staining in MSCs after 28 days of culture without nanoicking. Values were calculated using threshold analysis of the FITC channel. (n=3, error bars indicate SD, $p<0.05$)

Again, as with the Von Kossa staining, positive OPN staining was demonstrated for all nanokicked samples (fig. 5.15). As the antagomiR treated non-kicked sample did not show any presence of OPN in non-kicked samples, the positive staining is due to nanokicking. This is corroborated in fig. 5.16.

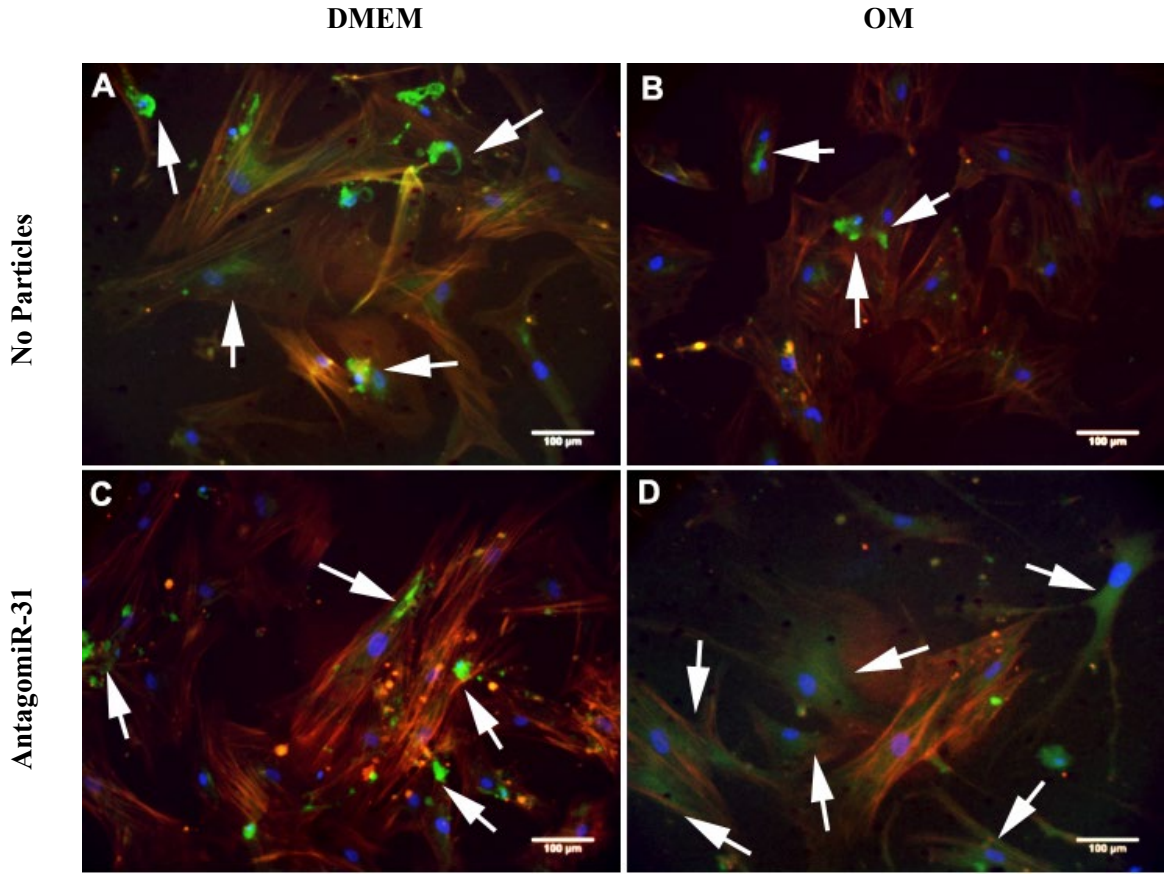

Fig. 5.15: Immunofluorescence staining of osteopontin in MSCs after 28 days of culture after nanokicking. MSCs were cultured in (A) DMEM media, (B) osteogenic media, (C) DMEM with antagomiR-31 and (D) osteogenic media with antagomiR-31. (Green = osteopontin (OPN), Blue = DAPI (nuclei), Red = actin staining). Arrowheads indicate positive staining.

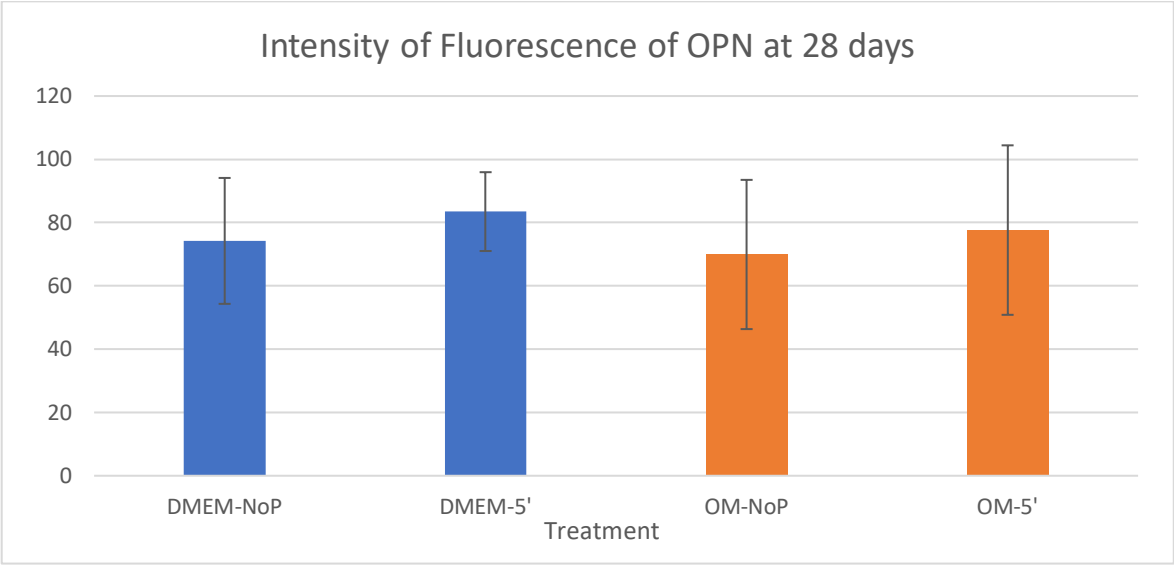

Fig. 5. 16: Semi-quantification of osteopontin staining in MSCs after 28 days of culture with nanokicking. Values were calculated using threshold analysis of the FITC channel. (n=3, error bars indicate SD, $p<0.05$)

5.4 Discussion:

In chapter 4, it was shown that whilst delivering miRNA sequences alone to MSCs did not strongly influence differentiation, a combination approach (i.e. delivery of miRNA sequences in combination with differentiation media) did appear to enhance the effect of either cue on its own. Therefore, this chapter aimed to use a positive method of stimulating differentiation, in this case, osteogenesis, in combination with delivery of miRNA sequences to determine whether a synergistic effect is produced.

MicroRNAs have been shown to impact important cell processes including differentiation. MiR-31 is a highly studied miRNA that is touted to repress osteogenesis by targeting SATB2. Studies using both miR-31 mimics and antagomiRs demonstrate its role in osteogenesis via targeting of SATB2 (Xie *et al.*, 2014; McCully *et al.*, 2018). In chapter 3, both Fluidigm and qPCR studies verified the expression of miR-31 in both Promocell and Stro-1 MSC populations. Here, miR-31 gene expression was shown to decrease during osteogenesis (figs 3.9 and 3.12 for Promocells; fig. 3.11 and 3.14 for Stro-1). These results, taken collectively with a previous publication from our group showing the delivery of antagomiR-31 to MSCs increased bone marker expression (McCully *et al.*, 2018), supported the use of miR-31 as a target for osteogenesis. Therefore, miR-31 antagomiRs were designed and conjugated on to PEGylated gold nanoparticles (GNPs) for delivery to MSCs.

Nanokicking is a novel technique that uses nanovibrations to exploit the physical properties of the cell to stimulate osteogenesis. By causing stresses and strains on the cell cytoskeleton, the cell responds by enhancing osteoblast formation. We aim to exploit this mechanotransduction response in combination with the delivery of antagomiR-31 to determine any synergistic effects on osteogenesis.

5.4.1 AntagomiR-31 +/- nanokicking: Impact at the RNA level

The gene expression levels for three different osteogenic markers were assessed at three time points (days 7, 14 and 28). With regards to the data, any increases in expression levels indicate an increase in the MSC osteogenic response.

Surprisingly, the osteogenic media did not give a positive response for any of the markers, this was unusual, as typically chemical induction works well (as shown in previous chapters). The antagomiR-31 application did not increase marker expression either. If the experiment had not included nanokicking, it may have been assumed that the MSC phenotype was

compromised and the cells were unable to differentiate. However, the nanokicked MSCs clearly demonstrated an increase for all three marker expression levels at all time points, supporting the ability of the MSC population to differentiate. A slight increase in expression is seen for DMEM samples when compared to OM samples. The reason behind this is not understood as we expect a higher increase for the differentiation media. Possible contamination during qPCR for either DMEM or OM samples may have contributed to this. A repeat experiment in a more sterilized environment may provide the expected result. The OM may have degraded in its function, but there would still be either an equal or higher expression. As such, this can be ruled out.

In terms of synergistic effects, there was no strong evidence to support that using two different osteogenic cues simultaneously enhanced osteogenesis. The hypothesis behind the theory of multiple cues acting synergistically is logical. The co-regulation of stem cell function by multi-variant stimuli occurs *in vivo* and the replication of this, using different approaches *in vitro,* may provide interesting information regarding the main stimulus that cells respond to (e.g. chemical or physical) (Kshitiz *et al.*, 2012). Cells interpret multiple signals from their microenvironment and it is most likely that a combination of stimuli drive MSc self-renewal and differentiation (Kumar, Placone and Engler, 2017). A lack of evidence to support this occurring *in vitro* in this chapter does not disprove the theory, but perhaps suggests that experiments can be further planned and expanded to gather as much information as possible at various timelines during differentiation.

5.4.2 AntagomiR-31 +/- nanokicking: Impact at the protein level

Following on from the gene study, the protein expression changes for three osteogenic markers were assessed over time in culture. Each approach used to stimulate osteogenesis was presented individually, with a combined graph for antagomiR-31 +/- osteogenic media and antagomiR-31 +/- nanokicking.

The only results which demonstrated positive changes in bone marker expression in response to osteogenic media, antagomiR-31 and nanokicking were at day 7 with Runx2; no changes were observed at days 14 and 28 with ALP or osteocalcin respectively. Whilst Runx2 protein expression at day 7 was not influenced by the addition of antagomiR-31 alone, there was a trend for increased expression when MSCs were treated with both osteogenic media and antagomiR-31 (fig. 5.3A). This potentially could support the notion of a synergistic

effect of the antagomiR and the osteogenic media. However, when comparing the nanokicked cells +/- antagomiR-31, there was no difference (fig. 5.3B).

The increase of Runx2 at the early time points does suggest an effect of miR-31, but since the antagomiRs are only added 24 hours after seeding, it may not be sufficient to cause a response at later stages. Refreshing the amount of miR-31 antagomiRs at regular intervals may potentially provide a stronger and more consistent response.

Interestingly, alongside a trend for increasing Runx2 expression, there was a clear increase in stemness marker CD90 for MSCs treated with antagomiR-31 and with osteogenic media. Whilst this only happened at the early time points of day 7, this is surprisingly, as in theory if cells are committing to differentiate towards the osteoblastic lineage, a decrease in stemness may be expected. However, it may just reflect that within the cultured MSCs there may be different populations of cells responding to treatments.

As quoted by the Genevier group in York, who specialise in MSC heterogeneity, biological processes are dynamic, adaptive and variable. Heterogeneity will always exist or emerge within even the most rigorously sorted clonal cell populations (Wilson *et al.*, 2019). This is especially true for MSCs, where the term is used to describe a heterogeneous population of stromal cells. Many studies have shown that MSCs are largely tissue-committed progenitors and may display varied tissue antigen that categorise the cells into subpopulations (Liu *et al.*, 2019). This heterogeneity can be demonstrated during chemical induction of differentiation, where only a population of the cells will actually differentiate as shown in chapter 3 (i.e. 100% of the cells are not differentiating). Therefore, perhaps for subtle changes in expression profiles, in this work in particular where small concentration of miRNAs are used in a single application, only small subsets of the entire population are responding.

The histology (Von Kossa) and immunofluorescence staining demonstrated positive osteogenesis for both osteogenic media and nanokicking, both alone and in combination. Unfortunately, the antagomiR treated DMEM samples did not show any signs of osteogenesis. Adding antagomiRs at multiple time points may provide an increased response for treated samples. Deng and co. used transfection reagents to deliver miR-31 antagomiRs (Deng *et al.*, 2014). Every 3 days the antagomiRs were added again and they showed the importance of miR-31 in osteogenesis up to the 21st day of culture. Other studies used plasmids to deliver changes to osteogenic genes (Runx2, OCN, etc.) to silence the effect of miR-31 (Deng *et al.*, 2013; Xie *et al.*, 2014). The study in this chapter can be compared to Deng's work, with the key difference being the delivery method and number of applications.

The use of transfection agents has been well studied and although they have high rates of successful delivery, they cannot be used as therapeutics, as these reagents cannot be used in the human body, due to their toxicity and possible off target effects.

5.4.3 Manipulating miR-31 levels in MSCs alongside nanokicking: Conclusion

This chapter showed that antagomiR-31 had an effect at the early time point during differentiation, but perhaps due to the exhaustion of antagomiRs on the GNPs and eventual release of GNPs from the cells, the addition of miR-31 antagomiRs at the early time point may not be enough. Introducing the antagomiRs at multiple time points may potentially increase osteogenesis. In addition, the use of GNPs as delivery platforms should be addressed. The benefits of GNPs, such as low toxicity and release rates, make them a good potential candidate for use in regenerative medicine.

MiR-31 has been studied mainly in cancer relate research and its pleiotropy in tumour progression in pancreatic cancer (among others) and tumour apoptosis in ovarian cancer (and others) is not understood (Yu *et al.*, 2018). As such it may not be the ideal candidate for therapeutic use, but due to their relevance in osteogenesis, studies can be conducted to see whether we can induce differentiation and carry over the methodology with better candidates.

The protein studies showed that nanokicked samples produced a higher expression of osteo-specific proteins such as Runx2, ALP, OCN and OPN. The Von Kossa staining also showed the increased response due to nanokicking. The cell's ability to react to changes in the environment, whether chemical or physical is vital for developing new forms of therapy. Dalby *et al.* has previously shown that nanoscale change to the environment using nanopatterning techniques led to changes in differentiation and proliferation of MSCs (Dalby, Gadegaard and Oreffo, 2014). The cell motor proteins, such as filopodia or blebs react to the patterning and the stresses caused by this led to changes in the cell to achieve homeostasis.

This ability of the cell can be exploited using nanovibrations. By using piezoelectric conductors, nanoscale vibrations can be produced, affecting the Rho-kinase (ROCK) pathways due to the tension created from actin-myosin contractions, leading to activation of SMAD proteins (Attisano and Wrana, 2002). These proteins are essential for triggering the BMP/TGFβ pathway. The ROCK pathway promotes dimerization of these SMAD proteins and their eventual translocation the nucleus. This leads to a cascade of events promoting

osteogenesis. Nanokick bioreactors are able to provide these nanovibrations and studies have shown their role in osteogenesis (Nikukar *et al.*, 2013). We also showed that using this technique increases the expression of osteogenic proteins and confirmed their importance as a new form of inducing bone formation. A representation of the proposed processes involved is shown in fig. 5.17.

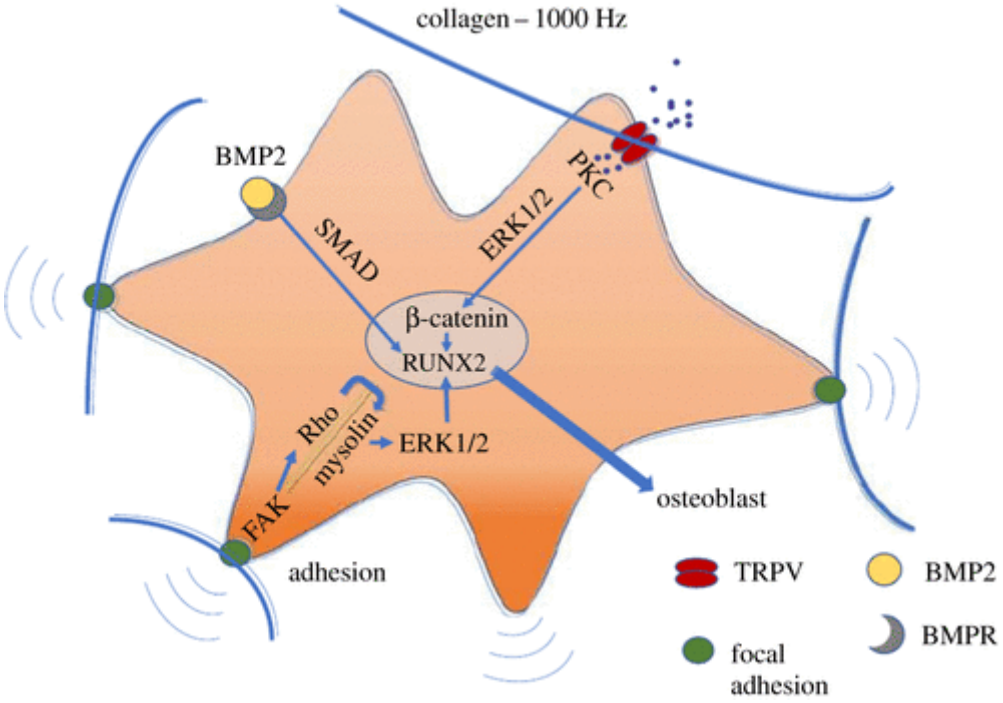

Fig. 5.17: The proposed processes involved in stimulating osteogenesis through nanokicking (Robertson *et al.*, 2018)**.**

As mentioned in the previous chapter, ribosome profiling can also be conducted to see the mRNA changes brought upon by preventing miR-31 function. Any variations from the nanovibrations to mRNA translation can also be studied.

Whilst some results may support a potential theory, clear evidence for a synergistic approach enhancing osteogenesis was not demonstrated. By introducing the antagomiRs at regular intervals, we may see an increase in the expression of other osteogenic proteins. The use of nanokicking at this juncture may provide an even larger effect and this avenue of research may be promising for regenerative therapy.

Chapter 6: Final Discussion

6.1 Gold nanoparticles

With the advent of biological and medical research, new and complex forms of therapy have been in the forefront. Gold is one of the oldest forms of medicine in the world, with Chinese texts suggesting its use as a curative for measles, small pox and removal of mercury from the skin (Huaizhi and Yuantao, 2001). Although these 'cures' were not based on scientific research, the properties of gold lent itself to these situations.

Being a noble metal, the main property of gold is its inertness. Being mostly unaffected by its surroundings, this property also lends itself to the reverse; it has minimal impact on the biological environment. As such, research was conducted to potentially exploit this property for medical applications. Biodistribution studies of GNPs have shown that very small sizes tend to be equally distributed within the body, but larger sizes accumulate within the liver and spleen (Park *et al.*, 2010). It can take up to 6 months to completely drain the system of GNPs so accounting for biodistribution and dosage is of paramount importance.

Gold nanoparticles (GNPs) were first formed as colloidal particles by Michael Faraday. He also noticed that this solution was red in colour. This was due to the absorption and scattering properties of the GNPs, which are different from its natural state. Depending on the size structure and aggregation state, they can absorb and scatter light of different wavelengths (Dreaden, Austin, *et al.*, 2012). This has been capitalized for use in imaging techniques as dark field microscopy illuminates GNPs without the use of fluorescent tags. The photothermal properties of GNPs have found use as a potential for tumour apoptosis through ablation (Dreaden *et al.*, 2011). The GNPs themselves could exhibit anti-angiogenic properties in studies (Arvizo *et al.*, 2011). Further research discovered that GNPs could be functionalized, and this would lend itself for use as a delivery vehicle for drugs and small sequences.

The sequences we used in our study were delivered by poly-ethylene glycol (PEG) coated GNPs. This is necessary to passivate the GNPs against the bodies natural defences and also protect its cargo (Berry, 2013). Thiolated sequences can be loaded on to gold surfaces due to formation of an Au-S bond. This bond is essential as a means of release. We aimed to utilize a glutathione mediated release to release these sequences. Glutathione is an antioxidant present within the cytoplasm that cleaves the Au-S bond releasing its cargo into the cell cytoplasm (McCully *et al.*, 2015).

Our work consisted of using these antagomiR/mimic functionalized GNPs to trigger differentiation of MSCs. Most research involving miRNAs use transfection agents such as

Lipofectamine 2000 to deliver their sequences. Although powerful, their toxicity to cells and tissue make translating their work *in vivo* difficult. By using gold nanoparticles as a delivery platform, we aimed to circumvent this problem. Xue *et al.* used miR-375 functionalized GNPs in mice to suppress tumour growth (Xue *et al.*, 2016). They found that miR-375 succeeded in this function and showed that the GNPs was cleared from the system after 7 days. There was no damage to the organ systems or adverse effects. Another group used miR-20a functionalized GNPs to promote cell survival in human prostate cancer cells (Hao *et al.*, 2011). Although not as popular as transfection agents, the need to be biologically compatible has led researches away from transfection agents and towards GNPs and biological compounds such as dendrimers.

Our work showed the possible use of functionalized GNPs in MSC differentiation. By enhancing the body's natural recovery processes through miRNAs, a new therapeutic agent can be brought to the forefront. Out of all our results, miR-143, miR-145 and miR-31 seem promising for further research. By using multiple treatments at the correct time point, we might be able to circumvent some of the issues we faced. Newer delivery methods such as dendrimers or hydrogel-based delivery platforms may provide a more efficient system, but the imaging properties, inertness and relative cost of production may help to bring GNPs into the spotlight.

6.2 MiRNA as potential candidates

MicroRNAs (miRNA) are small (around 22nt) single stranded RNAs that are involved in the regulatory mechanisms of nearly 60% of all genes in the human body. They function by binding to mRNAs, and either through perfect or imperfect complementarity, degrade or silence their function respectively. They were initially studied due to their involvement in cancer, but as more and more functions were discovered, their potential in medical therapies has increased.

Their role in MSC differentiation is an ongoing research field with profiling studies picking up several miRNAs that have important targets. All differentiation pathways of MSCs have a few miRNAs that either positively or negatively influence the process (fig. 3.1). By manipulating the levels of these miRNAs, we aimed to direct the lineage of MSCs to certain fates.

The manipulation of miRNAs for MSC differentiation is a burgeoning field due to their important role as regulators (Jonas and Izaurralde, 2015). Several studies have shown the importance of miRNAs in MSC pathways by targeting the various transcription factors involved in these processes (Clark *et al.*, 2014). Table 1.1 shows a small list of completed studies for MSC differentiation. Through the use of either transfection agents, delivery vehicles or gene constructs, the levels of miRNAs are altered leading to changes in the cell system (Wang *et al.*, 2015).

One main issue in miRNA therapeutics is that miRNAs have multiple targets of action. As their emergence due to involvement in cancer progression has been established, it is essential to confirm their impact on other systems through *in vivo* studies. Even if the delivery system is perfect, the miRNAs may still trigger oncogenic pathways. Increase in miR-21 levels has been linked to transformation of normal fibroblasts to cancer-associated fibroblasts (Pan, Wang and Wang, 2010). It has also been shown that it positively influences osteogenesis (Li *et al.*, 2017). This can lead to potential issues in therapy if taken to that step. A large number of miRNAs have functions that have yet to be documented. As such, it is imperative to recognize the threats posed by this area and steps must be taken to ensure utmost safety of the patients.

6.3 MiRNA for chondrogenesis and adipogenesis

Cartilage repair is an important area of research due to the difficulty of reaching and maintaining the chondrocyte phenotype. Current research includes using hydrogels or scaffolds with chondrogenesis promoting growth factors to stimulate cartilage growth (Ahmed *et al.*, 2015; Kubosch *et al.*, 2016; Legendre *et al.*, 2017). Novel techniques such as using lipid coated bubbles and even genetically enhanced fruits have shown promising results (Aliabouzar, Zhang and Sarkar, 2016; Choudhary *et al.*, 2016). The use of miRNAs in this field is just emerging and most research focuses on finding ideal targets for manipulation.

MiR-145 and miR-140 are play an essential role in chondrogenesis by targeting Sox9 and Wnt pathway respectively (Miyaki *et al.*, 2010; B. Yang *et al.*, 2011). Our Fluidigm study showed that miR-145 was downregulated with chondrogenesis. We functionalized the antagomiR-145 to GNPs to potentially prevent the downregulation of Sox9. Our results showed an increase in late stage gene expression of Aggrecan and Collagen X. Histology

and immunofluorescence also provided a further insight into the function of the antagomiR. The increase in the presence of proteoglycans and Collagen II, essential in cartilage matrix, indicated the success of the antagomiR. Although the levels of Collagen X were high, indicating possible hypertrophy, we were able to stimulate chondrogenesis and by potentially manipulating other miRNAs, we may be able to stunt the ossification of these chondrocytes. Further protein study is essential to confirm these results, but the initial outlook is positive.

Although promoting adipogenesis is not essential for therapy, any insight into controlling this process can be used for further research. By understanding the mechanisms involved in adipogenesis, alternate methods of bone-related therapy may open up.

Most studies consisted of discovering the upregulation or downregulation of miRNAs during adipocyte formation. One such miRNA, miR-27, was found to be downregulated in adipocytes. Through computational target prediction, it was shown to target PPARγ, the master regulator of adipogenesis (Takanabe *et al.*, 2008). Other miRNAs that were found to be significant in promoting adipogenesis were in fact miRNAs that targeted the osteogenic pathways. MiR-375, a repressor of osteogenesis, was shown to suppress the ERK pathway and miR-30a and miR-30d functioned by targeting Runx2 (Ling *et al.*, 2011; Zaragosi *et al.*, 2011).

The most studied miRNA for adipogenesis is miR-143. Several studies showed the role of miR-143 as a promoter of adipogenesis (Esau *et al.*, 2004; T. Sun *et al.*, 2009; Xie, Lim and Lodish, 2009). After our initial verification, we used miR-143 mimics with an aim to increase adipogenesis of MSCs. Our results did not work as expected, as we did not see any increases in adipogenic specific proteins after treatment with mimics, but this was due to the introduction of the mimics during the clonal expansion stage. Chen *et al.* showed that by introducing miR-143 during the terminal differentiation phase, ERK5 targeting helped to improve adipogenesis (Chen *et al.*, 2014). We might discover new findings by changing the time of addition. Although this may not be ideal in our study, as the MSCs require a push to shift towards adipogenesis, the introduction of miR-143 antagomiRs during the growth arrest stage of osteogenesis may help in directing the differentiation towards osteogenesis. We could also use the mimics in tandem with other approaches towards adipogenesis as a ‘promoter’.

6.4 MiRNA for osteogenesis

Osteoporosis and other low-bone density causing diseases are difficult ailments to live with. The quality of life becomes very arduous and most forms of treatment involves prevention of bone-density loss. As such, a therapy that can increase the density is very attractive and research is still ongoing to find a definite form of cure. Promoting osteogenesis of MSCs is viewed as a potential method of treatment. By using scaffolding to harbour growth factors or special nanopatterns, there seems to be a lot of promise in this field (Kilian *et al.*, 2010; Tsimbouri *et al.*, 2014). A way of non-invasive form is treatment is even more attractive.

MiRNAs have been shown to be involved in the differentiation of MSCs to osteoblasts. They are involved in all stages from the mesenchyme to osteoclast differentiation. Targets of Runx2 are especially attractive as being the master regulator of osteogenesis, any interference with its function could have profound impact down the line. Some of these miRNAs are miR-23a, miR-133, miR-205 (Hassan *et al.*, 2010; Liao *et al.*, 2013; Hu *et al.*, 2015). Other miRNAs that target important osteogenic factors are miR-31 (SATB2) and miR-214 (Osterix) (Shi *et al.*, 2013; Xie *et al.*, 2014).

Through our candidate identification study, we showed the downregulation of both miR-31 and miR-205 during osteogenesis. As important regulators of bone formation, repressing their function through antagomiRs may provide an insight into new forms of therapy.

MiR-205 did not show any promising results. It has been reported to target both Runx2 and SATB2. By targeting either, we should see an increase in the rate of osteogenesis, but our results could not match other conducted studies in strength. This may be due to the inefficacy of miR-205 as a target or the damage to the sequence by the cytoplasmic RNases. Although we do see evidences of osteopontin in the immunofluorescence studies, we are not able to show similar changes in other proteins. By possibly protecting miR-205 better, or by using a transfection agent, we may see an improved reaction from the MSCs.

Our final study conducted used miR-31 antagomiRs to again influence osteogenesis. This was done in tandem with another novel technique that uses nanovibrations, called ‘nanokicking’. Our results showed an increase at the early stages, wherein both Runx2 gene and protein expression was increased when the MSCs were treated with the antagomiRs across all samples. This was not reflected later on as there was no significant changes between the treated samples and controls. Studies by Deng’s and Xie’s group showed an increase in osteogenesis by using miR-31 antagomiRs. The main difference between their studies and our studies was the repeated addition of antagomiRs every 3 days. Although the

delivery platform was different (transfection agents), the refreshing of levels of miR-31 antagomiRs may have a significant impact on osteogenesis. By modifying our protocol, we may be able to carry on the progress of the early stages through to the final time point.

6.5 Nanokicking and combinational approaches

As mentioned previously, the need for new forms of treatments for osteoporosis is vital. By exploring new avenues of research, we may be able to discover exciting and innovative forms of therapy. A recently developing field is the use of the physical environment to trigger changes in the cell. By manipulating the stresses the cell undergoes, we may be able to initiate certain important pathways that can open the way for new areas of cell research. The use of patterning and scaffolding to act on the cytoskeleton proteins have shown to stimulate osteogenesis of MSCs. This has been carried on to other types of cells, again showing promising results. Through the use of nanovibrations, Dalby *et al.* has shown that manipulating the actin-myosin contractions of MSCs can direct the lineage of MSCs towards osteoblasts (Pemberton *et al.*, 2015).

We used a combination of nanokicking and antagomiRs to enhance the expression of osteo-specific genes and proteins, potentially leading to osteogenesis. Although our antagomiRs were not effective at a later stage, as mentioned previously, the use of nanokicking did show strong results. The expression of osteogenic proteins were higher for nanokicked samples, compared to non-kicked samples. The Von Kossa assay and immunofluorescence also showed deposits of silver phosphate and the presence of osteopontin respectively. Without the use of any osteogenic stimulants, we saw the signs of osteogenesis in the basal samples (MSCs cultured in DMEM). This confirms the already established impact of nanokicking on osteogenesis. By adding miR-31 antagomiRs at regular intervals and using the nanokicking bioreactor, we may see a synergistic effect that could be a new form of treatment or possible method to obtain osteoblasts for research.

Due to their targeted nature of action and size, antagomiR functionalized GNPs could be used with other techniques such as nanopatterning, scaffolding and growth factors to possibly see an increased rate and strength of osteogenesis.

6.6 Future Work

The research conducted in this study was able to exploit the function of miRNAs to induce differentiation of MSCs through functionalized GNPs. The potential for the use of GNPs in therapeutics is large and by using miRNAs to illicit changes in the cell system can be carried forward to other cell processes such as cancer. As such it is necessary to understand the mechanisms involved in cellular uptake and efficacy in the action of the functionalized sequences.

The cells used in the experiment were passage 3. This was done to obtain a large number of cells for multiple experiments. This can lead to loss of stemness and differentiation potential. It will be useful to conduct the experiments again for cells at the earlier passages to see if there is any improvement in the differentiation. Many studies are being conducted to see the role of miRNAs in cell function, but due to their varied role, it is difficult to pinpoint all their effects in cell processes. This can lead to potential side effects such as tumour growth. To circumvent this, *in vivo* studies are required to confirm off-target effects. Omic-based technologies (proteomics, metabolomics, etc.) can provide a deeper understanding of the processes involved, allowing a clear insight into the pathways being activated and also highlighting any unintended consequences. Ribosome profiling can also show if the sequences introduced are functioning accordingly and can show whether betterment in the sequences (such as improving targeting or protection) are required. The toxicity of GNPs have already been conducted and has shown its relatively low impact on body functions, it is still important to check for toxicity, biodistribution and dosage for further work.

6.7 Concluding Remarks

Our studies showed the promising nature of three out of four of our chosen targets:

- MiR-143 mimics decreased adipogenesis due to introduction at the early stage
- MiR-145 antagomiRs showed promising results as a promoter of chondrogenesis
- MiR-31 antagomiRs showed increased expression of the early stage marker

These results show the capabilities of miRNA therapeutics and the potential of using GNPs for therapy. This can be taken further by using miRNA mimics and antagomiRs to target other processes such an oncogenesis to prevent or treat tumours and cancerous cells. Other forms of differentiation and cell processes can also be viable targets of action.

Nanokicking has also lent its powerful use as an osteogenesis stimulator, with ongoing research being conducted to see its effect on other cell types and pathways.

Although these methods seem novel with great potential, it is necessary to look at improvements that could be made. GNPs have great use as a delivery platform, but it is essential to confirm the delivery of cargo and also confirm its biodistribution for *in vivo* studies. Although non-toxic, high amounts of GNPs in the liver or spleen can lead to complications. New forms of delivery such as dendrimers and liposomes are also potential delivery platforms that could prove viable and more effective than GNPs. The ease of production and functionalization are big pros for the use of GNPs, but efficiency is key for medicine. As such, we must look at the new vehicles being introduced and compare their efficacy.

With respect to the miRNAs, we must look at all possible targets for chosen miRNAs. MiR-31 has been implicated in oncogenesis and as such may prove to be a deterrent in its use as a therapeutic. Due to the short nature of miRNA sequences, there are multiple target sites that have not been identified for miRNAs. This can lead to off-target effects producing unintended consequences. Through tissue or animal studies, we may be able to confirm the effects of conserved miRNAs. Another point to note is the protection of miRNAs. By changing or adding certain sequences to the oligonucleotides, we may be better able to protect the sequence from its environment and even potentially allow specific targeting.

The ever-increasing list of miRNAs and their functions will provide novel forms of therapies for a multitude of ailments. By understanding its role, we can use multiple miRNA therapeutics in tandem, even with other forms of therapy, to reach new frontiers in medicine and therapy.

References

Abdoon, A. S. *et al.* (2016) 'Efficacy and toxicity of plasmonic photothermal therapy (PPTT) using gold nanorods (GNRs) against mammary tumors in dogs and cats', *Nanomedicine: Nanotechnology, Biology and Medicine*, 12(8), pp. 2291–2297. doi: https://doi.org/10.1016/j.nano.2016.07.005.

Abrahante, J. E. *et al.* (2003) 'The Caenorhabditis elegans hunchback-like Gene lin-57/hbl-1 Controls Developmental Time and Is Regulated by MicroRNAs', *Developmental Cell*, 4(5), pp. 625–637. doi: http://dx.doi.org/10.1016/S1534-5807(03)00127-8.

Acharya, A. *et al.* (2019) 'miR-26 suppresses adipocyte progenitor differentiation and fat production by targeting Fbxl19', *Genes & Development* . doi: 10.1101/gad.328955.119.

Adams, D. *et al.* (2018) 'Patisiran, an RNAi Therapeutic, for Hereditary Transthyretin Amyloidosis', *New England Journal of Medicine*. Massachusetts Medical Society, 379(1), pp. 11–21. doi: 10.1056/NEJMoa1716153.

Ahmed, M. *et al.* (2015) 'A combinatorial approach towards the design of nanofibrous scaffolds for chondrogenesis', *Scientific Reports*, 5(1), p. 14804. doi: 10.1038/srep14804.

Akinc, A. *et al.* (2010) 'Targeted Delivery of RNAi Therapeutics With Endogenous and Exogenous Ligand-Based Mechanisms', *Mol Ther*. The American Society of Gene & Cell Therapy, 18(7), pp. 1357–1364.

Akiyama, H. *et al.* (2002) 'The transcription factor Sox9 has essential roles in successive steps of the chondrocyte differentiation pathway and is required for expression of Sox5 and Sox6.', *Genes & development*. United States, 16(21), pp. 2813–2828. doi: 10.1101/gad.1017802.

Akiyama, H. (2008) 'Control of chondrogenesis by the transcription factor Sox9.', *Modern rheumatology / the Japan Rheumatism Association*. Japan, 18(3), pp. 213–219. doi: 10.1007/s10165-008-0048-x.

Akkiraju, H. and Nohe, A. (2015) 'Role of Chondrocytes in Cartilage Formation, Progression of Osteoarthritis and Cartilage Regeneration', *Journal of developmental biology*. 2015/12/18, 3(4), pp. 177–192. doi: 10.3390/jdb3040177.

Alberti, C. and Cochella, L. (2017) 'A framework for understanding the roles of miRNAs in animal development.', *Development (Cambridge, England)*. England, 144(14), pp. 2548–2559. doi: 10.1242/dev.146613.

Aliabouzar, M., Zhang, L. G. and Sarkar, K. (2016) 'Lipid Coated Microbubbles and Low Intensity Pulsed Ultrasound Enhance Chondrogenesis of Human Mesenchymal Stem Cells in 3D Printed Scaffolds', *Scientific Reports*, 6(1), p. 37728. doi: 10.1038/srep37728.

Alkilany, A. M. and Murphy, C. J. (2010) 'Toxicity and cellular uptake of gold nanoparticles: what we have learned so far?', *Journal of Nanoparticle Research*. Dordrecht: Springer Netherlands, 12(7), pp. 2313–2333. doi: 10.1007/s11051-010-9911-8.

Amendola, V. and Meneghetti, M. (2009) 'Laser ablation synthesis in solution and size manipulation of noble metal nanoparticles', *Physical Chemistry Chemical Physics*. The Royal Society of Chemistry, 11(20), pp. 3805–3821. doi: 10.1039/B900654K.

An, X. *et al.* (2016) 'miR-17, miR-21, and miR-143 Enhance Adipogenic Differentiation from Porcine Bone Marrow-Derived Mesenchymal Stem Cells.', *DNA and cell biology*. United States, 35(8), pp. 410–416. doi: 10.1089/dna.2015.3182.

Arner, P. and Kulyté, A. (2015) 'MicroRNA regulatory networks in human adipose tissue and obesity', *Nature Reviews Endocrinology*. Nature Publishing Group, a division of Macmillan Publishers Limited. All Rights Reserved., 11, p. 276. Available at: https://doi.org/10.1038/nrendo.2015.25.

Arvizo, R. R. *et al.* (2011) ‘Mechanism of anti-angiogenic property of gold nanoparticles: role of nanoparticle size and surface charge’, *Nanomedicine : nanotechnology, biology, and medicine*. 2011/02/17, 7(5), pp. 580–587. doi: 10.1016/j.nano.2011.01.011.

Attisano, L. and Wrana, J. L. (2002) ‘Signal transduction by the TGF-beta superfamily.’, *Science (New York, N.Y.)*. United States, 296(5573), pp. 1646–1647. doi: 10.1126/science.1071809.

Augello, A. and De Bari, C. (2010) ‘The Regulation of Differentiation in Mesenchymal Stem Cells’, *Human Gene Therapy*. Mary Ann Liebert, Inc., publishers, 21(10), pp. 1226–1238. doi: 10.1089/hum.2010.173.

Avior, Y., Sagi, I. and Benvenisty, N. (2016) ‘Pluripotent stem cells in disease modelling and drug discovery’, *Nature Reviews Molecular Cell Biology*. Nature Publishing Group, a division of Macmillan Publishers Limited. All Rights Reserved., 17, p. 170. Available at: https://doi.org/10.1038/nrm.2015.27.

Axtell, M. J., Westholm, J. O. and Lai, E. C. (2011) ‘Vive la diff{é}rence: biogenesis and evolution of microRNAs in plants and animals’, *Genome Biology*, 12(4), pp. 1–13. doi: 10.1186/gb-2011-12-4-221.

Baglìo, S. R. *et al.* (2013) ‘MicroRNA expression profiling of human bone marrow mesenchymal stem cells during osteogenic differentiation reveals Osterix regulation by miR-31’, *Gene*, 527(1), pp. 321–331. doi: http://dx.doi.org/10.1016/j.gene.2013.06.021.

Bartel, D. P. (2004) ‘MicroRNAs: Genomics, Biogenesis, Mechanism, and Function’, *Cell*, 116(2), pp. 281–297. doi: http://dx.doi.org/10.1016/S0092-8674(04)00045-5.

Bartel, D. P. (2009) ‘MicroRNAs: target recognition and regulatory functions’, *Cell*, 136. doi: 10.1016/j.cell.2009.01.002.

Benthien, J. P. and Behrens, P. (2010) ‘Autologous Matrix-Induced Chondrogenesis (AMIC): Combining Microfracturing and a Collagen I/III Matrix for Articular Cartilage Resurfacing’, *Cartilage*. SAGE Publications, 1(1), pp. 65–68. doi: 10.1177/1947603509360044.

Berry, C. (2013) *Gold nanoparticles in biomedicine*, *Biochemical Society*.

Bhaskar, B. *et al.* (2014) ‘Role of signaling pathways in mesenchymal stem cell differentiation.’, *Current stem cell research & therapy*. United Arab Emirates, 9(6), pp. 508–512.

Bianco, P. (2014) ‘“Mesenchymal” stem cells.’, *Annual review of cell and developmental biology*. United States, 30, pp. 677–704. doi: 10.1146/annurev-cellbio-100913-013132.

Bianco, P. and Robey, P. G. (2001) ‘Stem cells in tissue engineering’, *Nature*, 414(6859), pp. 118–121. doi: 10.1038/35102181.

Bieback, K. *et al.* (2008) ‘Clinical Protocols for the Isolation and Expansion of Mesenchymal Stromal Cells’, *Transfusion medicine and hemotherapy : offizielles Organ der Deutschen Gesellschaft fur Transfusionsmedizin und Immunhamatologie*. 2008/07/17. S. Karger GmbH, 35(4), pp. 286–294. doi: 10.1159/000141567.

BOHNSACK, M. T., CZAPLINSKI, K. and GÖRLICH, D. (2004) ‘Exportin 5 is a RanGTP-dependent dsRNA-binding protein that mediates nuclear export of pre-miRNAs’, *RNA* , 10(2), pp. 185–191. doi: 10.1261/rna.5167604.

Bonewald, L. F. (2007) ‘Osteocytes as dynamic multifunctional cells.’, *Annals of the New York Academy of Sciences*. United States, 1116, pp. 281–290. doi: 10.1196/annals.1402.018.

Bruderer, M. *et al.* (2014) ‘Role and regulation of RUNX2 in osteogenesis.’, *European cells & materials*. Scotland, 28, pp. 269–286.

Burr, D. B., Bellido, T. and White, K. E. (2015) ‘6 - Bone structure and function’, in Hochberg, M. C. et al. (eds). Philadelphia: Content Repository Only!, pp. 42–55. doi: https://doi.org/10.1016/B978-0-323-09138-1.00006-1.

Callis, T. E. *et al.* (2009) 'MicroRNA-208a is a regulator of cardiac hypertrophy and conduction in mice', *The Journal of clinical investigation*. 2009/08/10. American Society for Clinical Investigation, 119(9), pp. 2772–2786. doi: 10.1172/JCI36154.

Campsie, P. *et al.* (2019) 'Design, construction and characterisation of a novel nanovibrational bioreactor and cultureware for osteogenesis', *Scientific Reports*, 9(1), p. 12944. doi: 10.1038/s41598-019-49422-4.

Caplan, A. I. *et al.* (1997) 'Principles of cartilage repair and regeneration', *Clinical orthopaedics and related research*. Department of Biology, Case Western Reserve University, Cleveland, OH 44106-7080, USA., (342), pp. 254–269. Available at: http://europepmc.org/abstract/MED/9308548.

Carter, D. R. *et al.* (1987) 'Influences of mechanical stress on prenatal and postnatal skeletal development.', *Clinical orthopaedics and related research*. United States, (219), pp. 237–250.

Chamberlain, G. *et al.* (2007) 'Concise Review: Mesenchymal Stem Cells: Their Phenotype, Differentiation Capacity, Immunological Features, and Potential for Homing', *STEM CELLS*. John Wiley & Sons, Ltd., 25(11), pp. 2739–2749. doi: 10.1634/stemcells.2007-0197.

Chaudhuri, O. and Mooney, D. J. (2012) 'Anchoring cell-fate cues', *Nature Materials*. Nature Publishing Group, a division of Macmillan Publishers Limited. All Rights Reserved., 11, p. 568. Available at: https://doi.org/10.1038/nmat3366.

Chen, C. W. *et al.* (2005) 'Type I and II collagen regulation of chondrogenic differentiation by mesenchymal progenitor cells', *Journal of Orthopaedic Research*. John Wiley & Sons, Ltd, 23(2), pp. 446–453. doi: 10.1016/j.orthres.2004.09.002.

Chen, K. and Rajewsky, N. (2007) 'The evolution of gene regulation by transcription factors and microRNAs', *Nat Rev Genet*, 8. doi: 10.1038/nrg1990.

Chen, L. *et al.* (2014) 'MicroRNA-143 Regulates Adipogenesis by Modulating the MAP2K5–ERK5 Signaling', *Scientific Reports*. The Author(s), 4, p. 3819. Available at: http://dx.doi.org/10.1038/srep03819.

Chendrimada, T. P. *et al.* (2005) 'TRBP recruits the Dicer complex to Ago2 for microRNA processing and gene silencing.', *Nature*. England, 436(7051), pp. 740–744. doi: 10.1038/nature03868.

Chiu, Y.-L. and Rana, T. M. (2003) 'siRNA function in RNAi: A chemical modification analysis', *RNA*, 9(9), pp. 1034–1048. doi: 10.1261/rna.5103703.

Chou, C.-L. *et al.* (2013) 'Micrometer scale guidance of mesenchymal stem cells to form structurally oriented cartilage extracellular matrix', *Tissue engineering. Part A*. 2012/12/31. Mary Ann Liebert, Inc., 19(9–10), pp. 1081–1090. doi: 10.1089/ten.TEA.2012.0177.

Choudhary, D. *et al.* (2016) 'Genetically engineered flavonol enriched tomato fruit modulates chondrogenesis to increase bone length in growing animals', *Scientific Reports*, 6(1), p. 21668. doi: 10.1038/srep21668.

Christodoulides, C. *et al.* (2009) 'Adipogenesis and WNT signalling', *Trends in Endocrinology & Metabolism*, 20(1), pp. 16–24. doi: https://doi.org/10.1016/j.tem.2008.09.002.

Clapé, C. *et al.* (2009) 'miR-143 Interferes with ERK5 Signaling, and Abrogates Prostate Cancer Progression in Mice', *PLOS ONE*. Public Library of Science, 4(10), p. e7542. Available at: https://doi.org/10.1371/journal.pone.0007542.

Clark, E. A. *et al.* (2014) 'Concise review: MicroRNA function in multipotent mesenchymal stromal cells.', *Stem cells (Dayton, Ohio)*. United States, 32(5), pp. 1074–1082.

De Cola, A. *et al.* (2015) 'miR-205-5p-mediated downregulation of ErbB/HER receptors in breast cancer stem cells results in targeted therapy resistance', *Cell Death & Disease*, 6(7), pp. e1823–e1823. doi: 10.1038/cddis.2015.192.

Collino, F. *et al.* (2011) 'MicroRNAs and mesenchymal stem cells.', *Vitamins and hormones*. United States, 87, pp. 291–320. doi: 10.1016/B978-0-12-386015-6.00033-0.

Concepcion, C. P., Bonetti, C. and Ventura, A. (2012) 'The microRNA-17-92 family of microRNA clusters in development and disease', *Cancer journal (Sudbury, Mass.)*, 18(3), pp. 262–267. doi: 10.1097/PPO.0b013e318258b60a.

Conde, J. *et al.* (2012) 'Design of Multifunctional Gold Nanoparticles for In Vitro and In Vivo Gene Silencing', *ACS Nano*. American Chemical Society, 6(9), pp. 8316–8324. doi: 10.1021/nn3030223.

Cordeiro-Spinetti, E., Taichman, R. S. and Balduino, A. (2015) 'The Bone Marrow Endosteal Niche: How Far from the Surface?', *Journal of Cellular Biochemistry*. John Wiley & Sons, Ltd, 116(1), pp. 6–11. doi: 10.1002/jcb.24952.

Crowe, N. *et al.* (no date) 'Detecting new microRNAs in human osteoarthritic chondrocytes identifies miR-3085 as a human, chondrocyte-selective, microRNA', *Osteoarthritis and Cartilage*. doi: http://dx.doi.org/10.1016/j.joca.2015.10.002.

D'Alimonte, I. *et al.* (2013) 'Wnt Signaling Behaves as a "Master Regulator" in the Osteogenic and Adipogenic Commitment of Human Amniotic Fluid Mesenchymal Stem Cells', *Stem Cell Reviews and Reports*, 9(5), pp. 642–654. doi: 10.1007/s12015-013-9436-5.

Dalby, M. J. *et al.* (2007) 'The control of human mesenchymal cell differentiation using nanoscale symmetry and disorder', *Nat Mater*. Nature Publishing Group, 6(12), pp. 997–1003.

Dalby, M. J., Gadegaard, N. and Oreffo, R. O. C. (2014) 'Harnessing nanotopography and integrin-matrix interactions to influence stem cell fate', *Nat Mater*. Nature Publishing Group, a division of Macmillan Publishers Limited. All Rights Reserved., 13(6), pp. 558–569. Available at: http://dx.doi.org/10.1038/nmat3980.

Daraee, H. *et al.* (2016) 'Application of gold nanoparticles in biomedical and drug delivery', *Artificial Cells, Nanomedicine, and Biotechnology*. Taylor & Francis, 44(1), pp. 410–422. doi: 10.3109/21691401.2014.955107.

Darlington, G. J., Ross, S. E. and MacDougald, O. A. (1998) 'The Role of C/EBP Genes in Adipocyte Differentiation ', *Journal of Biological Chemistry* , 273(46), pp. 30057–30060. doi: 10.1074/jbc.273.46.30057.

Dawson, J. I. *et al.* (2014) 'Concise review: bridging the gap: bone regeneration using skeletal stem cell-based strategies - where are we now?', *Stem cells (Dayton, Ohio)*. United States, 32(1), pp. 35–44. doi: 10.1002/stem.1559.

Deans, R. J. and Moseley, A. B. (2000) 'Mesenchymal stem cells: Biology and potential clinical uses', *Experimental Hematology*, 28(8), pp. 875–884. doi: https://doi.org/10.1016/S0301-472X(00)00482-3.

Deng, Y. *et al.* (2013) 'The role of miR-31-modified adipose tissue-derived stem cells in repairing rat critical-sized calvarial defects', *Biomaterials*, 34(28), pp. 6717–6728. doi: http://dx.doi.org/10.1016/j.biomaterials.2013.05.042.

Deng, Y. *et al.* (2014) 'Repair of critical-sized bone defects with anti-miR-31-expressing bone marrow stromal stem cells and poly(glycerol sebacate) scaffolds.', *European cells & materials*. Scotland, 27, pp. 13–15.

Ding, D.-C. et al. (2011) 'Mesenchymal Stem Cells', *Cell Transplantation*, 20(1), pp. 5–14.

Ding, Y. *et al.* (2014) 'Gold Nanoparticles for Nucleic Acid Delivery', *Mol Ther*. The American Society of Gene & Cell Therapy, 22(6), pp. 1075–1083. Available at: http://dx.doi.org/10.1038/mt.2014.30.

Djuranovic, S., Nahvi, A. and Green, R. (2012) 'miRNA-Mediated Gene Silencing by Translational Repression Followed by mRNA Deadenylation and Decay', *Science*, 336(6078), pp.

237–240.

Doan, T. K. P. *et al.* (2012) ‘Inhibition of JNK and ERK pathways by SP600125- and U0126-enhanced osteogenic differentiation of bone marrow stromal cells’, *Tissue Engineering and Regenerative Medicine*, 9(6), pp. 283–294. doi: 10.1007/s13770-012-0352-6.

Dobreva, G. *et al.* (2006) ‘SATB2 Is a Multifunctional Determinant of Craniofacial Patterning and Osteoblast Differentiation’, *Cell*, 125(5), pp. 971–986. doi: http://dx.doi.org/10.1016/j.cell.2006.05.012.

Dominici, M. *et al.* (2006) ‘Minimal criteria for defining multipotent mesenchymal stromal cells. The International Society for Cellular Therapy position statement.’, *Cytotherapy*. England, 8(4), pp. 315–317. doi: 10.1080/14653240600855905.

Dorrance, A. M. *et al.* (2015) ‘Targeting Leukemia Stem Cells in vivo with AntagomiR-126 Nanoparticles in Acute Myeloid Leukemia’, *Leukemia*, 29(11), pp. 2143–2153. doi: 10.1038/leu.2015.139.

Dreaden, E. C. *et al.* (2011) ‘Beating cancer in multiple ways using nanogold.’, *Chemical Society reviews*. England, 40(7), pp. 3391–3404. doi: 10.1039/c0cs00180e.

Dreaden, E. C., Austin, L. A., *et al.* (2012) ‘Size matters: gold nanoparticles in targeted cancer drug delivery’, *Therapeutic delivery*, 3(4), pp. 457–478. Available at: http://www.ncbi.nlm.nih.gov/pmc/articles/PMC3596176/.

Dreaden, E. C., Alkilany, A. M., *et al.* (2012) ‘The golden age: gold nanoparticles for biomedicine’, *Chemical Society Reviews*. The Royal Society of Chemistry, 41(7), pp. 2740–2779. doi: 10.1039/C1CS15237H.

Duarte Campos, D. F. *et al.* (2014) ‘The Stiffness and Structure of Three-Dimensional Printed Hydrogels Direct the Differentiation of Mesenchymal Stromal Cells Toward Adipogenic and Osteogenic Lineages’, *Tissue Engineering Part A*. Mary Ann Liebert, Inc., publishers, 21(3–4), pp. 740–756. doi: 10.1089/ten.tea.2014.0231.

Dy, P. *et al.* (2012) ‘Sox9 directs hypertrophic maturation and blocks osteoblast differentiation of growth plate chondrocytes.’, *Developmental cell*. United States, 22(3), pp. 597–609. doi: 10.1016/j.devcel.2011.12.024.

Dykman, L. A. and Khlebtsov, N. G. (2014) ‘Uptake of engineered gold nanoparticles into mammalian cells.’, *Chemical reviews*. United States, 114(2), pp. 1258–1288. doi: 10.1021/cr300441a.

Dzmitruk, V. *et al.* (2018) ‘Dendrimers Show Promise for siRNA and microRNA Therapeutics’, *Pharmaceutics*. MDPI, 10(3), p. 126. doi: 10.3390/pharmaceutics10030126.

Eastment, C. *et al.* (1982) ‘In vitro proliferation of hematopoietic stem cells in the absence of an adherent monolayer’, *Blood*, 60(1), pp. 130 LP – 135. Available at: http://www.bloodjournal.org/content/60/1/130.abstract.

Ebert, M. S., Neilson, J. R. and Sharp, P. A. (2007) ‘MicroRNA sponges: competitive inhibitors of small RNAs in mammalian cells’, *Nat Meth*, 4(9), pp. 721–726.

Ebert, M. S. and Sharp, P. A. (2010) ‘MicroRNA sponges: Progress and possibilities’, *RNA* , 16(11), pp. 2043–2050. doi: 10.1261/rna.2414110.

Engler, A. J. *et al.* (2006) ‘Matrix elasticity directs stem cell lineage specification.’, *Cell*. United States, 126(4), pp. 677–689. doi: 10.1016/j.cell.2006.06.044.

Esau, C. *et al.* (2004) ‘MicroRNA-143 Regulates Adipocyte Differentiation’, *Journal of Biological Chemistry* , 279(50), pp. 52361–52365. doi: 10.1074/jbc.C400438200.

Fiume, R. *et al.* (2012) ‘Nuclear Phosphoinositides: Location, Regulation and Function BT - Phosphoinositides II: The Diverse Biological Functions’, in Balla, T., Wymann, M., and York, J.

D. (eds). Dordrecht: Springer Netherlands, pp. 335–361. doi: 10.1007/978-94-007-3015-1_11.

Fontaine, C. *et al.* (2008) 'Hedgehog Signaling Alters Adipocyte Maturation of Human Mesenchymal Stem Cells', *STEM CELLS*. John Wiley & Sons, Ltd, 26(4), pp. 1037–1046. doi: 10.1634/stemcells.2007-0974.

Formstecher, E. *et al.* (2006) 'Combination of active and inactive siRNA targeting the mitotic kinesin Eg5 impairs silencing efficiency in several cancer cell lines.', *Oligonucleotides*. United States, 16(4), pp. 387–394. doi: 10.1089/oli.2006.16.387.

Freiesleben, S. *et al.* (2016) 'Analysis of microRNA and Gene Expression Profiles in Multiple Sclerosis: Integrating Interaction Data to Uncover Regulatory Mechanisms', *Scientific Reports*, 6(1), p. 34512. doi: 10.1038/srep34512.

Friedenstein, A. J., Chailakhjan, R. K. and Lalykina, K. S. (1970) 'THE DEVELOPMENT OF FIBROBLAST COLONIES IN MONOLAYER CULTURES OF GUINEA-PIG BONE MARROW AND SPLEEN CELLS', *Cell Proliferation*. John Wiley & Sons, Ltd (10.1111), 3(4), pp. 393–403. doi: 10.1111/j.1365-2184.1970.tb00347.x.

Friedenstein, A. J., Chailakhyan, R. K. and Gerasimov, U. V (1987) 'Bone marrow osteogenic stem cells: in vitro cultivation and transplantation in diffusion chambers', *Cell Proliferation*. John Wiley & Sons, Ltd (10.1111), 20(3), pp. 263–272. doi: 10.1111/j.1365-2184.1987.tb01309.x.

Friedman, R. C. *et al.* (2009) 'Most mammalian mRNAs are conserved targets of microRNAs.', *Genome research*. United States, 19(1), pp. 92–105. doi: 10.1101/gr.082701.108.

Fu, J.-D. *et al.* (2013) 'Direct Reprogramming of Human Fibroblasts toward a Cardiomyocyte-like State', *Stem Cell Reports*. Elsevier, 1(3), pp. 235–247. doi: 10.1016/j.stemcr.2013.07.005.

Funk, J. R. *et al.* (2000) 'Biomechanical evaluation of early fracture healing in normal and diabetic rats', *Journal of Orthopaedic Research*. John Wiley & Sons, Ltd, 18(1), pp. 126–132. doi: 10.1002/jor.1100180118.

Galván, J. A. *et al.* (2014) 'Validation of COL11A1/procollagen 11A1 expression in TGF-β1-activated immortalised human mesenchymal cells and in stromal cells of human colon adenocarcinoma', *BMC cancer*. BioMed Central, 14, p. 867. doi: 10.1186/1471-2407-14-867.

Gao, J. *et al.* (2011) 'MicroRNA expression during osteogenic differentiation of human multipotent mesenchymal stromal cells from bone marrow', *Journal of Cellular Biochemistry*. Wiley Subscription Services, Inc., A Wiley Company, 112(7), pp. 1844–1856. doi: 10.1002/jcb.23106.

Ghosh, P. *et al.* (2008) 'Gold nanoparticles in delivery applications', *Advanced Drug Delivery Reviews*, 60(11), pp. 1307–1315. doi: http://dx.doi.org/10.1016/j.addr.2008.03.016.

Giner-Casares, J. J. *et al.* (2016) 'Inorganic nanoparticles for biomedicine: where materials scientists meet medical research', *Materials Today*, 19(1), pp. 19–28. doi: https://doi.org/10.1016/j.mattod.2015.07.004.

Grayson, W. L. *et al.* (2015) 'Stromal cells and stem cells in clinical bone regeneration', *Nature Reviews Endocrinology*. Nature Publishing Group, a division of Macmillan Publishers Limited. All Rights Reserved., 11, p. 140. Available at: https://doi.org/10.1038/nrendo.2014.234.

Guilak, F. *et al.* (2009) 'Control of Stem Cell Fate by Physical Interactions with the Extracellular Matrix', *Cell Stem Cell*, 5(1), pp. 17–26. doi: https://doi.org/10.1016/j.stem.2009.06.016.

Guillotin, B. *et al.* (2004) 'Human primary endothelial cells stimulate human osteoprogenitor cell differentiation.', *Cellular physiology and biochemistry : international journal of experimental cellular physiology, biochemistry, and pharmacology*. Germany, 14(4–6), pp. 325–332. doi: 10.1159/000080342.

Guo, H. *et al.* (2010) 'Mammalian microRNAs predominantly act to decrease target mRNA levels', *Nature*, 466. doi: 10.1038/nature09267.

Gupta, R. K. (2014) ‘Adipocytes.’, *Current biology : CB*. England, 24(20), pp. R988-93. doi: 10.1016/j.cub.2014.09.003.

Ha, M. and Kim, V. N. (2014) ‘Regulation of microRNA biogenesis’, *Nat Rev Mol Cell Biol*. Nature Publishing Group, a division of Macmillan Publishers Limited. All Rights Reserved., 15(8), pp. 509–524.

Hall, B. K. (1979) ‘Selective proliferation and accumulation of chondroprogenitor cells as the mode of action of biomechanical factors during secondary chondrogenesis.’, *Teratology*. United States, 20(1), pp. 81–91. doi: 10.1002/tera.1420200112.

Hao, L. *et al.* (2011) ‘Nucleic Acid–Gold Nanoparticle Conjugates as Mimics of microRNA’, *Small*. John Wiley & Sons, Ltd, 7(22), pp. 3158–3162. doi: 10.1002/smll.201101018.

Hassan, M. Q. *et al.* (2010) ‘A network connecting Runx2, SATB2, and the miR-23a~27a~24-2 cluster regulates the osteoblast differentiation program.’, *Proceedings of the National Academy of Sciences of the United States of America*. United States, 107(46), pp. 19879–19884. doi: 10.1073/pnas.1007698107.

Hayes, J., Peruzzi, P. P. and Lawler, S. (2014) ‘MicroRNAs in cancer: biomarkers, functions and therapy’, *Trends in Molecular Medicine*. Elsevier, 20(8), pp. 460–469. doi: 10.1016/j.molmed.2014.06.005.

Hayrapetyan, A., Jansen, J. A. and van den Beucken, J. J. J. P. (2014) ‘Signaling Pathways Involved in Osteogenesis and Their Application for Bone Regenerative Medicine’, *Tissue Engineering Part B: Reviews*. Mary Ann Liebert, Inc., publishers, 21(1), pp. 75–87. doi: 10.1089/ten.teb.2014.0119.

He, X. *et al.* (2014) ‘Enhanced Healing of Rat Calvarial Defects with MSCs Loaded on BMP-2 Releasing Chitosan/Alginate/Hydroxyapatite Scaffolds’, *PLOS ONE*. Public Library of Science, 9(8), p. e104061. Available at: https://doi.org/10.1371/journal.pone.0104061.

Herlofsen, S. R. *et al.* (2011) ‘Chondrogenic differentiation of human bone marrow-derived mesenchymal stem cells in self-gelling alginate discs reveals novel chondrogenic signature gene clusters.’, *Tissue engineering. Part A*. United States, 17(7–8), pp. 1003–1013. doi: 10.1089/ten.TEA.2010.0499.

Heydari Asl, S. *et al.* (2018) ‘Physical stimulation and scaffold composition efficiently support osteogenic differentiation of mesenchymal stem cells’, *Tissue and Cell*, 50, pp. 1–7. doi: https://doi.org/10.1016/j.tice.2017.11.001.

Higuchi, A. *et al.* (2013) ‘Physical Cues of Biomaterials Guide Stem Cell Differentiation Fate’, *Chemical Reviews*. American Chemical Society, 113(5), pp. 3297–3328. doi: 10.1021/cr300426x.

Hu, N. *et al.* (2015) ‘Regulative Effect of Mir-205 on Osteogenic Differentiation of Bone Mesenchymal Stem Cells (BMSCs): Possible Role of SATB2/Runx2 and ERK/MAPK Pathway’, *International Journal of Molecular Sciences*. Edited by M. Pichler. MDPI, 16(5), pp. 10491–10506. doi: 10.3390/ijms160510491.

Huaizhi, Z. and Yuantao, N. (2001) ‘China’s ancient gold drugs’, *Gold Bulletin*, 34(1), pp. 24–29. doi: 10.1007/BF03214805.

Huang, S. *et al.* (2012) ‘miR-143 and miR-145 inhibit stem cell characteristics of PC-3 prostate cancer cells.’, *Oncology reports*. Greece, 28(5), pp. 1831–1837. doi: 10.3892/or.2012.2015.

Hulkoti, N. I. and Taranath, T. C. (2014) ‘Biosynthesis of nanoparticles using microbes—A review’, *Colloids and Surfaces B: Biointerfaces*, 121, pp. 474–483. doi: http://dx.doi.org/10.1016/j.colsurfb.2014.05.027.

Hwang, K.-C. *et al.* (2008) ‘Chemicals that modulate stem cell differentiation’, *Proceedings of the National Academy of Sciences of the United States of America*. 2008/05/14. National Academy of Sciences, 105(21), pp. 7467–7471. doi: 10.1073/pnas.0802825105.

Ito, T. *et al.* (2008) 'FGF-2 increases osteogenic and chondrogenic differentiation potentials of human mesenchymal stem cells by inactivation of TGF-beta signaling', *Cytotechnology*. 2007/10/18. Springer Netherlands, 56(1), pp. 1–7. doi: 10.1007/s10616-007-9092-1.

James, A. W. (2013) 'Review of Signaling Pathways Governing MSC Osteogenic and Adipogenic Differentiation.', *Scientifica*. Egypt, 2013, p. 684736. doi: 10.1155/2013/684736.

Jensen, K., Anderson, J. A. and Glass, E. J. (2014) 'Comparison of small interfering RNA (siRNA) delivery into bovine monocyte-derived macrophages by transfection and electroporation', *Veterinary Immunology and Immunopathology*. Elsevier Scientific, 158(3–4), pp. 224–232. doi: 10.1016/j.vetimm.2014.02.002.

Ji, H. *et al.* (2014) 'Rho/Rock cross-talks with transforming growth factor-beta/Smad pathway participates in lung fibroblast-myofibroblast differentiation.', *Biomedical reports*. England, 2(6), pp. 787–792. doi: 10.3892/br.2014.323.

Ji, X. *et al.* (2007) 'Size Control of Gold Nanocrystals in Citrate Reduction: The Third Role of Citrate', *Journal of the American Chemical Society*. American Chemical Society, 129(45), pp. 13939–13948. doi: 10.1021/ja074447k.

Jing, D. *et al.* (2015) 'The role of microRNAs in bone remodeling', *In J Oral Sci*. West China School of Stomatology, 7(3), pp. 131–143. Available at: http://dx.doi.org/10.1038/ijos.2015.22.

Jonas, S. and Izaurralde, E. (2015) 'Towards a molecular understanding of microRNA-mediated gene silencing', *Nat Rev Genet*. Nature Publishing Group, a division of Macmillan Publishers Limited. All Rights Reserved., 16(7), pp. 421–433.

Kafshgari, M. H., Harding, F. J. and Voelcker, N. H. (2015) 'Insights into cellular uptake of nanoparticles.', *Current drug delivery*. United Arab Emirates, 12(1), pp. 63–77.

Kamaly, N. and Miller, A. D. (2010) 'Paramagnetic liposome nanoparticles for cellular and tumour imaging', *International journal of molecular sciences*. Molecular Diversity Preservation International (MDPI), 11(4), pp. 1759–1776. doi: 10.3390/ijms11041759.

Kamon, J. *et al.* (2003) '[The mechanisms by which PPARgamma and adiponectin regulate glucose and lipid metabolism]', *Nihon yakurigaku zasshi. Folia pharmacologica Japonica*, 122(4), p. 294—300. doi: 10.1254/fpj.122.294.

Kanellopoulou, C. *et al.* (2005) 'Dicer-deficient mouse embryonic stem cells are defective in differentiation and centromeric silencing.', *Genes & development*. United States, 19(4), pp. 489–501. doi: 10.1101/gad.1248505.

Kang, L. *et al.* (2016) 'MicroRNA-23a-3p promotes the development of osteoarthritis by directly targeting SMAD3 in chondrocytes', *Biochemical and Biophysical Research Communications*, 478(1), pp. 467–473. doi: https://doi.org/10.1016/j.bbrc.2016.06.071.

Kapinas, K., Kessler, C. B. and Delany, A. M. (2009) 'miR-29 suppression of osteonectin in osteoblasts: Regulation during differentiation and by canonical Wnt signaling', *Journal of Cellular Biochemistry*. Wiley Subscription Services, Inc., A Wiley Company, 108(1), pp. 216–224. doi: 10.1002/jcb.22243.

Karbiener, M. *et al.* (2009) 'microRNA miR-27b impairs human adipocyte differentiation and targets PPARγ', *Biochemical and Biophysical Research Communications*, 390(2), pp. 247–251. doi: http://dx.doi.org/10.1016/j.bbrc.2009.09.098.

Kasper, G. *et al.* (2007) 'Mesenchymal stem cells regulate angiogenesis according to their mechanical environment.', *Stem cells (Dayton, Ohio)*. United States, 25(4), pp. 903–910. doi: 10.1634/stemcells.2006-0432.

Kavalkovich, K. W. *et al.* (2002) 'Chondrogenic differentiation of human mesenchymal stem cells within an alginate layer culture system.', *In vitro cellular & developmental biology. Animal*. Germany, 38(8), pp. 457–466.

Kenyon, J. D. *et al.* (2019) ‘Analysis of -5p and -3p Strands of miR-145 and miR-140 During Mesenchymal Stem Cell Chondrogenic Differentiation.’, *Tissue engineering. Part A*. United States, 25(1–2), pp. 80–90. doi: 10.1089/ten.TEA.2017.0440.

Khan, H. A. *et al.* (2018) ‘14 - Nanoparticles for biomedical applications: An overview’, in Narayan, R. B. T.-N. (ed.). Woodhead Publishing, pp. 357–384. doi: https://doi.org/10.1016/B978-0-08-100716-7.00014-3.

Khan, M. S., Vishakante, G. D. and Siddaramaiah, H. (2013) ‘Gold nanoparticles: a paradigm shift in biomedical applications.’, *Advances in colloid and interface science*. Netherlands, 199–200, pp. 44–58. doi: 10.1016/j.cis.2013.06.003.

Kharissova, O. V *et al.* (2013) ‘The greener synthesis of nanoparticles’, *Trends in Biotechnology*, 31(4), pp. 240–248. doi: http://dx.doi.org/10.1016/j.tibtech.2013.01.003.

Khlebtsov, N. and Dykman, L. (2011) ‘Biodistribution and toxicity of engineered gold nanoparticles: a review of in vitro and in vivo studies.’, *Chemical Society reviews*. England, 40(3), pp. 1647–1671. doi: 10.1039/c0cs00018c.

Kilian, K. A. *et al.* (2010) ‘Geometric cues for directing the differentiation of mesenchymal stem cells’, *Proceedings of the National Academy of Sciences of the United States of America*. National Academy of Sciences, 107(11), pp. 4872–4877. doi: 10.1073/pnas.0903269107.

Kim, K.-Y. *et al.* (2005) ‘Disease-associated mutations and alternative splicing alter the enzymatic and motile activity of nonmuscle myosins II-B and II-C.’, *The Journal of biological chemistry*. United States, 280(24), pp. 22769–22775. doi: 10.1074/jbc.M503488200.

Knight, S. W. and Bass, B. L. (2001) ‘A Role for the RNase III Enzyme DCR-1 in RNA Interference and Germ Line Development in Caenorhabditis elegans’, *Science*. American Association for the Advancement of Science, 293(5538), pp. 2269–2271. doi: 10.1126/science.1062039.

Knoblich, J. A. (2008) ‘Mechanisms of Asymmetric Stem Cell Division’, *Cell*, 132(4), pp. 583–597. doi: https://doi.org/10.1016/j.cell.2008.02.007.

Koh, W. *et al.* (2010) ‘Analysis of deep sequencing microRNA expression profile from human embryonic stem cells derived mesenchymal stem cells reveals possible role of let-7 microRNA family in downstream targeting of hepatic nuclear factor 4 alpha.’, *BMC genomics*. England, 11 Suppl 1, p. S6. doi: 10.1186/1471-2164-11-S1-S6.

van der Kraan, P. M. *et al.* (2009) ‘TGF-beta signaling in chondrocyte terminal differentiation and osteoarthritis: Modulation and integration of signaling pathways through receptor-Smads’, *Osteoarthritis and Cartilage*, 17(12), pp. 1539–1545. doi: http://dx.doi.org/10.1016/j.joca.2009.06.008.

Krutzfeldt, J. *et al.* (2005) ‘Silencing of microRNAs in vivo with “antagomirs”.’, *Nature*. England, 438(7068), pp. 685–689. doi: 10.1038/nature04303.

Kshitiz *et al.* (2012) ‘Control of stem cell fate and function by engineering physical microenvironments’, *Integrative biology : quantitative biosciences from nano to macro*, 4(9), pp. 1008–1018. doi: 10.1039/c2ib20080e.

Kubosch, E. J. *et al.* (2016) ‘Clinical outcome and T2 assessment following autologous matrix-induced chondrogenesis in osteochondral lesions of the talus.’, *International orthopaedics*. Germany, 40(1), pp. 65–71. doi: 10.1007/s00264-015-2988-z.

Kumar, A., Placone, J. K. and Engler, A. J. (2017) ‘Understanding the extracellular forces that determine cell fate and maintenance’, *Development (Cambridge, England)*. The Company of Biologists Ltd, 144(23), pp. 4261–4270. doi: 10.1242/dev.158469.

Kumar, D., Meenan, B. J. and Dixon, D. (2012) ‘Glutathione-mediated release of Bodipy® from PEG cofunctionalized gold nanoparticles’, *International journal of nanomedicine*. 2012/07/25. Dove Medical Press, 7, pp. 4007–4022. doi: 10.2147/IJN.S33726.

Kumar, R. M. *et al.* (2014) 'Deconstructing transcriptional heterogeneity in pluripotent stem cells', *Nature*, 516(7529), pp. 56–61. doi: 10.1038/nature13920.

Kuznetsov, S. A. *et al.* (1997) 'Single-Colony Derived Strains of Human Marrow Stromal Fibroblasts Form Bone After Transplantation In Vivo', *Journal of Bone and Mineral Research*. John Wiley & Sons, Ltd, 12(9), pp. 1335–1347. doi: 10.1359/jbmr.1997.12.9.1335.

Kwak, P. B. and Tomari, Y. (2012) 'The N domain of Argonaute drives duplex unwinding during RISC assembly', *Nat Struct Mol Biol*. Nature Publishing Group, a division of Macmillan Publishers Limited. All Rights Reserved., 19(2), pp. 145–151.

Lai, E. C. *et al.* (2003) 'Computational identification of Drosophila microRNA genes', *Genome Biol*, 4. doi: 10.1186/gb-2003-4-7-r42.

Lai, P.-L. *et al.* (2017) 'Efficient Generation of Chemically Induced Mesenchymal Stem Cells from Human Dermal Fibroblasts', *Scientific Reports*. The Author(s), 7, p. 44534. Available at: https://doi.org/10.1038/srep44534.

Lamond, A. I. and Sproat, B. S. (1993) 'Antisense oligonucleotides made of 2'-O-alkylRNA: their properties and applications in RNA biochemistry.', *FEBS letters*. NETHERLANDS, 325(1–2), pp. 123–127.

Landthaler, M., Yalcin, A. and Tuschl, T. (2004) 'The Human DiGeorge Syndrome Critical Region Gene 8 and Its D. melanogaster Homolog Are Required for miRNA Biogenesis', *Current Biology*, 14(23), pp. 2162–2167. doi: http://dx.doi.org/10.1016/j.cub.2004.11.001.

Langenbach, F. and Handschel, J. (2013) 'Effects of dexamethasone, ascorbic acid and beta-glycerophosphate on the osteogenic differentiation of stem cells in vitro.', *Stem cell research & therapy*. England, 4(5), p. 117. doi: 10.1186/scrt328.

Lee, S. K.-W. *et al.* (2011) 'MicroRNA-145 regulates human corneal epithelial differentiation.', *PloS one*. United States, 6(6), p. e21249. doi: 10.1371/journal.pone.0021249.

Leeman, K. T. *et al.* (2019) 'Mesenchymal Stem Cells Increase Alveolar Differentiation in Lung Progenitor Organoid Cultures', *Scientific Reports*, 9(1), p. 6479. doi: 10.1038/s41598-019-42819-1.

Lefebvre, V. and de Crombrugghe, B. (1998) 'Toward understanding SOX9 function in chondrocyte differentiation.', *Matrix biology : journal of the International Society for Matrix Biology*. Netherlands, 16(9), pp. 529–540. doi: 10.1016/s0945-053x(98)90065-8.

Lefebvre, V. and Smits, P. (2005) 'Transcriptional control of chondrocyte fate and differentiation', *Birth Defects Research Part C: Embryo Today: Reviews*. Wiley Subscription Services, Inc., A Wiley Company, 75(3), pp. 200–212. doi: 10.1002/bdrc.20048.

Lefterova, M. I. *et al.* (2008) 'PPARγ and C/EBP factors orchestrate adipocyte biology via adjacent binding on a genome-wide scale', *Genes & Development* , 22(21), pp. 2941–2952. doi: 10.1101/gad.1709008.

Legendre, F. *et al.* (2017) 'Enhanced chondrogenesis of bone marrow-derived stem cells by using a combinatory cell therapy strategy with BMP-2/TGF-β1, hypoxia, and COL1A1/HtrA1 siRNAs', *Scientific Reports*, 7(1), p. 3406. doi: 10.1038/s41598-017-03579-y.

Li, D. *et al.* (2011) 'Role of mechanical factors in fate decisions of stem cells', *Regenerative medicine*, 6(2), pp. 229–240. doi: 10.2217/rme.11.2.

Li, H. *et al.* (2016) 'Isolation and characterization of primary bone marrow mesenchymal stromal cells', *Annals of the New York Academy of Sciences*. John Wiley & Sons, Ltd (10.1111), 1370(1), pp. 109–118. doi: 10.1111/nyas.13102.

Li, X. *et al.* (2017) 'MicroRNA-21 promotes osteogenesis of bone marrow mesenchymal stem cells via the Smad7-Smad1/5/8-Runx2 pathway.', *Biochemical and biophysical research communications*. United States, 493(2), pp. 928–933. doi: 10.1016/j.bbrc.2017.09.119.

Li, Z. and Rana, T. M. (2014) 'Therapeutic targeting of microRNAs: current status and future challenges', *Nat Rev Drug Discov*. Nature Publishing Group, a division of Macmillan Publishers Limited. All Rights Reserved., 13(8), pp. 622–638. Available at: http://dx.doi.org/10.1038/nrd4359.

Liao, J. *et al.* (2014) 'Sox9 Potentiates BMP2-Induced Chondrogenic Differentiation and Inhibits BMP2-Induced Osteogenic Differentiation', *PLoS ONE*. Public Library of Science, 9(2), pp. 1–13. doi: 10.1371/journal.pone.0089025.

Liao, X.-B. *et al.* (2013) 'MiR-133a Modulates Osteogenic Differentiation of Vascular Smooth Muscle Cells', *Endocrinology*. The Endocrine Society, 154(9), pp. 3344–3352. doi: 10.1210/en.2012-2236.

Lim, L. P. *et al.* (2005) 'Microarray analysis shows that some microRNAs downregulate large numbers of target mRNAs', *Nature*, 433. doi: 10.1038/nature03315.

Lin, E. A. *et al.* (2009) 'miR-199a, a bone morphogenic protein 2-responsive MicroRNA, regulates chondrogenesis via direct targeting to Smad1.', *The Journal of biological chemistry*. United States, 284(17), pp. 11326–11335. doi: 10.1074/jbc.M807709200.

Lin, G. *et al.* (2011) 'Tissue Distribution of Mesenchymal Stem Cell Marker Stro-1', *Stem Cells and Development*. Mary Ann Liebert, Inc., publishers, 20(10), pp. 1747–1752. doi: 10.1089/scd.2010.0564.

Lin, G. L. and Hankenson, K. D. (2011) 'Integration of BMP, Wnt, and notch signaling pathways in osteoblast differentiation', *Journal of Cellular Biochemistry*. John Wiley & Sons, Ltd, 112(12), pp. 3491–3501. doi: 10.1002/jcb.23287.

Lin, H.-Y. *et al.* (2010) 'Fibronectin and laminin promote differentiation of human mesenchymal stem cells into insulin producing cells through activating Akt and ERK', *Journal of Biomedical Science*, 17(1), p. 56. doi: 10.1186/1423-0127-17-56.

Lin, Q. *et al.* (2009) 'A role of miR-27 in the regulation of adipogenesis', *FEBS Journal*. Blackwell Publishing Ltd, 276(8), pp. 2348–2358. doi: 10.1111/j.1742-4658.2009.06967.x.

Ling, H.-Y. *et al.* (2011) 'MicroRNA-375 promotes 3T3-L1 adipocyte differentiation through modulation of extracellular signal-regulated kinase signalling', *Clinical and Experimental Pharmacology and Physiology*. John Wiley & Sons, Ltd (10.1111), 38(4), pp. 239–246. doi: 10.1111/j.1440-1681.2011.05493.x.

Liu, K. *et al.* (2016) 'Chemical Modulation of Cell Fate in Stem Cell Therapeutics and Regenerative Medicine', *Cell Chemical Biology*, 23(8), pp. 893–916. doi: https://doi.org/10.1016/j.chembiol.2016.07.007.

Liu, X. *et al.* (2019) 'Heterogeneity of MSC: Origin, Molecular Identities, and Functionality', *Stem cells international*. Hindawi, 2019, p. 9281520. doi: 10.1155/2019/9281520.

Liu, Y. *et al.* (2011) 'MiR-17 modulates osteogenic differentiation through a coherent feed-forward loop in mesenchymal stem cells isolated from periodontal ligaments of patients with periodontitis.', *Stem cells (Dayton, Ohio)*. United States, 29(11), pp. 1804–1816. doi: 10.1002/stem.728.

Llopis-Hernández, V. *et al.* (2015) 'Material-based strategies to engineer fibronectin matrices for regenerative medicine', *International Materials Reviews*. Taylor & Francis, 60(5), pp. 245–264. doi: 10.1179/1743280414Y.0000000049.

Loo, C. *et al.* (2004) 'Nanoshell-enabled photonics-based imaging and therapy of cancer.', *Technology in cancer research & treatment*. United States, 3(1), pp. 33–40. doi: 10.1177/153303460400300104.

Loo, C. *et al.* (2005) 'Immunotargeted nanoshells for integrated cancer imaging and therapy.', *Nano letters*. United States, 5(4), pp. 709–711. doi: 10.1021/nl050127s.

Lou, G. *et al.* (2015) 'Differential distribution of U6 (RNU6-1) expression in human carcinoma tissues demonstrates the requirement for caution in the internal control gene selection for microRNA quantification.', *International journal of molecular medicine*. Greece, 36(5), pp. 1400–1408. doi: 10.3892/ijmm.2015.2338.

Macia, E. *et al.* (2006) 'Dynasore, a cell-permeable inhibitor of dynamin.', *Developmental cell*. United States, 10(6), pp. 839–850. doi: 10.1016/j.devcel.2006.04.002.

Mackie, E. J. *et al.* (2008) 'Endochondral ossification: How cartilage is converted into bone in the developing skeleton', *The International Journal of Biochemistry & Cell Biology*, 40(1), pp. 46–62. doi: https://doi.org/10.1016/j.biocel.2007.06.009.

Magne, D. *et al.* (2005) 'Mesenchymal stem cell therapy to rebuild cartilage', *Trends in Molecular Medicine*, 11(11), pp. 519–526. doi: https://doi.org/10.1016/j.molmed.2005.09.002.

Manning, C. N. *et al.* (2015) 'Adipose-derived mesenchymal stromal cells modulate tendon fibroblast responses to macrophage-induced inflammation in vitro', *Stem cell research & therapy*. BioMed Central, 6(1), p. 74. doi: 10.1186/s13287-015-0059-4.

Manochantr, S. *et al.* (2017) 'The Effects of BMP-2, miR-31, miR-106a, and miR-148a on Osteogenic Differentiation of MSCs Derived from Amnion in Comparison with MSCs Derived from the Bone Marrow', *Stem cells international*. 2017/11/19. Hindawi, 2017, p. 7257628. doi: 10.1155/2017/7257628.

Manoharan, M. (1999) '2′-Carbohydrate modifications in antisense oligonucleotide therapy: importance of conformation, configuration and conjugation', *Biochimica et Biophysica Acta (BBA) - Gene Structure and Expression*, 1489(1), pp. 117–130. doi: http://dx.doi.org/10.1016/S0167-4781(99)00138-4.

Manson, J. *et al.* (2011) 'Polyethylene glycol functionalized gold nanoparticles: the influence of capping density on stability in various media', *Gold Bulletin*, 44(2), pp. 99–105. doi: 10.1007/s13404-011-0015-8.

Mariani, E., Pulsatelli, L. and Facchini, A. (2014) 'Signaling pathways in cartilage repair.', *International journal of molecular sciences*. Switzerland, 15(5), pp. 8667–8698. doi: 10.3390/ijms15058667.

Marie, P. J. (2008) 'Transcription factors controlling osteoblastogenesis', *Archives of Biochemistry and Biophysics*, 473(2), pp. 98–105. doi: http://dx.doi.org/10.1016/j.abb.2008.02.030.

Martinez-Sanchez, A., Dudek, K. A. and Murphy, C. L. (2012) 'Regulation of Human Chondrocyte Function through Direct Inhibition of Cartilage Master Regulator SOX9 by MicroRNA-145 (miRNA-145)', *The Journal of Biological Chemistry*. 9650 Rockville Pike, Bethesda, MD 20814, U.S.A.: American Society for Biochemistry and Molecular Biology, 287(2), pp. 916–924. doi: 10.1074/jbc.M111.302430.

Masanobu, K. (2013) 'Adipose tissue and bone: role of PPARγ in adipogenesis and osteogenesis', *Hormone Molecular Biology and Clinical Investigation*, p. 105. doi: 10.1515/hmbci-2013-0036.

Masè, M. *et al.* (2017) 'Selection of reference genes is critical for miRNA expression analysis in human cardiac tissue. A focus on atrial fibrillation', *Scientific Reports*, 7(1), p. 41127. doi: 10.1038/srep41127.

McBeath, R. *et al.* (2004) 'Cell shape, cytoskeletal tension, and RhoA regulate stem cell lineage commitment.', *Developmental cell*. United States, 6(4), pp. 483–495. doi: 10.1016/s1534-5807(04)00075-9.

McCully, M. *et al.* (2015) 'Significance of the balance between intracellular glutathione and polyethylene glycol for successful release of small interfering RNA from gold nanoparticles', *Nano Research*, 8(10), pp. 3281–3292. doi: 10.1007/s12274-015-0828-5.

McCully, M. *et al.* (2018) 'Nanoparticle-antagomiR based targeting of miR-31 to induce osterix and osteocalcin expression in mesenchymal stem cells', *PLOS ONE*. Public Library of Science,

13(2), p. e0192562. Available at: https://doi.org/10.1371/journal.pone.0192562.

McGregor, R. A. and Choi, M. S. (2011) 'microRNAs in the regulation of adipogenesis and obesity.', *Current molecular medicine*. Netherlands, 11(4), pp. 304–316.

McIntosh, C. M. *et al.* (2001) 'Inhibition of DNA Transcription Using Cationic Mixed Monolayer Protected Gold Clusters', *Journal of the American Chemical Society*. American Chemical Society, 123(31), pp. 7626–7629. doi: 10.1021/ja015556g.

McNamara, L. E. *et al.* (2010) 'Nanotopographical Control of Stem Cell Differentiation', *Journal of Tissue Engineering*. SAGE-Hindawi Access to Research, 2010, p. 120623. doi: 10.4061/2010/120623.

Mehlem, A. *et al.* (2013) 'Imaging of neutral lipids by oil red O for analyzing the metabolic status in health and disease', *Nat. Protocols*. Nature Publishing Group, a division of Macmillan Publishers Limited. All Rights Reserved., 8(6), pp. 1149–1154. Available at: http://dx.doi.org/10.1038/nprot.2013.055.

Meister, G. *et al.* (2004) 'Human Argonaute2 mediates RNA cleavage targeted by miRNAs and siRNAs', *Mol Cell*, 15. doi: 10.1016/j.molcel.2004.07.007.

Metzger, C. E. and Narayanan, S. A. (2019) 'The Role of Osteocytes in Inflammatory Bone Loss ', *Frontiers in Endocrinology* , p. 285. Available at: https://www.frontiersin.org/article/10.3389/fendo.2019.00285.

Michigami, T. (2014) 'Current Understanding on the Molecular Basis of Chondrogenesis', *Clinical Pediatric Endocrinology*, 23(1), pp. 1–8. doi: 10.1297/cpe.23.1.

Miyaki, S. *et al.* (2010) 'MicroRNA-140 plays dual roles in both cartilage development and homeostasis', *Genes & Development* , 24(11), pp. 1173–1185. doi: 10.1101/gad.1915510.

Molofsky, A. V, Pardal, R. and Morrison, S. J. (2004) 'Diverse mechanisms regulate stem cell self-renewal.', *Current opinion in cell biology*. England, 16(6), pp. 700–707. doi: 10.1016/j.ceb.2004.09.004.

Moreau, M. P. *et al.* (2013) 'Chronological Changes in MicroRNA Expression in the Developing Human Brain', *PLOS ONE*. Public Library of Science, 8(4), p. e60480. Available at: https://doi.org/10.1371/journal.pone.0060480.

Morrissey, D. V *et al.* (2005) 'Potent and persistent in vivo anti-HBV activity of chemically modified siRNAs', *Nat Biotech*. Nature Publishing Group, 23(8), pp. 1002–1007.

Muruganandan, S., Roman, A. A. and Sinal, C. J. (2009) 'Adipocyte differentiation of bone marrow-derived mesenchymal stem cells: cross talk with the osteoblastogenic program.', *Cellular and molecular life sciences : CMLS*. Switzerland, 66(2), pp. 236–253. doi: 10.1007/s00018-008-8429-z.

Mushahary, D. *et al.* (2018) 'Isolation, cultivation, and characterization of human mesenchymal stem cells', *Cytometry Part A*. John Wiley & Sons, Ltd, 93(1), pp. 19–31. doi: 10.1002/cyto.a.23242.

Narayanan, A. *et al.* (2019) 'Regulation of Runx2 by MicroRNAs in osteoblast differentiation', *Life Sciences*, 232, p. 116676. doi: https://doi.org/10.1016/j.lfs.2019.116676.

Nayerossadat, N., Maedeh, T. and Ali, P. A. (2012) 'Viral and nonviral delivery systems for gene delivery.', *Advanced biomedical research*. India, 1, p. 27. doi: 10.4103/2277-9175.98152.

Neve, A., Corrado, A. and Cantatore, F. P. (2011) 'Osteoblast physiology in normal and pathological conditions.', *Cell and tissue research*. Germany, 343(2), pp. 289–302. doi: 10.1007/s00441-010-1086-1.

Neves, R. P. P., Fernandes, P. A. and Ramos, M. J. (2017) 'Mechanistic insights on the reduction of glutathione disulfide by protein disulfide isomerase.', *Proceedings of the National Academy of*

Sciences of the United States of America. United States, 114(24), pp. E4724–E4733. doi: 10.1073/pnas.1618985114.

Nikukar, H. *et al.* (2013) 'Osteogenesis of mesenchymal stem cells by nanoscale mechanotransduction.', *ACS nano*. United States, 7(3), pp. 2758–2767. doi: 10.1021/nn400202j.

Nilesh Kumar Pathak, Alok Ji, R. P. S. (2014) 'Tunable Properties of Surface Plasmon Resonances: The Influence of Core–Shell Thickness and Dielectric Environment', *R.P. Plasmonics*, 9(3), pp. 651–657. doi: https://doi.org/10.1007/s11468-014-9677-4.

Nithianandarajah-Jones, G. N. *et al.* (2012) 'ERK5: structure, regulation and function.', *Cellular signalling*. England, 24(11), pp. 2187–2196. doi: 10.1016/j.cellsig.2012.07.007.

Noël, D. *et al.* (2004) 'Short-Term BMP-2 Expression Is Sufficient for In Vivo Osteochondral Differentiation of Mesenchymal Stem Cells', *STEM CELLS*. John Wiley & Sons, Ltd, 22(1), pp. 74–85. doi: 10.1634/stemcells.22-1-74.

Odorico, J. S., Kaufman, D. S. and Thomson, J. A. (2001) 'Multilineage Differentiation from Human Embryonic Stem Cell Lines', *STEM CELLS*. John Wiley & Sons, Ltd, 19(3), pp. 193–204. doi: 10.1634/stemcells.19-3-193.

Oskowitz, A. Z. *et al.* (2008) 'Human multipotent stromal cells from bone marrow and microRNA: regulation of differentiation and leukemia inhibitory factor expression.', *Proceedings of the National Academy of Sciences of the United States of America*. United States, 105(47), pp. 18372–18377. doi: 10.1073/pnas.0809807105.

Palliser, D. *et al.* (2006) 'An siRNA-based microbicide protects mice from lethal herpes simplex virus 2 infection', *Nature*, 439(7072), pp. 89–94.

Pan, X., Wang, Z.-X. and Wang, R. (2010) 'MicroRNA-21: a novel therapeutic target in human cancer.', *Cancer biology & therapy*. United States, 10(12), pp. 1224–1232. doi: 10.4161/cbt.10.12.14252.

Parekh, S. H. *et al.* (2011) 'Modulus-driven differentiation of marrow stromal cells in 3D scaffolds that is independent of myosin-based cytoskeletal tension.', *Biomaterials*. Netherlands, 32(9), pp. 2256–2264. doi: 10.1016/j.biomaterials.2010.11.065.

Park, J. *et al.* (2010) 'Intra-organ Biodistribution of Gold Nanoparticles Using Intrinsic Two-photon Induced Photoluminescence.', *Lasers in surgery and medicine*. United States, 42(7), pp. 630–639. doi: 10.1002/lsm.20935.

Pelham, R. J. J. and Wang, Y. l (1997) 'Cell locomotion and focal adhesions are regulated by substrate flexibility.', *Proceedings of the National Academy of Sciences of the United States of America*. United States, 94(25), pp. 13661–13665. doi: 10.1073/pnas.94.25.13661.

Pemberton, G. D. *et al.* (2015) 'Nanoscale stimulation of osteoblastogenesis from mesenchymal stem cells: nanotopography and nanokicking', *Nanomedicine*. Future Medicine, 10(4), pp. 547–560. doi: 10.2217/nnm.14.134.

Peng, Y. and Croce, C. M. (2016) 'The role of MicroRNAs in human cancer', *Signal Transduction and Targeted Therapy*, 1(1), p. 15004. doi: 10.1038/sigtrans.2015.4.

Phinney, D. G. and Prockop, D. J. (2007) 'Concise Review: Mesenchymal Stem/Multipotent Stromal Cells: The State of Transdifferentiation and Modes of Tissue Repair—Current Views', *STEM CELLS*. John Wiley & Sons, Ltd, 25(11), pp. 2896–2902. doi: 10.1634/stemcells.2007-0637.

Pittenger, M. F. (1998) 'No Title'.

Pittenger, M. F. *et al.* (1999) 'Multilineage Potential of Adult Human Mesenchymal Stem Cells', *Science*, 284(5411), pp. 143 LP – 147. doi: 10.1126/science.284.5411.143.

Pizzorno, J. (2014) 'Glutathione!', *Integrative medicine (Encinitas, Calif.)*. InnoVision Professional Media, 13(1), pp. 8–12. Available at:

https://www.ncbi.nlm.nih.gov/pubmed/26770075.

Polte, Jorg *et al.* (2010) 'Mechanism of gold nanoparticle formation in the classical citrate synthesis method derived from coupled in situ XANES and SAXS evaluation.', *Journal of the American Chemical Society*. United States, 132(4), pp. 1296–1301. doi: 10.1021/ja906506j.

Polte, Jörg *et al.* (2010) 'Nucleation and Growth of Gold Nanoparticles Studied via in situ Small Angle X-ray Scattering at Millisecond Time Resolution', *ACS Nano*. American Chemical Society, 4(2), pp. 1076–1082. doi: 10.1021/nn901499c.

Qiao, W., Chen, L. and Zhang, M. (2014) 'MicroRNA-205 regulates the calcification and osteoblastic differentiation of vascular smooth muscle cells.', *Cellular physiology and biochemistry : international journal of experimental cellular physiology, biochemistry, and pharmacology*. Germany, 33(6), pp. 1945–1953. doi: 10.1159/000362971.

Qu, F. *et al.* (2013) 'WNT3A modulates chondrogenesis via canonical and non-canonical Wnt pathways in MSCs', *Frontiers in bioscience (Landmark edition)*, 18, p. 493—503. doi: 10.2741/4116.

Ramalingam, P. *et al.* (2014) 'Biogenesis of intronic miRNAs located in clusters by independent transcription and alternative splicing', *RNA*. Cold Spring Harbor Laboratory Press, 20(1), pp. 76–87. doi: 10.1261/rna.041814.113.

Retting, K. N. *et al.* (2009) 'BMP canonical Smad signaling through Smad1 and Smad5 is required for endochondral bone formation.', *Development (Cambridge, England)*. England, 136(7), pp. 1093–1104. doi: 10.1242/dev.029926.

Reubinoff, B. E. *et al.* (2000) 'Embryonic stem cell lines from human blastocysts: somatic differentiation in vitro', *Nature Biotechnology*, 18(4), pp. 399–404. doi: 10.1038/74447.

Richardson, S. M. *et al.* (2010) 'Mesenchymal stem cells in regenerative medicine: opportunities and challenges for articular cartilage and intervertebral disc tissue engineering.', *Journal of cellular physiology*. United States, 222(1), pp. 23–32. doi: 10.1002/jcp.21915.

de Rie, D. *et al.* (2017) 'An integrated expression atlas of miRNAs and their promoters in human and mouse.', *Nature biotechnology*. United States, 35(9), pp. 872–878. doi: 10.1038/nbt.3947.

Riffo-Campos, Á. L., Riquelme, I. and Brebi-Mieville, P. (2016) 'Tools for Sequence-Based miRNA Target Prediction: What to Choose?', *International journal of molecular sciences*. MDPI, 17(12), p. 1987. doi: 10.3390/ijms17121987.

Robertson, S. N. *et al.* (2018) 'Control of cell behaviour through nanovibrational stimulation: nanokicking.', *Philosophical transactions. Series A, Mathematical, physical, and engineering sciences*. England, 376(2120). doi: 10.1098/rsta.2017.0290.

Roca, M. and Haes, A. J. (2008) 'Probing cells with noble metal nanoparticle aggregates.', *Nanomedicine (London, England)*. England, 3(4), pp. 555–565. doi: 10.2217/17435889.3.4.555.

Rodríguez-Carballo, E., Gámez, B. and Ventura, F. (2016) 'p38 MAPK Signaling in Osteoblast Differentiation', *Frontiers in cell and developmental biology*. Frontiers Media S.A., 4, p. 40. doi: 10.3389/fcell.2016.00040.

Romero, G. and Moya, S. E. (2012) 'Chapter 4 - Synthesis of Organic Nanoparticles', in de la Fuente, J. M. and Grazu, V. B. T.-F. of N. (eds) *Nanobiotechnology*. Elsevier, pp. 115–141. doi: https://doi.org/10.1016/B978-0-12-415769-9.00004-2.

van Rooij, E. and Olson, E. N. (2012) 'MicroRNA therapeutics for cardiovascular disease: opportunities and obstacles', *Nat Rev Drug Discov*. Nature Publishing Group, a division of Macmillan Publishers Limited. All Rights Reserved., 11(11), pp. 860–872. Available at: http://dx.doi.org/10.1038/nrd3864.

Rosen, E. D. and MacDougald, O. A. (2006) 'Adipocyte differentiation from the inside out.', *Nature reviews. Molecular cell biology*. England, 7(12), pp. 885–896. doi: 10.1038/nrm2066.

Rowlands, A. S., George, P. A. and Cooper-White, J. J. (2008) 'Directing osteogenic and myogenic differentiation of MSCs: interplay of stiffness and adhesive ligand presentation', *American Journal of Physiology-Cell Physiology*. American Physiological Society, 295(4), pp. C1037–C1044. doi: 10.1152/ajpcell.67.2008.

Royle, S. J. (2006) 'The cellular functions of clathrin', *Cellular and molecular life sciences : CMLS*, 63(16), pp. 1823–1832. doi: 10.1007/s00018-005-5587-0.

Ruby, J. G. *et al.* (2007) 'Evolution, biogenesis, expression, and target predictions of a substantially expanded set of Drosophila microRNAs', *Genome Res*, 17. doi: 10.1101/gr.6597907.

Samsonraj, R. M. *et al.* (2015) 'Establishing Criteria for Human Mesenchymal Stem Cell Potency', *STEM CELLS*. John Wiley & Sons, Ltd, 33(6), pp. 1878–1891. doi: 10.1002/stem.1982.

Schaap-Oziemlak, A. M. *et al.* (2010) 'MicroRNA hsa-miR-135b regulates mineralization in osteogenic differentiation of human unrestricted somatic stem cells.', *Stem cells and development*. United States, 19(6), pp. 877–885. doi: 10.1089/scd.2009.0112.

Scott, M. A. *et al.* (2011) 'Current Methods of Adipogenic Differentiation of Mesenchymal Stem Cells', *Stem Cells and Development*. 140 Huguenot Street, 3rd FloorNew Rochelle, NY 10801USA: Mary Ann Liebert, Inc., 20(10), pp. 1793–1804. doi: 10.1089/scd.2011.0040.

Seferos, D. S. *et al.* (2009) 'Polyvalent DNA nanoparticle conjugates stabilize nucleic acids.', *Nano letters*. United States, 9(1), pp. 308–311. doi: 10.1021/nl802958f.

Shen, G. (2005) 'The role of type X collagen in facilitating and regulating endochondral ossification of articular cartilage.', *Orthodontics & craniofacial research*. England, 8(1), pp. 11–17. doi: 10.1111/j.1601-6343.2004.00308.x.

Shi, K. *et al.* (2013) 'MicroRNA-214 suppresses osteogenic differentiation of C2C12 myoblast cells by targeting Osterix', *Bone*, 55(2), pp. 487–494. doi: https://doi.org/10.1016/j.bone.2013.04.002.

Simon, T. M. and Jackson, D. W. (2018) 'Articular Cartilage: Injury Pathways and Treatment Options', *Sports Medicine and Arthroscopy Review*, 26(1). Available at: https://journals.lww.com/sportsmedarthro/Fulltext/2018/03000/Articular_Cartilage__Injury_Pathways_and_Treatment.6.aspx.

Smith, C.-A. M. *et al.* (2010) 'The effect of static magnetic fields and tat peptides on cellular and nuclear uptake of magnetic nanoparticles', *Biomaterials*, 31(15), pp. 4392–4400. doi: https://doi.org/10.1016/j.biomaterials.2010.01.096.

Sperling, R. A. and Parak, W. J. (2010) 'Surface modification, functionalization and bioconjugation of colloidal inorganic nanoparticles', *Philosophical Transactions of the Royal Society of London A: Mathematical, Physical and Engineering Sciences*, 368(1915), pp. 1333–1383.

Steele, J. A. M. *et al.* (2012) 'Encapsulation of protein microfiber networks supporting pancreatic islets', *Journal of Biomedical Materials Research Part A*. John Wiley & Sons, Ltd, 100A(12), pp. 3384–3391. doi: 10.1002/jbm.a.34281.

Stewart, K. *et al.* (1999) 'Further characterization of cells expressing STRO-1 in cultures of adult human bone marrow stromal cells.', *Journal of bone and mineral research : the official journal of the American Society for Bone and Mineral Research*. United States, 14(8), pp. 1345–1356. doi: 10.1359/jbmr.1999.14.8.1345.

Suk, J. S. *et al.* (2016) 'PEGylation as a strategy for improving nanoparticle-based drug and gene delivery', *Advanced Drug Delivery Reviews*, 99, Part A, pp. 28–51. doi: http://dx.doi.org/10.1016/j.addr.2015.09.012.

Sun, F. *et al.* (2009) 'Characterization of function and regulation of miR-24-1 and miR-31.', *Biochemical and biophysical research communications*. United States, 380(3), pp. 660–665. doi: 10.1016/j.bbrc.2009.01.161.

Sun, T. *et al.* (2009) 'MicroRNA let-7 Regulates 3T3-L1 Adipogenesis', *Molecular Endocrinology*, 23(6), pp. 925–931. doi: 10.1210/me.2008-0298.

Sun, Z. and Komarova, N. L. (2015) 'Stochastic control of proliferation and differentiation in stem cell dynamics.', *Journal of mathematical biology*. Germany, 71(4), pp. 883–901. doi: 10.1007/s00285-014-0835-2.

Tabruyn, S. P. *et al.* (2013) 'MiR-205 is downregulated in hereditary hemorrhagic telangiectasia and impairs TGF-beta signaling pathways in endothelial cells.', *Angiogenesis*. Germany, 16(4), pp. 877–887. doi: 10.1007/s10456-013-9362-9.

Takanabe, R. *et al.* (2008) 'Up-regulated expression of microRNA-143 in association with obesity in adipose tissue of mice fed high-fat diet', *Biochemical and Biophysical Research Communications*, 376(4), pp. 728–732. doi: https://doi.org/10.1016/j.bbrc.2008.09.050.

Takarada, T. *et al.* (2013) 'An analysis of skeletal development in osteoblast-specific and chondrocyte-specific runt-related transcription factor-2 (Runx2) knockout mice.', *Journal of bone and mineral research : the official journal of the American Society for Bone and Mineral Research*. United States, 28(10), pp. 2064–2069. doi: 10.1002/jbmr.1945.

Tamayol, A. *et al.* (2013) 'Fiber-based tissue engineering: Progress, challenges, and opportunities', *Biotechnology Advances*, 31(5), pp. 669–687. doi: https://doi.org/10.1016/j.biotechadv.2012.11.007.

Thomson, J. M., Parker, J. S. and Hammond, S. M. (2007) 'Microarray analysis of miRNA gene expression.', *Methods in enzymology*. United States, 427, pp. 107–122. doi: 10.1016/S0076-6879(07)27006-5.

Thote, A. J. and Gupta, R. B. (2005) 'Formation of nanoparticles of a hydrophilic drug using supercritical carbon dioxide and microencapsulation for sustained release', *Nanomedicine: Nanotechnology, Biology and Medicine*, 1(1), pp. 85–90. doi: http://dx.doi.org/10.1016/j.nano.2004.12.001.

Trohatou, O. *et al.* (2014) 'Sox2 suppression by miR-21 governs human mesenchymal stem cell properties.', *Stem cells translational medicine*. United States, 3(1), pp. 54–68. doi: 10.5966/sctm.2013-0081.

Tsimbouri, P. *et al.* (2014) 'Nanotopographical Effects on Mesenchymal Stem Cell Morphology and Phenotype', *Journal of Cellular Biochemistry*, 115(2), pp. 380–390. doi: 10.1002/jcb.24673.

Tsimbouri, P. M. *et al.* (2017) 'Stimulation of 3D osteogenesis by mesenchymal stem cells using a nanovibrational bioreactor', *Nature Biomedical Engineering*, 1(9), pp. 758–770. doi: 10.1038/s41551-017-0127-4.

Uccelli, A., Moretta, L. and Pistoia, V. (2008) 'Mesenchymal stem cells in health and disease', *Nature Reviews Immunology*. Nature Publishing Group, 8, p. 726. Available at: https://doi.org/10.1038/nri2395.

Ullah, I., Subbarao, R. B. and Rho, G. J. (2015) 'Human mesenchymal stem cells - current trends and future prospective', *Bioscience Reports*, 35(2), p. e00191. doi: 10.1042/BSR20150025.

Vaidya, A. and Kale, V. (2015) 'Hematopoietic Stem Cells, Their Niche, and the Concept of Co-Culture Systems: A Critical Review.', *Journal of stem cells*. United States, 10(1), pp. 13–31.

Vaidyanathan, R., Curtis, A. and Mullin, M. (2011) 'Entry of large nanoparticles into cells aided by nanoscale mechanical stimulation', *Journal of Nanoparticle Research*, 13(10), pp. 5301–5309. doi: 10.1007/s11051-011-0516-7.

Valinezhad Orang, A., Safaralizadeh, R. and Kazemzadeh-Bavili, M. (2014) 'Mechanisms of miRNA-Mediated Gene Regulation from Common Downregulation to mRNA-Specific Upregulation.', *International journal of genomics*. Egypt, 2014, p. 970607. doi: 10.1155/2014/970607.

Vasudevan, S. (2012) ‘Posttranscriptional upregulation by microRNAs.’, *Wiley interdisciplinary reviews. RNA*. United States, 3(3), pp. 311–330. doi: 10.1002/wrna.121.

Verma, S. and Eckstein, F. (1998) ‘Modified oligonucleotides: synthesis and strategy for users.’, *Annual review of biochemistry*. UNITED STATES, 67, pp. 99–134. doi: 10.1146/annurev.biochem.67.1.99.

Vickers, K. C. and Remaley, A. T. (2012) ‘Lipid-based carriers of microRNAs and intercellular communication’, *Current opinion in lipidology*, 23(2), pp. 91–97. doi: 10.1097/MOL.0b013e328350a425.

Vimalraj, S. *et al.* (2015) ‘Runx2: Structure, function, and phosphorylation in osteoblast differentiation’, *International Journal of Biological Macromolecules*, 78, pp. 202–208. doi: http://dx.doi.org/10.1016/j.ijbiomac.2015.04.008.

Vinatier, C. *et al.* (2009) ‘Cartilage engineering: a crucial combination of cells, biomaterials and biofactors.’, *Trends in biotechnology*. England, 27(5), pp. 307–314. doi: 10.1016/j.tibtech.2009.02.005.

Viti, F. *et al.* (2016) ‘Osteogenic Differentiation of MSC through Calcium Signaling Activation: Transcriptomics and Functional Analysis’, *PLoS ONE*. Edited by S. Gronthos. San Francisco, CA USA: Public Library of Science, 11(2), p. e0148173. doi: 10.1371/journal.pone.0148173.

Wahid, F. *et al.* (2010) ‘MicroRNAs: Synthesis, mechanism, function, and recent clinical trials’, *Biochimica et Biophysica Acta (BBA) - Molecular Cell Research*, 1803(11), pp. 1231–1243. doi: http://dx.doi.org/10.1016/j.bbamcr.2010.06.013.

Wang, H. *et al.* (2015) ‘Recent progress in microRNA delivery for cancer therapy by non-viral synthetic vectors’, *Advanced Drug Delivery Reviews*, 81, pp. 142–160. doi: http://dx.doi.org/10.1016/j.addr.2014.10.031.

Wang, S., Qu, X. and Zhao, R. C. (2012) ‘Clinical applications of mesenchymal stem cells’, *Journal of Hematology & Oncology*, 5(1), p. 19. doi: 10.1186/1756-8722-5-19.

Wang, W. *et al.* (2013) ‘Role of thiol-containing polyethylene glycol (thiol-PEG) in the modification process of gold nanoparticles (AuNPs): stabilizer or coagulant?’, *Journal of colloid and interface science*. United States, 404, pp. 223–229. doi: 10.1016/j.jcis.2013.04.020.

Wang, X. *et al.* (2013) ‘Effect of RGD nanospacing on differentiation of stem cells’, *Biomaterials*, 34(12), pp. 2865–2874. doi: https://doi.org/10.1016/j.biomaterials.2013.01.021.

Wang, Y.-K. and Chen, C. S. (2013) ‘Cell adhesion and mechanical stimulation in the regulation of mesenchymal stem cell differentiation’, *Journal of Cellular and Molecular Medicine*. John Wiley & Sons, Ltd (10.1111), 17(7), pp. 823–832. doi: 10.1111/jcmm.12061.

Wang, Y. *et al.* (2007) ‘DGCR8 is essential for microRNA biogenesis and silencing of embryonic stem cell self-renewal.’, *Nature genetics*. United States, 39(3), pp. 380–385. doi: 10.1038/ng1969.

Wang, YanHong *et al.* (2019) ‘A Zfp609 circular RNA regulates myoblast differentiation by sponging miR-194-5p’, *International Journal of Biological Macromolecules*, 121, pp. 1308–1313. doi: https://doi.org/10.1016/j.ijbiomac.2018.09.039.

Wechsler, M. E., Hermann, B. P. and Bizios, R. (2016) ‘Adult Human Mesenchymal Stem Cell Differentiation at the Cell Population and Single-Cell Levels Under Alternating Electric Current.’, *Tissue engineering. Part C, Methods*. United States, 22(2), pp. 155–164. doi: 10.1089/ten.TEC.2015.0324.

Wei, W. *et al.* (2017) ‘miR-130a regulates differential lipid accumulation between intramuscular and subcutaneous adipose tissues of pigs via suppressing PPARG expression’, *Gene*, 636, pp. 23–29. doi: https://doi.org/10.1016/j.gene.2017.08.036.

Wen, J. H. *et al.* (2014) ‘Interplay of matrix stiffness and protein tethering in stem cell differentiation’, *Nature Materials*. Nature Publishing Group, 13, p. 979. Available at:

https://doi.org/10.1038/nmat4051.

Wilson, A. *et al.* (2019) 'Multiplicity of Mesenchymal Stromal Cells: Finding the Right Route to Therapy ', *Frontiers in Immunology* , p. 1112. Available at: https://www.frontiersin.org/article/10.3389/fimmu.2019.01112.

Wolfrum, C. *et al.* (2007) 'Mechanisms and optimization of in vivo delivery of lipophilic siRNAs', *Nat Biotech*. Nature Publishing Group, 25(10), pp. 1149–1157.

Wrobel, E., Leszczynska, J. and Brzoska, E. (2016) 'The Characteristics Of Human Bone-Derived Cells (HBDCS) during osteogenesis in vitro', *Cellular & molecular biology letters*. BioMed Central, 21, p. 26. doi: 10.1186/s11658-016-0027-8.

Wu, H. *et al.* (2009) 'Alternative Processing of Primary microRNA Transcripts by Drosha Generates 5? End Variation of Mature microRNA', *PLoS ONE*. Public Library of Science, 4(10), p. e7566.

Wuelling, M. and Vortkamp, A. (2010) 'Transcriptional networks controlling chondrocyte proliferation and differentiation during endochondral ossification.', *Pediatric nephrology (Berlin, Germany)*. Germany, 25(4), pp. 625–631. doi: 10.1007/s00467-009-1368-6.

Xie, H., Lim, B. and Lodish, H. F. (2009) 'MicroRNAs Induced During Adipogenesis that Accelerate Fat Cell Development Are Downregulated in Obesity', *Diabetes*, 58(5), pp. 1050 LP – 1057. doi: 10.2337/db08-1299.

Xie, Q. *et al.* (2014) 'Effects of miR-31 on the osteogenesis of human mesenchymal stem cells.', *Biochemical and biophysical research communications*. United States, 446(1), pp. 98–104. doi: 10.1016/j.bbrc.2014.02.058.

Xue, H.-Y. *et al.* (2016) 'Gold nanoparticles delivered miR-375 for treatment of hepatocellular carcinoma', *Oncotarget*. Impact Journals LLC, 7(52), pp. 86675–86686. doi: 10.18632/oncotarget.13431.

Yang, B. *et al.* (2011) 'MicroRNA-145 regulates chondrogenic differentiation of mesenchymal stem cells by targeting Sox9.', *PloS one*. United States, 6(7), p. e21679. doi: 10.1371/journal.pone.0021679.

Yang, J. *et al.* (2014) 'Nanotopographical Induction of Osteogenesis through Adhesion, Bone Morphogenic Protein Cosignaling, and Regulation of MicroRNAs', *ACS Nano*. American Chemical Society, 8(10), pp. 9941–9953. doi: 10.1021/nn504767g.

Yang, J. *et al.* (2015) 'The Hedgehog signalling pathway in bone formation', *International Journal Of Oral Science*. The Author(s), 7, p. 73. Available at: https://doi.org/10.1038/ijos.2015.14.

Yang, R. *et al.* (2016) 'Monte Carlo Simulation of Microscopic Dose Enhancement of Glucose Conjugated Gold Nanoparticles for the I-125 Radioactive Seeds Brachytherapy', *International Journal of Radiation Oncology • Biology • Physics*. Elsevier, 96(2), p. S170. doi: 10.1016/j.ijrobp.2016.06.427.

Yang, X. *et al.* (2003) 'Induction of human osteoprogenitor chemotaxis, proliferation, differentiation, and bone formation by osteoblast stimulating factor-1/pleiotrophin: osteoconductive biomimetic scaffolds for tissue engineering.', *Journal of bone and mineral research : the official journal of the American Society for Bone and Mineral Research*. United States, 18(1), pp. 47–57. doi: 10.1359/jbmr.2003.18.1.47.

Yang, Z. *et al.* (2011) 'MicroRNA hsa-miR-138 inhibits adipogenic differentiation of human adipose tissue-derived mesenchymal stem cells through adenovirus EID-1.', *Stem cells and development*. United States, 20(2), pp. 259–267. doi: 10.1089/scd.2010.0072.

Ye, D. *et al.* (2012) 'MiR-138 promotes induced pluripotent stem cell generation through the regulation of the p53 signaling.', *Stem cells (Dayton, Ohio)*. United States, 30(8), pp. 1645–1654. doi: 10.1002/stem.1149.

Ye, L. *et al.* (2018) 'A Simple System for Differentiation of Functional Intestinal Stem Cell-like Cells from Bone Marrow Mesenchymal Stem Cells', *Molecular Therapy - Nucleic Acids*. Elsevier, 13, pp. 110–120. doi: 10.1016/j.omtn.2018.08.017.

Yguerabide, J. and Yguerabide, E. E. (1998) 'Light-scattering submicroscopic particles as highly fluorescent analogs and their use as tracer labels in clinical and biological applications.', *Analytical biochemistry*. United States, 262(2), pp. 137–156. doi: 10.1006/abio.1998.2759.

Yoo, J. U. *et al.* (1998) 'The Chondrogenic Potential of Human Bone-Marrow-Derived Mesenchymal Progenitor Cells*', *JBJS*, 80(12). Available at: https://journals.lww.com/jbjsjournal/Fulltext/1998/12000/The_Chondrogenic_Potential_of_Human.4.aspx.

Young, H. E. *et al.* (1995) 'Mesenchymal stem cells reside within the connective tissues of many organs', *Developmental Dynamics*. John Wiley & Sons, Ltd, 202(2), pp. 137–144. doi: 10.1002/aja.1002020205.

Younger, S. T. and Corey, D. R. (2011) 'Transcriptional gene silencing in mammalian cells by miRNA mimics that target gene promoters', *Nucleic Acids Research*, 39(13), pp. 5682–5691. doi: 10.1093/nar/gkr155.

Yu, F. *et al.* (2010) 'Mir-30 reduction maintains self-renewal and inhibits apoptosis in breast tumor-initiating cells.', *Oncogene*. England, 29(29), pp. 4194–4204. doi: 10.1038/onc.2010.167.

Yu, T. *et al.* (2018) 'Functions and mechanisms of microRNA-31 in human cancers', *Biomedicine & Pharmacotherapy*, 108, pp. 1162–1169. doi: https://doi.org/10.1016/j.biopha.2018.09.132.

Yuan, L. *et al.* (2013) 'Low-level shear stress induces human mesenchymal stem cell migration through the SDF-1/CXCR4 axis via MAPK signaling pathways.', *Stem cells and development*. United States, 22(17), pp. 2384–2393. doi: 10.1089/scd.2012.0717.

Zaragosi, L.-E. *et al.* (2011) 'Small RNA sequencing reveals miR-642a-3p as a novel adipocyte-specific microRNA and miR-30 as a key regulator of human adipogenesis.', *Genome biology*. England, 12(7), p. R64. doi: 10.1186/gb-2011-12-7-r64.

Zhang, J. *et al.* (2011) 'Roles of SATB2 in Osteogenic Differentiation and Bone Regeneration', *Tissue Engineering Part A*. Mary Ann Liebert, Inc., publishers, 17(13–14), pp. 1767–1776. doi: 10.1089/ten.tea.2010.0503.

Zhang, L. *et al.* (2010) 'Chondrogenic differentiation of human mesenchymal stem cells: a comparison between micromass and pellet culture systems.', *Biotechnology letters*. Netherlands, 32(9), pp. 1339–1346. doi: 10.1007/s10529-010-0293-x.

Zhang, Q. *et al.* (2015) 'Honokiol inhibits bladder tumor growth by suppressing EZH2/miR-143 axis', *Oncotarget*. Impact Journals LLC, 6(35), pp. 37335–37348. doi: 10.18632/oncotarget.6135.

Zhang, X. *et al.* (2006) 'Runx2 Overexpression Enhances Osteoblastic Differentiation and Mineralization in Adipose - Derived Stem Cells in vitro and in vivo', *Calcified Tissue International*, 79(3), pp. 169–178. doi: 10.1007/s00223-006-0083-6.

Zhang, Y. *et al.* (2011) 'A program of microRNAs controls osteogenic lineage progression by targeting transcription factor Runx2', *Proceedings of the National Academy of Sciences of the United States of America*. 2011/05/31. National Academy of Sciences, 108(24), pp. 9863–9868. doi: 10.1073/pnas.1018493108.

Zhao, J. *et al.* (2015) 'Down-regulation of miR-205 promotes stemness of hepatocellular carcinoma cells by targeting PLCβ1 and increasing CD24 expression', *Neoplasma*, 62(4), pp. 567–573. doi: 10.4149/neo_2015_068.

Zhao, X. *et al.* (2014) 'The role of SATB2 in skeletogenesis and human disease', *Cytokine & Growth Factor Reviews*, 25(1), pp. 35–44. doi: http://dx.doi.org/10.1016/j.cytogfr.2013.12.010.

Zhou, C. *et al.* (2011) 'Luminescent Gold Nanoparticles with Efficient Renal Clearance',

Angewandte Chemie (International ed. in English), 50(14), pp. 3168–3172. doi: 10.1002/anie.201007321.

Zhu, H. *et al.* (2014) 'Role of extracellular signal-regulated kinase 5 in adipocyte signaling.', *The Journal of biological chemistry*. United States, 289(9), pp. 6311–6322. doi: 10.1074/jbc.M113.506584.

Zhuang, L. *et al.* (2019) 'miR-205 targets runt-related transcription factor 2 to inhibit human pancreatic cancer progression', *Oncology letters*. 2018/11/12. D.A. Spandidos, 17(1), pp. 843–848. doi: 10.3892/ol.2018.9689.